AD-A044 174 ARMY ELECTRONICS COMMAND FORT MONMOUTH N J F/G 9/1
TRANSMISSION-LINE ANALOGS FOR PIEZOELECTRIC LAYERED STRUCTURES.(U)
MAY 76 A BALLATO

UNCLASSIFIED ECOM-4413 NL

1 OF 3
ADA
044174

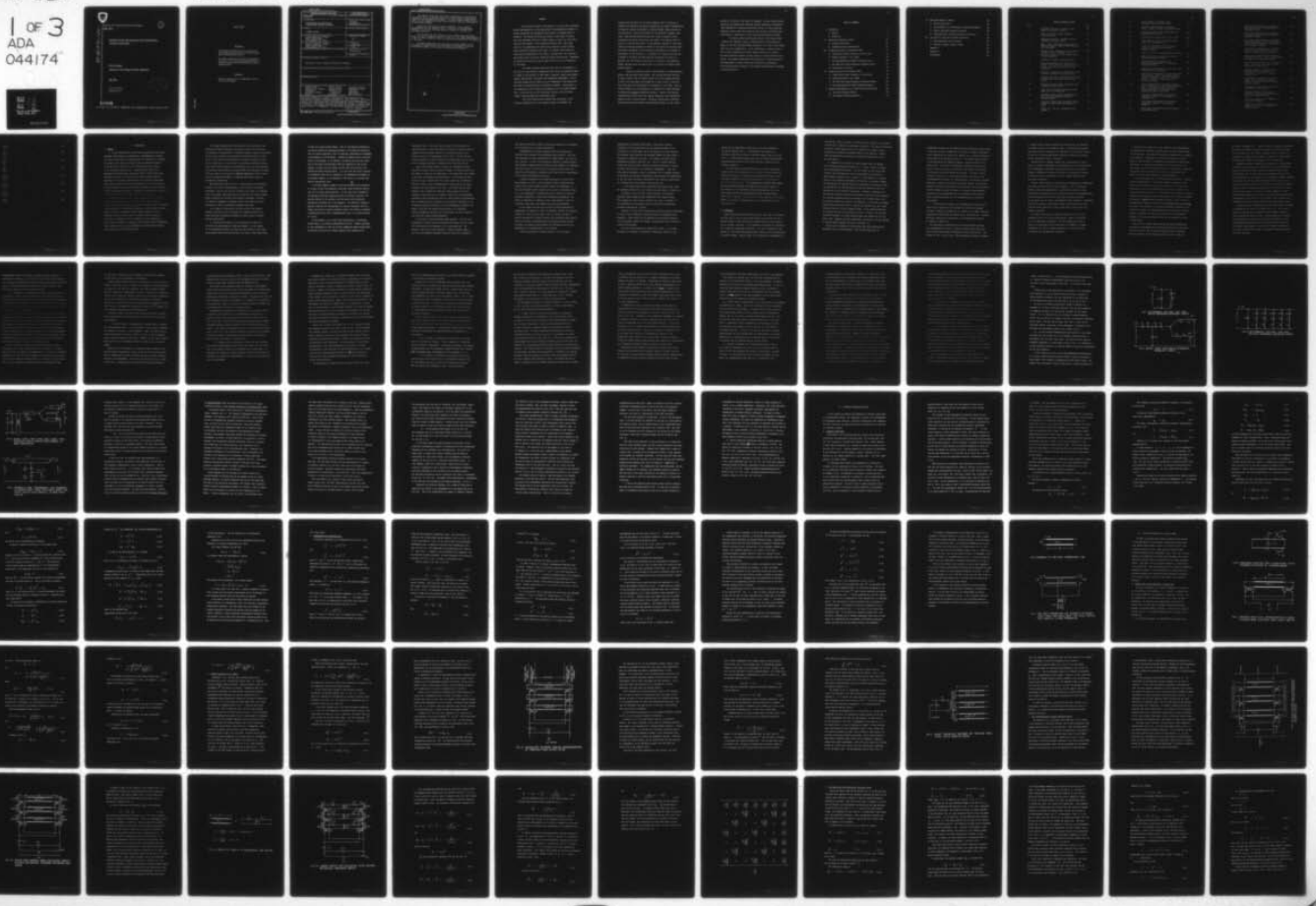

Research and Development Technical Report

ECOM -4413

AD A044174

TRANSMISSION-LINE ANALOGS FOR PIEZOELECTRIC LAYERED STRUCTURES

Arthur Ballato

Electronics Technology & Devices Laboratory

May 1976

ECOM

US ARMY ELECTRONICS COMMAND FORT MONMOUTH, NEW JERSEY 07703

NOTICES

Disclaimers

The findings in this report are not to be construed as an official Department of the Army position, unless so designated by other authorized documents.

The citation of trade names and names of manufacturers in this report is not to be construed as official Government indorsement or approval of commercial products or services referenced herein.

Disposition

Destroy this report when it is no longer needed. Do not return it to the originator.

UNCLASSIFIED

SECURITY CLASSIFICATION OF THIS PAGE *(When Data Entered)*

REPORT DOCUMENTATION PAGE		READ INSTRUCTIONS BEFORE COMPLETING FORM
1. REPORT NUMBER ECOM-4413	2. GOVT ACCESSION NO.	3. RECIPIENT'S CATALOG NUMBER
4. TITLE *(and Subtitle)* TRANSMISSION-LINE ANALOGS FOR PIEZOELECTRIC LAYERED STRUCTURES		5. TYPE OF REPORT & PERIOD COVERED Doctoral Dissertation 6. PERFORMING ORG. REPORT NUMBER
7. AUTHOR(s) ARTHUR BALLATO		8. CONTRACT OR GRANT NUMBER(s)
9. PERFORMING ORGANIZATION NAME AND ADDRESS US Army Electronics Command ATTN: DRSEL-TL-ML Fort Monmouth, NJ 07703		10. PROGRAM ELEMENT, PROJECT, TASK AREA & WORK UNIT NUMBERS N/A
11. CONTROLLING OFFICE NAME AND ADDRESS US Army Electronics Command ATTN: DRSEL-TL-ML Fort Monmouth, NJ 07703		12. REPORT DATE May 1976 13. NUMBER OF PAGES 252
14. MONITORING AGENCY NAME & ADDRESS(if different from Controlling Office)		15. SECURITY CLASS. (of this report) Unclassified 15a. DECLASSIFICATION/DOWNGRADING SCHEDULE

16. DISTRIBUTION STATEMENT *(of this Report)*

Approved for public release; distribution unlimited.

17. DISTRIBUTION STATEMENT *(of the abstract entered in Block 20, if different from Report)*

18. SUPPLEMENTARY NOTES

19. KEY WORDS *(Continue on reverse side if necessary and identify by block number)*

Acoustic waves	Filter crystals	Equivalent circuits
Piezoelectric crystals	Crystal Filters	Transmission Lines
Transducers	Reflection and refraction	Resonators
Oscillator crystals	Acoustics	Ultrasonics
Filters		Mode conversion

20. ABSTRACT *(Continue on reverse side if necessary and identify by block number)*

This report comprises a doctoral dissertation in electrophysics at the Polytechnic Institute of Brooklyn, Brooklyn, NY 11201, June 1972. This study derives exact equivalent network representations for the electromechanical behavior of crystal stacks that are piezoelectrically driven in thickness modes of vibration. The stacked structure may consist of any number of layers; each layer consists of a homogeneous, but arbitrarily anisotropic crystal medium.

(Cont'd on reverse)

DD FORM 1 JAN 73 1473 EDITION OF 1 NOV 65 IS OBSOLETE

UNCLASSIFIED

SECURITY CLASSIFICATION OF THIS PAGE *(When Data Entered)*

The analysis shows that each layer is represented by three acoustic transmission lines; in general, these lines possess unequal characteristic immittances and propagation wavenumbers. At the interface between any two layers, the six transmission lines (three from each side) are interconnected by transformer elements.

The circuit descriptions obtained constitute a first rigorous representation for the canonical cases of thickness- and lateral-field excitation of the three thickness modes of vibration of crystals with arbitrary anisotropy.

The circuits have been realized in such a fashion that the overall result for a multi-layered structure is built up by the simple interconnection of basic blocks of identical form, with each block accounting for the behavior of one layer.

An example demonstrates the application of these networks to the development of actual devices and illustrates the systematic, efficient and practical aspects of the network characterization developed.

SUMMARY

The principal purpose of this study is to derive exact equivalent network representations for the quasi-static electromechanical behavior of crystal stacks that are piezoelectrically driven in thickness modes of vibration. The stacked structure may consist of any number of layers, which are considered infinite in lateral extent, so that all field variations are with respect to the thickness coordinate only. Each layer consists of a homogeneous, but arbitrarily anisotropic crystal medium, whose constitutive equations are linear. No further restrictions are placed upon the magnitudes of the elastic, piezoelectric, and dielectric coefficients other than those imposed by energy considerations. Thickness- or lateral-field excitation may be used to drive one or any combination of the plates.

The present analysis shows that each layer is represented, in the bulk, by three acoustic transmission lines, which are physically equal in length to the thickness of that layer; in general, these lines possess unequal characteristic immittances and propagation wavenumbers. At the interface between any two layers, the six transmission lines (three from each side) are interconnected by transformer elements. Incorporation of the piezoelectric drive mechanism requires an additional simple network that is connected only at the transformer terminals, thus providing further coupling between the transmission lines.

The circuit descriptions obtained here constitute a first rigorous representation for the canonical cases of thickness- and

lateral-field excitation of the three thickness modes of vibration of crystals with arbitrary anisotropy; furthermore, the network representation includes the complete development of coupling between these modes due to the piezoelectric effect and accounts for all mechanical boundary conditions. What has thus been attained is not simply a complete circuit equivalence that holds port-to-port, but rather a true analog, which is valid on a point-to-point basis. As the physical processes of the actual problem are thereby accurately mirrored in the quantities associated with the network equivalent, which is spatially distributed to correspond to the geometry of the structure, it is possible to visualize and trace the interplay of the waves involved simply by inspecting the circuit; in addition, the full effects arising from the coupling at the boundaries between adjacent media are made evident in a succinct and readily interpretable manner.

Apart from physical insight, the development of these equivalent networks has additional significance. The circuits have been realized in such a fashion that the overall result for a multi-layered structure is built up by the simple interconnection of basic blocks of identical form, with each block accounting for the behavior of one layer. When an actual structure is to be analyzed, it is therefore no longer necessary to perform an <u>ab initio</u> mathematical analysis. Instead, the complete characterizing circuit can be put down by inspection, thus reducing the problem to one of network theory. Similarly, synthesizing a structure that realizes given performance specifications reduces, via the circuit

analog, to a problem in the domain of networks. In fact, almost without exception, the mechanically vibrating, layered system here considered is itself embedded in a completely electrical circuit, so that having the mechanical portion cast into electrical form provides a uniformity that lends itself to optimization of the overall electromechanical system.

The general network description derived in this study yields a powerful and immediate access to computer-aided circuit design programs, so that the lead-time between conception of an idea to the working model can be cut dramatically. As an illustration, a computer simulation is used to generate the filter response function for a simple two-layer structure composed of quartz plates of varying relative orientation. This example demonstrates the application of these concepts to the development of actual devices and illustrates the systematic, efficient and practical aspects of the network characterization developed in the present work.

TABLE OF CONTENTS

TABLE OF FIGURES & TABLES

I. INTRODUCTION

A. GENERAL

1. In this dissertation we derive exact equivalent circuit representations that describe the quasi-static electromechanical behavior of crystal stacks driven in thickness modes of vibration. The structure may consist of any number of layers; these are considered infinite in lateral extent, so that all field variations are with respect to the thickness coordinate only. Comprising each stratum is an homogeneous, but arbitrarily anisotropic crystal, whose constitutive equations are linear. No further restrictions are placed upon the magnitudes of the elastic, piezoelectric, and dielectric coefficients other than are imposed by energy considerations, so that the analysis includes materials with high piezoelectric coupling; such are currently of great technological interest. Thickness- or lateral-field excitation may be used to drive one or any combination of the plates.

Our analysis shows that each layer is represented, in the bulk, by three acoustic transmission lines, physically equal in length to the thickness of that layer, but having, in general, unequal characteristic immittances and propagation wavenumbers. Each interface, however, appears as lumped transformer elements coupling together the six transmission lines incident upon that boundary from the strata on both sides. Incorporation of the piezoelectric drive mechanism is further shown to require an additional simple network and interconnection, which appears also only at the boundaries, and which provides further coupling between the transmission lines.

For various combinations of layer material and orientation, plus mechanical interface conditions and electric driving field direction, the mechanical and piezoelectric interfacial networks simplify considerably. Of the crystal vibrator devices conceived and utilized over the years, which fit into the class of structures we describe, virtually all are of this latter type. In such cases, the equivalent electrical circuits which result from specializing our formulation yield the same mechanical and electrical port-relations as obtained from the traditional equivalent circuits; indeed, the circuits are formally identical but for the piezoelectric transformer placement, a seemingly minor detail, shown to be important conceptually.

When conditions allow little or no simplification of the boundary networks, the circuit representations we give here most distinguish themselves. They are the first set covering, with rigor, the canonical cases of thickness- and lateral-field excitation of the three thickness modes of vibration of crystals with arbitrary anisotropy, including the complete development of coupling between these modes due to the piezoelectric effect and mechanical boundary conditions.

As an example and application of these circuits and concepts, computer simulation is used to generate the response function of a simple two-layer configuration composed of quartz plates of varying relative orientations.

2. The objectives sought in this dissertation go beyond the derivation and presentation of these new networks. It will appear, as the development proceeds, that what has been attained is not simply an equivalence which holds port-to-port, but rather a true analog which

is valid on a point-to-point basis. That is, the physical processes of the actual problem are accurately mirrored in the quantities associated with the circuit equivalent, which is spatially distributed to correspond to the geometry of the structure. Because the network and the structure accord in this manner, it is possible to visualize and trace the interplay of the waves involved simply from the inspection of the circuit diagram, including the full effects arising from the coupling at the boundaries between adjacent media. It is true that the circuit contains no information other than is contained in the mathematical statement of the problem; however, it is contained in the circuit in a succinct and readily interpretable form.

In the more complex classes of vibrating systems we are discussing, it is easy to have the mathematics describing these situations obscure just what is taking place physically. On the other hand, reference to the analogous electrical equivalent places in evidence, directly, the physical content of the problem, with the details and intricacies individually accounted for in the schematic. The effects of changes in physical condition and configuration are readily visualized, such as a change from welded to sliding interface contact; the effect of replacing a piezoelectric plate with a nonpiezoelectric one, or a crystal stratum by a fluid.

We thus present, for a given layer configuration, an equivalent network which is a pictorial representation as well. Another advantage of this development is that the circuits themselves suggest applications and devices that are not so readily apparent when considering the

mathematics alone. This comes about because of the similarity the equivalents bear to others describing the behavior of existing types of components whose operation depends on a different principle, e.g., microwave filters or electromagnetic delay lines. Not only are new devices suggested, but their realization and optimization can be guided by the techniques developed in connection with the older devices.

Apart from valuable physical insight, the development of these equivalent circuits serves additional purposes. We stated earlier that any number of strata can be accommodated. This stems from a key feature of the work, the concept of building blocks. The circuits have been realized in such a fashion that the overall result for a structure is built up, simply, by the interconnection of basic blocks, each block accounting for the behavior of one layer. All blocks have the same canonical form, although the numerical values associated with the elements of each block will, in general, differ, and, as we mentioned previously, certain particular cases will bring further simplifications. When a suitable physical structure is to be analyzed, therefore, it is no longer necessary to perform an ab initio mathematical analysis, but merely to put down the network characterizing it by inspection. Numerical parameters need still to be calculated, but this is done for the individual network blocks separately.

At this point, other advantages become apparent. Not only is it unnecessary to analyze each new arrangement over again, layer by layer, but such analysis as is necessary is of a particular sort. The problem is now one of network analysis, a highly developed subject, and all of the powerful techniques from this field can be brought to

bear upon the equivalent network to obtain such measures of performance as are required for the intended application.

Complementing the analysis problem is that of synthesizing a structure which realizes given performance specifications. Here also the procedures are highly systematized in network theory, which may be used directly. In fact, the mechanically vibrating, layered system we here consider is almost without exception itself embedded in a completely electrical circuit, so that having the mechanical portion cast into electrical form provides a uniformity which lends itself to optimization of the overall electromechanical system.

A further advantage of the network description, and one of the most important, is that it gives immediate access to computer-aided circuit design (CAD) programs currently coming into prominence, so that the lead-time between conception of an idea to the working device can be cut dramatically. Working either from a new idea in terms of structure or materials, or from given performance requirements, the device is simulated on a computer, using a CAD program to arrive at a physical design which then becomes the basis for experiments.

In this regard, the fact that, subject to rather unrestrictive assumptions, the analysis is exact, is important, because the simulated behavior of a device is also exact. When the results are used to produce experimental or practical models, any deviations from predicted results may justly be ascribed solely to empirical factors, whereas otherwise, the question arises whether the divergence is due to the experiments or to approximations in the analysis.

A further application of these circuits is to the accurate

determination of material coefficients. Prior uses of stacked resonators for this purpose have had mixed success because of the restriction to a single mode, and to the absence of an exact analysis. Our networks clearly describe the interplay between the three modes as experimental conditions are varied. For example, the effect of one experimental parameter variation, viz., that of a relative rotation between two adjacent plates, about the thickness direction, is simply to change turns ratios in the interfacial transformers. This, and other similar procedures, taken in conjunction with a suitable sequence of immittance and frequency measurements, should permit the determination of the full array of elastic, piezoelectric and dielectric coefficients of a substance with high precision and relative ease.

3. Our results arise from a combination of separate ideas; these are discussed briefly here, and covered in greater detail in Section I B.

We observe, first, that for a given direction, an arbitrary, unbounded crystal supports three independent plane acoustic waves. This suggests that three modes, instead of one, have, in general, to be incorporated into equivalent circuits describing one-dimensional thickness vibrations of a crystal.

Secondly, the idea that the physically vibrating system is distributed in nature is most graphically conveyed by means of transmission-line schematics. These carry over the important idea of spatial extension to the equivalent networks and suggest an analog which might be valid on a point-to-point basis.

The next notion concerns the piezoelectric effect. It is often discussed as a volumetric, distributed, interaction; however, it may

equally well be considered to arise only at the layer boundaries. Two results support this: a. a piezoelectric rod excited by a microwave cavity field is found to initiate acoustic waves at the end face; b. a traction-free crystal plate has its three thickness modes piezoelectrically coupled at the free boundaries, whereas they are otherwise uncoupled.

The final aspect requiring treatment, when casting the physical situation into circuit theory terms, is that of the purely mechanical boundary conditions. In addition to the piezoelectric effect, these also couple together the three thickness modes at the interfaces in all but the simplest cases. It is apparent that networks which account for the mechanical boundary conditions might be placed directly at the interfaces in the equivalent circuit representation, but it is less obvious how they are associated there with the piezoelectric drive circuit elements. We show that each effect appears in the overall network as a separate interconnection of ideal transformers at each layer interface.

B. HISTORICAL

Having mentioned very briefly what has been done, some of the motivation for doing it, and the main ideas involved, we turn now to a more detailed account of the background and sources from which this problem, and its solution, have come. It is convenient to organize the discussion into a number of overlapping categories. The topic of analogs is first touched on, after which the analogy between acoustics and electromagnetics is briefly reviewed. Network theory as an outgrowth of electromagnetics

then follows. Next, past work on acoustic waves in crystals is considered, followed by the subject of piezoelectric excitation. The topic of equivalent electrical circuits growing out of the combination of acoustic waves, piezoelectric excitation and network theory is then taken up. Finally, areas of application are indicated, with general references to all of the above topics.

1. Networks will be derived in later chapters which are analogs of the vibrating structures described in I A. above, insofar as regards their electromechanical behavior. To make clearer our use of the word "analog", and also because the idea of representing one physical or ideal system by another, which is alike it in some respect, is a common thread in the historical development sketched here, we indicate a number of distinctions. Two physical systems are considered true analogs if both are described by the same mathematical relations everywhere within the systems and at their respective boundaries. Sometimes, irrespective of the physical processes interior to two systems, which may not be analogous, the relations characterizing their behavior at the boundary ports, such as terminal voltages and currents, are identical. In this case the analogy extends only port-to-port and is a limited and imperfect one, but in many practical cases it is still extremely useful. A true analog corresponds at the ports and also in the interior, so that it is valid, for spatially distributed systems, on a point-to-point basis; our networks are of this latter type. Analogs, and their experimental realization, have been applied to various elastic problems by Mindlin & Salvadori (1).

One may talk of analogies in senses other than that understood when describing true or limited analogs. Thus, without regard for the

mathematics involved, one can consider physical models as analogs insofar as they may be used to demonstrate a principle, as Maxwell's mechanical model illustrating the induction of currents (2), or Kelvin's string and spring model of an anisotropic solid (3). Yet another form of analog is that represented by schematic drawings. Here the analogy is of a subtler sort. We have now a diagrammatic, shorthand, depiction of a physical situation, wherein the essence of the problem is abstracted and idealized by means of symbols and topology. Electrical circuit schematic elements, e.g., are analogs of certain limiting cases of electromagnetic situations; the correspondence is one between a physical system and a drawing, not between two physical systems. The physical problems we treat are characterized in this manner, but as the schematic circuits themselves always correspond to a physical electromagnetic realization, the correspondence can be considered to exist between pairs of physical systems, and our representations are, therefore, true analogs.

2. The subjects of acoustics and electromagnetics are both very large. We will simply note that because they share the phenomenon of waves in common, the possibility of a common, or at least a similar, explanation or description has always been an intriguing one. A general reference, covering both disciplines, is the comprehensive article by Truesdell & Toupin (4).

One difficulty in establishing a true analogy between acoustics and electromagnetics is that, in general, acoustic plane waves have three polarizations whereas electromagnetic waves have only two. Mac Cullagh (5) did, in fact, force a true mathematical analogy by assuming

an "elastic strain" energy function which involved only the components of rotation relative to an absolute frame; the constitutive equations then relate stress to rotations, the equations for the "elastic" motion of light in a vacuum become formally identical to Maxwell's equations, and the longitudinal mode is eliminated.

Another avenue of approach consists not in suppressing the third mode in an acoustic formulation of electromagnetics, but in generalizing the electromagnetic formulation to provide light with a third polarization. Although of theoretical interest (6), experimental evidence is lacking (6,7) for this approach, and the analogy cannot be made more than a similarity.

The most recent attempts at displaying the mathematical correspondences which exist have also been the most successful. Auld (8) considers acoustic plane wave propagation in a piezoelectric medium and shows that whereas the equations are not identical to those for electromagnetics, the field operators in each case bear certain analogous relations to each other. Peng (9) uses a transformation which promotes the electromagnetic field vectors to second-rank tensors, and obtains equation sets which are nearly identical, so that a good deal of insight into both systems is achieved.

An analog in the form of a mechanical model of the "ether" was proposed by Kelvin (10), which would require a number of gyroscopes in a very complicated arrangement. The very complexity of such a model is an indication of the artificiality of attempts at a common explanation, or even of a common description, in the strict sense, of acoustic and electromagnetic phenomena.

The crux of the difficulty is that acoustics and electromagnetics are fundamentally different in nature; while they have certain common, or similar traits, the differences prohibit an analogy which is complete in all respects. Fortunately, the areas of similarity do permit a number of true analogs to be formulated, particularly as regards wave properties. The analogy which concerns us has to do with the fact that uniform, plane, waves of both types may be represented by spatially distributed circuit schematics in the form of transmission lines. These will be discussed subsequently in greater detail.

3. As we indicated earlier, electrical network theory is a limiting form of electromagnetics. The network components appearing in the theory are both lumped (11-14) and distributed (15). Of particular importance for us is the transmission-line, which is principally the creation of Heaviside (16-17). It incorporates those aspects of electromagnetic waves required to provide true analogs of the acoustic problems we consider. Beyond providing analogous systems, the use of network representations allows us to employ circuit schematics as visual analogs to assist in the portrayal of the physical processes involved; this is particularly helpful for understanding transient operation of layered devices. Therefore, not only do we carry over the electromagnetic analogs to our acoustic problems, but we use the schemata for visual interpretations.

Added to this, network theory provides specialized mathematical techniques and procedures which have been tailored for the very ends we wish to achieve, such as realizing specified filter responses. General references are the texts by Guillemin (18-19), Cauer (20)

and Carlin & Giordano (21). Network theory with specific applications to filters is discussed by Ruston & Bordogna (22), Mason (23), Youla (24) and Zverev (25). The subject of crystal filters is dealt with in Herzog (26), Mason (23) and Kosowsky & Hurtig (27), while crystal oscillators are treated in Groszkowski (28) and Hafner (29).

Although Heaviside is responsible for almost all of transmission-line theory in its present form, inclusion of the finite transmission line as an additional circuit element for network synthesis began with Richards (30), in 1948; since then conventional circuit theory has been enriched by an increasing use of distributed networks, primarily for filters, but also for broad-band transformers and delay lines. The recent articles by Carlin (31), and Koga (32) indicate the current status and contain additional references to the literature. As our circuit results appear in the form of networks composed of lumped and distributed elements, the synthesis procedures now actively being investigated can be applied, via the analogs, to the realization of piezoelectric layered crystal structures having prescribed behavior.

We mention, lastly, computer-aided circuit design (CAD) as a means of implementing the results of network theory (33). This field is developing rapidly, and CAD programs are now becoming available to handle distributed-element circuits. These programs are a necessity when considering the analysis of many-layered structures, or even configurations consisting of only two or three layers except when the crystal plates possess a great deal of intrinsic symmetry and are simply oriented with respect to the common thickness coordinate and with each other.

4. We take up now the topic of plane acoustic waves propagating in crystals. The discussion is divided into four parts: propagation in media which are a.) unbounded and nonpiezoelectric, b.) unbounded and piezoelectric, c.) bounded and nonpiezoelectric and d.) bounded and piezoelectric.

a.) George Green, in 1839, gave the first general theory for the propagation of plane acoustic waves in anisotropic media (34). He showed that three types of waves are possible, that they in general have different velocities, and that the directions of particle motion are mutually perpendicular. It was he who, in an earlier paper (35), also showed that twenty-one elastic constants are required for the characterization of an arbitrary crystal. This was deduced from the conservation of energy principle which he was the first to state. In both of these papers he was seeking equations governing the behavior of light, so we have here yet another example of how closely light was associated with mechanical motion, and how steadfastly analogous explanations were pursued.

In 1877 Christoffel published a long article on the same subject (36). He cast the equations in terms of strain instead of stress, and gave the formulation which is still followed today.

Lord Kelvin (37) built upon the work of Green, clarified parts of his work, and extended it. Here, again, it appears that the motivation for these acoustical researches was to obtain a clearer understanding of optical phenomena, although he did pronounce the topic of elastic waves in a solid "a fine subject for investigation."

Musgrave (38-42) presents very fine discussions of the behavior of elastic waves in anisotropic substances using the projective geometrical

correspondences between the velocity, slowness and wave surfaces. He summarizes the situation as it stood after Kelvin's work, but spurred by the availability of experimental data which was all but absent in Kelvin's time, he investigates specific features of the elastic surfaces, and calculates a number of them for various materials.

b.) Historically, consideration of acoustic wave propagation in piezoelectric crystals arose from experiments upon vibrating plates of quartz, of which more will be said in d.) below; from those investigations of of particular cases, involving the more difficult problem of reflections of waves in a bounded plate, we find the origins of the development of propagation in unbounded piezoelectric media.

Lawson (43), in 1941, showed that the extensive experimental results of Atanasoff & Hart (44) on vibrating quartz plates required a piezoelectric correction to make them consistent. He gave the correct general differential equations and secular equation, which involved piezoelectrically stiffened elastic constants. Bechmann (45-47), who was also interested in plate vibrations, gave a complete discussion of the unbounded propagation problem, including the effect of the piezoelectric constants on the particle motions, and the effect of an exciting field on the effective piezoelectric constant driving a given thickness mode.

In 1949, Kyame (48) treated the more difficult problem of wave propagation in an infinite medium where both the acoustic and electromagnetic effects are coupled by piezoelectricity. The theory he developed incorporates the full Maxwell's equations, and predicts five plane waves, three of which become the acoustic modes, in the absence of piezoelectricity, while the remaining two become the usual electromagnetic waves.

He also gives an expression for the complete Poynting vector composed of both elastic and electromagnetic contributions.

Similar analyses were carried out by Pailloux (49) in 1958, and Alda, Hruška & Tichý (50) in 1963. Hruška (51-52) compared the results obtained by keeping the full Maxwell's equations, with those of Lawson's method, where the quasi-static approximation is made. He was able to separate the effects, and to show that, whereas a quasi-static piezoelectric correction to the elastic constants and velocities can amount to a difference measured in per cent, the result of the quasi-static approximation differs from the exact electromagnetic calculation by less than 10^{-8} percent, and so is completely negligible for our purposes here.

We mention, lastly, that Auld (8) has derived reciprocity relations for the piezoelectric medium in both the exact case and the quasi-static approximation.

c.) Now we come to a consideration of acoustic waves in bounded, but nonpiezoelectric media. It is appropriate to look first at reflection and refraction of waves at a single boundary. Knott (53) first gave the solution for isotropic solids in contact, in 1899. In the intervening years, additional treatments were given. Musgrave (41-42) gives a recent account of the case of anisotropic bodies in contact, with a practical example.

Passing on to the situation of an isotropic material bounded by two parallel planes, constituting a plate, one can do no better than to consult the comprehensive article by Mindlin (54) which includes historical references and developments. We take note of only one fact now, to make a point later. Although Rayleigh and Lamb gave the formal solution to

the traction-free plate problem in 1889, it was not until 1954 that it was recognized that the plate waves could be decomposed into pairs of longitudinal and shear waves reflecting from the boundaries (54).

The history of high frequency waves and vibrations in anisotropic plates begins with the work of Koga (55-56) who solved the thickness mode problem for the case of an infinite nonpiezoelectric plate in which he independently rediscovered Christoffel's method. In applying the theory to plate resonators of quartz and tourmaline, he recognized the influence of the piezoelectric effect in altering the effective elastic stiffness, but his treatment takes the form of an ad hoc addition.

Corresponding to Rayleigh's (57) solution, for the isotropic plate, is Ekstein's (58) solution for the two-dimensional vibrations of a monoclinic plate, which was elaborated on by Newman & Mindlin (59) in 1957. Since then a great variety of results for bounded crystal plates has become available, notably through the work of Mindlin and his colleagues. They have had considerable success in applying methods of power-series expansions in the thickness-coordinate, originally due to Poisson & Cauchy, to arrive at approximate, two-dimensional, plate equations which may then, very often, be solved exactly.

d.) Inclusion of the piezoelectric effect into the thickness-vibrations of plate-resonators was carried out by Cady (60) in 1936 who gave a more rigorous analysis of its influence for a single mode. He considered the crystal as a lumped mechanical system in the vicinity of resonance, and included the consequences of a finite air gap between the plate and electrodes.

Following this, Lawson (43), as mentioned earlier, gave the correct quasi-static equations for acoustic plane wave propagation in an infinite piezoelectric plate, forming the basis of a rigorous theory of piezoelectric vibrations, instead of considering the plate a lumped system, as had Cady. However, his assumed solutions do not individually satisfy the proper boundary conditions, except in simple instances, but application of the results to the experiments of Atanasoff & Hart (44) was adequate to resolve their inconsistencies, largely due to neglect of stiffening. In 1942 Lawson (61) took up the problem more fully, considering a driving electric field oriented in the thickness direction, and arrived at results which were believed to be exact, including the influence of an air gap. The effect of piezoelectricity, additional to stiffening, was incorporated into an "effective thickness," different for each of the three modes, and from the geometrical thickness.

Ekstein (62), in 1946, and Mindlin (63), in 1952, treated the much more difficult problem of the finite crystal plate. Our work concerns only unbounded plates, so we will pass over the main results of their papers, except to indicate how they proceeded, and return to them in connection with equivalent circuits. Ekstein used perturbation theory to investigate forced vibrations. The plate problem is first solved approximately in this manner assuming the piezo-effect is absent; the procedure is then used again to take piezoelectricity into account. Mindlin's work treated forced vibrations of monoclinic crystals by an extension of his approximate two-dimensional plate equations to include piezoelectricity.

The publications of Bechmann (45-47), already referred to, apply

also to the vibrations of piezo-plates, but are more properly considered in the context of equivalent circuits.

Tiersten (64) in 1963, reconsidered Lawson's problem (61), and discovered that the solution given does not satisfy the proper boundary conditions. He solved the problem exactly. Tiersten found that the three thickness-modes are, in general, coupled at the two traction-free boundaries, by virtue of the piezoelectric effect. Only in simple situations will they be uncoupled, in which case the solution reduces to that of Koga (55). It is upon these results that our construction of analog circuits is, in large measure, based; the results provide an interpretation for certain network features which is simple and physically satisfying.

In 1970, Yamada & Niizeki (65) recast Tiersten's exact solution into normal coordinate form, and calculated the input admittance of the plate vibrator for the cases of traction-free, mass loading and air-gap boundary conditions. We will retain certain features of their derivation, specifically the normal-coordinate transformation, in our analysis.

e.) The analysis and networks to be given here will assume that the structures are lossless. This is adopted as a convenience, but is not really a restriction. In practical situations, the presence of loss usually has to be considered; methods for doing this, starting from the lossless case, are described in the literature (66-72).

f.) We conclude our discussion of piezoelectrically driven crystal plates with an aspect that is of fundamental importance for our developments; that is the effect of the mechanical boundaries when two crystals are juxtaposed to form a layered structure.

From the work on reflection and refraction of acoustic waves, going back to Green and even earlier, it has been long recognized that the mechanical boundary conditions provide for mode coupling, and that, in general, all modes are involved, even for normal incidence, corresponding to the one-dimensional thickness-modes of interest to us. The usual case in practice, however, is to use materials and geometries in layered configurations which result in a single mode-type (73-85), although occasionally (86) mode coupling is taken into consideration.

Our development represents the coupling, completely, in our circuits, in such a way that the phenomenon appears in a readily interpretable form to those familiar with network schematics.

5. A basic aspect of the work to be described in succeeding chapters depends upon an interpretation of the piezoelectric effect in terms of a force acting at surfaces rather than throughout a volume. For the class of problems we treat, this interpretation turns out to have a very clear, physical, meaning, when regarded in network equivalent terms. The usual formulation of piezoelectric driving as a volumetric effect is given by Cady (87); the alternative of surface forcing grew out of work by Cook (88), who in 1956 gave an analysis of a piezo-transducer used for generating transients, and by Slater (89), and Arenberg (90), who described microwave cavity excitation in piezoelectric crystals. Cook clearly stated the equivalence of the two ways of regarding the excitation, and showed that application of a voltage to an initially quiescent transducer produces two elastic waves that propagate from the two plate surfaces inward toward each other. This effect was used by Bömmel & Dransfeld (91-93) to produce hypersonic acoustic waves in quartz

rods, by introducing one end of the rod into a microwave cavity, there to interact with the cavity field. A similar arrangement at the output allowed the waves to be detected. Experiments and analysis, carried out in 1960 by Jacobsen (94-95) led to a more complete understanding of the surface-volume equivalence. He showed, as did Bömmel & Dransfeld (93), that acoustic waves are produced at all spatial discontinuities of the (volumetric) piezoelectric stress, the abrupt discontinuity which occurs at the end face of a rod or plate being only a special case. For us, it is a very important one.

Treatments of the case of distributed sources arising from discontinuities within the piezoelectric medium have been confined to the case of one mode, and are discussed in Mitchell & Redwood (96-97), and Leedom et al. (98). Variations in the piezo-stress throughout the specimen is a practical concern with ceramic transducers but much less so with quartz and substances with small piezoelectric coupling. In fact, the fringing field in a microwave cavity produces a continuous distribution of acoustic sources within a quartz rod in Jacobsen's experiments (95), but he shows their effect to be inconsequential compared to the impulse-like source created at the rod end-face. Transient problems, wherein the surface forcing effect shows up most prominently, were additionally considered by Redwood (99-100) and Peterson & Rosen (101).

Replacement of the volumetric piezoelectric driving stress by the surface forcing equivalent was fruitfully applied by Holland (102-104) to a variety of ceramic vibrator problems involving complex configurations. He emphasized the simple physical interpretation which could be given

to this formulation; the same interpretation will arise in our treatment.

The finding, by Tiersten (64), that the three thickness-modes are coupled, by the piezoelectric effect, at the plate surfaces, is another manifestation of the part the boundary discontinuities play. It will be shown that both Tiersten's boundary coupling, and the initiation of acoustic waves from the end face of a piezoelectric rod in a microwave cavity, are both aspects of the same phenomenon, and both follow from a consideration of the appropriate equivalent circuit.

6a. Circuit theory is conceptually, if not historically, the offspring of Maxwell's field theory. Some of the advantages of this idealization have been pointed out previously. In view of them it's not surprising that circuit theory should be used to model physical electromagnetic systems; that is, to be used as analog representations for them. This has been done with great success, beginning principally in the early 1940's in connection with the development of radar systems (105-108), and continues to the present time to be applied to a large variety of problems (109-111). In fact, it is just the carry-over of network representations of field problems from the electromagnetic to acoustic domains which is beginning to prove so fruitful today, and this carry-over depends upon the analogous aspects of these fields.

b. The work of Rayleigh (112) contains implicitly the notion of an acoustic transmission line, but it was the pioneering work of Mason (113-114) who introduced the concept in connection with crystal vibrators. He stated explicitly that, to take into account the wave motion, the representation would have to be a transmission line.

A fuller account of his work will be given in c., below, but we note his contribution here in connection with acoustic transmission lines. Also in this connection, we mention that it was Redwood & Lamb (115) who first redrew Mason's lumped transmission-line network in spatially distributed form. Here we have the germ of the network ideas we will develop later.

In the work of Oliner (116-117) and his colleagues (118), we find the first systematic application of microwave network methodology to the representation of acoustic wave reflection and refraction at a plane boundary; specifically, the representation of the physical problem in terms of transmission lines coupled together at the boundary by a network. An isotropic medium is considered, but the waves may make any angle with respect to the boundary. We consider anisotropic media, but limit the discussion to normal incidence.

The power of carrying over a network description and microwave electromagnetic techniques of analysis may be illustrated here by a few remarks. We noted above that it wasn't until 1954 that it was realized plate waves could be decomposed into pairs of longitudinal and shear waves reflecting at the boundaries, whereas the analytic solution was given sixty-five years earlier. The reason for the time span is largely because the physical features of the problem are obscured by the mathematics. In Oliner's formulation, using acoustic transmission lines coupled by boundary circuits, the decomposition follows immediately, by inspection, as does the separation of the mode types into symmetric and antisymmetric families. The physical meaning is at once evident, as is the role of the free boundaries of the plate. In addition to

the pictorial and physical clarity achieved, the building-block approach was also introduced. This means that equivalent networks are found for transmission regions and discontinuities separately, and the overall network realization for a given structure is then obtained by attachment of the individual network components, each representing a portion of that structure. We use the building-block approach to arrive at results which hold for an arbitrary number of strata, after having solved a simpler set of problems.

c. We come now to a discussion of the background and development of equivalent circuits to represent piezoelectric vibrating systems. Because this topic is closest to the new analogs we shall present, it is considered at somewhat greater length. In so doing we hope to indicate more clearly our points of departure from these past developments, but also, how the various features we find in these networks are subsumed into our equivalent circuit analogs.

i). The case of a single, isolated resonance is treated first. A mechanically vibrating system with a single degree of freedom, driven by exposure to the electric field of a capacitor, can be represented, at the capacitor terminals, by an electrical equivalent circuit. This was first shown by Butterworth (119) in 1914. In 1922, Cady (120) described experiments on quartz resonators, and represented the behavior near a resonance by giving the equivalent series and parallel resistance and capacitance, which are then functions of frequency.

This was followed, in 1925, by Van Dyke's note (121), wherein he gave a circuit which consisted of constant-value elements; it turned out to be identical with Butterworth's. The Butterworth-Van Dyke

circuit is shown in Fig. 1. It was subsequently verified experimentally in a series of thorough investigations (122-126) by Dye in 1926, Van Dyke in 1928, and Watanabe in 1928-1930. It is still in use today (127).

Another path to the same result is via Mindlin's (63) approximate plate equations; it may be shown that when the plate is allowed to become laterally unbounded, the input immittance in the region near the thickness-shear mode is also realized by the circuit of Fig. 1.

As long as a vibrating piezoelectric system is confined to a frequency at, or near, an isolated resonance, then the input impedance is adequetely described, for the majority of cases, by this simple circuit. If it is desired to use the vibrator to couple mechanical motion, then the device is no longer a one-port, and mechanical terminals must be added. This was done by Mason (128), who, in 1935, gave an equivalent network, valid near a single resonance; it consisted of one electrical and two mechanical ports, and is shown in Fig. 2.

ii). We now consider representations which describe a single mode, but which take into account all of the resonances associated with it. Butterworth (129) was first, here, also. His circuit for the family of resonances belonging to a single mode is given in Fig. 3; it consists of a single capacitor shunted by an infinite number of series RLC combinations, one for each resonance.

In 1939, Mason (130) gave an exact electromechanical representation of a crystal vibrator having one mode of motion, driven by an electric field normal to the direction of propagation of the acoustic waves. His differed from Butterworth's, which is also exact, in that the infinity of

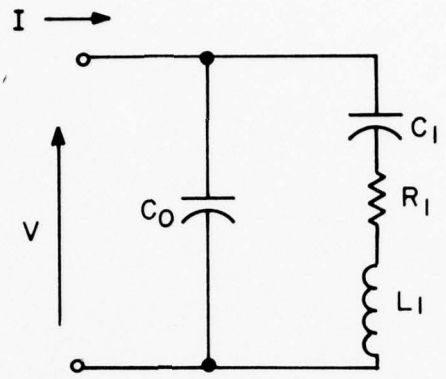

FIG. 1. BUTTERWORTH - VAN DYKE : ONE - PORT, SINGLE RESONANCE, EQUIVALENT CIRCUIT.

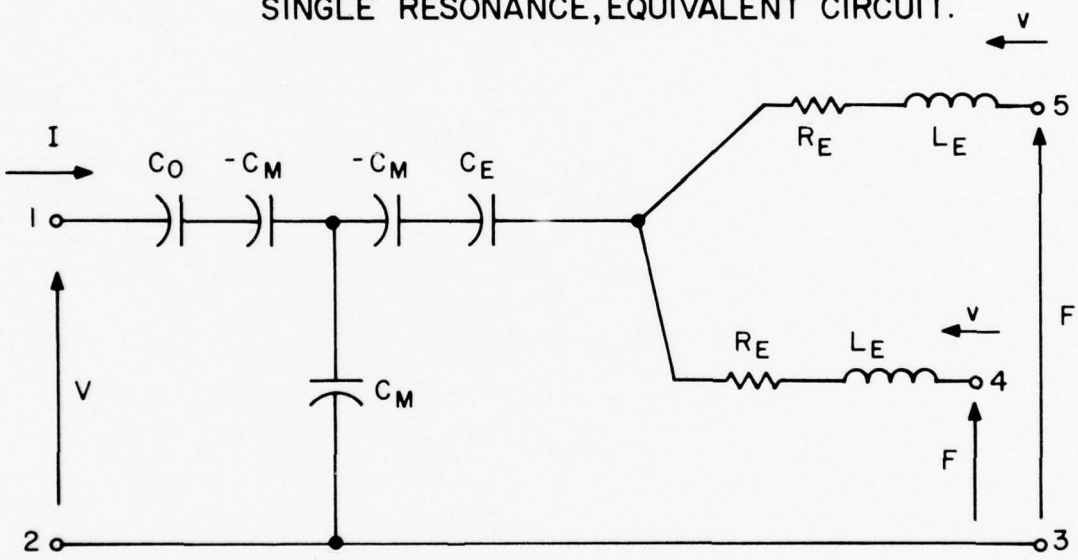

FIG. 2. MASON : THREE - PORT, SINGLE RESONANCE, EQUIVALENT CIRCUIT.

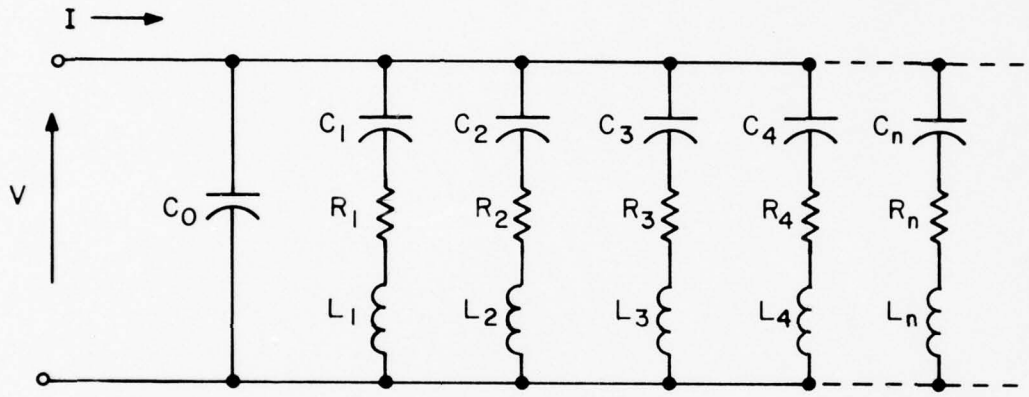

FIG. 3. BUTTERWORTH - VAN DYKE : ONE PORT, MULTIPLE RESONANCE, EQUIVALENT CIRCUIT.

resonances, instead of being individually displayed as RLC circuits, are lumped together into frequency sensitive transcendental functions. Mason also made allowance for the two mechanical ports for the purpose of mechanical coupling at the boundary faces. More specialized limiting forms, such as represent single-resonance operation, and mechanical clamping of one face, etc., are deduced from the exact form. The exact form, as Mason gave it, is shown in Fig. 4.

An excellent overall introduction to equivalent circuits of Mason's type, for the various types of modes of motion used in practice today, is given by Berlincourt, Curran & Jaffe (131).

Additional, exact, equivalent representations have been given by Roth (132-133). These networks also contain lumped circuit elements which are transcendental functions of frequency, and provision is made for two mechanical ports, but the topology differs from those of Mason's. Other results are due to Ekstein (62), who obtained a circuit for the bounded crystal plate, corresponding to his approximate solution, of the same form as Butterworth's (129).

Bechmann (134), in 1940, considered thickness modes of plates excited with an electric field in the thickness direction, and arrived at very accurate results for the elements of Butterworth's 1915 circuit, including the effects of damping and air-gap. These results hold for a crystal plate of any orientation. In 1952 he gave a formulation of the Christoffel method wherein he showed clearly how the piezoelectric stiffening modifies the eigenvectors, and gave some additional considerations not given in Lawson (61); the element values of the equivalent circuit (129) were also calculated using an approximate expression for

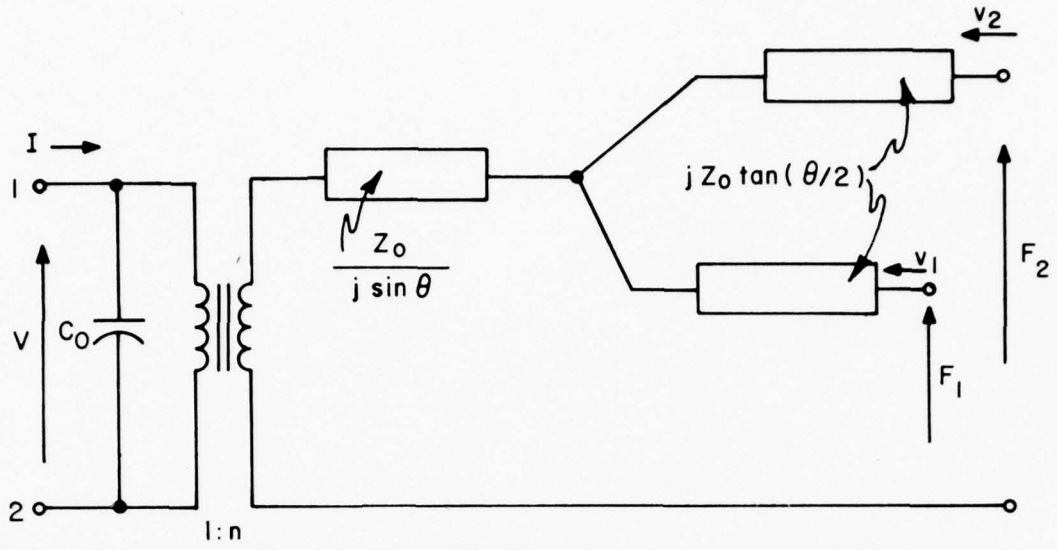

FIG. 4. MASON: EXACT, THREE-PORT, SINGLE MODE-TYPE, EQUIVALENT CIRCUIT. APPLIED FIELD NORMAL TO WAVE PROPAGATION.

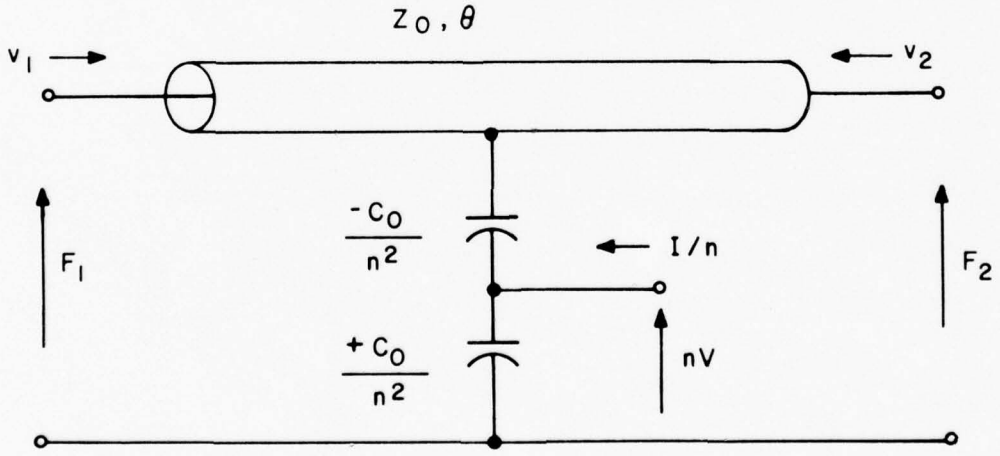

FIG. 5. REDWOOD & LAMB: TRANSMISSION-LINE SCHEMATIC OF MASON'S EXACT, THREE-PORT, SINGLE MODE-TYPE, CIRCUIT. APPLIED FIELD PARALLEL TO WAVE PROPAGATION.

laterally finite plates. A 1953 addendum (46), treated the case of an electric driving field at an arbitrary direction to the crystal, and the effective piezoelectric constant, forcing a thickness mode, is given in general.

Holland has applied his Green's function techniques (103, 104), which we referred to in connection with piezoelectric surface driving, to compute general N-port circuits valid near a resonance. He and Eer Nisse (135, 136) have also been successful in using variational procedures to achieve the same end.

iii). Let us now pick up the threads of two ideas which will bring us, at last, to the heart of the matter of piezoelectric crystal equivalent circuits as they stand today. The threads are themselves entwined, so they will be discussed together. The first idea concerns the transcendental nature of the circuit elements referred to in various places above, while the second pertains to the direction of the electric forcing field.

It turns out that, for acoustic plane wave propagation in a piezoelectric crystal, the electric field associated with the wave, in the quasistatic approximation, must be purely longitudinal. This is shown clearly by Auld (8). In the general case, when the quasi-static approximation is not used, the field may have a transverse component (48), but this is not of interest for us. This fact, that a longitudinal electric field is associated with the acoustic wave, requires a distinction to be made as to the direction of the applied forcing field, or, alternately, as to the electroding arrangement on a plate, and shows up in the equivalent networks. Two cases are distinguished: electric field in the plate thickness direction, called here <u>thickness excitation</u>

of thickness modes (TETM) and electric field lateral to the unique, thickness direction, called lateral excitation of thickness modes (LETM).

We described Mason's 1939 exact circuit, containing transcendental, lumped, elements (Fig. 4). The situation corresponded to the LETM case. Bechmann's 1940 analysis (134) covered the TETM case. Both of them arrived at transcendental frequency equations of slightly different form, as befits the two cases of excitation. What these analyses showed, apart from the differences between the two canonical types of excitation, was that the presence of the piezoelectric effect produces a non-harmonic relationship between the overtones of the modes. Furthermore, the effect, for each mode type, is contained in a single constant, the piezoelectric coupling coefficient, which is a function of the mode type, the vibrator material, and orientation of the specimen with respect to the crystallographic axes. Gradually, the fundamental importance of this coefficient, and of the meaning to be attached to the departure of the overtones of a single mode from a harmonic ratio, have become generally understood (137-143). This understanding was materially aided by Tiersten's 1963 paper (64) which contains a rigorous analysis of Lawson's problem and a clear explanation of the non-harmonic effect in the TETM case.

Having remarked that the frequencies of natural vibration of a piezo-resonator are derived from the non-harmonic roots of a transcendental equation, of slightly different form for the two cases TETM and LETM, we may also recall that Mason's 1939 lumped, exact equivalent network contained transcendental elements, and further, that he clearly stated this was necessary to account for wave transmission in the medium. A finite transmission line, by itself, has immittance poles

and zeros which are harmonic, but a length of line with a lumped circuit element attached to one end has a relation for the critical frequencies which is of the same form as the piezo-resonator's. When the piezoelectric coupling coefficient vanishes, the plate problem reduces to that of Koga (55), and has the same, harmonic, frequencies as a length of transmission line with nothing attached. This situation begins to appear very similar to the discussion of the piezo-plate by Lawson (61) where he introduced an "effective thickness" due to the piezoelectric effect. If only one mode is present, this would be similar to the electrical length of the loaded transmission line just mentioned. In terms of Tiersten's (64) complete analysis, the lumped circuit is a manifestation of the piezo-coupling which takes place at the boundary. The justification for this line of reasoning and the establishment of the transmission-line analogs for the LETM and TETM cases for a single resonator plate, and for any number of layers of such plates, will be given in this dissertation.

The transcendental frequency equations obtained in the single-mode case, for both TETM and LETM, have been approximated by a variety of algebraic formulas (142, 144-146), which hold in the region of any one resonance. Marutake's method is to make partial-fractions expansions of the immittances. In the LETM case, (144) this decomposition is shown to be realized by Butterworth's (129) exact circuit.

Onoe and Jumonji (142), discuss a large variety of modes of ceramic plates, bars, and other configurations, and show that they can be classified into one or other of the canonic types which we have called (in the case of thickness modes of plates), TETM and LETM.

The terminology they have used is "stiffened" and "unstiffened" respectively; this refers to the effect on the elastic constant due to the piezoelectric nature of the material. We do not adopt this nomenclature, because, as we shall show later, generally all modes are stiffened, but there are other subtle differences which make a distinction between these two classes of modes essential. Because we deal only with thickness modes of plates we shall stick with the names TETM and LETM exclusively.

iv). Our discussions have brought us to the last, and most important part of the equivalent network picture as it concerns us. We have alluded to it here and there in the previous paragraphs, and now take it up.

In his works, Mason has always regarded his equivalent circuit containing transcendental elements as representing the wave transmission properties of the transducer he is characterizing. The circuit is always given in lumped form, however, possibly because numerical calculations are facilitated thereby; the transcendental immittance elements are the only hint at a spatially distributed circuit. In 1956, Redwood & Lamb (115) redrew Mason's lumped circuit by using a piece of transmission line to replace the transcendental components, which they recognized as the tee form of the distributed network, and they have continued to use the pictorially new circuit in succeeding papers (147, 99, 100, 146). We present their representation, corresponding to the TETM case (as indicated by the negative capacitor), in Fig. 5.

Investing the electrical schematic with a physical length was an important step forward in the development of a true analog such as we will give. Use of the transmission-line element in schematic networks

for crystals is still a very infrequent occurrence, however, aside from the works of Redwood, Lamb, and their colleagues, referred to above. One representation was given by Franx (148). They have also been used in schematic form by Leedom, Krimholtz & Matthaei (98, 149).

The latest representations, those of Leedom, Krimholtz and Matthaei, in 1970-1971, stress the desirability of a transmission-line schematic. They give three-port circuits, using transmission lines, having forms quite different from those of Mason as redrawn by Redwood & Lamb. In these new networks the electrical port is connected to the center of a purely acoustic transmission line of length equal to the frequency determining length of the vibrator. Some of the circuit elements in the networks are not constant but are frequency sensitive, and no attempt is made to produce a true analog, but simply one which is valid at the three ports. One motivation for the development of the circuits of Leedom et al. is the fact that a Mason-Redwood & Lamb network schematic shows the boundary acoustic forces to be developed, not across the transmission line alone, but partly across the transmission line and partly across the piezoelectric transformer which connects the transmission line to the electrical port. This is a valid criticism, and Leedom et al. have succeeded in separating the acoustic and electrical effects, but at a cost of greater complications elsewhere in the circuits.

The network picture of Redwood & Lamb does appear to be somewhat unphysical in the form they gave it. We will show subsequently that, by splitting the transformers representing the piezoelectric coupling, and removing them to the two boundaries of each of our plates, the Mason-Redwood & Lamb circuit schematic which results is capable of a strict analog interpretation. That is, we invest the graphical

representation not only with a length, but endow it also with a spatial coordinate corresponding point for point with that of the physical problem - we shall have a true analog, and the network schematic, therefore, will take on a significance it has never had before.

One last point remains to be made here. In all of the discussions under c. we have confined our attention to the case of a single mode in the resonant system. This is simply because, while coupled-mode equivalent circuits have been described in the literature (150), they seem all to be concerned only with operation in the vicinity of two coupled resonances, rather than a coupling between circuits of Mason's type (Fig. 4).

From what we have described in earlier sections, it is known that there are three thickness modes, and they couple mechanically and piezoelectrically at each boundary. Redwood (100) remarks that a number of circuits (Fig. 5) would have to be combined to obtain a truly representative network for transient conditions. We shall show that three such elementary circuits are required, for our problem, and will give interface networks which represent both types of coupling in a form which is physically meaningful. The transmission lines are conventional, and the lumped elements are all constant; the difference between the cases of TETM and LETM is also simply indicated by the presence or absence of a negative capacitor in just the form usually given (131) in single-mode situations.

7. Some of the practical uses to which stacks of plate vibrators have been put are described above (73-86). We wish here to indicate a number of references which pertain to the use of acoustic methods for

measurement of material properties, either of a single resonator by itself, or as a stacked combination. Huntington (151) gives additional references to the use of "composite oscillator" measurements for determination of unknown material parameters. The paper by Bolef & Menes (85) gives an example of elastic constant measurement by measuring acoustic resonances; the layers are represented by transmission lines. Cook & Van Valkenburg (152) use resonances to determine the thickness of a specimen. In McSkimin (153) is a very good outline of methods used for measurements, with a generous bibliography of the pertinent literature. The specific area of crystal vibrator measurements is discussed in the IEEE Standards (154-155) and in Horton & Boor (156).

8. General background information relating to various areas we touch upon in later chapters is given in references (157-189). The subject of elasticity is covered in (157-163, 165-167, 172, 173, 178, 184, 187 & 189); propagation of waves in solids may be found in (159, 160, 163, 165, 167, 171-173, 187 & 189). The characterization of material properties is described, with data, in (164, 165, 179-181, 186 & 203), while references (161, 162, 176, 177, 185 & 188) treat practical vibrating systems and devices; equivalent circuits of devices are given in (168-170, 180 & 185). Normal coordinate transformations may be found in (158, 174, 179, & 187), and general history relating to our subject is found in (159, 160, 175, 182 & 183).

II. UNBOUNDED PIEZOELECTRIC MEDIA

In this chapter we consider the propagation of acoustic plane waves in a piezoelectric medium. The propagation is shown to be representable by transmission-line equations. Equivalent transmission-line schematics are then introduced, and form the basis for the networks to be described in subsequent chapters.

A. Acoustic Plane Waves.

Our notation, and definitions regarding crystal axial conventions, orientation, and constitutive relations agree, for the most part, with the 1949 "Standards on Piezoelectric Crystals" (154). Tensor notation is used almost exclusively (64), although we shall have occasion to use matrices (65) as well. Equation numbers will be enclosed in parentheses, as are references to the Bibliography; however, equations will be described by two numbers separated by a decimal point. The first number denotes the chapter number.

In describing plane acoustic wave propagation in piezoelectric crystals, two main approaches are found in the literature. The first is the traditional Christoffel-Green formulation, perhaps best presented by Bechmann (45,46), as augmented for inclusion of piezoelectricity. In this formulation, everything is referred to a set of coordinate axes which coincide with the crystallographic axes, insofar as this is geometrically possible. This set of axes is almost invariably used to specify components of the material tensors determined by measurement (181,186), since the presence of crystal symmetry elements leads to

simplifications in this frame, and such symmetry is more readily apparent in an inspection of the term schemes for a given crystal class (139, 166, 179, 180).

The direction of wave propagation is generally oblique to this axial set, and is specified by its projections. For any assumed propagation direction, one must solve an eigenvalue problem to determine the three phase velocities and the corresponding particle displacement directions. In setting up the problem, the elements Γ_{ij}^{E} , of the secular equation, called Christoffel's moduli, are simply determined in terms of the elastic stiffnesses and the known (or assumed) propagation direction. A similar remark applies to the inclusion of the piezo-effect into the secular equation. From the presence or absence of various terms, one can see at a glance whether the different components of motion are coupled, and whether the coupling is elastic, piezoelectric, or both. One also sees immediately if a given mode can be excited for a driving field parallel to the wave propagation direction, corresponding to TETM for us.

When dealing with our problem, these advantages are offset by the fact that the plate boundaries are, generally, oblique, and the analysis becomes less straightforward and clear. Hence we shall follow Lawson (61), Kyame (66), and Tiersten (64), and choose, without loss in generality, the direction of wave propagation as a coordinate axis, which we take to be the $+x_3$ axis. For our purposes now, it is sufficient to prescribe only that x_1 and x_2 are chosen to form a right-handed orthogonal system with x_3 , and that the transformation between our x_i and the crystallographic X,Y,Z system specified in (154) is known. Transformations are described

in (165&190). With the problem set up in the x_i system one has to refer all of the required material coefficient components to this system, and then set up the secular equation.

Because the problem is inherently one-dimensional, with no variations taking place in the plane lateral to the wave progression, the eigenvalues are independent of a coordinate rotation about x_3 . However, the orientation of the x_1 and x_2 axes enters into the expressions for transforming the material coefficient components, and so, while everything comes out properly in the x_i frame, it is harder to recognize certain simplifications that are easily noted in the other formulation. Nevertheless, transforming the problem to the x_i system presents no conceptual difficulties, nor does it result in any loss of generality. As it simplifies the analysis, we shall adopt it here. On the other hand, we shall give some tables in the Appendices which are more readily understood in the X,Y,Z frame, so we have need for both sets of coordinates in what follows.

We use the conventions that a subscripted index preceded by a comma indicates differentiation with respect to the space coordinate having that subscript, dot notation indicates time differentiation, and the summation convention for repeated indices is employed.

The pertinent sets of equations which have to be solved together are (see (64,191)):

The stress equations of motion, corresponding to Newton's equations

$$T_{ij,i} = \rho \ddot{u}_j \quad . \tag{2.1}$$

The equations defining mechanical strain

$$S_{kl} = 1/2(u_{k,l} + u_{l,k}) \quad . \tag{2.2}$$

The divergence relation from Maxwell's equations, in the absence of free charge

$$D_{i,i} = 0. \tag{2.3}$$

The electric field-electric potential relations, in the quasi-static approximation

$$E_k = -\varphi_{,k} . \tag{2.4}$$

The linear, piezoelectric constitutive relations, characterizing the medium (154)

$$T_{ij} = c^{E}_{ijkl} S_{kl} - e_{kij} E_k \tag{2.5}$$

and

$$D_i = e_{ikl} S_{kl} + \epsilon^{S}_{ik} E_k . \tag{2.6}$$

Equation (2.5) is Hooke's Law, extended to take into account piezoelectricity.

In these equations: T_{ij} , u_j , S_{ij} , D_i , E_i are the components of stress, mechanical displacement, strain, electric displacement, and electric field, respectively, while ρ and φ are the mass-density and electric potential, respectively. The material parameters c^{E}_{ijkl} , e_{kij} and ϵ^{S}_{ik} are the elastic stiffnesses at constant electric field, the piezoelectric stress constants, and dielectric permittivities at constant strain, respectively. All Latin indices have the range 1, 2 and 3.

Assuming that there are no field variations in the lateral directions, x_1 and x_2 , but only along the direction of propagation, x_3 , and assuming a time factor exp $(+j\omega t)$ henceforth omitted, equations (2.1) through (2.6) become

$$T_{3j,3} = -\rho\omega^2 u_j \quad , \tag{2.7}$$

$$2S_{3\ell} = u_{\ell,3} + u_{3,\ell} \quad , \tag{2.8}$$

$$D_{3,3} = 0 \quad , \tag{2.9}$$

$$E_3 = -\varphi_{,3} \quad , \tag{2.10}$$

$$T_{3j} = c^{E}_{3jk3} S_{k3} - e_{33j} E_3 \quad , \tag{2.11}$$

$$D_3 = e_{3k3} S_{k3} + \epsilon^{S}_{33} E_3 \quad . \tag{2.12}$$

All other components of the elastic strain vanish, from (2.2) and our assumption of field variations with x_3 only. Additional stress components are generally present, but as they do not play any part in the problems treated subsequently, we do not consider them further. They may be calculated from (2.5) when the strain and electric field components are determined.

Auld has shown (8) that there can be no electric field components, associated with the wave, transverse to its direction of propagation. A uniform lateral field may, however, be imposed upon a region by sources other than the wave; we will have occasion to consider this in Chapter IV. Lateral electric displacement components may be associated with plane waves, and are calculated from (2.6); these also arise in Chapter IV.

Equations (2.8) and (2.10) may be used to eliminate the strain and electric field from (2.11) and (2.12), to give

$$T_{3j} = c^{E}_{3jk3} u_{k,3} + e_{33j} \varphi_{,3} \tag{2.13}$$

and

$$D_3 = e_{3k3} u_{k,3} - \epsilon^{S}_{33} \varphi_{,3} \quad . \tag{2.14}$$

Substitution of (2.14) into (2.9) then yields

$$D_{3,3} = e_{3k3}\, u_{k,33} - \epsilon^{S}_{33}\, \varphi_{,33} = 0 , \tag{2.15}$$

so that

$$\varphi_{,33} = (e_{3k3} / \epsilon^{S}_{33})\, u_{k,33} . \tag{2.16}$$

Integration of (2.16) gives

$$\varphi = (e_{3k3} / \epsilon^{S}_{33})\, u_k + a_3 x_3 + b_3 . \tag{2.17}$$

When this is inserted into (2.13) there results

$$T_{3j} = \bar{c}_{3jk3}\, u_{k,3} + e_{33j}\, a_3 \tag{2.18}$$

where

$$\bar{c}_{3jk3} = c^{E}_{3jk3} + e_{33j}\, e_{3k3} / \epsilon^{S}_{33} \tag{2.19}$$

are the "piezoelectrically stiffened" elastic stiffnesses at constant normal electric displacement and constant tangential electric field.

Insertion of (2.17) into (2.14) shows D_3 to be a spatial constant,

$$D_3 = - \epsilon^{S}_{33}\, a_3 , \tag{2.20}$$

that is, the longitudinal component of the electric displacement cannot vary with x_3 .

The equations of motion are obtained from (2.18) and (2.7) as

$$\bar{c}_{3jk3}\, u_{k,33} + \rho \omega^2 u_j = 0 , \tag{2.21}$$

which shows the motions u_k to be coupled through the elastic constants.

Equation set (2.21) may be solved by assuming the u_k to be proportional to $\exp(\pm j\chi x_3)$ which will satisfy (2.21) provided

$$(\bar{c}_{3jk3} - c\,\delta_{jk})\beta_k = 0 \,, \tag{2.22}$$

with

$$c = \rho\omega^2/\varkappa^2 \,, \tag{2.23}$$

and the β_k are the proportionality constants.

To obtain a nontrivial solution to (2.22) requires that

$$\left| \bar{c}_{3jk3} - c\,\delta_{jk} \right| = 0 \,. \tag{2.24}$$

Equation (2.24) is a cubic in c, and gives three real, positive roots $c^{(i)}$, from which three real wavenumbers $\varkappa^{(i)}$ may be obtained from (2.23) for a specified value of ω. Each $c^{(i)}$ also determines a set of ratios among the components $\beta_k^{(i)}$ of the corresponding eigenvector; if the components for each (i) are normalized by

$$\beta_k \beta_k = 1 \,, \tag{2.25}$$

then the $\beta_k^{(i)}$ are the direction cosines of the particle displacement for each of the three modes (i). The β_k also have the property

$$\beta_j^{(i)} \beta_k^{(i)} = \beta_m^{(j)} \beta_m^{(k)} = \delta_{jk} \,, \tag{2.26}$$

where δ_{jk} is the Kronecker delta. In matrix terminology, one would say that the modal matrix is orthogonal (192-193), a property which will prove useful.

At this point we introduce a transformation to normal coordinates (194,65) by defining the quantities:

$$T_{3j}^{\circ} = \beta_i^{(j)} T_{3i} \,, \tag{2.27}$$

$$u_j^{\circ} = \beta_i^{(j)} u_i \,, \tag{2.28}$$

$$e_{33j}^{\circ} = \beta_i^{(j)} e_{33i} \,. \tag{2.29}$$

Because the $\beta_i^{(j)}$ are orthonormal, the inverse transformations are

$$T_{3j} = \beta_j^{(i)} T_{3i}^{\circ} \quad , \tag{2.30}$$

$$u_j = \beta_j^{(i)} u_i^{\circ} \quad , \tag{2.31}$$

$$e_{33j} = \beta_j^{(i)} e_{33i}^{\circ} \quad . \tag{2.32}$$

In terms of the new quantities, (2.7) becomes

$$T_{3j,3}^{\circ} = -\rho \omega^2 u_j^{\circ} \quad , \tag{2.33}$$

while (2.18) is transformed as follows. We rewrite (2.22) as

$$\left(\bar{c}_{3jk3} - c^{(i)} \delta_{jk}\right) \beta_k^{(i)} = 0 \quad , \tag{2.34}$$

to emphasize the mode index (i), (which is not summed here) and then multiply through (2.18) by $\beta_j^{(i)}$. Substituting from (2.34), while making use of the symmetry of $\bar{c}_{3jk3}$ gives

$$T_{3i}^{\circ} = \beta_j^{(i)} T_{3j} = \bar{c}_{3jk3} \beta_j^{(i)} u_{k,3} + \beta_j^{(i)} e_{33j} a_3 \tag{2.35}$$

$$T_{3i}^{\circ} = c^{(i)} \delta_{kj} \beta_j^{(i)} u_{k,3} + e_{33i}^{\circ} a_3 \tag{2.36}$$

$$T_{3i}^{\circ} = c^{(i)} \beta_j^{(i)} u_{j,3} + e_{33i}^{\circ} a_3 \tag{2.37}$$

$$T_{3i}^{\circ} = c^{(i)} u_{i,3}^{\circ} + e_{33i}^{\circ} a_3 \quad , \tag{2.38}$$

which is the required form.

Substitution of this into (2.33) gives

$$c^{(i)} u_{i,33}^{\circ} + \rho \omega^2 u_i^{\circ} = 0 \quad , \tag{2.39}$$

so that the motions u_i° are now uncoupled in the differential equations (2.39).

Equations (2.33) and (2.38) will be associated below with the equations of a uniform transmission line (195).

For future reference, we note that

$$e_{3k3}\, u_k = e^{\circ}_{3k3}\, u^{\circ}_k \tag{2.40}$$

is invariant under the transformation, because

$$\begin{aligned} e_{3k3}\, u_k &= (\beta_k^{(i)}\, e^{\circ}_{3i3})\ (\beta_k^{(m)}\, u^{\circ}_m) \\ &= \beta_k^{(i)}\, \beta_k^{(m)}\, e^{\circ}_{3i3}\, u^{\circ}_m \\ &= \delta_{im}\ e^{\circ}_{3i3}\, u^{\circ}_m \\ &= e^{\circ}_{3i3}\, u^{\circ}_i \ . \end{aligned}$$

The equation for the potential (2.17) simply becomes

$$\varphi = (e^{\circ}_{3k3} / \epsilon^{S}_{33})\, u^{\circ}_k + a_3 x_3 + b_3 \ . \tag{2.41}$$

It is seen from (2.41) that the x_3 -directed component of electric field arising from the particle displacement due to the passage of a wave reverses direction when the wave direction reverses.

In the above, we have given a short description of plane acoustic waves traveling in an homogeneous, linear, but arbitrarily anisotropic, piezoelectric substance. The three modes which are allowed for any assumed propagation direction have motions which are coupled by the elastic constants; a normal coordinate transformation uncouples them, and provides a set of first order differential equations which are to be compared with the Heaviside equations for a transmission line. This

will now be done.

B. Transmission-Line Representation.

Heaviside's equations for a transmission line are (195, 110):

$$V_{,3}^{(i)} = -j \varkappa^{(i)} Z_o^{(i)} I^{(i)} , \tag{2.42}$$

and

$$I_{,3}^{(i)} = -j \varkappa^{(i)} Y_o^{(i)} V^{(i)} , \tag{2.43}$$

where $V^{(i)}$ and $I^{(i)}$ are the voltage and current, respectively, associated with mode (i); $Z_o^{(i)}$ and $Y_o^{(i)}$ are, in like manner the respective transmission-line characteristic impedance and admittance, with

$$Z_o^{(i)} = 1 / Y_o^{(i)} . \tag{2.44}$$

The wavenumber $\varkappa^{(i)}$, for each mode (i), which governs propagation along x_3, is defined as

$$\varkappa^{(i)} = \omega / v^{(i)} , \tag{2.45}$$

when there is no transverse wavenumber component, as in our situation. In (2.45), $v^{(i)}$ is the phase velocity along x_3. The symbol $\varkappa$ has been used in (2.23) in connection with the elastic wave discussion. Inasmuch as the elastic wave velocity for mode (i) is

$$v^{(i)} = \sqrt{c^{(i)} / \rho} , \tag{2.46}$$

where $c^{(i)}$ is the i^{th} root of (2.24), it follows that we have implicitly already made this identification between the acoustic

waves and the equivalent transmission lines. That the velocity is given by (2.46) follows from the wave equation (2.21) or (2.39), so (2.23) is the same as (2.45). We are free to make the corresponding wavenumbers equal; it amounts to positing three transmission lines (one for each (i)), each supporting a wave propagating with velocity $v^{(i)}$ from (2.46). It remains to be seen whether this assumption, and the pertinent acoustic equations, are then consistent with Heaviside's equations (2.42) and (2.43). We take up this question next.

First we repeat (2.33) and (2.38) here.

$$T^{\circ}_{3i,3} = -\rho\omega^2 u^{\circ}_i \quad , \tag{2.33}$$

$$T^{\circ}_{3i} = c^{(i)} u^{\circ}_{i,3} + e^{\circ}_{33i}\, a_3 \quad . \tag{2.38}$$

Note that the term $e^{\circ}_{33i}\, a_3$, which is piezoelectric in nature, is a spatial constant. Apart from this term, the above set of coupled first-order, ordinary differential equations is very similar to the set (2.42), (2.43). Our immediate goal is to make this similarity an identity, after which the piezoelectric term will be taken up.

To this end, we separate the stresses T°_{3i} into two groups by defining

$$T^{\circ}_{3i} = \tilde{T}^{\circ}_{3i} + \bar{T}^{\circ}_{3i} \quad , \tag{2.47}$$

with

$$\bar{T}^{\circ}_{3i} = e^{\circ}_{33i}\, a_3 \quad . \tag{2.48}$$

Because $\bar{T}^{\circ}_{3i}$ is a constant,

$$\bar{T}^{\circ}_{3i,3} = 0 \quad , \tag{2.49}$$

so that (2.33) and (2.38) now can be written

$$\tilde{T}^{\circ}_{3i,3} = -\rho\omega^2 u_i^{\circ} \quad , \tag{2.50}$$

$$\mathcal{C}^{(i)} u^{\circ}_{i,3} = \tilde{T}^{\circ}_{3i} \quad , \tag{2.51}$$

which set now has a structure the same as (2.42), (2.43).

In order to arrive at an analogy, corresponding quantities must be paired. Formally, there is quite some latitude in doing this, for, apart from the fact that either $I^{(i)}$ or $V^{(i)}$ can be made analogous to u_i°, and similarly for $\tilde{T}^{\circ}_{3i}$, factors of proportionality can be inserted, as between $V^{(i)}$ and $\tilde{T}^{\circ}_{3i}$, or incorporated into the definition of $Z_o^{(i)}$, etc. As a practical matter, certain choices appear more natural than others. Another consideration is the desirability of having our results accord with past work.

It is both natural, and in accordance with results we have described in Figures 2, 4 and 5, to choose $\tilde{T}^{\circ}_{3i}$ proportional to $V^{(i)}$ and u_i° proportional to $I^{(i)}$. We specifically make the following choices of analogous quantities:

$$V^{(i)} = A\,\tilde{T}^{\circ}_{3i} \quad , \tag{2.52}$$

$$I^{(i)} = -\dot{u}_i^{\circ} \quad . \tag{2.53}$$

$I^{(i)}$ is thus the negative of the particle velocity in the transformed system. We shall denote this velocity by v_i°; it should be clearly

distinguished from the wave phase velocity $v^{(i)}$. As both quantities take the same symbol in the current literature, it seems best to retain it for both uses with the foregoing caveat.

With the choices (2.52) and (2.53), plus (2.44), (2.45) and (2.46), the equations become consistent if we make

$$Z_o^{(i)} = A \rho v^{(i)} \quad , \tag{2.54}$$

as may be verified by straightforward substitution.

The factor "A" which appears as the proportionality constant in (2.52), and again in (2.54), shall be taken equal to a portion of area perpendicular to the phase progression of the waves, i.e., normal to x_3. This allows the voltages on the lines to represent forces, and in so doing, makes our representation accord with usual practice, without any loss in generality.

A word should be said about the minus sign appearing in (2.53), which looks somewhat mysterious at first. It comes about as a result of the definitions and conventions regarding power flow in acoustics and electromagnetics, and is amply discussed in the literature (8, 9, 48, 71, 196-199). Taking a simple case, power flows into an elastic body when a positive tensile force is applied, producing a positive, outward-directed particle velocity. The outward velocity associated with the inward power flow produces the negative sign. By precisely the same argument that leads to the invariance expressed by (2.40) we have as an invariant

$$T_{3k} u_k = T_{3i}^{\circ} u_i^{\circ} \quad ,$$

which leads to the invariance of the x_3-directed power flow.

Another aspect of interest is that of the symmetry properties of the transmission-line variables, in particular, the reflection properties relating positive-traveling and negative-traveling waves. Heaviside's equations require that two waves progressing in opposite directions must differ in the sign of one, and only one, of the variables, voltage or current. For isotropic materials, it is shown in (118) that a reflection-symmetry argument decides in favor of a reversal of the current directions between oppositely directed image waves, while the voltages are unchanged.

When arbitrary anisotropy is present this argument can no longer be invoked to choose between the variables. In fact, the normal coordinate transformation we have introduced places both sets of mechanical variables on the same footing, because it amounts to projecting the stress and velocity components upon the eigenvector of each mode. The basis of the eigenvectors provides a preferred axial set to which symmetry arguments must be referred.

The important point for us is that Heaviside's equations are obeyed by the variables $A\tilde{T}^{\circ}_{3i}$ and $-\dot{u}^{\circ}_{i}$. This, by itself, implies the reversal of one, but not both, of these quantities for an image wave; we are free to choose this, and we make the choice (2.55), taking u°_{i} to reverse direction when the wave is reversed, so that the usual mirror reflection symmetry is present on the transmission lines when considered in terms of $V^{(i)}$ and $I^{(i)}$.

Because the same transformation is applied to the piezoelectric constants to obtain e°_{33i}, it also lacks, in general, the symmetry properties possessed by e_{33k}.

We have now established the analogy with the Heaviside equations in the form we will use. To recapitulate, we take

$$V^{(i)} = A \tilde{T}^{\circ}_{3i} \quad , \tag{2.52}$$

$$I^{(i)} = -j\omega u^{\circ}_{i} \quad , \tag{2.55}$$

$$Z_o^{(i)} = A \rho v^{(i)} \quad , \tag{2.54}$$

$$\kappa^{(i)} = \rho \left[v^{(i)} \right]^2 , \tag{2.56}$$

$$Z_o^{(i)} = 1 / Y_o^{(i)} \quad , \tag{2.44}$$

$$\varkappa^{(i)} = \omega / v^{(i)} \quad , \tag{2.45}$$

which makes (2.50), (2.51) equivalent to (2.42), (2.43).

Returning now to the piezoelectric term $\bar{T}^{\circ}_{3i}$, we have noted that it is a constant throughout space, and simply adds everywhere to the "wavy" portion of the stress $\tilde{T}^{\circ}_{3i}$ which one may associate with motion on the transmission lines. It arises mathematically from the integration of (2.16), and is independent of waves propagating in an unbounded medium. The introduction of finite boundaries into the problem is a different matter. To illustrate the effect of boundaries we will discuss a modification of Fig. 5. In so doing we will attain other objectives, also: it will serve as a preview of Chapter III, will introduce a different way of drawing transmission lines which is more useful and illuminating for our purposes, and establish continuity between past work and the new network results to be presented.

The schematic representation of the transmission line of Fig. 5 suggests an idealized version of a coaxial line (198), which is shown with the outer sheath connected, through capacitors, to the electrical terminal and mechanical datum. An alternative schematic form is that of the two-wire line (198), which is in current usage (31, 11, 117). A section of line drawn in this manner is shown in Fig. 6. There is no sheath in this case, and the only points of entry, or attachment, are at the ends. Figure 7 is a redrawn version of Fig. 5, using the two-wire format, with the piezoelectric transformer reintroduced, as in Fig. 4.

Drawn in this fashion, the equivalent circuit is more suggestive of the fact that the piezoelectric excitation may be considered to arise at the ends, instead of being extended throughout the volume. It will appear in Chapters III and IV that this is the case, and that (2.48) is the driving term which simply adds to the wave stress to produce the total mechanical stress at the plate surface.

In this chapter we have obtained equations for plane acoustic waves in an homogeneous, but arbitrarily anisotropic, piezoelectric material, in a form that we found to be representable as elastic motions on acoustic transmission lines. A set of analogous relationships between the parameters of the line and the acoustic wave was determined, thus setting the stage for the considerations of the next chapters.

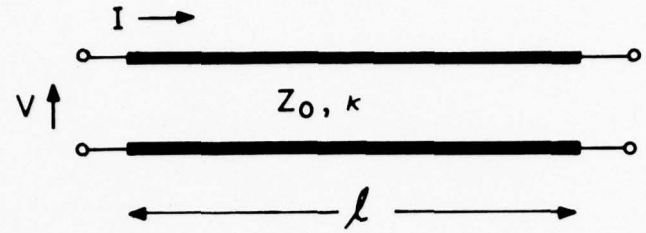

FIG. 6. SCHEMATIC OF TWO-WIRE TRANSMISSION LINE.

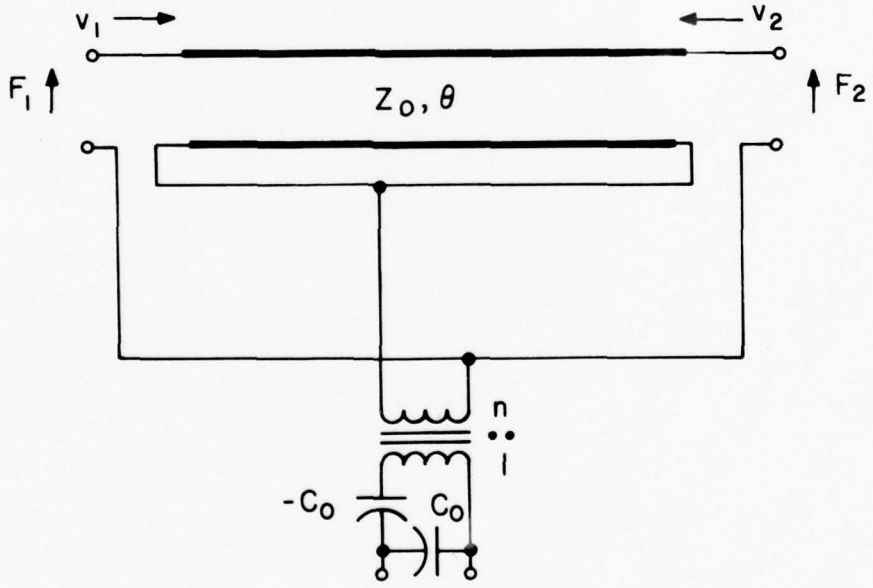

FIG. 7. TWO-WIRE TRANSMISSION LINE SCHEMATIC OF MASON'S EXACT, THREE-PORT, SINGLE MODE TYPE, CIRCUIT. APPLIED FIELD PARALLEL TO WAVE PROPAGATION.

III. THICKNESS EXCITATION OF THICKNESS MODES

We begin by presenting the analytic solution of the problem of thickness modes of an electroded, piezoelectric crystal plate with traction-free surfaces, driven by an electric field in the thickness direction (64,65), after which we synthesize exact network equivalents using transmission lines. Then, with a view to removing the restriction to traction-free boundaries, the electromechanical impedance matrix is determined in the normal coordinate system. This matrix is then realized rigorously, in transmission-line circuit form. When taken together with the network developments presented in Chapter V, the TETM problem for a single plate with arbitrary boundary-port conditions becomes completely represented by the overall network, which is a true analog of the physical situation.

A. Single-Plate Crystal Resonator, Traction-Free.

Our plate is presumed to be laterally unbounded, of thickness 2h, the upper and lower surfaces at $x_3 = +h$ and $-h$, respectively, are further presumed to be maintained at potentials $+\varphi_0$ and $-\varphi_0$, also respectively, the time factor $\exp(+j\omega t)$ being, as usual, suppressed. The electrodes for accomplishing this are not of interest now; let them simply be perfect electrical conductors, massless, and without elastic stiffness. A sketch of the situation is given in Fig. 8. The lateral coordinates are, likewise, of no interest now.

At the plate boundaries, the conditions to be satisfied are

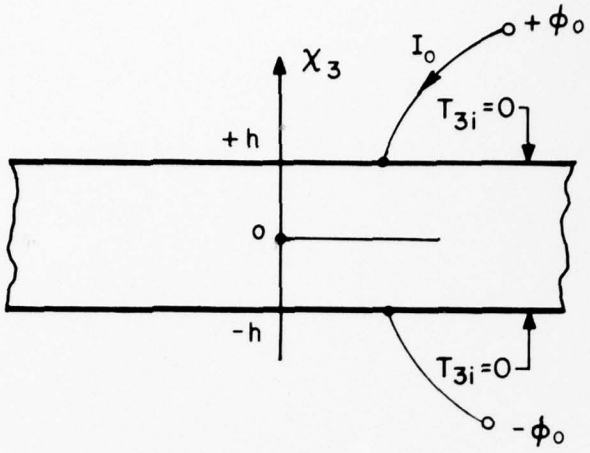

FIG 8. UNBOUNDED, TRACTION-FREE, PIEZOELECTRIC PLATE. THICKNESS EXCITATION OF THICKNESS MODES.

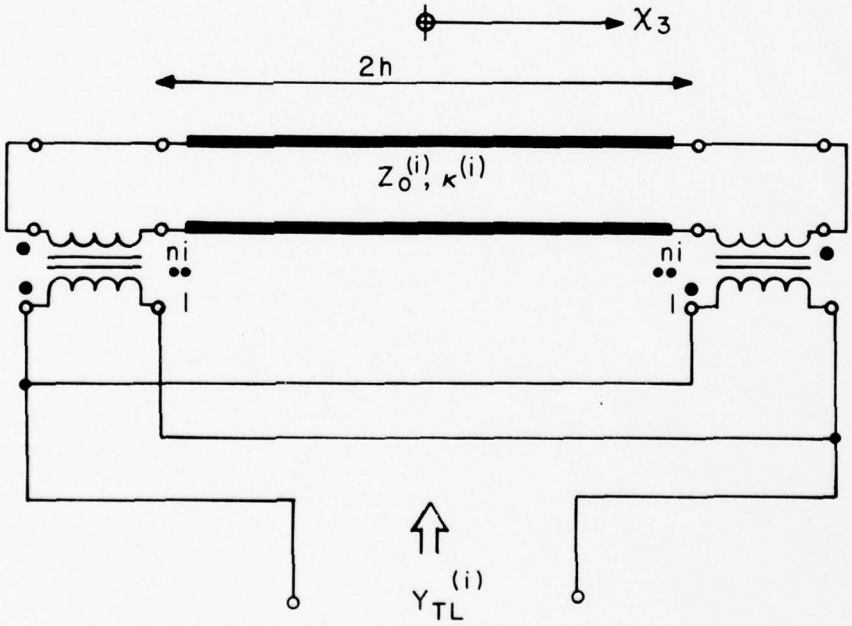

FIG. 9. TRACTION-FREE PLATE. REPRESENTATION OF SINGLE THICKNESS MODE, ELECTRICAL INPUT CIRCUIT OMITTED.

$$T_{3j} = 0 , \quad \text{at} \quad x_3 = \pm h, \tag{3.1}$$

and

$$\varphi = \pm \varphi_0, \quad \text{at} \quad x_3 = \pm h. \tag{3.2}$$

Because the untransformed stresses T_{3j} vanish at the surfaces, the transformed stresses T°_{3j} also vanish:

$$T^{\circ}_{3i} = 0 , \quad \text{at} \quad x_3 = \pm h. \tag{3.3}$$

This is a consequence of (2.27) and the fact that $\beta_i^{(j)}$ is nonsingular; it has a determinant equal to unity.

We now seek a solution to (2.39) which satisfies the boundary conditions (3.2) and (3.3) when inserted into (2.41) and (2.38). In keeping with the symmetry of the problem, we select

$$u^{\circ}_i = U_i \sin \varkappa^{(i)} x_3 , \tag{3.4}$$

which satisfies (2.39), and put it into (2.38), using (3.3):

$$\begin{aligned} T^{\circ}_{3i} &= \mathcal{C}^{(i)} u^{\circ}_{i,3} + e^{\circ}_{33i} a_3 \\ &= \mathcal{C}^{(i)} \varkappa^{(i)} U_i \cos \varkappa^{(i)} h + e^{\circ}_{33i} a_3 \\ &= 0 \quad \text{at} \quad x_3 = \pm h, \end{aligned}$$

hence,

$$U_i = \frac{- e^{\circ}_{33i} a_3}{\mathcal{C}^{(i)} \varkappa^{(i)} \cos \varkappa^{(i)} h} . \tag{3.5}$$

The quantity a_3 is determined by substitution of (3.4) and (3.5) into (2.41) and using (3.2). This also fixes b_3 appearing

in (2.41). These manipulations result in

$$b_3 = 0 ,$$

and

$$a_3 = \frac{+ \varphi_0 / h}{\left\{ 1 - \sum_{i=1}^{3} (k^{(i)})^2 \frac{\tan x^{(i)} h}{x^{(i)} h} \right\}} , \tag{3.6}$$

where

$$(k^{(i)})^2 = \frac{e^{\circ}_{3i3} \; e^{\circ}_{33i}}{\epsilon^{S}_{33} \; c^{(i)}} , \quad \text{(no sum)} \tag{3.7}$$

and $k^{(i)}$ is the piezoelectric coupling coefficient for mode (i) in the TETM case. Because of the symmetry of the e°_{ijk}, the last two indices can be interchanged, so the numerator of (3.7) is simply the square of the appropriate transformed piezoelectric constant.

From the expressions given, one has

$$T^{\circ}_{3i} = e^{\circ}_{33i} \; a_3 \cdot \left\{ 1 - \frac{\cos x^{(i)} x_3}{\cos x^{(i)} h} \right\} , \quad \text{(no sum)} \tag{3.8}$$

and

$$u^{\circ}_i = \frac{- e^{\circ}_{33i} \sin x^{(i)} x_3}{c^{(i)} x^{(i)} h \cos x^{(i)} h} \cdot \frac{\varphi_0}{\left\{ 1 - \sum_{j=1}^{3} (k^{(j)})^2 \frac{\tan x^{(j)} h}{x^{(j)} h} \right\}} . \tag{3.9}$$

Equation (2.20) is

$$D_3 = - \epsilon^{S}_{33} \; a_3 , \tag{2.20}$$

therefore, we get

$$D_3 = \frac{-\epsilon_{33}^{S}\,\varphi_0/h}{\left\{1-\sum_{j=1}^{3}\left(k^{(j)}\right)^2\,\frac{\tan x^{(j)}h}{x^{(j)}h}\right\}} \,. \tag{3.10}$$

Now consider a portion of the plate having lateral area A. This is the same area introduced in (2.52). The current, I_o, intercepted by this area, is equal to

$$I_o = -A\,\dot{D}_3 \,, \tag{3.11}$$

$$I_o = -j\omega A D_3 \,. \tag{3.12}$$

The minus sign is a consequence of the fact that, at the positive (upper) electrode, the surface normal points in the direction of minus x_3 within the crystal.

Looking into the electrical port, one sees an admittance

$$Y_{in\,(TETM)} = I_o/(2\varphi_o) \,, \tag{3.13}$$

with I_o given by (3.12).

Defining the capacitance Co by

$$C_o = A\,\epsilon_{33}^{S}/(2h) \,, \tag{3.14}$$

and using (3.10), (3.12) and (3.13), we arrive at the input admittance (65):

$$Y_{in\ (TETM)} = \frac{j\omega C_o}{\left\{1 - \sum_{p=1}^{3} (k^{(p)})^2 \frac{\tan \varkappa^{(p)} h}{\varkappa^{(p)} h}\right\}} . \qquad (3.15)$$

B. Network Synthesis of Y_{in} (TETM).

Expression (3.15), for the input admittance seen at the electrical port of the traction-free crystal plate, is a function of three tangents having, generally, different periods, since all the wavenumbers $\varkappa^{(p)}$ will usually be distinct. Remembering what was said earlier concerning the three acoustic eigen-modes satisfying transmission-line equations, and also the discussions in the Introduction about piezoelectric coupling of the modes at boundaries, and viewing (3.15) in this light, we might expect that (3.15) could be realized by a generalization of Fig. 7, involving three transmission lines. Such is indeed the case, and this simple problem has been selected here with just this end in mind. It will introduce a three-transmission-line network with the least amount of additional detail, so that the increased complexity will not obscure the ties our circuits have with those previously given in the literature.

To begin the synthesis, recall that Fig. 7 represents a mode driven by an applied field parallel to the wave propagation direction, which is also true in our case. Circuits for the field normal to the wave propagation, on the other hand, are distinguished in the literature (131) by the absence of the negative C_o. With this hint, we extract from Y_{in} (TETM) in (3.15) a shunt capacitor of value C_o, and then a series capacitor of value minus C_o. This fragment of the TETM network has been called the "electrical input

circuit" by Schüssler (143); we will retain the name.

When the electrical input circuit, described above, has been extracted from Y_{in} (TETM), the remainder, Y_{TL}, say, is

$$Y_{TL} = j\omega C_o \left\{ \sum_{p=1}^{3} (k^{(p)})^2 \frac{\tan \varkappa^{(p)} h}{\varkappa^{(p)} h} \right\}. \tag{3.16}$$

This means that we have the sum of three admittances in parallel, and each admittance contains one tangent function.

We next notice that, because of the mechanical boundary conditions, the surface stresses, both T_{3i} and T°_{3i}, vanish, while the corresponding displacements are allowed to develop freely. Equations (2.52) and (2.53) then suggest as a consequence that the mechanical ports are short circuited.

Let us first consider one of the three admittances comprising Y_{TL}, for if we can formulate an appropriate network for one of the three terms, we have only to add, in parallel, two others which are alike it save for the mode index number. Call this admittance $Y^{(i)}_{TL}$.

With Fig. 7 in mind, we are thus led to Fig. 9, wherein, to be consistent with Chapter II, we have used

$$Z^{(i)}_{o} = A \rho v^{(i)}, \tag{2.54}$$

$$\varkappa^{(i)} = \omega / v^{(i)}, \tag{2.45}$$

which then requires that the piezoelectric transformer turns ratios, n_i, become

$$n_i = + A e^{\circ}_{33i} / (2h), \tag{3.17}$$

and the transformer dots to be located as given. The fact that the dots are adjacent at one end, and opposite at the other end is a manifestation of the polar nature of the piezoelectric effect; the circuit is mechanically symmetric.

In drawing Fig. 9 with the transformers as shown, we emphasize the concept of boundary excitation. We have given in the figure a representation with the transformer primaries in parallel; one can as well redraw it with a single primary winding, and two secondary windings with a common flux, so that the secondaries are in parallel.

Figure 9 may be verified by reverting back to the equivalent tee circuit for a transmission line, as given, for example, in Fig. 4. We shall omit doing it here, and go on instead to the complete network, since we have accumulated all of the pieces. We require three networks as in Fig. 9, in parallel, plus the electrical input circuit, attached to the electrical port. Figure 10 shows the assembled network.

Equation (2.47) tells us that, because the T°_{3i} vanish at the plate surfaces, the partial stresses $\tilde{T}^{\circ}_{3i}$ and $\bar{T}^{\circ}_{3i}$ add to zero there. According to our discussions in Chapter II, $A\,\tilde{T}^{\circ}_{3i}$ are the voltage variables associated with the waves on the transmission lines, while the $A\,\bar{T}^{\circ}_{3i}$ are piezoelectric in nature, since

$$A\bar{T}^{\circ}_{3i} = A\, e^{\circ}_{33i}\, a_3 , \tag{3.18}$$

which follows from (2.48). We see that Fig. 10 provides just these interpretations when the $A\,\bar{T}^{\circ}_{3i}$ are identified with the secondary voltages produced by the piezo-transformers located at the ends of the transmission lines.

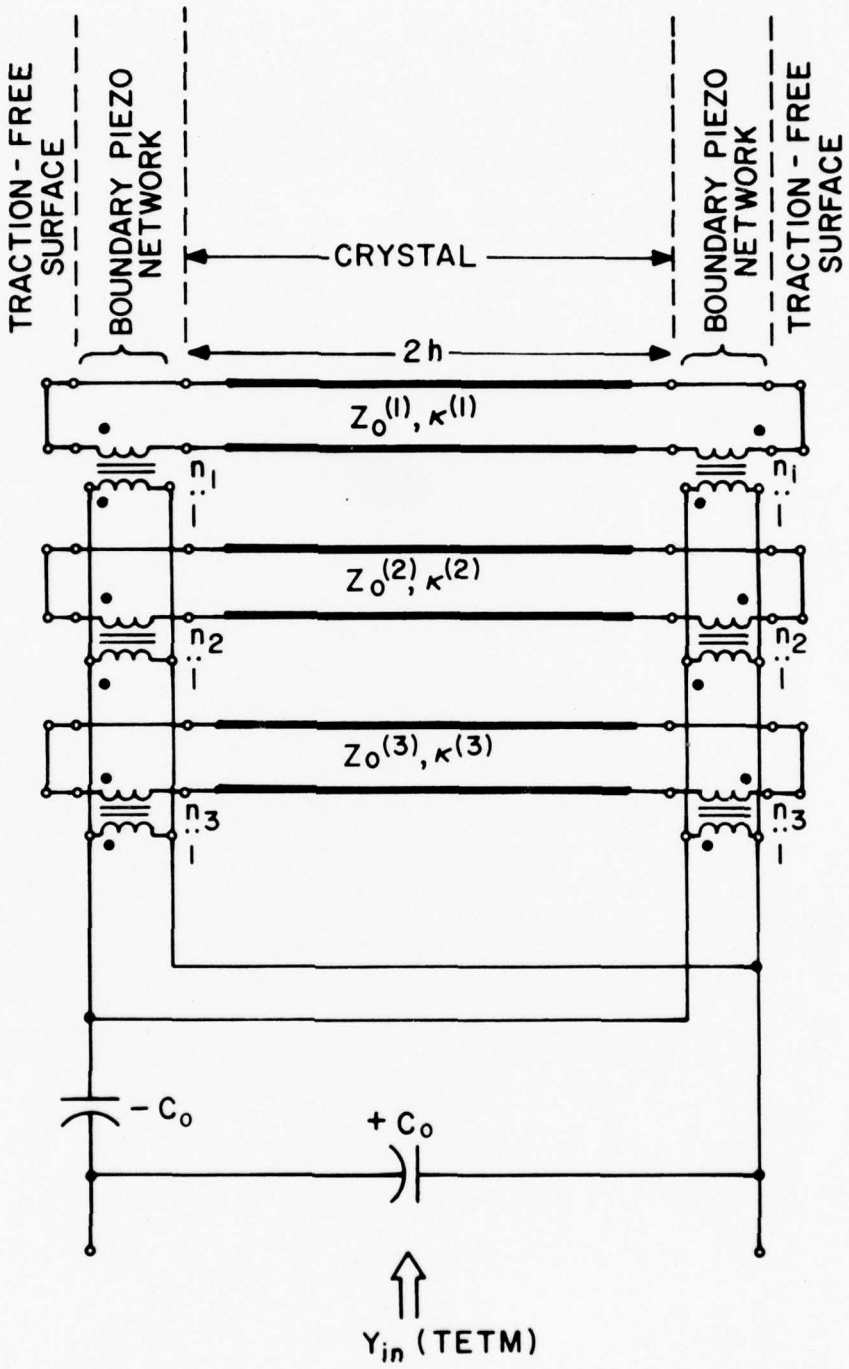

FIG. 10. EQUIVALENT NETWORK ANALOG REPRESENTATION OF TRACTION-FREE PLATE, TETM.

The structure of Fig. 10 also furnishes a simple, visual, interpretation to Tiersten's finding (64) that, even in the traction-free case, all three modes are coupled, piezoelectrically, at the boundary. It is clear that, if the electrical port is left open, the positive and negative capacitors combine to short-circuit the piezotransformers, and the three eigen-modes are then decoupled. In any other case, where the electrical port is attached to a finite immittance, the three modes are boundary-coupled.

Other insights may be obtained through a study of the schematic, but it is not our intent to be exhaustive about this aspect of the problem; we desire to derive networks which are rigorously analogous to the problems stated, and make a few observations about them. Once they are understood, and some facility is obtained in manipulating them, they speak for themselves.

We will confine ourselves, now, to the following remarks in regard to Fig. 10 and the physical problem it represents.

Equation (3.15) is an exact result, and Fig. 10 realizes it exactly. The figure, therefore, can be used for time-domain analyses, even though it was developed from a frequency-domain synthesis. Consider this aspect briefly. One can see that a transient excitation applied to the electrical port produces two waves in each transmission line, each wave starting at the surface and propagating inwardly. Each pair of waves is of equal strength and the stresses have the same polarity, so, consequently, no net mechanical current will flow across the center line of the resonator plate.

When two of the three piezoelectric turns ratios n_i are zero,

only a single transmission line remains coupled to the electrical input circuit, and, in this simpler case, the time-domain response reduces to that given in the literature (88, 99-101). If two n_i are zero, and only one mode is driven piezoelectrically, (3.15) shows that the critical frequencies, corresponding to poles and zeros of Y_{in} (TETM), are obtained from the roots of

$$\tan \varkappa h = \infty \,, \tag{3.19}$$

which gives the harmonically-related antiresonant frequencies, and from the roots of

$$\tan \varkappa h = +\varkappa h / k^2 \,, \tag{3.20}$$

which gives the non-harmonically-related resonant frequencies. Since only one mode is now considered, the mode superscript is dropped. Tiersten (64) has given a discussion of the meaning of (3.20); it was first derived by Bechmann (134), in 1940, for a single mode.

Reverting back to the case of three modes, the exact result (3.15) may be used down to DC in which limit the effective capacitance becomes

$$C_{DC} = \frac{C_o}{\left[1 - \sum_{p=1}^{3} (k^{(p)})^2\right]} \,, \tag{3.21}$$

whereas, in the absence of piezoelectricity, the limit would be simply C_o. The piezo-coupling factors $k^{(p)}$ have the effect, therefore, of increasing the effective permittivity. This has been shown, also by Bechmann (200). Because the crystal plate is passive, moreover, it is necessary that the limiting capacitance at DC be positive,

which implies the constraint on the coupling factors

$$\sum_{p=1}^{3} (k^{(p)})^2 < 1 . \tag{3.22}$$

Additional relations of this sort may be derived from the necessity that the stored energy density be positive. This, in turn, requires that the overall material constant matrix formed from (2.5) and (2.6) be positive definite (164), and leads to a variety of results. Some general considerations relating to coupling factors are given in the paper by Baerwald (201).

The network of Fig. 10 degenerates, at DC, into a simple capacitor circuit that consists of the TETM electrical input circuit (C_o in shunt, followed by $-C_o$ in series) and three capacitors in parallel, one for each transmission line, each of value $C_o(k^{(p)})^2$. In the high frequency limit the input capacitance approaches C_o, the piezoelectrically induced motion becoming "frozen."

We now use the symmetry of Fig. 10 to simplify it. Because of the transformer dot array, the mechanical voltages produced at the ends of each transmission line have the same polarity, as noted earlier, and the mid-point of the lines, corresponding to the plane $x_3 = 0$, of the crystal plate, is a node of mechanical current. We may therefore bisect the network of three transmission lines at their centers (19). The bisection produces six lines, each of length h, open circuited at the ends at which the bisections were made. The six lines consist of three sets of identical twins, which are all connected in parallel through their piezo-transformers. Each set of twin lines can be further reduced to a single line, having twice the characteristic admittance of the individual lines. Our manipulations lead us thus to Fig. 11.

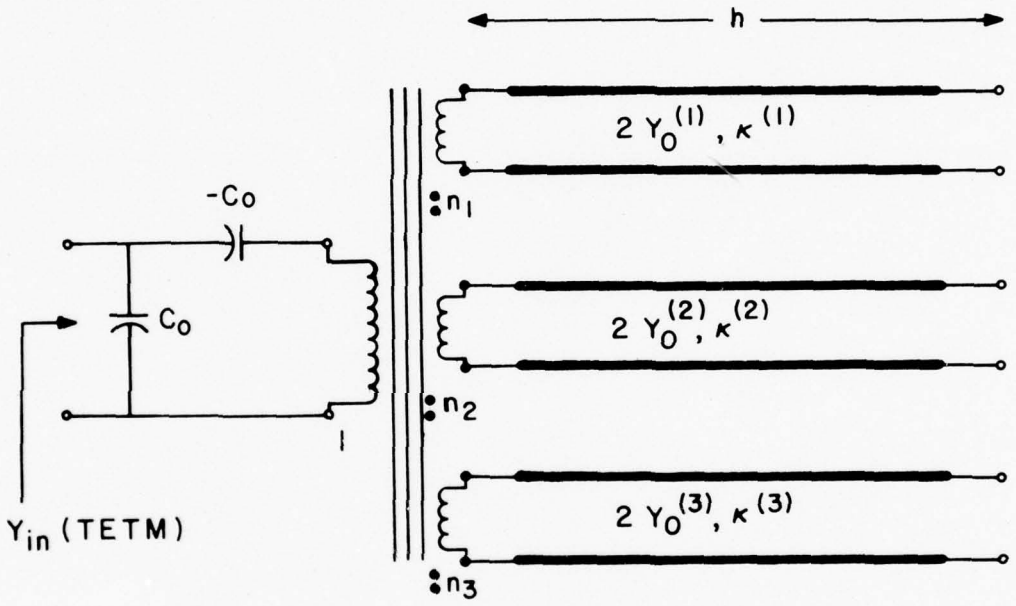

FIG. 11. EXACT EQUIVALENT NETWORK FOR TRACTION-FREE PLATE, TETM. BISECTED BASIS.

Here, the three modal transmission lines have been connected via a common core transformer, so that the secondaries are in parallel.

Although we have not shown it yet, Fig. 10 is a true analog representation where the vibrating plate parameters, such as the displacements, u_i , may be determined exactly as a function of coordinate x_3 , from a consideration of the network. Figure 11, on the other hand, has lost this intimate physical meaning, because of the circuit manipulations that have been carried out. The important thing to be emphasized will vary with the situation, usually; at first, the analogous aspects of the representations provide insight into the physics, while at a later stage, after insight has been attained, circuit simplifications can be sought to reduce the network configuration to more tractable forms for application.

We leave the one-port, traction-free plate now, and pass on to a more general treatment of the TETM-driven plate which will lead, in Chapter V, to a complete seven-port network for handling arbitrary boundary conditions.

C. The Electromechanical Network Impedance Matrix.

Our network of Fig. 10 realizes input admittance (3.15) exactly. It was obtained by a one-port synthesis, and no other constraints were imposed other than that (3.15) be satisfied. As we indicated toward the close of the last section, and this is significant, the network of Fig. 10 actually is valid on a point-to-point basis, and not simply valid only at the electrical port. Because this is so, it can be generalized to arbitrary boundary conditions, as we shall shortly show. The traction-free-boundary plate, chosen to introduce our new results because of its simplicity, led to the imposition of short circuits

at the mechanical ports; in more general instances the shorts will be replaced by mechanical boundary networks, coupling the three transmission lines to each other, and to the mechanical impedances, seen at the boundary, arising from adjacent strata, lumped loads, or other mechanical influences.

We thus anticipate the more general network of Fig. 12. The construction of the mechanical boundary networks will be given in Chapter V. In the figure the negative capacitance, associated with TETM, has been disposed symmetrically in the electrical input circuit, and placed more explicitly at the crystal interfaces, whereas the shunt capacitance is clearly associated with the crystal in the bulk. It is understood that the shunt capacitor plates coincide with the plate surfaces for a complete analog; they are drawn using the conventional circuit symbol as a convenience. We mention in passing that one may look upon this static capacitance C_o, as a vestige of the two electromagnetic modes in the quasi-static approximation, so that, additional to the three acoustic transmission lines, a fourth line exists, representing these two coalesced modes, the velocity on which line is infinite.

Our object here is twofold. We must provide a link between the traction-free case of Fig. 10 and the anticipated picture of Fig. 12 for general mechanical boundary conditions. At the same time, we must show these general circuit forms to be true analogs, i.e., we must investigate the correspondence of the picture with the spatial coordinate, and treat the network as a seven-port, rather than as a one-port, because the three stress and three displacement (or velocity) components at each of the two surfaces are generally interrelated.

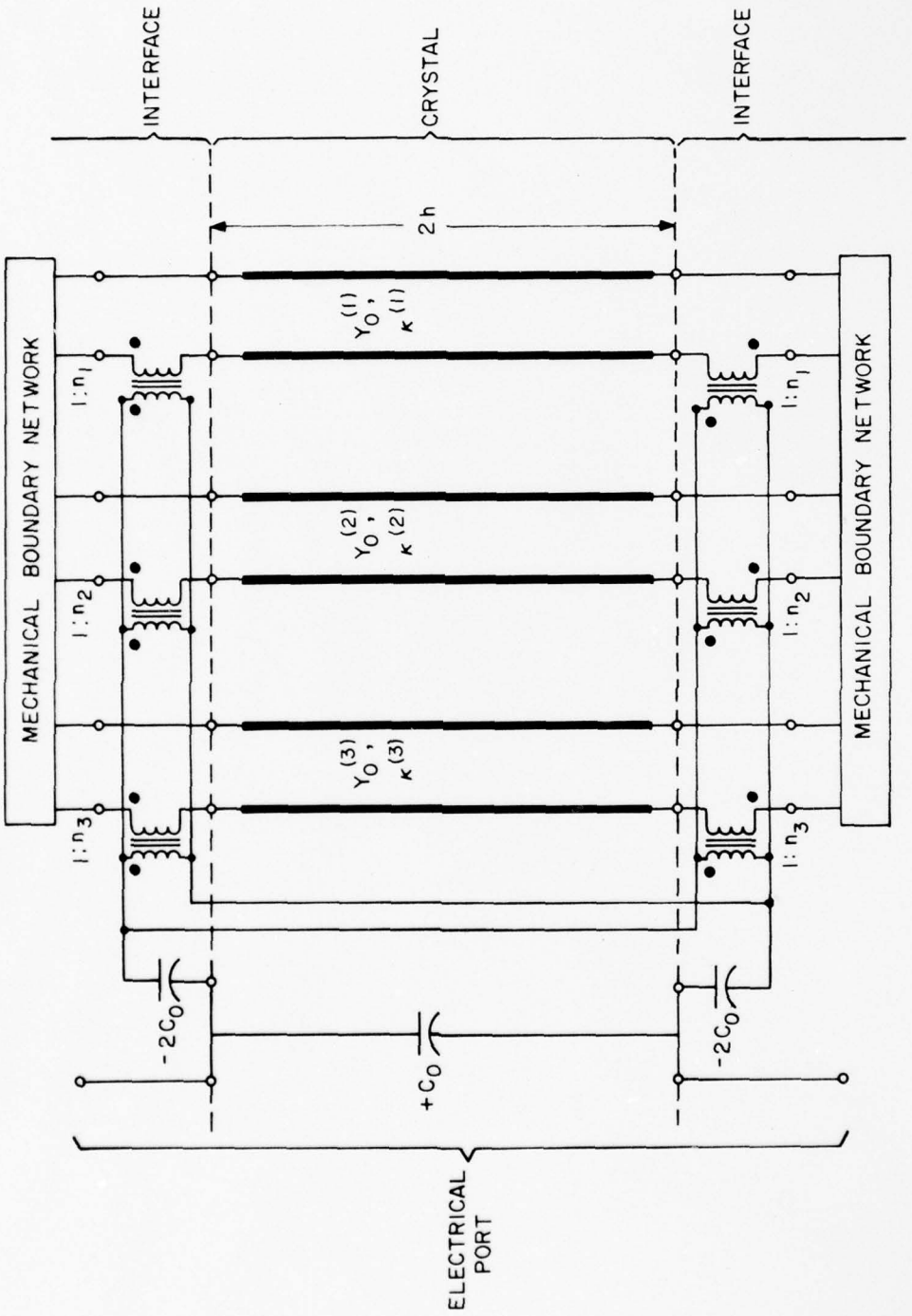

FIG. 12. EQUIVALENT NETWORK ANALOG REPRESENTATION OF TETM PLATE WITH ARBITRARY MECHANICAL BOUNDARY LOADINGS.

To accomplish these ends most easily, we take the following course. We will reverse our procedure of solving the physical problem first and then realizing its network, as we did in Sections III A and B above; instead we provisionally adopt the circuit of Fig. 13, examine it from a network standpoint, and then carry out the corresponding operations on the equations describing the physics.

In Fig. 13, the short circuits of Fig. 10 have been removed, and the mechanical boundary networks are also absent. We shall obtain the impedance matrix for this seven-port, and, after its validity has been established by recourse to the equations of the physical problem, use the matrix in conjunction with the mechanical networks, established in like manner, to arrive at an overall realization. This approach leads to a relatively simple analytical form for the impedance matrix of the complete network, and one which is easy to obtain, whereas inclusion of the mechanical networks and arbitrary mechanical loads at the outset greatly complicates the analysis.

Consider the posited Fig. 13. Because it pertains to normal coordinates, the port-variables are superscripted with the degree sign, as shown. The ports are numbered so that the left side (bottom of the crystal) of the transmission line supporting mode (i) leads to port (i°), while the right side (top of the crystal) of the same transmission line leads to port $((i + 3)^{\circ})$; ports (1°) to (6°) are the mechanical ports, while port (7°) is the electrical port. We also define V_{π}° and I_{π}° $(\pi = 1,2,\ldots,7)$ as the voltages and currents appropriate to port number (π°), with conventions as shown in Fig. 13. At present we do not have to match these variables with the stresses and displacements.

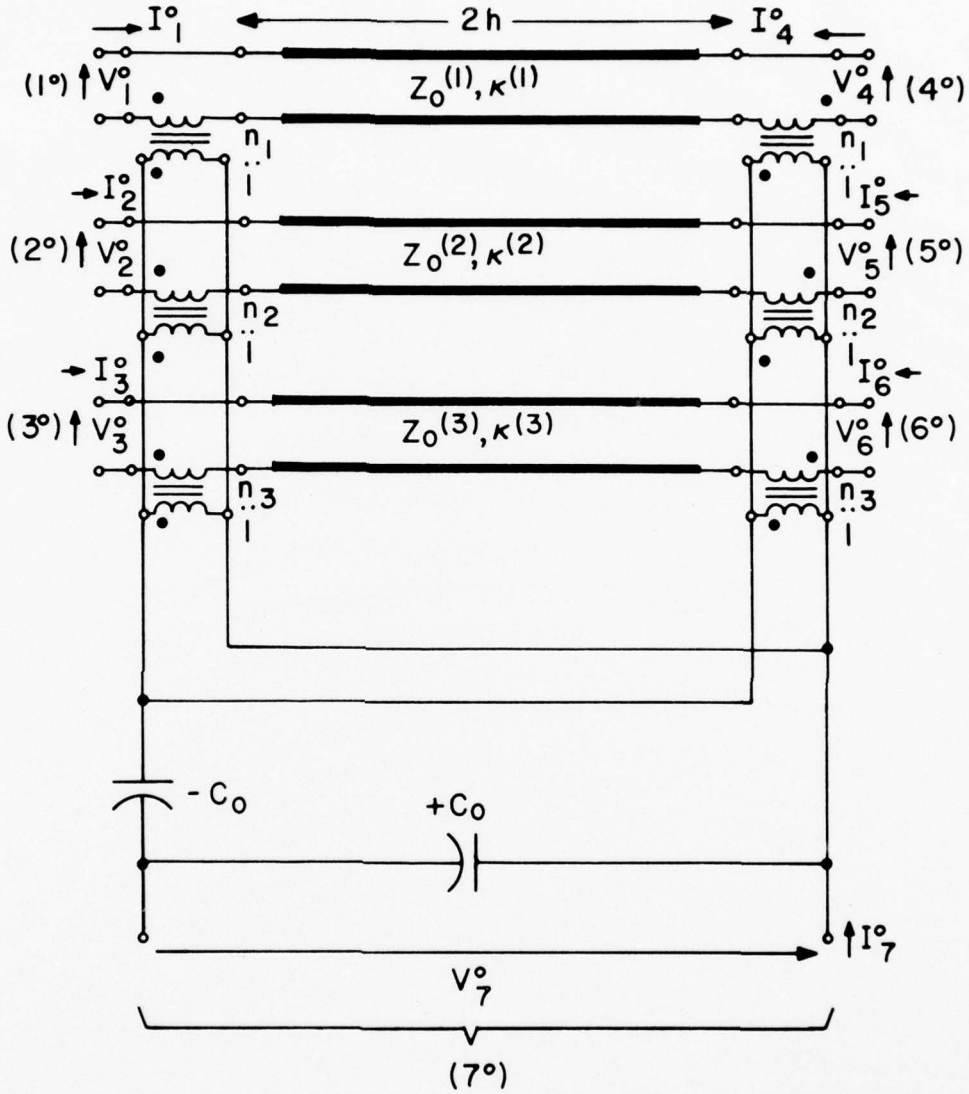

FIG. 13. SEVEN-PORT, NORMAL-MODE, EQUIVALENT CIRCUIT, WITHOUT MECHANICAL BOUNDARY NETWORKS AND LOADS.

In order to carry out the analysis of the circuit of Fig. 13, it is convenient to replace the distributed lines by their equivalent lumped tee form. This form is shown in Fig. 14 for a single line, and the substitution of three such tees for the lines in Fig. 13 produces the network of Fig. 15.

We seek to determine the quantities $Z^{\circ}_{\pi\varsigma}$ in the relations

$$V^{\circ}_{\pi} = Z^{\circ}_{\pi\varsigma} \; I^{\circ}_{\varsigma} \tag{3.23}$$

where the Greek indices have the range 1 to 7. Our task is reduced in size by a number of considerations. First, as a consequence of the fact that the network is composed of linear, passive and bilateral elements, and because we will choose our loop current definitions to coincide with our choice of loops for application of Kirchhoff's voltage law, the parameter matrices will be symmetrical (202). We notice, also, that the impedances break up into four types, viz., driving-point impedances, which are electrical or mechanical, and transfer impedances, which connect either two mechanical ports or a mechanical port to the electrical port. Apart from the mode index number, all the driving-point mechanical impedances will be equal, as will the mutual mechanical impedances between the two ports of a single transmission line. Again, mutatis mutandis, all of the electrical-mechanical transfer impedances will be equal. Finally, all of the mechanical impedances, whether driving point or transfer become almost trivially simple to evaluate by virtue of the two capacitances, which together produce a shorting of the piezo-transformers, when port (7°) is open, thereby decoupling the transmission lines from each other.

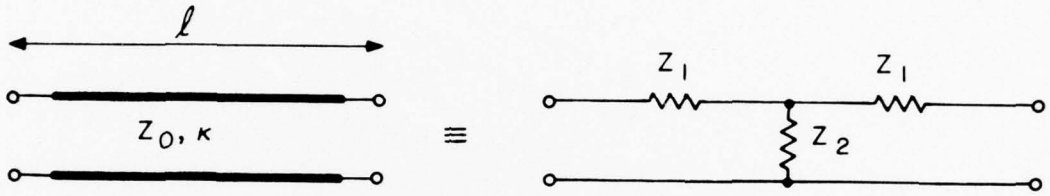

$$Z_1 = \frac{Z_0}{j \sin\theta} (\cos\theta - 1) = j Z_0 \tan(\theta/2)$$

$$Z_2 = \frac{Z_0}{j \sin\theta} \quad ; \quad \theta = \kappa \ell$$

FIG. 14. LUMPED, TEE, FORM OF A TRANSMISSION-LINE SECTION.

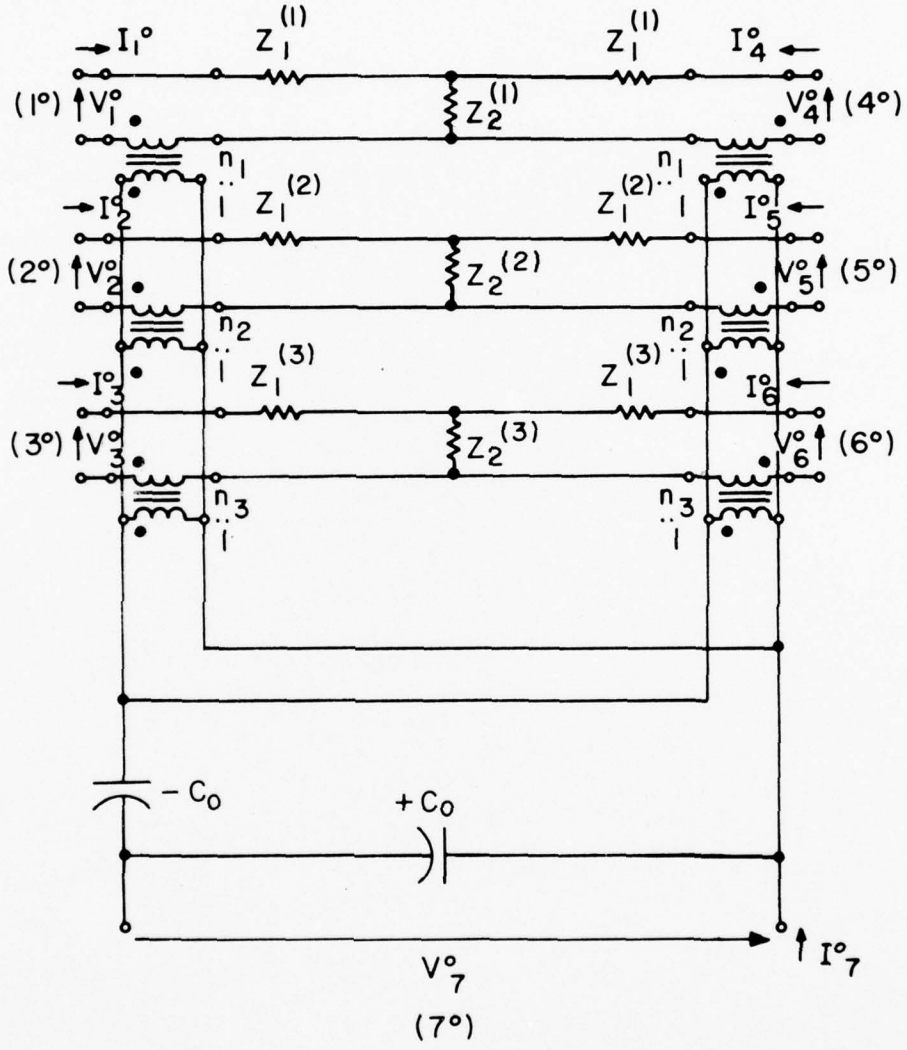

FIG. 15. LUMPED CIRCUIT FOR EVALUATING TETM ELECTRO-MECHANICAL IMPEDANCE MATRIX.

This last-mentioned consideration has the effect of making vanish the impedance matrix elements with the following indices: 12,13,15,16, 23,24,26,34,35,45,46 and 56, plus, by symmetry, those with these indices in reverse order. These correspond to mechanical transfer impedances between different lines. The mechanical driving-point impedances are

$$Z_{11}^{\circ} = Z_{44}^{\circ} = Z_1^{(1)} + Z_2^{(1)} = \frac{Z_o^{(1)}}{j \tan \theta_1} , \tag{3.24}$$

$$Z_{22}^{\circ} = Z_{55}^{\circ} = Z_1^{(2)} + Z_2^{(2)} = \frac{Z_o^{(2)}}{j \tan \theta_2} , \tag{3.25}$$

and

$$Z_{33}^{\circ} = Z_{66}^{\circ} = Z_1^{(3)} + Z_2^{(3)} = \frac{Z_o^{(3)}}{j \tan \theta_3} , \tag{3.26}$$

where we have put

$$\theta_i = 2h \chi^{(i)} . \tag{3.27}$$

The mutual mechanical impedances that are not zero, are

$$Z_{14}^{\circ} = Z_{41}^{\circ} = Z_2^{(1)} = \frac{Z_o^{(1)}}{j \sin \theta_1} , \tag{3.28}$$

$$Z_{25}^{\circ} = Z_{52}^{\circ} = Z_2^{(2)} = \frac{Z_o^{(2)}}{j \sin \theta_2} , \tag{3.29}$$

and

$$Z^{\circ}_{36} = Z^{\circ}_{63} = Z^{(3)}_{2} = \frac{Z^{(3)}_{o}}{j \sin \theta_3} . \qquad (3.30)$$

With the mechanical ports (1°) to (6°) open-circuited, the impedance seen looking into the electrical port is

$$Z^{\circ}_{77} = \frac{1}{j\omega C_o} , \qquad (3.31)$$

which is consistent with the mechanical port conditions, since we shall find that open circuits at the mechanical ports mean zero velocities and displacements, so the crystal is clamped and the piezoelectric effect is prevented from contributing to the impedance seen at port (7°).

It remains to obtain the electro-mechanical transfer impedances. We pick z°_{71} as representative. Ports (2°) through (7°) are open, so a short is placed across all piezo-transformers, decoupling the three transmission lines. A current I_1° injected into port (1°) as shown, produces a current $n_1 I_1^{\circ}$ on the primary side of the piezoelectric drive transformer. This current flows through the positive and negative capacitors and produces a voltage at port (7°) of $n_1 I_1^{\circ}/(j\omega C_o)$, polarized as shown, hence

$$Z^{\circ}_{71} = \frac{n_1}{j\omega C_o} = Z^{\circ}_{74} . \qquad (3.32)$$

Similarly one obtains

$$Z^{\circ}_{72} = \frac{n_2}{j\omega C_o} = Z^{\circ}_{75} , \qquad (3.33)$$

and

$$Z^{\circ}_{73} = \frac{n_3}{j\omega C_o} = Z^{\circ}_{76} . \tag{3.34}$$

With the symmetry of the impedance matrix about the main diagonal, this completes the evaluation of the $Z^{\circ}_{\pi\varsigma}$. The entire array is given on the next page. If instead of three modes, only one is considered, the corresponding three-port impedance matrix is obtained from our seven-port matrix by eliminating any two of the first three rows and columns, and the same members of the second set of three rows and columns, then suppressing the mode index number in what remains. With a trivial renumbering of ports, it will be seen to be identical with that given by Auld (8).

$$
[z^{o}] = \begin{bmatrix}
\frac{Z_0^{(1)}}{j\tan\theta_1} & 0 & 0 & \frac{Z_0^{(1)}}{j\sin\theta_1} & 0 & 0 & \frac{n_1}{j\omega C_0} \\
0 & \frac{Z_0^{(2)}}{j\tan\theta_2} & 0 & 0 & \frac{Z_0^{(2)}}{j\sin\theta_2} & 0 & \frac{n_2}{j\omega C_0} \\
0 & 0 & \frac{Z_0^{(3)}}{j\tan\theta_3} & 0 & 0 & \frac{Z_0^{(3)}}{j\sin\theta_3} & \frac{n_3}{j\omega C_0} \\
\frac{Z_0^{(1)}}{j\sin\theta_1} & 0 & 0 & \frac{Z_0^{(1)}}{j\tan\theta_1} & 0 & 0 & \frac{n_1}{j\omega C_0} \\
0 & \frac{Z_0^{(2)}}{j\sin\theta_2} & 0 & 0 & \frac{Z_0^{(2)}}{j\tan\theta_2} & 0 & \frac{n_2}{j\omega C_0} \\
0 & 0 & \frac{Z_0^{(3)}}{j\sin\theta_3} & 0 & 0 & \frac{Z_0^{(3)}}{j\tan\theta_3} & \frac{n_3}{j\omega C_0} \\
\frac{n_1}{j\omega C_0} & \frac{n_2}{j\omega C_0} & \frac{n_3}{j\omega C_0} & \frac{n_1}{j\omega C_0} & \frac{n_2}{j\omega C_0} & \frac{n_3}{j\omega C_0} & \frac{1}{j\omega C_0}
\end{bmatrix}
$$

D. The TETM Plate Electromechanical Impedance Matrix

Having the matrix array for the posited Fig. 13, we now show that this same array appears from the equations governing the motion of the crystal plate, obtained in Chapter II, when the properly analogous quantities are paired. Once this has been done, an appeal to the fact that the acoustic and transmission-line waves obey the same equations of motion within the region $-h < x < h$ and have the same boundary values, will establish the fact that Fig. 13 constitutes a true analog up to the mechanical boundaries. After the mechanical boundary networks have been added, in Chapter V, the analogy for a single plate will be complete in all respects.

In keeping with (2.52) and (2.53) we adopt the choices

$$V_\pi^\circ = A\, T_{3i}^\circ(-h) , \qquad (\pi = i = 1,2,3) , \tag{3.35}$$

$$V_\pi^\circ = A\, T_{3i}^\circ(+h) , \qquad (\pi = i+3 = 4,5,6) , \tag{3.36}$$

$$V_\pi^\circ = V_7^\circ , \qquad (\pi = 7) , \tag{3.37}$$

where $T_{3i}^\circ(\pm h)$ refers to the value of T_{3i}° at the top, resp., bottom, of the plate.

Note that the choice here pertains to the total stress T_{3i}°, and not simply to the "wavy" portion, $\tilde{T}_{3i}^\circ$.

The currents are taken as

$$I_\xi^\circ = -\dot{u}_i^\circ(-h) = -j\omega u_i^\circ(-h), \qquad (\xi = i = 1,2,3), \tag{3.38}$$

$$I_\xi^\circ = +\dot{u}_i^\circ(+h) = +j\omega u_i^\circ(+h), \qquad (\xi = i+3 = 4,5,6), \quad (3.39)$$

$$I_\xi^\circ = I_7^\circ, \qquad (\xi = 7), \quad (3.40)$$

where, again, $u_i^\circ(\pm h)$ refers to the value of u_i° at $x_3 = \pm h$.

The reason for the sign difference between (3.38) and (3.39) is this: the transmission-line equations (2.42), (2.43) have a convention regarding the variables; the voltage and current are always measured in the same sense, and, as a wave progresses down the line, this sense does not change. On the other hand, we have chosen our port currents I_ξ°, in Fig. 13, to be always directed into the port at the terminal which is considered positive. The mechanical voltages have an unchanged sense along the transmission lines. Labeling in this manner is conventional for lumped networks, and preserves a nice symmetry between "input" and "output," but makes inevitable the reversal of signs elsewhere. It seems to us least undesirable to incorporate them, as we have done, in the distinction between (3.38) and (3.39).

Based upon these choices relating circuit variables and physical quantities, the impedance matrix elements will depend upon quotients of stress components and components of displacement, both in the normal-coordinate system.

By definition, the impedance element $Z_{\pi\xi}^\circ$ is obtained from

$$Z_{\pi\xi}^\circ = V_\pi^\circ / I_\xi^\circ, \quad (3.41)$$

with all currents equal to zero except for I_ξ°. The physical significance of having six of the seven currents equal to zero is this: since the first six currents have been taken to be proportional

to the displacement components at the bottom and top faces of the plate, in the normal coordinates, we see that if ξ is equal to seven, referring to the electrical port current, the fact that all mechanical currents are zero means the plate is completely clamped at the top and bottom surfaces, and, since the piezoelectric drive is located only there, the crystal plate cannot move. This statement parallels our remarks about the traction-free case where the stresses vanished in the normal coordinate system, because they vanished in the untransformed system, and $\beta_j^{(i)}$ is nonsingular. When ξ is not equal to seven, then only five of the six mechanical currents are zero, and only one plate surface is clamped and cannot move. The other surface has, in general, all components of motion in the untransformed system; however, these are not independent, but bear constant ratios to one another as dictated by the direction cosines of the transformation, since I_ξ^o is compounded of untransformed components of motion in the ratio of the $\beta_j^{(i)}$. This becomes more readily apparent when the impedance components are evaluated, as we now do.

As one would expect, the same conclusions we came to in the network case, regarding certain impedance components being identical save for change of mode index number, are valid here. This allows us to cut down on the number of elements to be evaluated.

Again, four categories of impedances are recognized. The first is the electrical input impedance z_{77}^o ; this differs from the reciprocal of (3.15) because, in that case, the tractions, but not the displacements, were forced to be zero. We take u_i^o (i = 1,2,3) to be identically zero everywhere. This satisfies (2.39).

Equation (2.41) becomes

$$\varphi = a_3 x_3 + b_3 \,. \tag{3.42}$$

Application of the boundary conditions (3.2) then gives

$$b_3 = 0,$$

and

$$a_3 = \varphi_0 / h \,. \tag{3.43}$$

From (2.20), (3.12), (3.43) and (3.14) we arrive at

$$Z^{\circ}_{77} = \left(V^{\circ}_7 / I^{\circ}_7 \right)_{u^{\circ}_i = 0} = 1 / j\omega C_0. \tag{3.44}$$

The remaining impedances may be obtained by assuming one of the u_i° to be finite and the other two to be identically zero. Because the u_i° are uncoupled in the bulk, they satisfy (2.39) separately. A value of zero satisfies (2.39), and makes four of the six mechanical currents vanish. The fifth is made to vanish by chosing the finite u_i° to be a solution of (2.39) in such a manner that it is zero at the appropriate surface, and non-zero at the other. Choosing

$$u^{\circ}_i = C_i \sin \varkappa^{(i)} (h \pm x_3) \tag{3.45}$$

accomplishes this; the sign being chosen to make u_i° vanish at $x_3 = \mp h$, respectively.

For definiteness, we take

$$u^{\circ}_2 = u^{\circ}_3 = 0 \tag{3.46}$$

everywhere, and, as a solution to (2.39),

$$u^{\circ}_1 = C_1 \sin \varkappa^{(1)} (h - x_3) \,. \tag{3.47}$$

As a consequence of the requirement that, now,

$$I_7^{\circ} = 0,$$

plus (3.12), we have

$$D_3 = 0;$$

and, by (2.20)

$$a_3 = 0,$$

so that, from (2.38), we get

$$T_{3i}^{\circ} = c^{(i)} u_{i,3}^{\circ} . \tag{3.48}$$

With (3.46) we obtain

$$T_{32}^{\circ} = T_{33}^{\circ} = 0, \tag{3.49}$$

which leads to

$$V_2^{\circ} = V_3^{\circ} = V_5^{\circ} = V_6^{\circ} = 0, \tag{3.50}$$

and, hence, the $Z_{\pi\xi}^{\circ}$ having the subscripts 21,31,51 and 61, are zero. We shall omit doing it, but it is very easily shown by changing the mode index number (i) of the u_i° that is chosen to remain finite, that the $Z_{\pi\xi}^{\circ}$ are symmetric, so that impedance elements with subscripts 12,13,15 and 16 are also zero. It also then appears that, additionally, the following-subscripted elements vanish, along with their symmetrically-related partners: 23,24,26,34,35,45,46 and 56.

We now continue to determine the finite impedance components stemming from our choice (3.46), (3.47). Using (3.48) and (3.47)

AD-A044 174 ARMY ELECTRONICS COMMAND FORT MONMOUTH N J F/G 9/1
TRANSMISSION-LINE ANALOGS FOR PIEZOELECTRIC LAYERED STRUCTURES.(U)
MAY 76 A BALLATO

UNCLASSIFIED ECOM-4413 NL

2 OF 3
ADA
044174

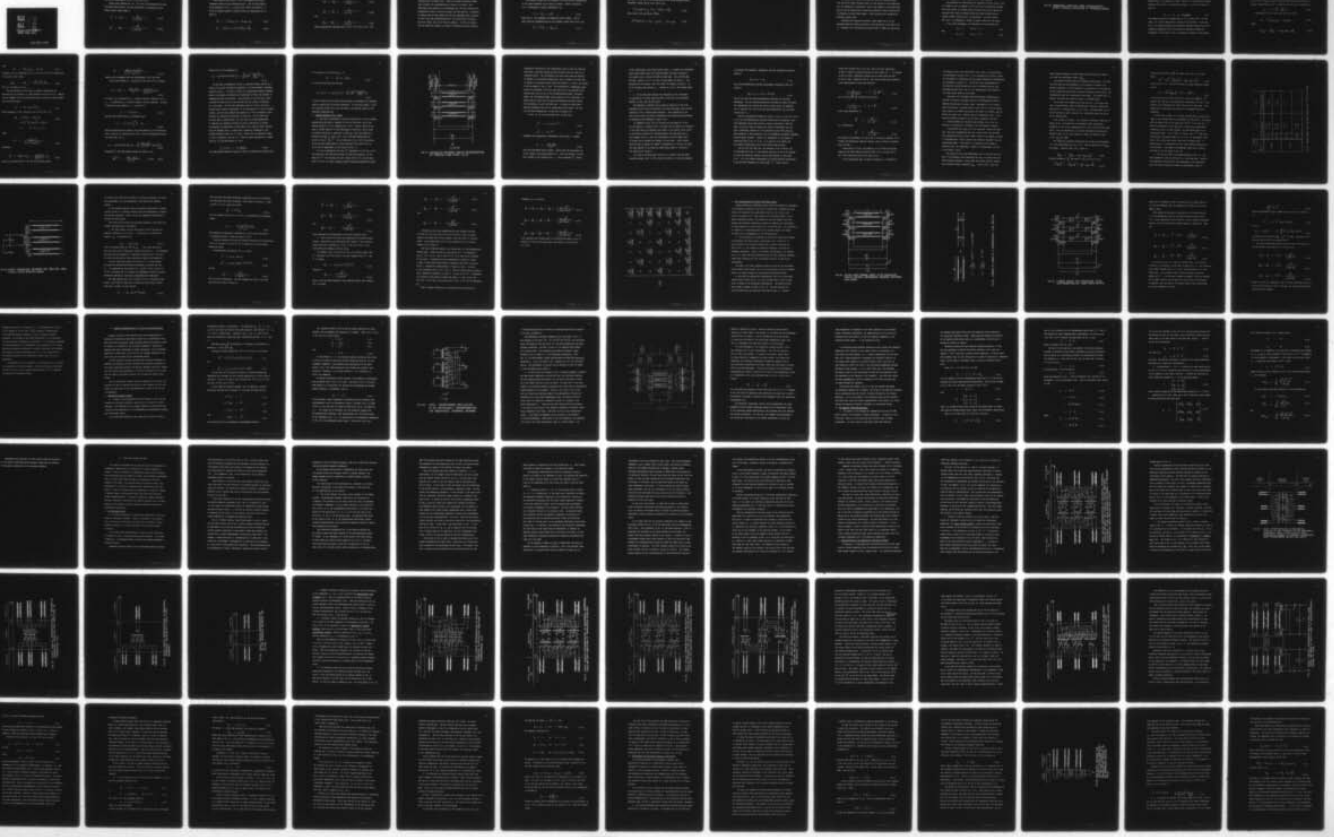

gives

$$T_{31}^{\circ} = -\alpha^{(1)} c^{(1)} G_1 \cos\alpha^{(1)}(h-x_3), \tag{3.51}$$

so that, by (3.35), (3.36), and (3.27),

$$V_1^{\circ} = -\alpha^{(1)} c^{(1)} G_1 A \cos\theta_1 , \tag{3.52}$$

and

$$V_4^{\circ} = -\alpha^{(1)} c^{(1)} G_1 A . \tag{3.53}$$

I_1° is obtained from (3.38) and (3.47):

$$I_1^{\circ} = -j\omega G_1 \sin\theta_1 , \tag{3.54}$$

so we have determined

$$Z_{11}^{\circ} = Z_o^{(1)} / (j \tan\theta_1) , \tag{3.55}$$

plus

$$Z_{41}^{\circ} = Z_o^{(1)} / (j \sin\theta_1) , \tag{3.56}$$

and use has been made of (2.45), (2.54) and (2.56).

Making other choices for (i) in (3.45), and using both the plus and minus signs therein, for each such choice, a repetition of the steps directly above leads to

$$Z_{11}^{\circ} = Z_{44}^{\circ} = \frac{Z_o^{(1)}}{j \tan\theta_1} , \tag{3.57}$$

$$Z_{22}^{\circ} = Z_{55}^{\circ} = \frac{Z_o^{(2)}}{j \tan\theta_2} , \tag{3.58}$$

$$Z_{33}^{\circ} = Z_{66}^{\circ} = \frac{Z_o^{(3)}}{j \tan \theta_3}, \tag{3.59}$$

which are the same as (3.24), (3.25) and (3.26); also

$$Z_{14}^{\circ} = Z_{41}^{\circ} = \frac{Z_o^{(1)}}{j \sin \theta_1}, \tag{3.60}$$

$$Z_{25}^{\circ} = Z_{52}^{\circ} = \frac{Z_o^{(2)}}{j \sin \theta_2}, \tag{3.61}$$

and

$$Z_{36}^{\circ} = Z_{63}^{\circ} = \frac{Z_o^{(3)}}{j \sin \theta_3}. \tag{3.62}$$

These are the same as (3.28), (3.29) and (3.30), while (3.44) is the same as (3.31).

All but the electro-mechanical transfer impedances have been obtained; this calculation follows next.

Once again we use (3.46), (3.47), and compute the voltage developed across the open electrical port. For the same reasons given following (3.47), a_3 is again zero, while the quantity b_3 is of no concern because it does not enter the expression for V_7°, which is

$$V_7^{\circ} = [\varphi(x_3 = +h) - \varphi(x_3 = -h)], \tag{3.63}$$

$$V_7^{\circ} = [u_1^{\circ}(+h) - u_1^{\circ}(-h)]\, e_{313}^{\circ} / \epsilon_{33}^{S}; \tag{3.64}$$

this last expression following from (2.41) with $a_3 = 0$ and the choices (3.46), (3.47) for the u_i^o. Substituting the particular form for u_1^o given by (3.47) makes V_7^o become

$$V_7^o = - C_1 \, e_{313}^o \sin\theta_1 \, / \, \epsilon_{33}^S \, . \tag{3.65}$$

The current I_1^o is obtained from (3.54), so the impedance z_{71}^o is

$$Z_{71}^o = e_{313}^o \, / \, (j\omega \, \epsilon_{33}^S) \, . \tag{3.66}$$

Recalling the definitions (3.14) and (3.17) allows us to put this in the form

$$Z_{71}^o = \frac{n_1}{j\omega \, C_o} \, , \tag{3.67}$$

which is seen to agree with (3.32).

Continuing exactly as we have proceeded above to determine z_{71}^o, but with interchanges of index numbers, one may similarly show that

$$Z_{71}^o = Z_{74}^o = \frac{n_1}{j\omega \, C_o} \, , \tag{3.68}$$

$$Z_{72}^o = Z_{75}^o = \frac{n_2}{j\omega \, C_o} \, , \tag{3.69}$$

and

$$Z_{73}^o = Z_{76}^o = \frac{n_3}{j\omega \, C_o} \, . \tag{3.70}$$

These relations are identical with (3.32), (3.33) and (3.34). The

symmetry of the $Z^{\circ}_{\pi\xi}$ about the main diagonal makes the determination complete, and, it is seen that our assignments (3.35) to (3.40) are, in every respect, consistent with the posited Fig. 13 and with the equations governing the physics of the system, so that the impedance matrices obtained from the physics and the figure are identical. The impedance matrix is further seen to have the property that all mechanical ports are on an equal footing, the only difference being the arbitrarily assigned port numbers; this property also follows at once from Fig. 13.

This section has developed the seven-port impedance matrix from the physical equations governing the problem. Upon comparison with the matrix of Section C, one sees they are identical. This justifies not only our choice of pairings of variables between the circuit and the problem, but proves that Figure 13 is an exact representation of the physical problem as seen at the ports (π^{0}). We remark again that the complete problem involves additional circuitry, so that the mechanical conditions at the layer surfaces can be expressed in untransformed variables, instead of those superscripted with the degree sign. Within the normal-coordinate framework, however, the representation of Figure 13 is exact. One additional topic remains to be considered yet, and this concerns the piezoelectric drive, to which we devote the next section. We mention in passing that we have marked out upon our unbounded plate a portion of area A and have characterized this; the entire plate is simply more such areas, with all of them in parallel. It will be noticed that the LETM case treated in Chapter IV presents the dual situation

of portions of a single plate characterized as being in series electrically.

E. Piezoelectric Tractions.

We noted in Section IB 5. the historical development of the concept of piezoelectric tractions taking place at discontinuities. In this regard, Holland's work (102) deserves special mention as it pertains to piezo-vibrators and stacks of plates, and he emphasized the surface-traction aspect in these situations.

We have arrived, in our work, at circuit representations which place just such an interpretation in evidence. That is, our circuits portray the piezo-drive effect as a phenomenon that takes place at the surfaces of the plate, and therefore the schematic shares this accordance with the nature of the physical problem.

This section discusses the drive mechanism further and leads up to a demonstration that the circuits, such as those of Fig. 10 and 13, are true analogs; they provide realizations not only at the seven ports, but are valid within the bulk of the layer, as well.

The physical reason for the location of the piezo-drive transformers at the layer boundaries can be seen as follows. Newton's equations (2.1), transformed to normal coordinates, are

$$F_i^\circ = T_{3i,3}^\circ = \rho \ddot{u}_i^\circ \quad , \tag{3.71}$$

where the F_i° are components of mechanical force density. The F_i° arise from the differentiation of the stresses, which from (2.38), are

$$T_{3i}^\circ = c^{(i)} u_{i,3}^\circ + e_{33i}^\circ a_3 \ . \tag{2.38}$$

The quantity a_3, in turn, is a uniform electric field, from (2.41), which depends for its value upon the boundary conditions imposed (see, e.g., (3.6), (3.43) and above (3.48)). Differentiation of (2.38) yields no contribution from the second term on the right within the bulk of the crystal, where $e^{\circ}_{33i}\, a_3$ is constant. However, each surface produces a discontinuity, so the differentiation yields a delta-function of force density, located at the surface. This will, in general, result in all three components of F°_i being produced there. In the event that the material comprising the plate is not piezoelectrically homogeneous, additional contributions to F°_i will be produced because the term $a_3\, e^{\circ}_{33i,3}$ is then not always zero. We do not consider this further, but it may be treated by the method set forth in Chapter VI.

The delta-functions of piezoelectric force density are represented by our transformers, which are located at the surface and exert finite forces, but have no spatial extensions.

The mechanical variables, represented by (3.35), (3.36), (3.38) and (3.39) as port voltages V°_{π} and port currents I°_{β} occur at the surfaces $x_3 = \pm h$, as do the piezoelectric drive terms discussed above. Therefore, making use of (2.47) and (2.52),

$$V^{(i)}(\text{at port } (\pi^{\circ})) = (V^{\circ}_{\pi} - A\bar{T}^{\circ}_{3i}) = A\tilde{T}^{\circ}_{3i} \,. \tag{3.72}$$

Also, from (2.53) and (2.38), (2.39),

$$I^{(i)}(\text{at port } (\pi^{\circ})) = I^{\circ}_{\pi} = -j\omega u^{\circ}_i \,, \quad (\pi = 1,2,3), \tag{3.73}$$

and

$$I^{(i)}(\text{at port}(\pi')) = -I_{\pi}^{\bullet} = -j\omega u_i^{\circ}, \quad (\pi = 4,5,6). \tag{3.74}$$

Since $V^{(i)}$ and $I^{(i)}$ are the transmission-line variables, these are then expressed directly in terms of known values at the surface. The boundary values at the transmission-line ends, expressed by (3.72), (3.73) and (3.74), are the same as those appearing at the plate surface in the physical problem. This, plus the fact that the network and the acoustic problem obey the same transmission-line equations within the bulk, as shown in Chapter II, guarantees that the network is a true analog, and that corresponding quantities are matched on a point-for-point basis along the spatial coordinate from -h to +h.

In the results of Chapter V we shall obtain suitable mechanical boundary networks to be attached to Fig. 13, which will then become complete.

IV. Lateral Excitation of Thickness Modes

Lateral excitation is the second canonical form of excitation of thickness modes. It has been the subject of recent interest (207-215), although use was made of it by Atanasoff & Hart (44), referenced in Cady's book (160). Also, excitation by an electric field lateral to the wave propagation direction is often used with vibrators in the form of bars. We have chosen the name given in the chapter title, (abbreviated as LETM) to characterize this type of excitation. As much confusion arises from other names that abound in the literature, it seems to us least ambiguous in this form.

In this chapter we will parallel the treatment given the TETM case in the last chapter, considering first a traction-free plate analytically, then obtaining a network that realizes the electrical port immittance. After this, the seven-port admittance matrix for the normal coordinate system is derived, analytically, and realized as a network, which is shown to be a true analog of the acoustic problem.

Our efforts are aided by similarities that this problem shares with the first (TETM) canonical form, so that certain of the properties will be recognized by inspection, such as the symmetry of the admittance matrix, and the possibility of obtaining additional matrix coefficients by permuting the mode index number. These features will therefore be discussed briefly only.

Concerning the analytical portion, there seems not to be any published material relating directly to the derivation as we shall give it. Schweppe (215) consideres two modes driven by LETM, but limits the

discussion to ceramics, (class 6mm), while the other publications treat of only one mode, or of a number of modes each of which is uncoupled to the others at the boundaries, in the manner of Lawson's TETM paper (61). What we shall give for the traction-free plate is patterned after Tiersten's treatment (216a,b).

A. Single-Plate Crystal Resonator, Traction-Free.

1. The plate under consideration is presumed to be laterally unbounded and of thickness 2h; the upper and lower surfaces at $x_3 = +h$ and $-h$, respectively, are further presumed to have no mechanical surface-tractions applied. A uniform electric field is applied in a direction perpendicular to the thickness coordinate. Without loss in generality, we take the field direction as the negative x_1 axis. This specification of a lateral field now requires the lateral coordinates to be distinguished, and the matter tensors specifying the phenomenological elastic, piezoelectric and dielectric properties have to be referred from the X,Y,Z system to the new x_i system, now established. In the TETM case, only such components as were referred to x_3 were required.

The mechanism for establishing the impressed electric field is not of interest to us; we suppose it to be set up by an electrode arrangement sufficiently far removed from the section of plate we focus our attention upon that any effects other than those arising from an assumed uniform lateral field, are negligible. The time factor, $\exp(j\omega t)$, is suppressed. Figure 16 shows a section of the plate.

At the plate boundaries, the conditions to be satisfied are

$$T_{3j} = 0, \qquad \text{at } x_3 = \pm h, \tag{3.1}$$

and

$$D_3 = 0, \qquad \text{at } x_3 = \pm h. \tag{4.1}$$

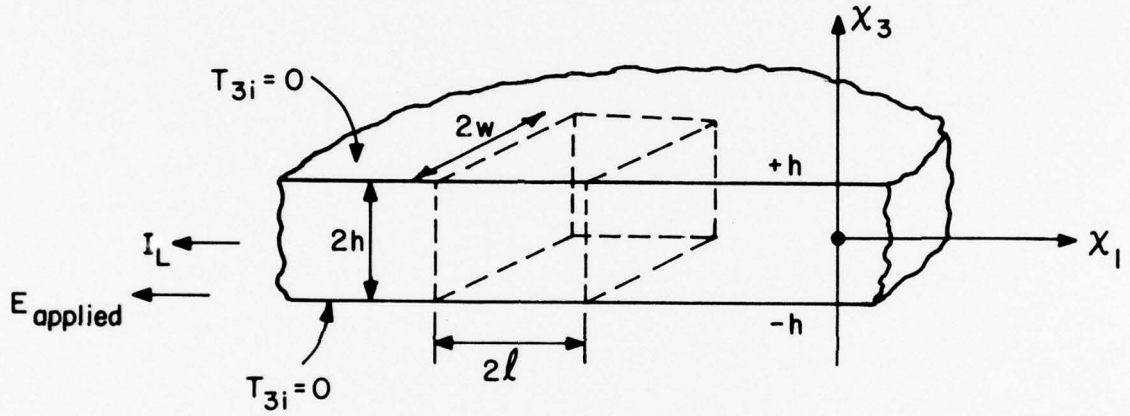

FIG. 16. UNBOUNDED, TRACTION - FREE, PIEZOELECTRIC PLATE. LATERAL EXCITATION OF THICKNESS MODES.

The mechanical condition (3.1) is the same as in the TETM case, and we also have, as a consequence,

$$T_{3i}^{\circ} = 0 , \qquad at\ x_3 = \pm h . \tag{3.3}$$

The condition (4.1) replaces (3.2). D_3 must still be a constant throughout the plate, and, because of (4.1), that constant must be zero, however, it cannot be shown from (2.20) because we shall find that the applied electric field modifies this expression. The assumption, in Chapter II, of no lateral field variations was valid both in Chapter III and here because E(applied)is uniform. This implies a laterally varying potential, however, which we take as

$$\varphi = (e_{3k3} / \epsilon_{33}^{S}) u_k + a_3 x_3 + a_1 x_1 + b_3 , \tag{4.2}$$

using (2.17) as a guide; (4.2) satisfies the completely general (2.16).

If we take the applied field to point in the negative x_1 direction, as the applied TETM field pointed in the negative x_3 direction, it follows that a_1 is positive in value. From (2.4), the positive-directed electric field in the x_1 direction is called E_1, and (4.2) gives its value as

$$E_1 = - a_1 = - E(applied) . \tag{4.3}$$

This added term must be included when (2.5) is written out. We will take E_1 as a given value which is fixed for the problem. It is seen that E_1 by itself satisfies the electrical boundary condition that the tangential component of the field shall be continuous across the boundaries, so the field in the x_1 direction, external to the crystal,

is likewise equal to E_1 .

When (2.5) is written out, we get, instead of (2.13),

$$T_{3j} = c^{E}_{3jk3}\, u_{k,3} + e_{33j}\, \varphi_{,3} - e_{13j} E_1 \; ; \tag{4.4}$$

and, similarly, (2.6) now gives

$$D_3 = e_{3k3}\, u_{k,3} - \epsilon^{S}_{33}\, \varphi_{,3} + \epsilon^{S}_{31} E_1 \; , \tag{4.5}$$

instead of (2.14). In the quantities e_{13j} and ϵ^{S}_{31} we have the first appearance of components of the material tensors referring to a lateral axis.

From (4.2) we have

$$\varphi_{,3} = \left(e_{3k3} / \epsilon^{S}_{33} \right) u_{k,3} + a_3 \; , \tag{4.6}$$

and when this is inserted into (4.5), D_3 becomes

$$D_3 = - \epsilon^{S}_{33}\, a_3 + \epsilon^{S}_{31} E_1 \; , \tag{4.7}$$

but, as (4.1) makes D_3 equal to zero, arising from the fact that no current can now flow in the x_3 direction, we are able to evaluate a_3 :

$$a_3 = + \left(\epsilon^{S}_{31} / \epsilon^{S}_{33} \right) E_1 \; . \tag{4.8}$$

Substitution of (4.6) and (4.8) into (4.4) gives

$$T_{3j} = \bar{c}_{3jk3}\, u_{k,3} - \underline{e}_{13j} E_1 \; , \tag{4.9}$$

where

$$\bar{c}_{3jk3} = c^{E}_{3jk3} + e_{33j}\, e_{3k3} / \epsilon^{S}_{33} \tag{2.19}$$

are the same piezoelectrically stiffened elastic stiffnesses encountered in Chapter II.

The quantities $\underline{e}_{13j}$ are given by

$$\underline{e}_{13j} = e_{13j} - (\epsilon^{S}_{31}/\epsilon^{S}_{33})\, e_{33j} \quad . \tag{4.10}$$

We will need D_1 in order to determine the current and admittance of this configuration. We use (2.6) to obtain

$$D_1 = e_{1k3}\, u_{k,3} - \epsilon^{S}_{13}\, \varphi_{,3} + \epsilon^{S}_{11}\, E_1 \,, \tag{4.11}$$

where (2.4) has also been used. When (4.6) and (4.8) are put into (4.11), we arrive at

$$D_1 = \underline{e}_{1k3}\, u_{k,3} + \underline{\epsilon}_{11}\, E_1 \quad . \tag{4.12}$$

In this expression $\underline{e}_{1k3}$ equals the following

$$\underline{e}_{1k3} = e_{1k3} - (\epsilon^{S}_{31}/\epsilon^{S}_{33})\, e_{3k3} \,, \tag{4.13}$$

and $\underline{\epsilon}_{11}$ is

$$\underline{\epsilon}_{11} = \epsilon^{S}_{11} - \epsilon^{S}_{13}\, \epsilon^{S}_{31}/\epsilon^{S}_{33} \,. \tag{4.14}$$

Because of the symmetry of e_{kij} to an interchange of the last two indices, and because ϵ^{S}_{ik} are likewise symmetric, (4.13) is the same as (4.10), and (4.14) can be written

$$\underline{\epsilon}_{11} = \epsilon^{S}_{11} - (\epsilon^{S}_{13})^2/\epsilon^{S}_{33} \,. \tag{4.15}$$

2. We now transform to normal coordinates to uncouple the motions. In the transformed system we have

$$T^{\circ}_{3i} = c^{(i)}\, u^{\circ}_{i,3} - \underline{e}^{\circ}_{13i}\, E_1 \,, \tag{4.16}$$

and

$$D_1 = \underline{\underline{e}}^{\circ}_{1i3}\, u^{\circ}_{i,3} + \underline{\underline{\epsilon}}_{11} E_1 . \qquad (4.17)$$

Equation (4.16) is obtained as in (2.35)-(2.38), and (4.17) comes from (4.12) and (2.40), where

$$\underline{\underline{e}}^{\circ}_{13i} = e^{\circ}_{13i} - (\epsilon^{s}_{31}/\epsilon^{s}_{33})\, e^{\circ}_{33i} , \qquad (4.18)$$

and $\underline{\underline{\epsilon}}_{11}$ is given by (4.15).

The wave equation (2.39) must, of course, additionally be satisfied by any solution u°_i that satisfies (4.16) and (3.3). Regarding the symmetry of the traction-free plate, we take the same solution as for the TETM case:

$$u^{\circ}_i = U_i \sin x^{(i)} x_3 , \qquad (3.4)$$

which satisfied (2.39), and use it with (4.16) and (3.3):

$$\begin{aligned} T^{\circ}_{3i} &= c^{(i)} u^{\circ}_{i,3} - \underline{\underline{e}}^{\circ}_{13i} E_1 \\ &= c^{(i)} x^{(i)} U_i \cos x^{(i)} h - \underline{\underline{e}}^{\circ}_{13i} E_1 \\ &= 0 \qquad \text{at} \quad x_3 = \pm h , \end{aligned} \qquad (4.16)$$

hence

$$U_i = \frac{+\,\underline{\underline{e}}^{\circ}_{13i} E_1}{c^{(i)} x^{(i)} \cos x^{(i)} h} . \qquad (4.19)$$

Therefore,

$$T^{\circ}_{3i} = -\,\underline{\underline{e}}^{\circ}_{13i} E_1 \left\{ 1 - \frac{\cos x^{(i)} x_3}{\cos x^{(i)} h} \right\} , \qquad (4.20)$$

which is the same form as (3.8) for the TETM case, while

$$u_i^\circ = \frac{\underline{\epsilon}_{13i}^\circ E_1 \sin x^{(i)} x_3}{c^{(i)} x^{(i)} \cos x^{(i)} h} , \tag{4.21}$$

which is to be compared with the corresponding (3.9) for TETM.

Now we can evaluate D_1 by putting (4.21) into (4.17), yielding

$$D_1 = \left\{ \underline{\epsilon}_{11} + \frac{\underline{\epsilon}_{13i}^\circ \underline{\epsilon}_{1i3}^\circ}{c^{(i)}} \cdot \frac{\cos x^{(i)} x_3}{\cos x^{(i)} h} \right\} E_1 , \tag{4.22}$$

so that D_1 is a function of x_3, instead of being a constant, as is D_3. To obtain the x_1-directed current, we must integrate. We take a portion of area normal to x_1, of width $2w$,

$$A_L = (2h)(2w) , \tag{4.23}$$

and find the current which it intercepts from

$$I_L = -j\omega (2w) \int_{-h}^{+h} D_1 \, dx_3 , \tag{4.24}$$

where the negative sign arises in the same manner as in the TETM case. With D_1 from (4.22) inserted into (4.24), and the integration carried out, one finds, for I_L,

$$I_L = -j\omega (2w) E_1 \left\{ 2h \, \underline{\epsilon}_{11} + \sum_{i=1}^{3} \frac{2 \underline{\epsilon}_{13i}^\circ \underline{\epsilon}_{1i3}^\circ}{c^{(i)} x^{(i)}} \tan x^{(i)} h \right\} . \tag{4.25}$$

Defining $\underline{k}^{(i)}$, the LETM coupling factor for mode (i), by

$$\left(\underline{k}^{(i)}\right)^2 = \frac{\underline{\epsilon}_{13i}^\circ \underline{\epsilon}_{1i3}^\circ}{\underline{\epsilon}_{11} c^{(i)}} , \quad \text{(no sum)} \tag{4.26}$$

allows (4.25) to be expressed as

$$I_L = -j\omega(2w)(2h)E_1 \in_{11} \left\{ 1 + \sum_{i=1}^{3} \left(\underline{k}^{(i)}\right)^2 \frac{\tan x^{(i)} h}{x^{(i)} h} \right\} . \tag{4.27}$$

We now have an expression for the x_1-directed current arising as a result of the plate vibrations responding to the time-harmonic impressed electric field E_1. In order to arrive at an equivalent network representation, we arrange our definition of admittance to take into account an elemental portion of the plate. This was done in the TETM case, where a portion of area of size A was selected and the current intercepted by it was found. For the TETM unbounded plate as a whole, the total current would itself be unbounded, so the calculation is a form of normalization, and the whole problem then appears as a sum of elemental plate portions all connected electrically in parallel. For the LETM case we again make a normalization, but this time it is more appropriate to consider the elemental sections as being electrically in series. We determine the admittance on this basis. To do this we first consider that the imposed field E_1 arises from a potential difference in the lateral direction equal to $(-E_1 (2\ell))$, where 2ℓ is an arbitrary length in the x_1 direction. See Fig. 16. Then the input admittance Y_{in} (LETM) would be, in the same manner as (3.13),

$$Y_{in}\ (\text{LETM}) = -I_L / (2\ell E_1) . \tag{4.28}$$

The capacitance between two plates of area A_L, separated by distance 2ℓ,

in a medium of permittivity ϵ_{11}, is

$$\underline{C}_o = \underline{\epsilon}_{11} A_L / (2\ell) , \tag{4.29}$$

so (4.28) can be put into the form

$$Y_{in}\,(LETM) = +j\omega \underline{C}_o \left\{ 1 + \sum_{i=1}^{3} (\underline{k}^{(i)})^2 \frac{\tan \chi^{(i)} h}{\chi^{(i)} h} \right\}. \tag{4.30}$$

It will be seen that the entire plate appears as an assembly of elemental areas in series such as we have considered. In the final result, (4.30), the tranverse length (2ℓ) does not appear, but appears instead in the tranverse capacitance $\underline{Co}$.

B. Network Synthesis of Y_{in} (LETM).

1. The task of performing a one-port synthesis of (4.30) is greatly simplified by the work of Chapter III for the TETM case, and by the simpler nature of (4.30), compared with (3.15). We see, first of all, that Y_{in} (LETM) consists of four admittances in parallel, one of which is simply realized by a capacitor of value $\underline{Co}$. What then remains is nothing more than Y_{TL} from (3.16), with a suitable substitution of $\underline{Co}$ for Co and $\underline{k}^{(i)}$ for $k^{(i)}$. But we know that Y_{TL} in (3.16) is realized by the parallel combination of three networks of the form of Fig. 9, so we are led immediately to the circuit of Fig. 17.

It is to be emphasized that the $\chi^{(i)}$ appearing in (3.15) and (4.30) are identical; both come from solving the same wave equation, (2.39), where the $c^{(i)}$ are the same for both, coming from (2.19) in each case. That is to say, the same stiffened elastic constants determine the wave

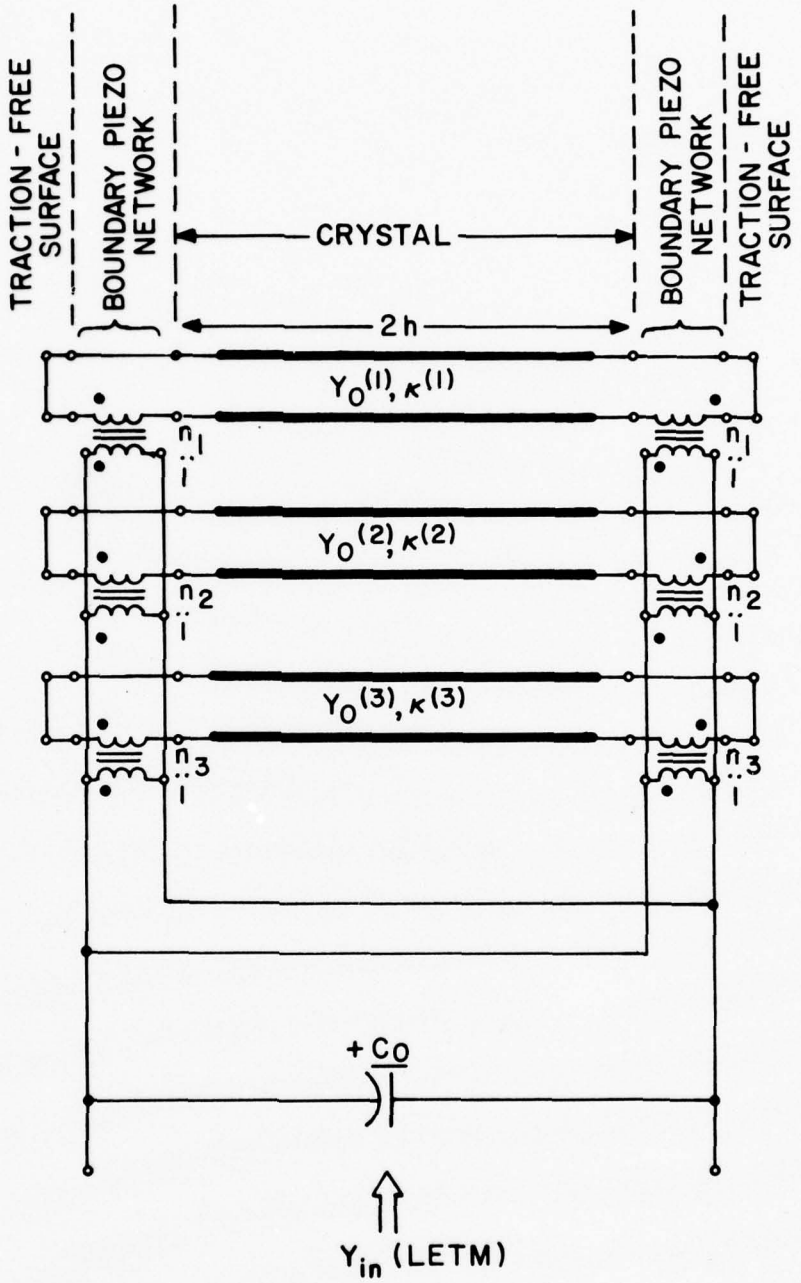

FIG. 17. EQUIVALENT NETWORK ANALOG REPRESENTATION OF TRACTION-FREE PLATE, LETM.

propagation velocities on the transmission lines in both the TETM and LETM cases, and these velocities are the same as for the case of an unbounded medium. The differences that exist come from the presence or absence of the negative capacitance, and, of course, the fact that Co refers to a capacitor whose plates are normal to x_3 while the plates of Co are normal to the x_1 axis. The piezoelectric transformer turns ratios are different in the two cases and this is an important fact, because here lies the key to the misunderstanding about "stiffened modes" and "unstiffened modes" which prevails in the literature. It should also be noted that the piezo-transformers have been located at the boundary, as with the TETM case. It cannot be shown from a one-port synthesis that this is indeed where they belong, but this will be shown subsequently, as was done in Chapter III.

In Fig. 17, as in our previous work, we have used

$$Y_o^{(i)} = 1/(A\rho v^{(i)}) , \tag{4.31}$$

$$\kappa^{(i)} = \omega / v^{(i)} , \tag{2.45}$$

whereupon the piezoelectric transformer turns ratios, n_i become

$$n_i = \frac{+A_L \, e^{\circ}_{13i}}{2h} , \tag{4.32}$$

with the transformer dots as shown. Notice that the area factor in (4.31) refers to the plane normal to x_3, while the factor in (4.32) has a normal in the direction of x_1. This is because $Y_o^{(i)}$ refers

to the transmission lines which extend along x_3, whereas the transformer turns ratios depend upon the cross sectional area which intercepts the current flow in either the TETM or LETM case. For the TETM case, the area factor in (3.17) is just A, whose normal is along x_3, the direction of the current, while for LETM, the current is along x_1 so (4.32) contains the quantity A_L, defined in (4.23), with normal along x_1.

2. We now make some remarks with reference to the literature; in particular, we review some past work in the light of our general results, so far, for the LETM plate.

The presence or absence of the negative capacitor is the first indication of the type of excitation; the LETM electrical input circuit consists of only a single shunt capacitor. This separation of the input circuit from the portion representing the vibration was mentioned in connection with Schüssler's paper (143).

In Schweppe's paper (215) he derives the equivalent of (4.30) for two modes in a ceramic plate. He shows that by means of a variation in the angle which the applied field makes in the lateral plane, which is the same as rotating the crystallographic XYZ axes about our x_3, with respect to our x_1 axis, the amplitudes of the two modes which he treats can be altered with respect to each other. Such a device could be used to reduce the number of resonators in a filter; the idea has been applied to the shear and quasi-shear modes in a rotated Y-cut quartz plate (214a,b).

The case of one mode being excited by a lateral field was first treated by Mason (130) in 1939, where the motion of a bar was analyzed.

He obtained the resonance frequencies from the harmonically-related roots of

$$\tan \pi h = \infty \,, \tag{4.33}$$

and the non-harmonically-related antiresonant frequencies from the roots of

$$\tan \pi h = -\pi h (1-k^2)/k^2 . \tag{4.34}$$

One can see that the TETM antiresonances coincide with the LETM resonances. For the situation where only one mode of either is driven, the construction for finding the roots is given nicely by Schüssler (143); Tiersten (64) first gave the TETM construction, and the other follows from it.

From the differences between the roots of (3.19), (3.20) and (4.33), (4.34) the electromechanical coupling factors may be determined (141). The differences which arise from the types of excitation, TETM and LETM, can also be used to explain the finding of Bechmann (208,210) that a production version of a high precision quartz TETM vibrator, when converted to LETM operation, had its fundamental resonance frequency shifted upward slightly. Viewed as a consequence of the change in conditions from (3.20) to (4.33), it is seen to be an effect due the coupling coefficient, which may be found from his data.

Just as with the TETM case, the solution (4.30) is exact, and the realization of Fig. 17 also exactly realizes (4.30) so the network is valid for transient studies, and can additionally be used down to DC. At DC the network degenerates to a simple parallel combination of $\underline{C}o$ and three capacitors of value $\underline{C}o(\underline{k}^{(i)})^2$. Notice that we

cannot say anything like (3.22) now, since the input capacitance of such a circuit is always positive for real values $\underline{k}^{(i)}$. If, however, we wish to make a comparison between the two cases TETM and LETM in the DC limit, supposing that Co = $\underline{Co}$, then we would have identical input capacitances in each case providing

$$\frac{1}{1 - \sum_{p=1}^{3} (k^{(p)})^2} = 1 + \sum_{i=1}^{3} (\underline{k}^{(i)})^2 , \tag{4.35}$$

or in the case of only one mode of each type,

$$\frac{1}{1 - k^2} = 1 + \underline{k}^2 , \tag{4.36}$$

which leads immediately to

$$\underline{k}^2 = \frac{k^2}{1 - k^2} , \tag{4.37}$$

or, alternatively

$$k^2 = \frac{\underline{k}^2}{1 + \underline{k}^2} . \tag{4.38}$$

An identical relationship, (4.36)-(4.38), is found by Bechmann (137), between one-dimensional coupling factors, from an entirely different point of view.

Coming back to (4.34), the quantity $(1-k^2)/k^2$ can be replaced simply by the LETM coupling factor $\underline{k}^{-2}$ from (4.37), so that (4.34) and (3.20) differ now only by the sign of χh.

In the single-mode case, we noted in Chapter I, in connection

with Mason's exact 1939 LETM network (130), that it was equivalent to Butterworth's circuit (129). It is instructive to think of these two alternates in connection with the normal-coordinate transformation we introduced in Chapter II. We saw that this transformation in the physical problem allowed us to put the network results into transmission-line form, that is, the transmission lines represent the three normal modes of the system.

Guillemin (217) discusses normal-coordinate transformations applied to circuits and shows that such a transformation leads to network realizations as Foster forms. Butterworth's 1915 circuit, which incidentally, predates Foster's work (217) is just one Foster form, wherein the normal coordinates are placed in evidence, and the method for doing this, starting from the transmission line, is the partial-fractions expansion, as was used by Marutake (144,145).

3. Having worked both traction-free problems, we are now in a position to consider the "stiffened" and "unstiffened" question.

A distinction has grown up in the literature between the TETM case (also the corresponding case for a bar or rod), and the LETM case (similarly for bar or rod), where a mode of the former is called a "stiffened mode," while a mode of the latter is referred to as an "unstiffened mode." That there is a distinction to be made is certainly true; the terminology, however, is unfortunate, and this is not merely a cavil.

The origin for the terms doubtlessly lies in the fact that for most of the popularly used substances and cuts, it arises that the TETM situation produces a driven mode whose phase velocity depends upon stiffened elastic constants $\bar{c}_{3j\ell3}$, (see (2.19)), while the

LETM situation produces a driven mode whose phase velocity depends only upon the unstiffened values c^{E}_{3jk3} .

Our general results permit the following observations. The TETM and LETM cases are distinguished by the presence or absence of a negative capacitor, by the difference in orientation of Co and $\underline{Co}$ and by the quantities which enter the piezo-transformer turns ratios. The transmission lines are identical for both cases. This means that, in general, both TETM and LETM will drive a "stiffened mode."

As we shall show a TETM-driven mode must be a "stiffened mode" and a "stiffened mode" must be TETM-drivable, whereas a LETM-driven mode may be a "stiffened mode" or not, and a "stiffened mode" may or not be drivable by LETM; likewise, an "unstiffened mode" may or may not be LETM-drivable.

This is seen as follows. The criterion of whether a mode can be driven or not, is whether the corresponding piezo transformer, connected to that modal transmission line, has a finite or zero turns ratio. This is determined by the proper transformed piezoelectric constant; from (3.17), this constant is e°_{33i} for TETM and, from (4.32), $\underline{e}^{\circ}_{13i}$ for LETM.

The effective stiffness determining the velocity and wavenumber $\kappa^{(i)}$, for transmission line (i) is $c^{(i)}$. We may relate this to $\bar{c}_{3j'k3}$ as follows: starting from (2.19), which is

$$\bar{c}_{3jk3} = c^{E}_{3j'k3} + e_{33j}\, e_{3k3} / \epsilon^{S}_{33} , \qquad (2.19)$$

multiply through by $\beta_j^{(i)}$ and apply (2.34) and (2.29) to get

$$\kappa^{(i)} \delta_{kj} \beta_j^{(i)} = c^{E}_{3jk3} \beta_j^{(i)} + e^{\circ}_{33i}\, e_{3k3} / \epsilon^{S}_{33} . \qquad (4.39)$$

Now multiply through by $\beta_k^{(i)}$ and apply (2.26) and (2.29) which gives

$$c^{(i)} = \beta_j^{(i)} c^E_{3jk3} \beta_k^{(i)} + e^0_{33i} e^0_{3i3} / \epsilon^S_{33} . \qquad (4.40)$$

By the use of (3.7), this can be written in other equivalent forms, such as

$$c^{(i)} = \beta_j^{(i)} c^E_{3jk3} \beta_k^{(i)} / \left(1 - (k^{(i)})^2\right) . \qquad (4.41)$$

It is enough for us to see, from (4.40), that the eigenvalue $c^{(i)}$ depends upon e^0_{33i} for its piezoelectric stiffening, and this is the quantity that determines the turns ratios for the TETM case. This proves that a TETM-driven mode must be a "stiffened mode" and conversely.

In the case of LETM, it is obvious that e^0_{13i} may be finite while e^0_{33i} is zero because they are independent of each other. This would make the second term on the right hand side of (4.40) zero and $c^{(i)}$ would be determined by the c^E_{3i3j} only, without any piezoelectric stiffening; hence, in this instance, the LETM-driven mode is an "unstiffened mode." But if e^0_{33i} is finite, then $c^{(i)}$ must have a piezoelectric stiffening term; so, by (4.18), if furthermore e^0_{13i} and/or ϵ^S_{3i} are/is also finite, then this "stiffened mode" is LETM-drivable, in contradiction to the usual notions prevailing in the literature. The general circumstances under which a mode is excitable or not are given in Fig. 18.

4. Let us go on now to the simplification of Fig. 17. The same arguments we gave in Section III B hold good here. Briefly, the symmetrical excitation of the transmission lines guarantees that the centers thereof are nodes of displacement, which is

e°_{33i} → / e°_{13i} ↓		FINITE	ZERO
		$C^{(i)}$ STIFFENED	$C^{(i)}$ UNSTIFFENED
FINITE	$\epsilon^{S}_{13}=0$	TETM LETM	—— LETM
	$\epsilon^{S}_{13}\neq 0$	TETM LETM	—— LETM
ZERO	$\epsilon^{S}_{13}=0$	TETM ——	—— ——
	$\epsilon^{S}_{13}\neq 0$	TETM LETM	—— ——

FIG. 18. CONDITIONS FOR DRIVING MODES BY TETM & LETM.

to say, of mechanical current. The same thing is, of course, to be seen from (3.4) as well. Therefore the transmission lines may be opened at this point. The two lines, each now of length h, belonging to mode (i), are then in parallel and may be replaced by one line of twice the characteristic admittance.

There thus results three lines on a bisected basis. In the resulting figure, Fig. 19, one has a circuit very much like that of Fig. 11, save for the absence of the negative capacitor, the replacement of Co by $\underline{Co}$ and the substitution of (4.32) for (3.17) in the turns ratios.

The establishment of the seven-port electromechanical admittance matrix will concern us next.

C. The LETM Plate Electromechanical Admittance Matrix.

We shall now continue in the fashion of Chapter III to establish the seven-port immittance matrix appropriate to the LETM problem. It will turn out that LETM and TETM are very nearly duals of one another, and that, just as the negative capacitor found to be present in the TETM case made it advantageous to work with the impedance matrix then, it will prove to our advantage to use the admittance formulation now.

It will be recalled that evaluation of the impedance matrix elements involved placing open circuits at all ports, and this had the result, in the TETM situation, that when port (7°) was opened, the negative capacitance, added to the positive, produced a short across the piezo-transformers which decoupled the transmission lines. This rendered the impedances easy to determine, whereas the admittance matrix elements, which involve short circuits at

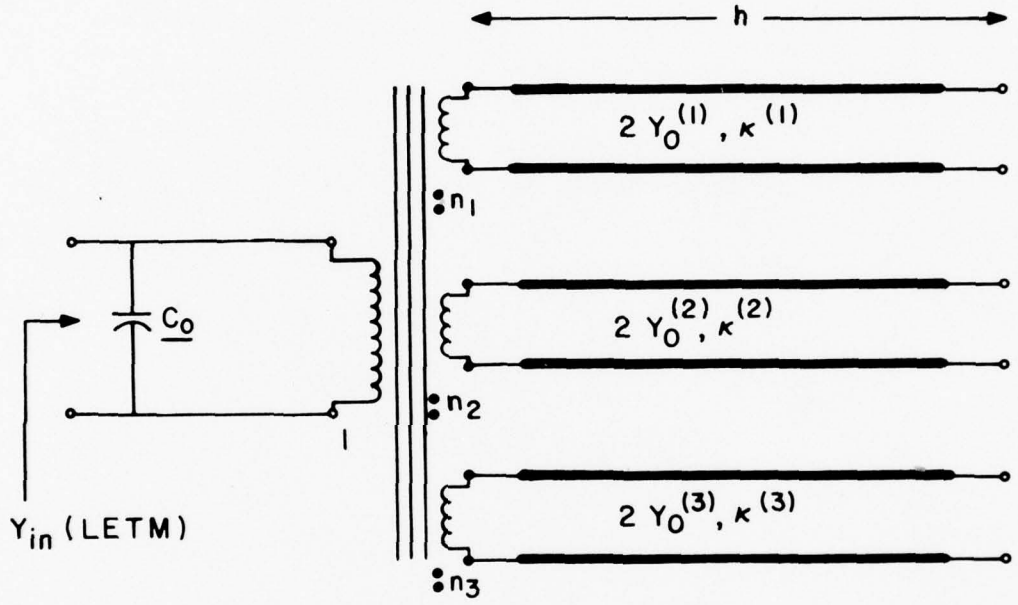

FIG. 19. EXACT EQUIVALENT NETWORK FOR TRACTION - FREE PLATE, LETM. BISECTED BASIS.

all ports, would have had the effect of placing the negative Co across the transformers, and the transmission lines would have remained coupled.

In the present instance, where the negative capacitance is absent, a short at port (7^{O}) reflects directly upon the transformers to produce the desired decoupling. Hence, we use the admittance formulation to express the LETM results.

This time we will start with the plate equations, after which the network realization will be obtained.

1. We again choose, for our definitions of port voltages and currents, equations (3.35)-(3.40). By definition, the admittance element $y^{O}_{\pi\xi}$ is obtained from

$$y^{\circ}_{\pi\xi} = I^{\circ}_{\pi} / V^{\circ}_{\xi} , \tag{4.42}$$

with all voltages equal to zero but V^{O}_{ξ} . This means physically that the plate will be completely traction-free when y^{O}_{77} is determined and have only one component of transformed stress applied, and that to only one side when the other admittance elements are determined.

Thus the conditions required to obtain y°_{77} we have already met when the traction-free plate was analyzed in Section IVA, and y^{O}_{77} is recognized as being equal to Y_{in} (LETM), which is given in (4.30). It remains for us to obtain the components of self and mutual mechanical admittance, and mutual electromechanical admittance.

The same argument that led to chosing (3.45) is applicable here, except, as we wish to force with a single non-zero voltage, rather than with a current, we take instead

$$T^{\circ}_{3i} = G_i \sin \alpha^{(i)}(h \pm x_3) . \tag{4.43}$$

When the self and mutual mechanical admittances are to be determined, the electrical port must be shorted. This leads to setting E_1 equal to zero in (4.16), which then reads

$$T_{3i}^{\circ} = c^{(i)} u_{i,3}^{\circ} \quad . \tag{4.44}$$

With the assumed form of T_{3i}° in (4.43), the transformed displacements become

$$u_i^{\circ} = \frac{\mp G_i \cos \chi^{(i)} (h \pm \chi_3)}{c^{(i)} \chi^{(i)}} \quad , \tag{4.45}$$

the constant of integration, amounting to a rigid body translation, is discarded because it does not satisfy (2.39).

From our choices of voltage and current variables and our definition (4.42), we can use (4.43) and (4.45) to obtain the self and mutual mechanical terms.

Straightforward calculation for i = 1 gives

$$V_1^{\circ} = A G_1 \sin \theta_1 \, , \tag{4.46}$$

$$I_1^{\circ} = -j\omega G_1 \cos \theta_1 / (c^{(1)} \chi^{(1)}) \, , \tag{4.47}$$

so that

$$y_{11}^{\circ} = \frac{Y_o^{(1)}}{j \tan \theta_1} \, , \tag{4.48}$$

with the usual definitions. The same arguments we used in the TETM case now can be used to arrive at

$$y_{11}^{o} = y_{44}^{o} = \frac{Y_o^{(1)}}{j \tan \theta_1}, \tag{4.49}$$

$$y_{22}^{o} = y_{55}^{o} = \frac{Y_o^{(2)}}{j \tan \theta_2}, \tag{4.50}$$

and

$$y_{33}^{o} = y_{66}^{o} = \frac{Y_o^{(3)}}{j \tan \theta_3}, \tag{4.51}$$

which completes the determination of the main diagonal terms.

2. From (4.44) we see that only mechanical off-diagonal matrix elements determined by the same mode index number (i) are non-zero, which means that, according to (3.35), (3.36) and (3.38), (3.39), those whose port numbers differ by three.

For example, with (4.46) for V_1^o, only I_4^o is finite (apart from I_1^o, obviously; but this leads to the main diagonal term y_{11}^o). For I_4^o we obtain,

$$I_4^{o} = +j\omega G_1 / (c^{(1)} x^{(1)}), \tag{4.52}$$

leading to

$$y_{41}^{o} = \frac{Y_o^{(1)}}{-j \sin \theta_1}. \tag{4.53}$$

Again we use the TETM arguments, about permuting modal index numbers, etc., to deduce

$$y^{\circ}_{14} = y^{\circ}_{41} = \frac{Y_o^{(1)}}{-j \sin \theta_1}, \tag{4.54}$$

$$y^{\circ}_{25} = y^{\circ}_{52} = \frac{Y_o^{(2)}}{-j \sin \theta_2}, \tag{4.55}$$

and

$$y^{\circ}_{36} = y^{\circ}_{63} = \frac{Y_o^{(3)}}{-j \sin \theta_3}. \tag{4.56}$$

Similarly we find that components with the following indices are zero: 12,13,15,16,23,24,26,34,35,45,46 and 56, plus, of course, those on the other side of the diagonal, with the digits in reversed order. This follows from (4.44), as we remarked in the discussion between (4.51) and(4.52).

One set of elements remains to be determined, the electromechanical mutual terms. These are found by application of V_7° and measuring the I_{ξ}° (ξ = 1 to 6). Now we take all T_{3i}° to be zero at the surfaces of the plate, a condition which we encountered in Section A, above. In fact, we can borrow those results, because we know that an applied field E_1 produces the displacements u_i° given by (4.21). We said, in the discussion after (4.27), that E_1 could be looked upon as arising from a potential difference $(-E_1(2\ell))$. If this is our V_7°, appropriate to a portion of the plate of length 2ℓ along x_1, then, by the use of (4.21), (4.23) and (4.32), along with (3.38), (3.39), we can determine $y^{\circ}_{\pi 7}$.

After a simple calculation, and applying our usual methods of

symmetry, etc., we obtain

$$y^{\circ}_{17} = y^{\circ}_{71} = y^{\circ}_{47} = y^{\circ}_{74} = \frac{n_1 \, Y_o^{(1)}}{j \cot(\theta_1/2)}, \tag{4.57}$$

$$y^{\circ}_{27} = y^{\circ}_{72} = y^{\circ}_{57} = y^{\circ}_{75} = \frac{n_2 \, Y_o^{(2)}}{j \cot(\theta_2/2)}, \tag{4.58}$$

and

$$y^{\circ}_{37} = y^{\circ}_{73} = y^{\circ}_{67} = y^{\circ}_{76} = \frac{n_3 \, Y_o^{(3)}}{j \cot(\theta_3/2)}. \tag{4.59}$$

This completes the determination of the admittance matrix, which is written out fully on the next page, the element y°_{77} being given by (4.30).

$$
[y^{o}] = \begin{bmatrix}
\frac{Y_0^{(1)}}{j\tan\theta_1} & 0 & 0 & \frac{Y_0^{(1)}}{-j\sin\theta_1} & 0 & 0 & \frac{n_1 Y_0^{(1)}}{j\cot(\theta_1/2)} \\
0 & \frac{Y_0^{(2)}}{j\tan\theta_2} & 0 & 0 & \frac{Y_0^{(2)}}{-j\sin\theta_2} & 0 & \frac{n_2 Y_0^{(2)}}{j\cot(\theta_2/2)} \\
0 & 0 & \frac{Y_0^{(3)}}{j\tan\theta_3} & 0 & 0 & \frac{Y_0^{(3)}}{-j\sin\theta_3} & \frac{n_3 Y_0^{(3)}}{j\cot(\theta_3/2)} \\
\frac{Y_0^{(1)}}{-j\sin\theta_1} & 0 & 0 & \frac{Y_0^{(1)}}{j\tan\theta_1} & 0 & 0 & \frac{n_1 Y_0^{(1)}}{j\cot(\theta_1/2)} \\
0 & \frac{Y_0^{(2)}}{-j\sin\theta_2} & 0 & 0 & \frac{Y_0^{(2)}}{j\tan\theta_2} & 0 & \frac{n_2 Y_0^{(2)}}{j\cot(\theta_2/2)} \\
0 & 0 & \frac{Y_0^{(3)}}{-j\sin\theta_3} & 0 & 0 & \frac{Y_0^{(3)}}{j\tan\theta_3} & \frac{n_3 Y_0^{(3)}}{j\cot(\theta_3/2)} \\
\frac{n_1 Y_0^{(1)}}{j\cot(\theta_1/2)} & \frac{n_2 Y_0^{(2)}}{j\cot(\theta_2/2)} & \frac{n_3 Y_0^{(3)}}{j\cot(\theta_3/2)} & \frac{n_1 Y_0^{(1)}}{j\cot(\theta_1/2)} & \frac{n_2 Y_0^{(2)}}{j\cot(\theta_2/2)} & \frac{n_3 Y_0^{(3)}}{j\cot(\theta_3/2)} & y^{o}_{77}
\end{bmatrix}
$$

D. The Electromechanical Network Admittance Matrix.

Having obtained the admittance matrix from the mathematical statement of the physical problem, we wish here to synthesize a transmission-line network that realizes this same matrix exactly, and, further, one that can be shown to be a true analog of the vibrating plate, in the normal coordinate system. The results of the next chapter will then provide the necessary additional circuitry to complete the development of true analogs for a single plate, and, at the same time, lead naturally, in Chapter VI, to generalizations of our results wherein any number of layers may be accommodated by our representations.

1. We may shorten the procedure of finding an appropriate network by considering our past results, particularly Fig. 13 and Fig. 17. Taken together, they strongly suggest that a circuit identical to that of Fig. 13, but lacking the negative capacitor, will meet the necessary conditions. And so, we consider, provisionally, the network of Fig. 20, which has those characteristics we have repeatedly stressed: three modal transmission lines and boundary-forcing, piezoelectric transformers.

One might go to more elaborate lengths to show why the admittance matrix leads to this figure, but it will save space to turn the process around, and simply analyze the conjectured configuration shown.

To this end, we replace each transmission line by its equivalent lumped circuit; shown in Fig. 21, this has been taken in the pi form, which is proper to an admittance determination. The complete seven-port, lumped, network is given in Fig. 22. The port voltage and current conventions are identical with those of Fig. 15. Element

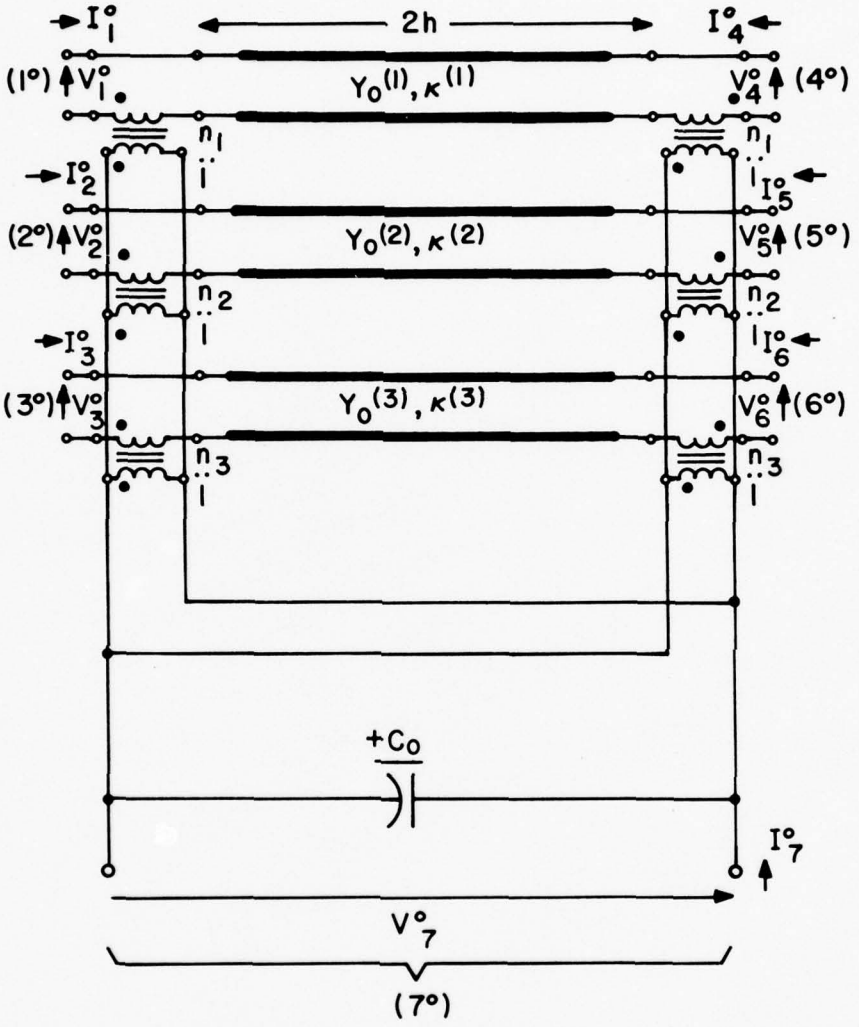

FIG. 20. SEVEN-PORT, NORMAL-MODE, LETM EQUIVALENT CIRCUIT, WITHOUT MECHANICAL BOUNDARY NETWORK AND LOADS.

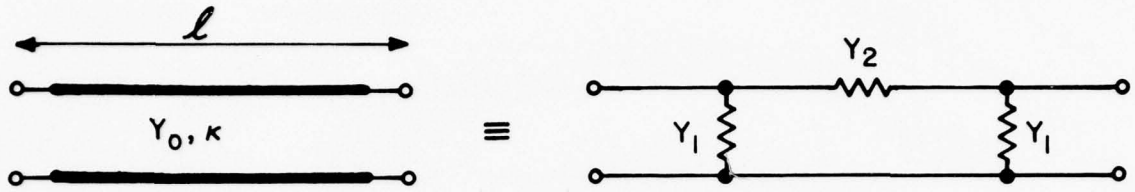

$$Y_1 = \frac{Y_0}{j \sin\theta} (\cos\theta - 1) = j\, Y_0 \tan(\theta/2)$$

$$Y_2 = \frac{Y_0}{j \sin\theta} \quad ; \quad \theta = \kappa\ell$$

FIG. 21. LUMPED, PI, FORM OF A TRANSMISSION - LINE SECTION

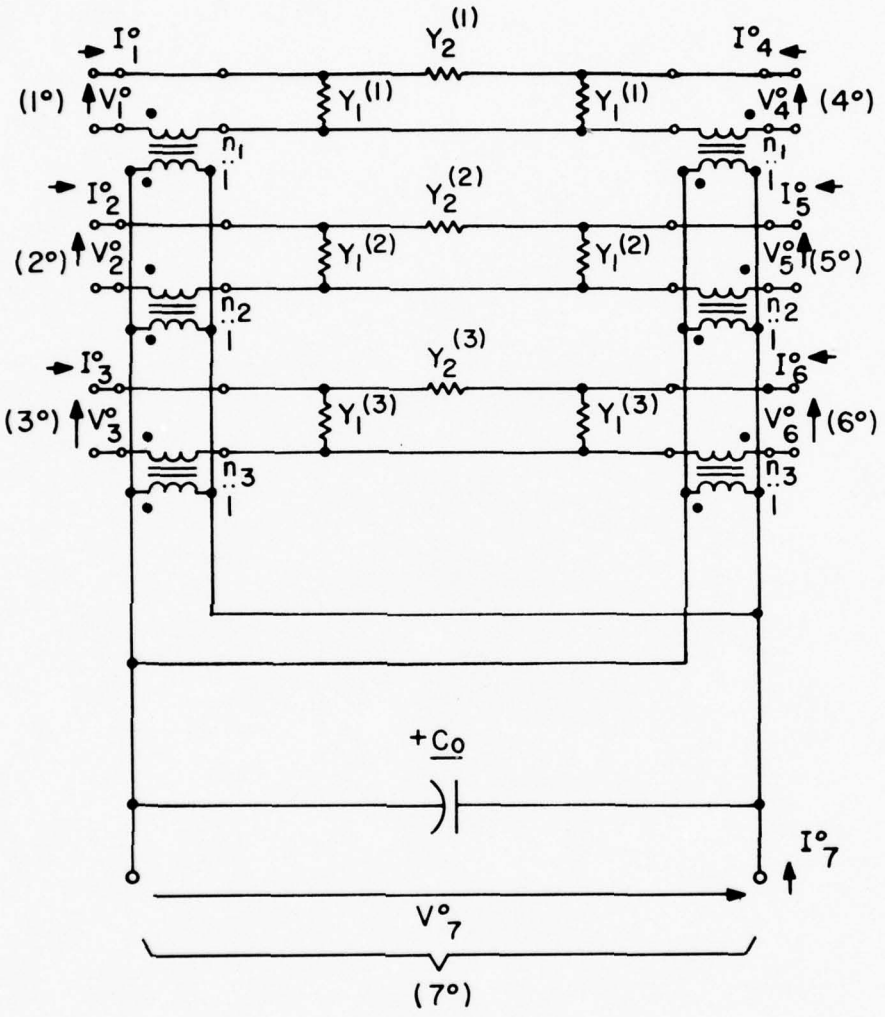

FIG. 22. LUMPED CIRCUIT FOR EVALUATING LETM ELECTROMECHANICAL ADMITTANCE MATRIX.

values for the members of the pi circuits are to be taken from Fig. 21, with the necessary sub- or superscripts, relating to the mode number, added.

What remains of our task is simplified, as it was in Section C, by the decoupling effect of the short circuit applied to port (7°). Using elementary circuit analysis, and the inherent symmetries present, we may write down the elements almost by inspection. They are:

$$y_{11}^{\circ} = y_{44}^{\circ} = Y_1^{(1)} + Y_2^{(1)} = \frac{Y_o^{(1)}}{j \tan \theta_1}, \tag{4.60}$$

$$y_{22}^{\circ} = y_{55}^{\circ} = Y_1^{(2)} + Y_2^{(2)} = \frac{Y_o^{(2)}}{j \tan \theta_2}, \tag{4.61}$$

$$y_{33}^{\circ} = y_{66}^{\circ} = Y_1^{(3)} + Y_2^{(3)} = \frac{Y_o^{(3)}}{j \tan \theta_3}. \tag{4.62}$$

To find the term y_{77}°, from the circuit given, it is easiest to resort to a bisection, as was done to obtain Fig. 19. The situation is the same, because ports (1°) to (6°) are now shorted, as in the former case. As no current flows through the three series arms, denoted as $Y_2^{(i)}$ in the figure, because of symmetry, they are bisected with an open circuit, and the result is three pairs of admittances in parallel, that are seen on the primary sides of the transformers as a total admittance of value

$$2 \cdot \sum_{i=1}^{3} n_i^2 \, Y_1^{(i)} \, . \tag{4.63}$$

When the admittance of Co is added to this, and we use, from Fig. 21,

$$Y_1^{(i)} = j \, Y_o^{(i)} \tan(\theta_i/2), \tag{4.64}$$

we get

$$y_{77}^{o} = j\omega C_o + j2 \sum_{i=1}^{3} n_i^2 \, Y_o^{(i)} \tan(\theta_i/2). \tag{4.65}$$

By using the definitions of Co, $n_i Yo^{(i)}$ and θ_i, this may be put into the form (4.30), the required result.

The finite mechanical mutual terms are simply the negative of the series arm of the proper pi, so that we have

$$y_{14}^{o} = y_{41}^{o} = -Y_2^{(1)} = \frac{Y_o^{(1)}}{-j \sin\theta_1}, \tag{4.66}$$

$$y_{25}^{o} = y_{52}^{o} = -Y_2^{(2)} = \frac{Y_o^{(2)}}{-j \sin\theta_2}, \tag{4.67}$$

$$y_{36}^{o} = y_{63}^{o} = -Y_2^{(3)} = \frac{Y_o^{(3)}}{-j \sin\theta_3}, \tag{4.68}$$

while it is seen, by inspection, that the terms subscripted 12,13,15, 16,23,24,26,34,35,45,46, and 56, are zero, as are the corresponding terms below the diagonal.

The remaining category is that of the electromechanical mutual terms; these are found by forcing with V_7^o . Symmetry was used to get y_{77}^o , and it is useful here also. We use the same bisection as previously, but reason that the full voltage appears across each transformer, so that secondary voltages of $n_i V_7^o$ serve as the sources in each of six simple loops, each consisting only of $Y_1^{(i)}$, producing currents of $n_i Y_1^{(i)}$, circulating, in every case, in the direction counter to the particular port current I_ξ^o ; thus the admittance elements are equal to

$$-n_i Y_1^{(i)} = \frac{n_i Y_o^{(i)}}{j \cot(\theta_i/2)} . \tag{4.69}$$

In particular

$$y_{17}^o = y_{47}^o = \frac{n_1 Y_o^{(1)}}{j \cot(\theta_1/2)} , \tag{4.70}$$

$$y_{27}^o = y_{57}^o = \frac{n_2 Y_o^{(2)}}{j \cot(\theta_2/2)} , \tag{4.71}$$

$$y_{37}^o = y_{67}^o = \frac{n_3 Y_o^{(3)}}{j \cot(\theta_3/2)} , \tag{4.72}$$

which, with the symmetry $y_{\pi\xi}^o = y_{\xi\pi}^o$ completes the evaluation. We see the results are in accordance with what we obtained from the equations of the plate, so the network of Fig. 20 represents the physics of the problem, insofar as may be seen from the seven ports (π^o).

2. That the network of Fig. 20 actually does more than represent the physical situation at the seven ports may be shown by following the

argument as we gave it in Section III E. The stresses are given by (4.16) instead of (2.38), with $-\overset{\circ}{e}_{13i} E_1$ suffering a discontinuity at the surface instead of $\overset{\circ}{e}_{33i} a_3$, but the conclusion remains unaltered: the placing of the piezo-transformers at the boundaries has this definite significance, as explained. The discussion regarding the identification of the transmission line variables with the plate mechanical voltages and currents is likewise unchanged, and therefore, quite simply, we have established that Fig. 20 is a true analog of the physical problem of the LETM-driven crystal plate, up to the boundaries.

A consideration of the situation at the boundaries is the subject for discussion in the next chapter. There we will obtain additional circuitry to place at the normal coordinate ports (π°) to complete the physical and network pictures.

V. Complete Representations of a Plate with Arbitrary Loads

Chapters III and IV have revealed that the thickness modes of vibration of arbitrarily anisotropic plates may be represented by networks that are true analogs; these represent exactly the physical state of affairs as a function of the thickness coordinate. Because the problems have been transformed to normal coordinates, and the networks described in these terms, one is left at the bounding surfaces of the plate with port variables in the transformed system.

In this chapter we provide the additional circuitry necessary to complete the conversion to port variables which exactly correspond to the actual quantities entering the physical boundary conditions, namely, the true stress and displacement (or velocity) components, and we also find the overall immittance matrices for the complete networks thus formed.

When the seven-port networks have been completed in this way, the analogs will also be complete and exact in every respect, and the networks can substitute for the electromechanical plates in any and all circumstances.

A. Mechanical Boundary Network

1. In most of the calculations of this chapter it will suit our purposes to use matrix notation, along with, or in place of, tensor notation. Our attention will be largely confined to the physical and electrical port quantities in the transformed and untransformed systems, and to the modal matrix.

As we have done previously, the degree sign is used to denote a

transformed variable or coefficient. The quantities T_{3_j} , $T^{\circ}_{3_j}$, u_j , u°_j , v_j and v°_j are taken as three-by-one column matrices, and written T, T° , u, u°, v and v°, respectively. Similarly, the V_{π} , V°_{π} , I_{π} and I°_{π} are taken as seven-by-one column matrices, respectively written V, V°, I and I°.

The modal matrix $\beta^{(j)}_i$ is written β ; a transpose is indicated by a subscript t, thus, $\beta^{(j)}_i$ is β_t .

According to these definitions, and (3.35)-(3.40), we can write

$$V^{\circ}_t = \left[A T^{\circ}_t(-h) \,\vdots\, A T^{\circ}_t(+h) \,\vdots\, V^{\circ}_7 \right] , \tag{5.1}$$

and

$$I^{\circ}_t = \left[-\upsilon_t(-h) \,\vdots\, +\upsilon_t(+h) \,\vdots\, I^{\circ}_7 \right] . \tag{5.2}$$

For the work of this section we require a relation between the mechanical port voltages and the currents appearing on a single side of the plate. That is, we wish to pair the matrices $AT^{\circ}(-h)$ and $-v^{\circ}(-h)$, and also $AT^{\circ}(+h)$ and $+v^{\circ}(+h)$.

It will make the notation simpler, and, incidentally, prevent v from being confused with a voltage, to introduce the abbreviations

$$A T^{\circ}(-h) = L^{\circ} , \tag{5.3}$$

$$A T^{\circ}(+h) = M^{\circ} , \tag{5.4}$$

$$-\upsilon^{\circ}(-h) = J^{\circ} , \tag{5.5}$$

and

$$+\upsilon^{\circ}(+h) = K^{\circ} , \tag{5.6}$$

and similarly for the corresponding untransformed matrices.

Our immediate object is now to see how these quantities are interrelated, and to implement the relations by a network. From (2.27), (2.28), (2.30) and (2.31) there follow

$$L = \beta L^{\circ} \quad , \tag{5.7}$$

$$M = \beta M^{\circ} \quad , \tag{5.8}$$

$$J = \beta J^{\circ} \quad , \tag{5.9}$$

and

$$K = \beta K^{\circ} \quad . \tag{5.10}$$

At the surface $x = -h$, the physical boundary conditions which have to be met are those of continuity of each stress and velocity (or displacement) component. This requires the specification of the quantities L and J, the three mechanical port voltages and currents, respectively. Similarly, at the upper surface $x = +h$, continuity of M and K are demanded.

We require one network at each surface, that converts our mechanical port variables from L° and J° to L and J, and from M° and K° to M and K. From Section II A, the matrix β relating the transformed and untransformed variables, is orthogonal, that is,

$$\beta_t = \beta^{-1} \quad . \tag{5.11}$$

A multi-winding, ideal transformer interconnection which realizes this transformation, which is discussed by Carlin & Giordano (218), is shown in Fig. 23, for the case of a three by three array, as is the case for β. The figure may be reversed, with the primaries labeled with the superscripted variables, upon interchanging sub- and super-scripts on the components of β, i.e., by substituting the corresponding components of β_t, for the transformer turns ratios. This ability will lead

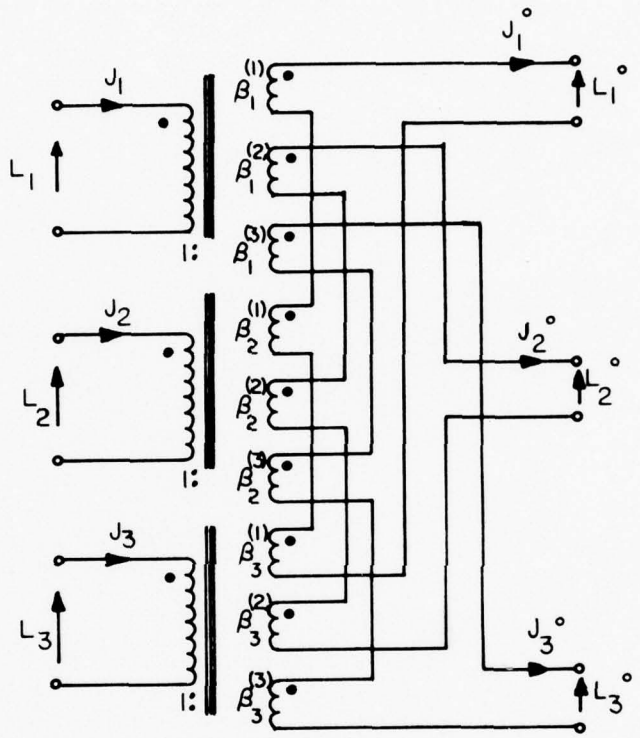

$$J = \beta J^{\circ}$$

$$L^{\circ} = \beta_t L$$

FIG. 23 IDEAL TRANSFORMER REALIZATION OF AN ORTHOGONAL TRANSFORMATION: THE MECHANICAL INTERFACE NETWORK.

to simplifications when two strata are connected mechanically together, as is done in Chapter VI.

When mechanical interface networks of the type given in Fig. 23 are attached to the ports (π°), $(\pi^{\circ})=(1^{\circ},2^{\circ},3^{\circ})$ and $(4^{\circ},5^{\circ},6^{\circ})$, the quantities which then appear at the new ports (π) are those required by the plate boundary conditions. We show, in Fig. 24, the complete TETM network for a single plate. The electrical port does not require a transformation, and is labeled (7) for notational consistency. From Fig. 24, the LETM network follows upon shorting the negative capacitors, replacing C_o by $\underline{C_o}$, and using (4.32), instead of (3.17) for the turns ratios. The orientation of $\underline{Co}$ must also be changed so that the normal to the electrodes points along x_1 .

2. At first sight the network of Fig. 24 appears somewhat intricate, but upon closer examination, one may see that the individual features are all separated from one another, and the entire structure is built up by the simple addition of all the parts. We shall see, in the next chapter, how practical boundary conditions very often lead to considerable simplifications of this network. Taking it as a whole, now, we see that the three plane acoustic waves in the piezoelectric crystal are accounted for by the three transmission lines. The applied electric field, which is imposed by a potential at port (7), appears in the shunt capacitance C_o . These are the only features that we attribute to the bulk of the crystal; what remains is described in terms of interfacial networks of two types. The first is due to the piezoelectric effect. This effect is expressed in our circuits by the presence of piezo-transformers, located only at the two boundaries, and connected into each of the three transmission lines in a simple manner. The

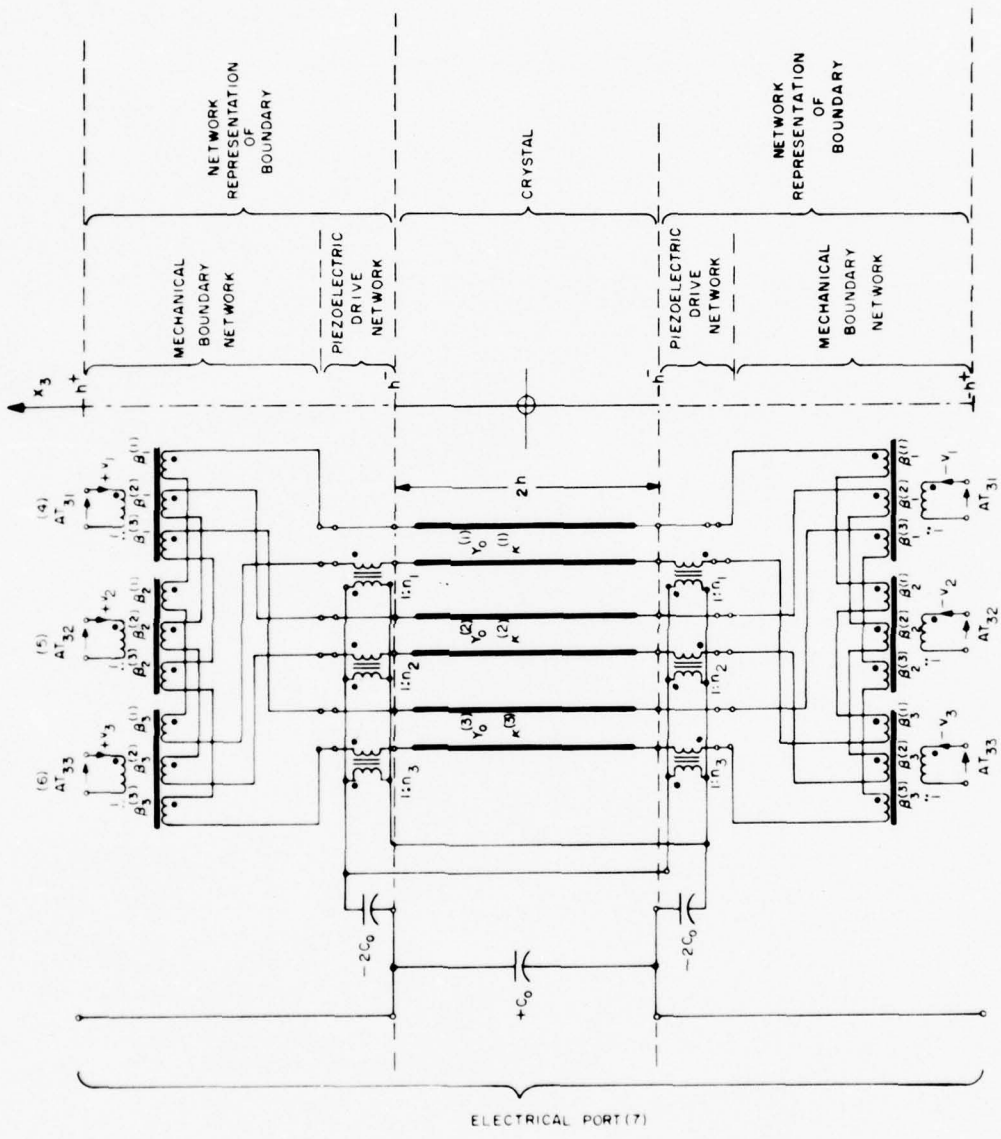

FIG. 24 EXACT ANALOG REPRESENTATION OF TETM PLATE, FOR ARBITRARY BOUNDARY CONDITIONS

manner of connection is this: from the electrical input network (shunt $\underline{C_o}$ for LETM, shunt C_o and series $-C_o$ for TETM) the six transformer primaries are in parallel. The six secondaries are simply placed in series with the ends of the three modal transmission lines, with dots in accordance with the polar nature of the excitation.

The third component is the mechanical boundary network, which also consists only of ideal transformers. Two such are required, one for each plate surface. As drawn in the figure, (which could be turned around by transposing the turns ratios), the three ports connecting the mechanical transformer secondaries together lead to the three modal transmission-line ends, where they are placed in series with the piezo-transformers. That the piezo-drive and the mechanical transformers are placed in series at the input to the transmission lines is a consequence, and a very important one, of (2.47), which can be written

$$\tilde{\overline{T}}_{3i}^{\circ} = T_{3i}^{\circ} - \overline{\overline{T}}_{3i}^{\circ} \quad . \tag{5.12}$$

The interpretation attached to this result was given in III E. It amounts to the fact that the mechanical and piezoelectric sources are in series and subtract to produce a resultant that propagates along the appropriate transmission line.

The mechanical transformer circuit itself accomplishes the transformation from the normal coordinate system of the transmission lines to the coordinate system established by the reference axes that describe the crystal orientation. In this way, the stresses and displacements (or velocities) that appear in the normal coordinates, and that are

there compounded of components of the same quantities in the untransformed (reference) coordinates, are reapportioned by the circuit configuration and turns ratios, so that the separate components of the reference system appear at the mechanical ports.

By introducing these boundary networks we have allowed the processes appearing in the interior of the crystal plate to be presented in a very simple and lucid manner, i.e., a single transmission line for each mode, and a simple capacitor to represent the dielectric behavior of the crystal with respect to an applied electric field. The price of such simplicity within the plate is the coordinate-tranformingˢ networks required at each boundary. It is a small price when one considers how explicit each of the interactions is made and how graphically they are reproduced in the topology of the schematic. Each and every detail has been accounted for, and the interplay of the various effects may be traced through the schematic.

Even within the crystal, and it is this key feature that makes the equivalent network also an analog, the values of the physical variables may be ascertained from the circuit, without returning to the elastic equations. All of the contents of the equations with which we started have been built into the circuit representation, that exactly, and truly, mirrors the physical situation, including its distributed nature.

B. The Complete Immittance Matrices.

1. In Chapter III we obtained the impedance matrix for the TETM plate vibrator in the system of normal coordinates. In Chapter IV the admittance matrix for the LETM plate was derived, also in normal coordinates. For both cases, we now obtain from these matrices

the complete immittance matrix with the mechanical ports referred to the laboratory coordinate system. These matrices describe the behavior of the TETM and LETM plates under all circumstances of electrical or mechanical forcing or loading.

Because we treated the two canonical problems separately, it has not been necessary to provide distinctive notation, and so only the symbols z° and y° were used, without special subscripts. We shall treat both together here, but the TETM plate will always be described in impedance terms, and the LETM in admittance terms, so that no confusion should arise.

Using (5.1), (5.3) and (5.4), we have

$$V_t^\circ = \left[L^\circ \mid M^\circ \mid V_7^\circ \right]_t \quad . \tag{5.13}$$

If V_t is defined to be the corresponding matrix when L°, M° and V_7° are replaced with their unsuperscripted counterparts, then we find by means of (5.7) and (5.8) the matrix relating V and V° to be

$$V = B V^\circ \quad , \tag{5.14}$$

with

$$B = \begin{bmatrix} \beta & 0 & 0 \\ 0 & \beta & 0 \\ 0 & 0 & 1 \end{bmatrix} \quad . \tag{5.15}$$

Thus B is a seven-by-seven array, which we have partitioned, as shown, into rows and columns having three, three, and one members, respectively.

When (5.2) is used with (5.5) and (5.6), we have

$$I_t^\circ = \left[J^\circ \mid K^\circ \mid I_7^\circ \right]_t \quad , \tag{5.16}$$

and if I_t is defined to be the corresponding matrix when J°, K° and I_7° are replaced by their unsuperscripted counterparts, we find, by using (5.9) and (5.10) in exactly the same manner as for V, that

$$\mathcal{I} = B\, \mathcal{I}^\circ, \tag{5.17}$$

where B is again given in (5.15).

Now that all our quantities are defined, the actual operations involved in arriving at the overall immittances are easily performed. What we desire is a relationship between the untransformed voltages and currents, i.e., we we wish to find, for the TETM case, the matrix z in the relation

$$V = \mathcal{Z}\, \mathcal{I}. \tag{5.18}$$

We already have z° in the relation

$$V^\circ = \mathcal{Z}^\circ\, \mathcal{I}^\circ, \tag{5.19}$$

which was obtained in III C. First we recognize that, because β is orthogonal, B is also orthogonal (219). Then the following steps follow at once

$$V = B\, V^\circ, \tag{5.14}$$

$$= B\, \mathcal{Z}^\circ\, \mathcal{I}^\circ, \tag{5.20}$$

$$= B\, \mathcal{Z}^\circ (B_t \mathcal{I}), \tag{5.21}$$

$$= \mathcal{Z}\, \mathcal{I}, \tag{5.22}$$

where

$$\mathcal{Z} = B\, \mathcal{Z}^\circ\, B_t, \tag{5.23}$$

$$= B\, \mathcal{Z}^\circ\, B^{-1}. \tag{5.24}$$

It will be seen, because (5.14) and (5.17) are the same relations with one variable written for the other, that an identical series of operations leads to the same result in the LETM case, using y°. Thus we are led to the relations

$$Z = B\, Z^\circ\, B^{-1}, \tag{5.24}$$

for TETM, and

$$y = B\, y^\circ\, B^{-1}, \tag{5.25}$$

for LETM. The overall immittance is related to the normal coordinate immittance by a similarity transformation.

2. By partitioning z and y in exactly the same fashion as we did for B, in (5.15), we may go into more detail in the determination of the elements of the overall matrices. To effect the partition we shall rename the elements of z in the following manner:

$$Z = \begin{bmatrix} Z_1 & Z_6 & Z_5 \\ Z_{6t} & Z_2 & Z_4 \\ Z_{5t} & Z_{4t} & Z_3 \end{bmatrix}, \tag{5.26}$$

with a similar numbering for the partitioned elements of y, z° and y°.

Application of (5.24), using the B and z° matrices in their three-by-three partitioned form then gives

$$Z = \begin{bmatrix} \beta Z_1^\circ \beta_t & \beta Z_6^\circ \beta_t & \beta Z_5^\circ \\ \beta Z_{6t}^\circ \beta_t & \beta Z_2^\circ \beta_t & \beta Z_4^\circ \\ Z_{5t}^\circ \beta_t & Z_{4t}^\circ \beta_t & Z_3^\circ \end{bmatrix}. \tag{5.27}$$

The z° matrix in Section III C. shows us that

$$\mathcal{Z}_1^{\circ} = \mathcal{Z}_2^{\circ} , \tag{5.28}$$

$$\mathcal{Z}_4^{\circ} = \mathcal{Z}_5^{\circ} . \tag{5.29}$$

Furthermore z° is symmetric, so we have only to determine the elements z_1, z_3, z_4 and z_6, since, because of the form of B, if z° is symmetric, z is also symmetric; furthermore, z_1 will equal z_2 and z_4 will equal z_5. By applying the relation, (5.27), we get

$$\mathcal{Z}_1 = \beta \, \mathcal{Z}_1^{\circ} \, \beta_t . \tag{5.30}$$

Hence we obtain for the elements $(z_1)mn$, of the three-by-three matrix z_1, the following

$$(\mathcal{Z}_1)_{mn} = \sum_{p=1}^{3} \frac{\beta_m^{(p)} \, \mathcal{Z}_o^{(p)} \, \beta_n^{(p)}}{j \tan \theta_p} . \tag{5.31}$$

In like fashion, the other quantities to be determined are

$$(\mathcal{Z}_3) = 1/(j\omega C_o) , \tag{5.32}$$

$$(\mathcal{Z}_4)_m = \sum_{p=1}^{3} \frac{\beta_m^{(p)} \, n_p}{j\omega C_o} , \tag{5.33}$$

and

$$(\mathcal{Z}_6)_{mn} = \sum_{p=1}^{3} \frac{\beta_m^{(p)} \, \mathcal{Z}_o^{(p)} \, \beta_n^{(p)}}{j \sin \theta_p} , \tag{5.34}$$

which completes the determination of all elements of the TETM overall impedance matrix.

For the determination of the corresponding quantities in the LETM case, we can start from (5.27) with the substitution of y for z, y^{o} for z^{o}. The difference comes in when the elements for the various submatrices are obtained from the y^{o} matrix, given in Section IV C. Once this is done, and the manipulations carried out, we find

$$(y_1)_{mn} = (y_2)_{mn} = \sum_{p=1}^{3} \frac{\beta_m^{(p)} Y_o^{(p)} \beta_n^{(p)}}{j \tan \theta_p}, \quad (5.35)$$

$$(y_4)_m = (y_5)_m = \sum_{p=1}^{3} \frac{\beta_m^{(p)} n_p Y_o^{(p)}}{j \cot(\theta_p/2)}, \quad (5.36)$$

$$(y_3) = y_{77} = y_{77}^{o} = Y_{in}(LETM), \quad (5.37)$$

and

$$(y_6)_{mn} = \sum_{p=1}^{3} \frac{\beta_m^{(p)} Y_o^{(p)} \beta_n^{(p)}}{-j \sin \theta_p}, \quad (5.38)$$

which completes the determination of all elements of the LETM overall admittance matrix.

We have now completed our treatment of single crystal plate. In this chapter the necessary circuitry was added to the networks already derived to provide a complete and exact analog characterization of both a TETM- and LETM- driven crystal layer, for completely arbitrary mechanical and electrical boundary conditions.

Expressions were obtained, for both canonic forms of excitation, for the overall immittance matrix elements, describing the behavior of the physical system and of the analogous networks.

VI. Multilayer Stacks of Plates

The results we obtained for one plate will now be generalized to encompass a description of the behavior of a stacked assembly of plates. It will be possible to characterize stacks without imposing any restrictions upon the number of layers, their relative thicknesses, type of crystal from layer to layer, or orientation of one with respect to the other. The general result is arrived at from a consideration of a stack of the simplest kind, consisting of only two strata. After the general result is established, we look at a number of special cases of interfacial contact and give their equivalent network representations. A section is devoted to general impedance boundary conditions, after which the chapter concludes with a section devoted to the problem of single-ended and distributed sources of piezoelectric excitation.

A. The Two-Layer Stack.

1. We seek to categorize a simple stack consisting of only two layers of arbitrary thickness. From our discussion it will appear that, once this has been done, the result may be extended, without further difficulty, to a stack consisting of an arbitrary number of strata.

In the multi-plate configuration, we make the same restriction as formerly in that no lateral variations are permitted. This means a limitation to unbounded plates for which our networks describe a section of area A.

Unbounded plates may seem to be an idealization wholly divorced

from practicality, but as may be seen in (72), a lateral extent less than one hundred thicknesses may be considered, for many purposes, to be unbounded; when plates are stacked, the presence of the layering acts additionally to suppress the effects of the lateral boundaries (84). This assumption, then, is not unrealistic, but is actually approached readily in practice.

Before going on to the two-layer stack proper, we deal with one other side issue, and that pertains to the method whereby the individual layers are excited. Our desire is to make the analysis as general as possible, but to indicate how close to practicality are such idealizations as we will make.

If we permit ourselves to use the idealizations of perfect electric and perfect magnetic conductors (198), then it is possible to have contiguousTETM- and LETM-driven plates, or LETM-driven plates without collinear electric fields. In this way we achieve a complete freedon in choosing how any layer is to be excited, and every layer can be treated separately, as regards the electrical port.

This is a useful artifice, and we shall adopt it; but is should also be borne in mind that, while a perfect magnetic conductor may not be realizable, and so one may not physically be able to force the desired boundary conditions in this manner, these same boundary conditions may be closely approximated in practice by other means. For example, a TETM plate may be in juxtaposition to a LETM plate if the latter has "wrap-around" electrodes and is overlaid at the interface by a thin film of high permittivity dielectric. This configuration may be approximated by having a TETM plate, coated with perfect electric

conductors on the two bounding surfaces, mate with a LETM plate similarly coated with perfect magnetic conductors.

We may employ similar means to approximate two LETM plates with the lateral fields not collinear, and/or of unequal strength; the common boundary would be idealized by a perfect magnetic conductor at the interface.

The idealizations we have described are, therefore, not without practical counterpart, so we employ them without a real sacrifice in the applicability of our results.

2. Let us now consider two plates joined together at the common surface. The mechanical boundary conditions to be satisfied are, in general, the continuity of the three stress and three displacement (or velocity) components. This is simply achieved in our analog network of Fig. 24, or the corresponding LETM network, by a direct connection of the three ports (1), (2), & (3) of the top plate to the ports (4), (5) and (6) of the bottom plate. We represent each plate by the analog in Fig. 24, or the corresponding LETM analog, adding suitable identifications to the quantities appearing thereon to distinguish between the two plates.

This connection presupposes that in the physical problem the two crystal plates have been referred to the same coordinate system, of course. In our treatments of a single plate of the LETM variety we have chosen the electric field always to be in the x_1 direction. This choice does not result in any loss of generality in the two layer case, but a certain caution must be exercised, as discussed below.

When both crystals have been referred to the same coordinate system, the connection of three mechanical ports of each, as detailed above, completes this aspect of the problem of joining two plates.

When the crystals have been referred to different x_1, x_2 coordinates, as, for example, when two LETM plates are to be joined with the lateral driving fields not parallel but with each field defining the x_1 axis in its own crystal, then an additional step must be taken. In this case we take one system (say the coordinates of the bottom crystal) as the reference, laboratory, frame. We then convert the mechanical components at each surface of the upper plate into the laboratory coordinate frame by means of a network of the form of Fig. 23, placed at each of the two sets of mechanical ports. As the x_3 axis has always been assumed the thickness coordinate, this component does not have to be transformed, and the network at each surface of the upper crystal degenerates into a direct feed-through for the longitudinal components of stress and displacement, plus a four-port interconnection. The turns ratios of this transformer four-port are given by the matrix specifying a two-dimensional rotation of axes. In any event, this additional network in the form of the circuit of Fig. 23, can be combined with the original into a network again of the same form, but with transformed turns ratios, given by the matrix product of the two transformations.

Notice that we do not have to transform any other part of the network representing the upper layer; these retain the values they have, referred to the coordinates of that layer. This means, also, that we retain for our definition of the electrical port of this

upper stratum, an association with the lateral area, A_L, whose normal then makes an angle with respect to the laboratory frame.

The foregoing considerations resolve the problem of lateral fields at an angle to the laboratory x_1 axis, and preserve the generality of our results without having to go back and reconsider the LETM case for the superposition of two fields, one along x_1 and the other along x_2.

3. Connecting ports (1), (2), (3) of the upper plate to ports (4), (5), (6), respectively, of the lower plate, completely satisfies the mechanical boundary conditions at the interface of contact, for the connection guarantees that the three stress components, referred to the same coordinate system, and the corresponding displacement (or velocity) components, are continuous. The only other condition to be satisfied relates to the electric field. As described above, use of perfect electric and magnetic conductors, as required for the particular type of excitation desired, allows the electrical port (port 7) of each layer, to be considered separately of any neighboring layer. In practice, this means that the electrical connections for each layer in the stack would be established, in general, by separate metallic tabs brought out to the edge of the stack, so that each electrode is externally available for whatever interconnections there are to be made.

Let us consider a number of types of connections that would be expected to occur frequently in practice. One of the simplest types consists of a two-layer stack driven in TETM by a single pair of

electrodes on the outer surfaces of each plate. Here the displacement component D_3 has a common value in both plates; any electric conductor present at the common interface may be removed. Another simple two-layer configuration again consists of TETM plates, but operated as an electrical two-port, with one layer being the input and the other the output, or else one port consisting of the electrode connections, top and bottom, of one plate, and the other port taken as the upper and lower electrodes of the stack. In this situation the stack requires three electrodes, the one at the interface of the two layers actually consists of one electrode from each plate united at the boundary. This internal electrode takes part in the driving scheme and cannot be removed as in the first case.

At the join of two plates, at least one of which is LETM-driven, a thin dielectric layer would be required practically, and flanking this, two metallic electrodes would be brought out from what would be considered a single interface (neglecting the influence of the dielectric layer).

All of these cases may be similarly understood with respect to the equivalent network of Fig. 24 for the TETM plate, and the corresponding LETM circuit. With reference to Fig. 24, the upper terminal in port (7) represents the electrode on the upper surface of the stratum, and carries the total electric current to the crystal. A portion of this is displacement current which flows through Co, while the remainder flows through the interconnections joining the upper and lower sets of piezo-transformers in parallel. The total electric current then flows to the lower terminal of port (7) whence it leaves the crystal. The current flowing through the two interconnections is the piezoelectric polariza-

tion current; the proportions flowing in the two interconnecting wires will not be equal, in general, unless the structure is symmetrically loaded.

If two TETM plates are joined, the union is accounted for electrically, in the circuit schematic, simply by connecting the upper terminal of port (7) of the lower plate to the lower terminal of port (7) of the upper plate. The node at which the connection is made may be left accessible for the external connection of sources or loads if desired, or it may be suppressed, as would be the case of an interface without an electrode.

Similar considerations apply to a two-layer configuration consisting of two LETM layers, or a stack consisting of one TETM and one LETM layer. In all cases, the electrical connections are made via the two terminals comprising port (7) for each layer in a manner which exactly corresponds to the physical situation.

From our discussions of two-layer stack we may conclude that the operations to be carried out on the two networks, one representing each layer, in order to characterize the process of joining the two plates, consist of a) joining together the three mechanical ports and b.) connecting the electrical terminals of port (7), in each network, as called for by the statement of the physical problem. By the nature of the steps taken to form the composite analog network from the networks of the two component layers, it is clear that the building-up of a general n - layer stack simply amounts to a repetition of these same steps for each layer added. The network of each stratum is the complete analog of that stratum, and at each cycle of the build-up the boundary conditions on all layers are accounted for, so a cascade

of such single-layer analog networks yields a composite network which remains a true, and exact analog of the complete n - layered structure.

Examples of multilayer stacks have been discussed in the literature, (73-86), already cited. Cady (220) treats the subject of a composite resonator, but his analysis, as in almost all of the others, is limited to a single mode-type; the necessity of keeping track of all the equations in even this relatively simple case rather obscures the physical picture. By means of the building-block approach applied to our schematic analogs, we retain the content of the mathematics, and gain a method of description which lends itself to physical insight.

The paper by Sittig (80) treats TETM-driven transducers for delay line applications. He shows various types of electrical connections between the different plates: series, parallel, and grouped series-parallel combinations, all of which may be used with our networks. As we are able to accommodate all three modes in our description, the way is now open to expand the capabilities of such stacked devices by making use of the interplay between the various modes that is made so evident by the circuit description. One such application is to the coding of information (82); another relates to filtering. In this latter category, a stack of crystal plates wherein two or three of the modes in each layer are used could result in an integrated crystal filter having an excellent shape factor combined with small size, and increased ruggedness due to its monolithic composition.

B. Specializations of the Mechanical Interfacial Network.

In Section A. it was shown that the electrical port of each layer could be treated separately from the mechanical ports when two layers were brought together to form a simple stack. The contiguous mechanical

ports had, however, to be connected at the interface to satisfy the mechanical boundary conditions.

We wish, in this section, to look at a single interface, in network terms, and to see what simplifications come about in certain limiting cases, that are, very often, important practically. Because of the independence of the electrical port, and the particular way the piezoelectric transformers are attached to the rest of the circuitry, as seen, for example, in Fig. 24, we may accomplish our objectives in this section with the greatest clarity by removing the piezoelectric coupling from our considerations. This is done with the understanding that our results in no way imply this restriction, and with the realization that we may reintroduce the piezo-drive into such schematics as with which we will now deal, simply by placing a piezo-transformer secondary in series with each transmission-line end. With this understanding, we may focus our attention solely upon the mechanical interface portion of the overall network.

1. Figure 24 gives the network for a single plate. When two plates are juxtaposed, continuity of the stress and displacement components, for rigid (welded) contact, requires the mechanical interfacial networks of both plates to be connected as we have described in Section A. This connection is given in Fig. 25. A circulating current flows in each of the three loops formed by the back-to-back attachment of the primaries of the six ports. These currents are equal to the actual particle velocity components v_i . As these six ports become inaccessible after the plates are joined, the three loops may be suppressed, and the interconnections of the six transmission lines incident upon the boundary may be exactly represented by the

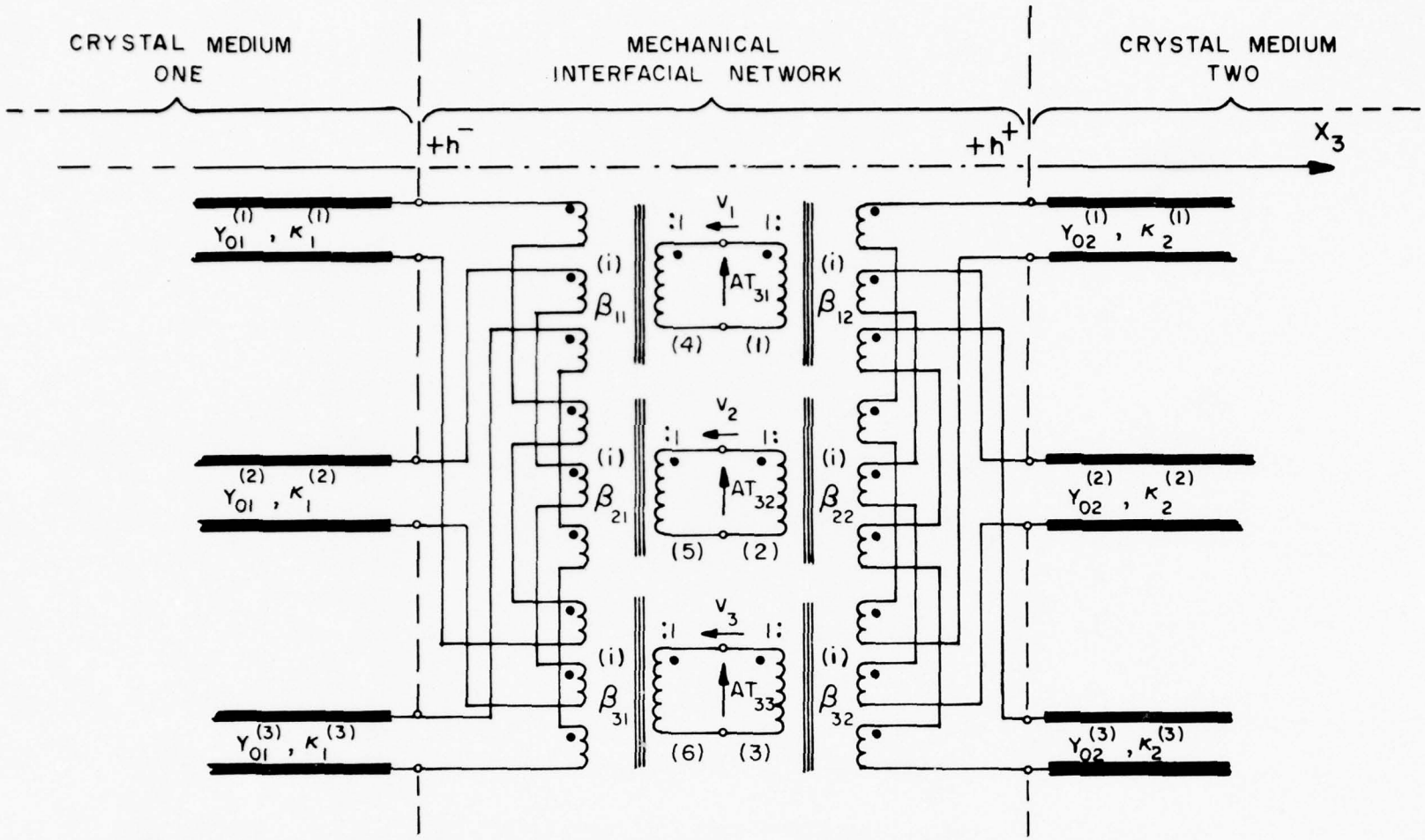

FIG. 25 EXACT ANALOG REPRESENTATION OF MECHANICAL INTERFACIAL COUPLING BETWEEN TWO CRYSTALS HAVING ARBITRARY ANISOTROPY. PLANE WAVE PROPAGATION NORMAL TO BOUNDARY. PIEZOELECTRIC DRIVE OMITTED FOR CLARITY.

diagram shown in Fig. 26.

Figure 26 represents the most involved situation that may occur. Even with the piezoelectric drive circuitry omitted for simplicity, the mechanical conditions require eighteen windings to account for the intricacies of the coupling. One sees that the network structure is completely symmetrical, and that in this general case each transmission line is coupled to every other, so that a disturbance propagating down one line toward the interface will produce, in addition to a reflected wave in that same line, outgoing waves in each of the other five lines. The ratios of the amplitudes will be governed by the transformer turns ratios, which are the components of the modal matrix, in each layer, referred to the same laboratory coordinate system.

Price & Huntington (86) refer to the mechanical coupling which takes place in crystals at an interface, at normal incidence, and treat the case where two modes from each medium are so coupled. We shall give a network later which shows their case schematically, as well as a number of other limiting forms of interest.

2. The network representing welded, (rigid), contact, has been given in Fig. 26. It obeys the boundary conditions requiring T_{3j} and u_j to be continuous at the interface. If we require that only T_{33} and u_3 be continuous, and make T_{31} & T_{32} vanish at the junction, with u_1 & u_2 allowed to develop freely, this corresponds to <u>transverse</u>, or <u>lateral, slip</u> (221). The diagram of Fig. 26 is modified in this instance by first going back to Fig. 25 and shorting the two primary loops across which are developed the voltages AT_{31} & AT_{32}. Doing this has the effect of shorting the secondaries on both sides, so those twelve windings are

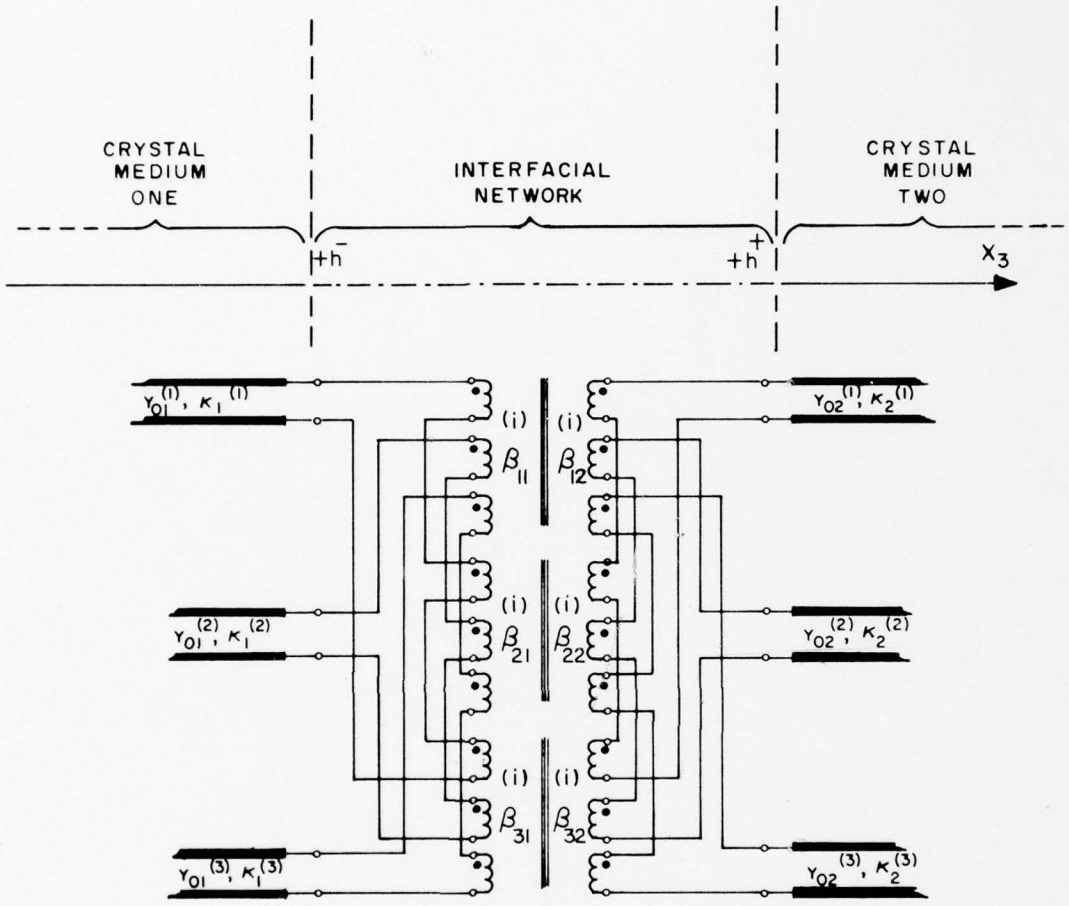

FIG. 26 EXACT REPRESENTATION OF MECHANICAL COUPLING AT THE INTERFACE OF TWO ARBITRARILY ANISOTROPIC MEDIA. PLANE ACOUSTIC WAVE PROPAGATION NORMAL TO BOUNDARY. PIEZOELECTRIC DRIVE TRANSFORMERS OMITTED FOR CLARITY.

replaced by short circuits. After a slight redrawing, the result for transverse slip is shown in Fig. 27. One sees that the six transmission lines are still coupled to one another, although the coupling circuitry assumes a simpler form, with only the connection between ports (3) and (6) remaining.

Two sub-categories of lateral, or transverse, slip of interest are the solid-fluid interface, and the interface between two fluids. We shall give both network descriptions. The solid-fluid interface is important because transducers are often used to operate into fluids, as in sonar, ultrasonic cleaning and level monitoring apparatus. It also describes a loss mechanism which occurs when resonators are operated in imperfectly evacuated enclosures. A fluid is distinguished from a solid, for our purposes, by the fact that it cannot support shear stresses, (nor can it be piezoelectric); only compressional waves are allowed. Therefore the fluid is represented by one transmission line only, while the solid retains the three lines interconnected as shown in either half of Fig. 27. The result, for the solid-fluid configuration is given as Fig. 28. If the density of the fluid tends toward zero, so will the characteristic impedance of the transmission line that represents it, by (2.54); in the limit of zero density, a short appears across the primary of the transformer in Fig. 28, uncoupling the three transmission lines of the solid, each of which becomes shorted. This limit corresponds to the solid-vacuum interface. For the fluid-fluid interface, a single transmission line on each side suffices; the transformer consists of only a two-winding unit with one-to-one turns ratios, so it can be replaced by a direct connection, as has been done in Fig. 29, (cf. (118)).

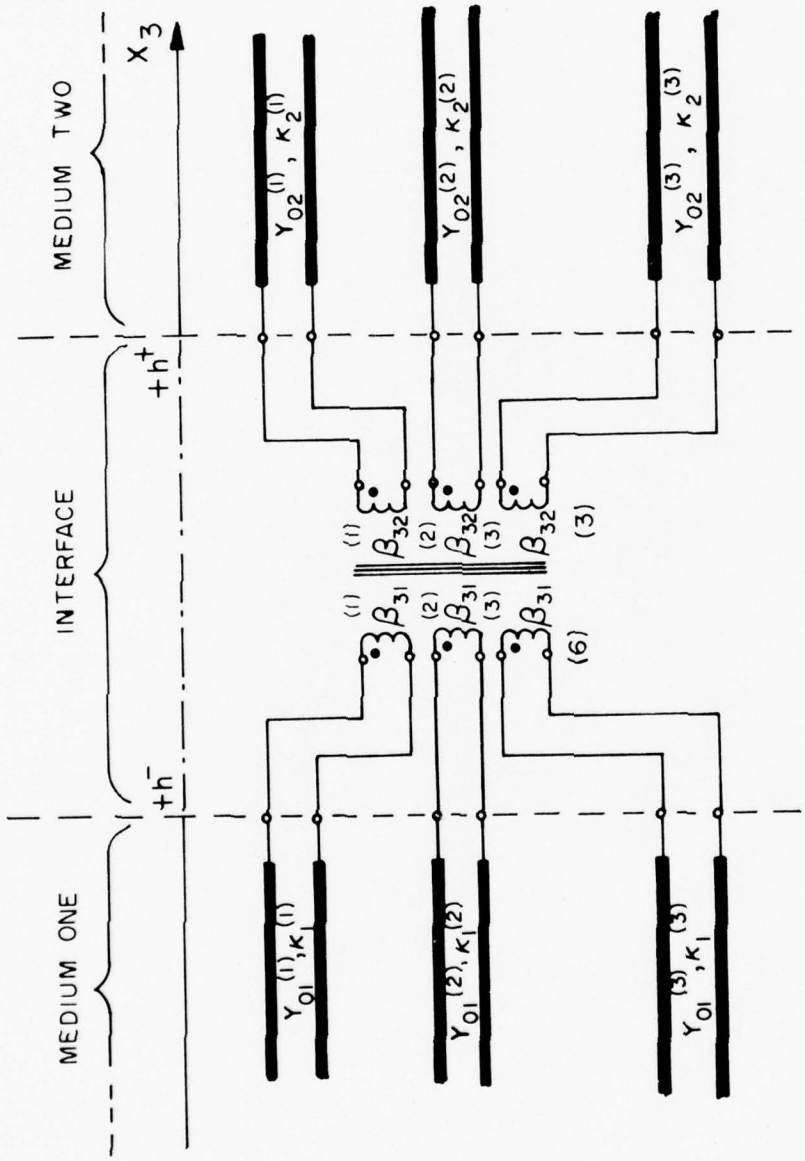

FIG. 27 EXACT ANALOG REPRESENTATION OF MECHANICAL INTERFACIAL COUPLING, FOR CONDITIONS OF TRANSVERSE SLIP.

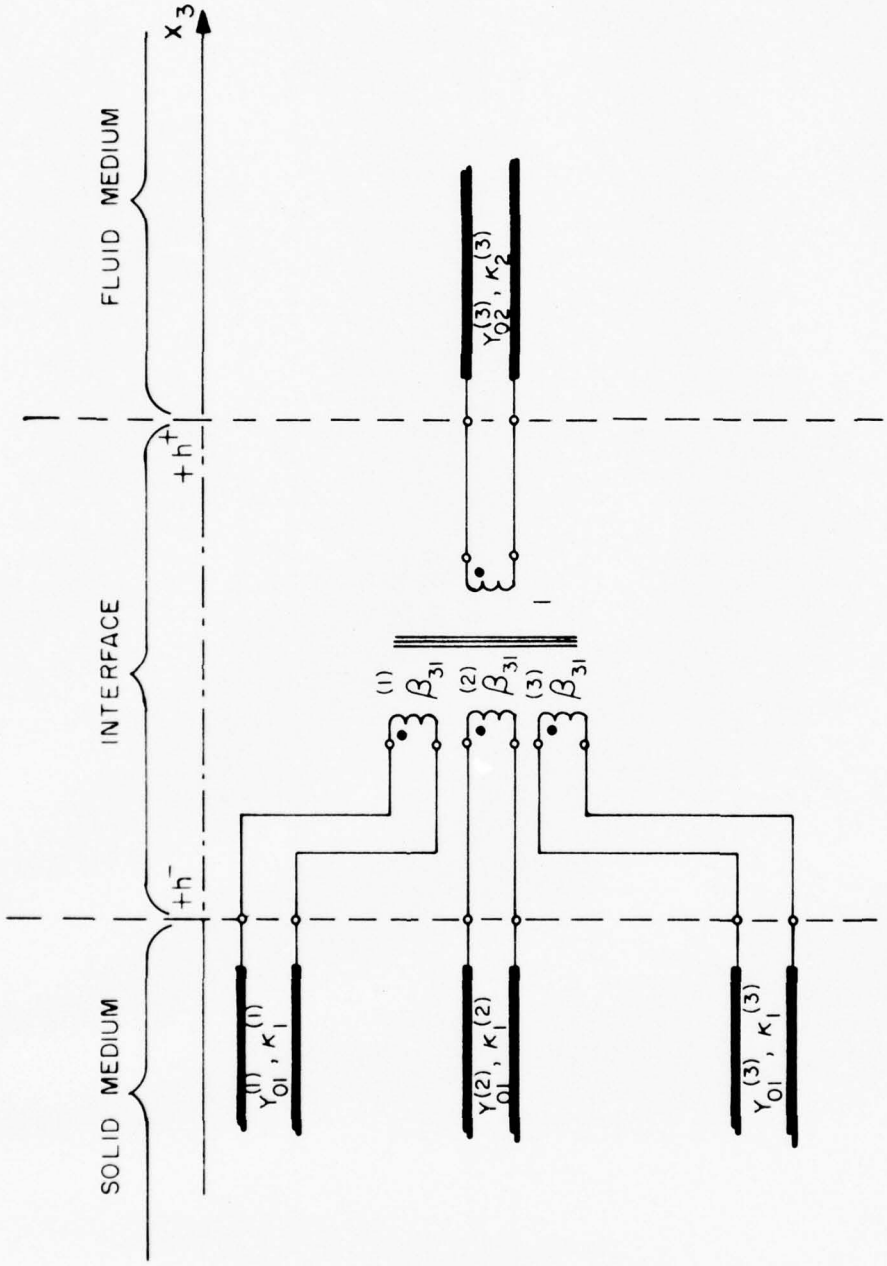

FIG. 28 EXACT ANALOG REPRESENTATION OF MECHANICAL INTERFACIAL COUPLING AT A SOLID-FLUID BOUNDARY.

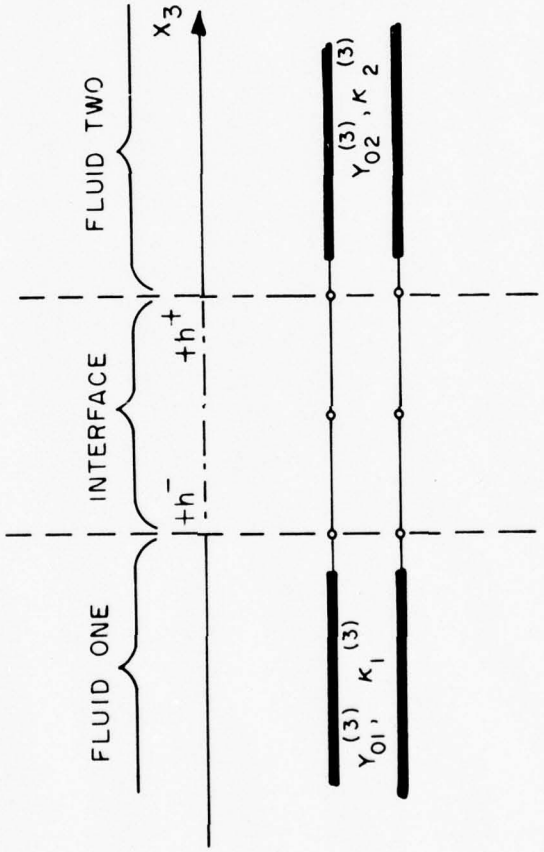

FIG. 29 EXACT ANALOG REPRESENTATION OF THE INTERFACE BETWEEN TWO FLUIDS.

3. Boundary conditions requiring T_{33} to vanish, and the continuity of the components T_{31}, T_{32}, u_1 and u_2 lead to the compressional slip interface (221). This is a generalization of the locally reacting surface condition of Brekhovskikh (222). Here the vanishing of the T_{33} stress component shorts the interconnections between ports (3) and (6), but two interconnections remain. Figure 30 gives a schematic of the boundary representation, that follows from Fig. 26 in the same way that the circuit of Fig. 27 was derived.

4. A different variety of boundary condition is that of blockage (221), where one or more components of displacement is/are zero. We give in Fig. 31 the equivalent circuit for transverse or lateral blockage, where T_{33} and u_3 are continuous, while u_1 and u_2 are zero. Longitudinal blockage, requiring continuity of T_{31}, T_{32}, u_1 and u_2, and the vanishing of u_3, is represented in Fig. 32.

When all displacements are forced to be zero, then it follows from (5.9) and (5.10) that, since J and K vanish, so do J° and K°. Hence, all six transmission lines incident upon the interface are open circuited. They are mechanically uncoupled, and, because of the open circuits, cannot be driven piezoelectrically: the crystals are completely clamped, and can only be excited by an internally applied mechanical force, which would appear as a voltage source on the transmission lines.

5. The foregoing situations arise from the particular boundary conditions stipulated at the interface between the media that are joined. Other particularizations of the general network of Fig. 26 come about because of the form taken by the modal matrix β in each medium. We take two cases to exemplify this. The first, shown in Fig. 33,

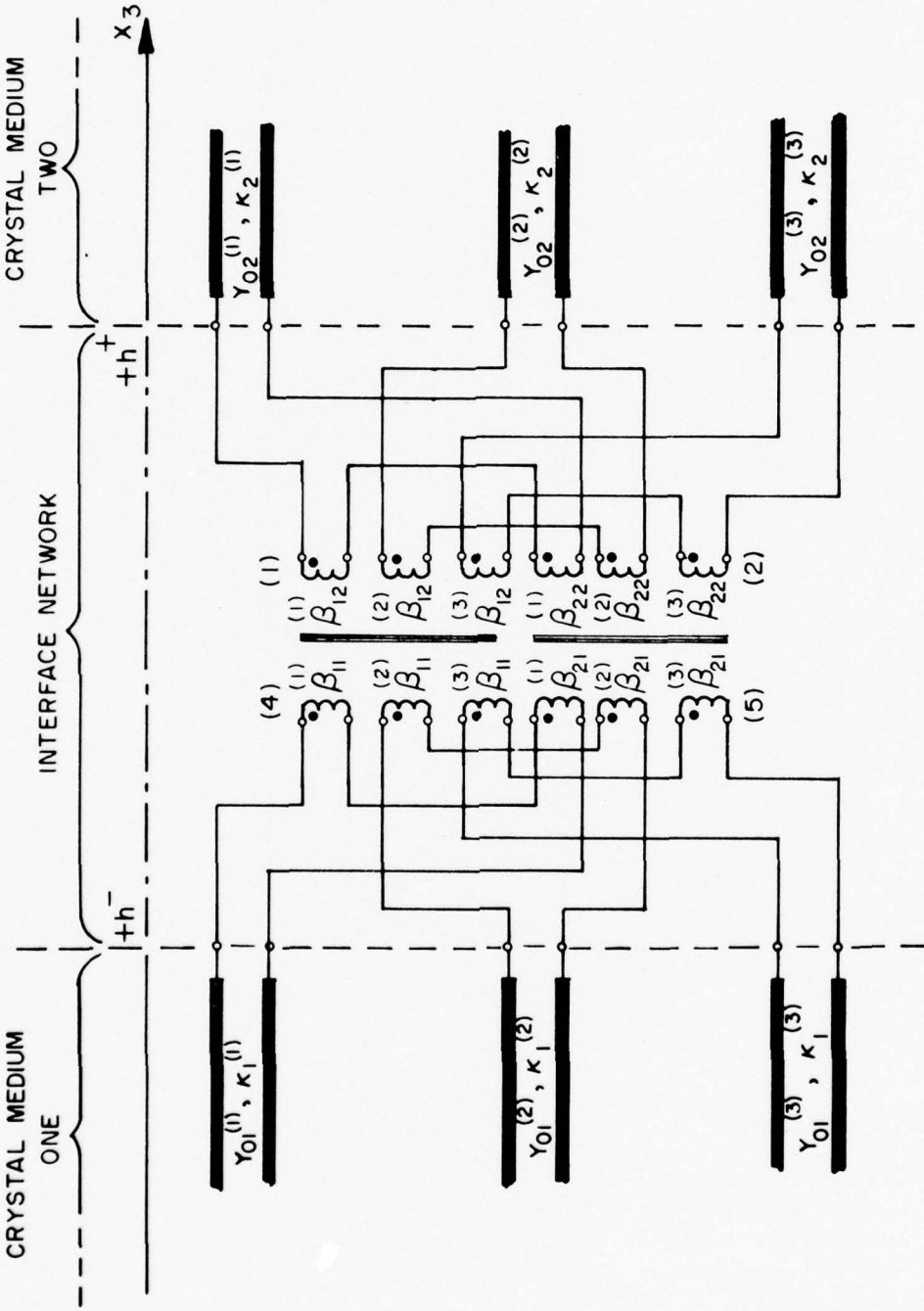

FIG. 30 EXACT ANALOG REPRESENTATION OF MECHANICAL INTERFACIAL COUPLING, FOR CONDITIONS OF COMPRESSIONAL SLIP.

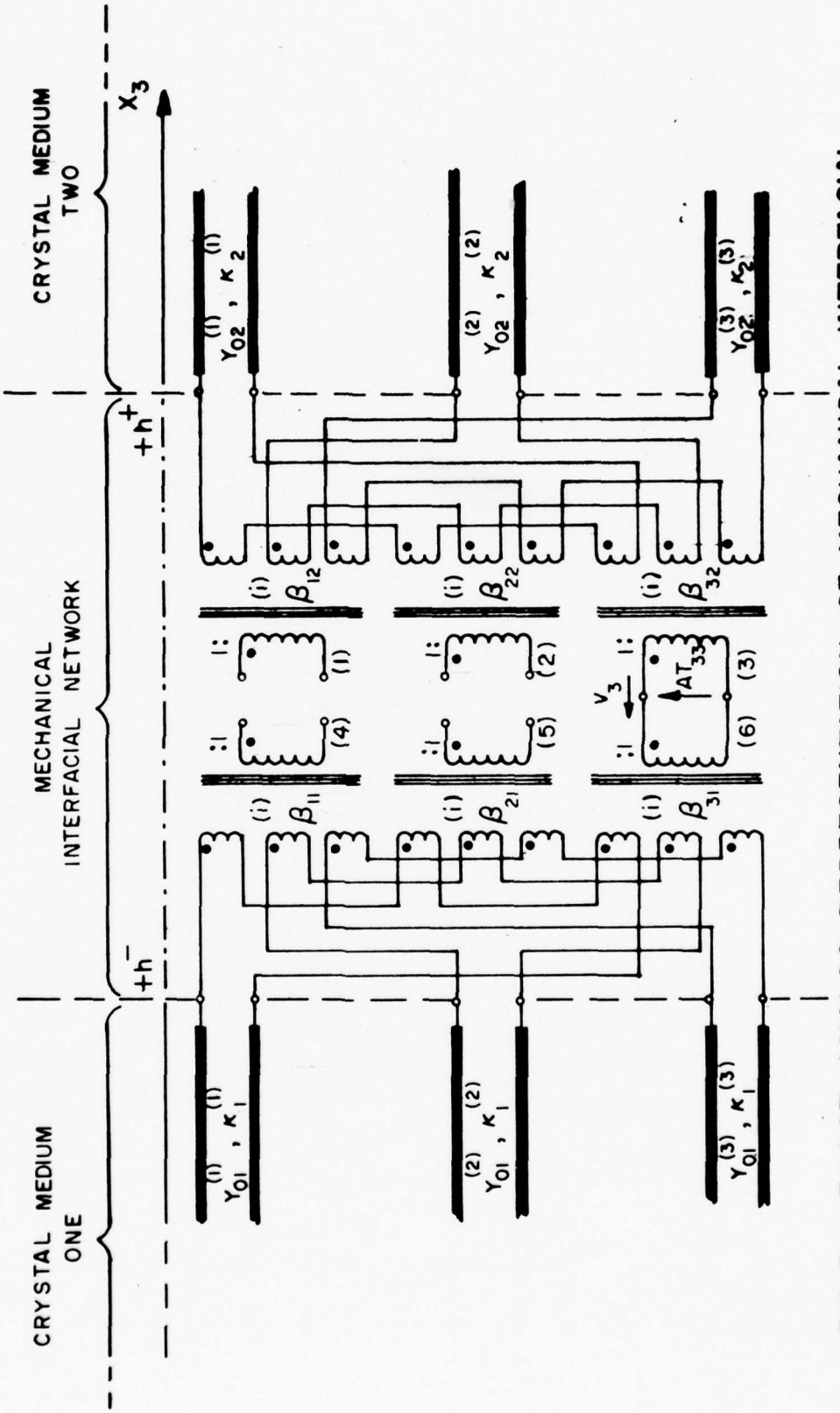

FIG. 31 EXACT ANALOG REPRESENTATION OF MECHANICAL INTERFACIAL COUPLING, FOR CONDITIONS OF TRANSVERSE BLOCKAGE.

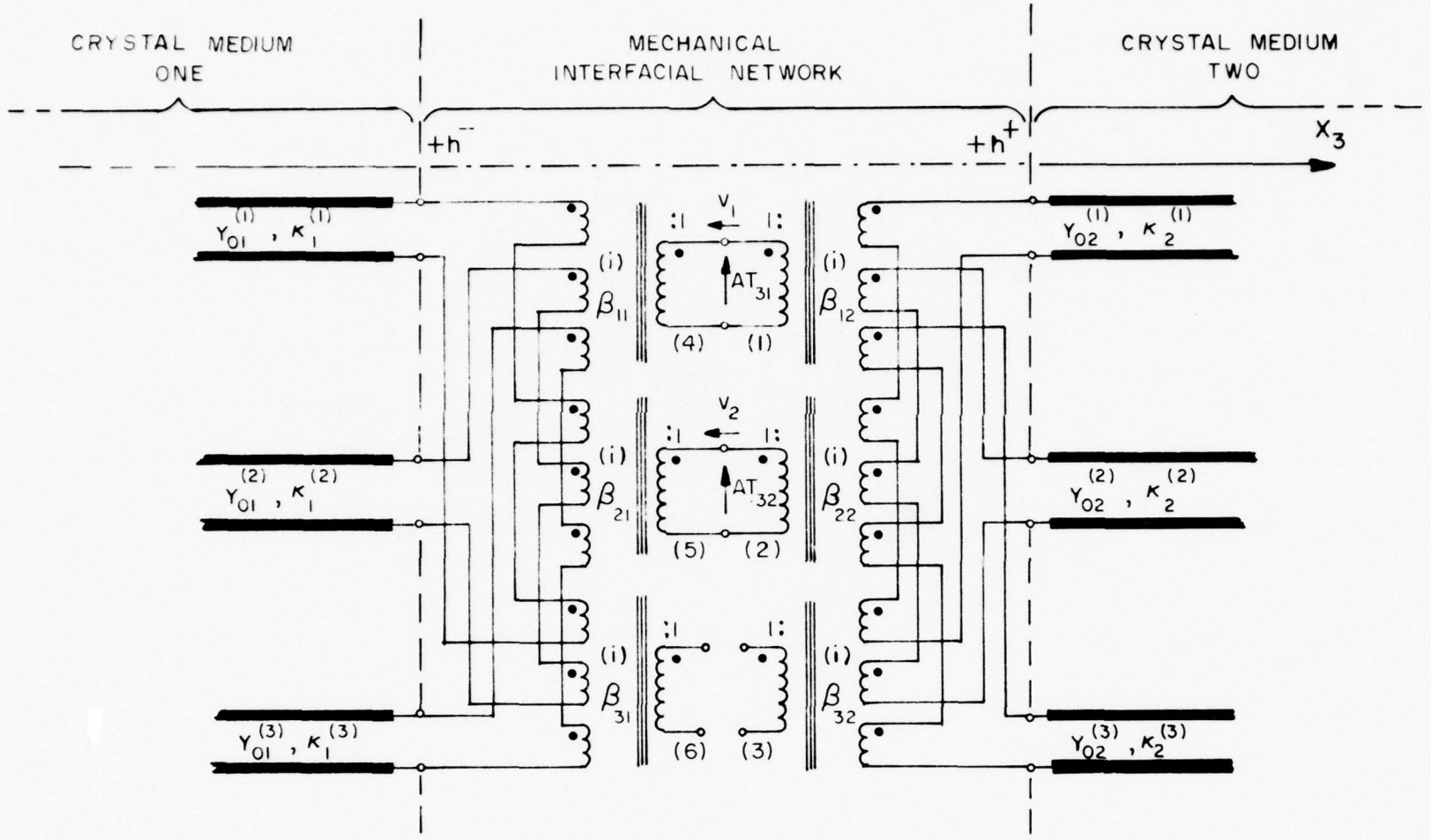

FIG. 32. EXACT ANALOG REPRESENTATION OF MECHANICAL INTERFACIAL COUPLING BETWEEN TWO CRYSTALS HAVING ARBITRARY ANISOTROPY, FOR CONDITIONS OF LONGITUDINAL BLOCKAGE.

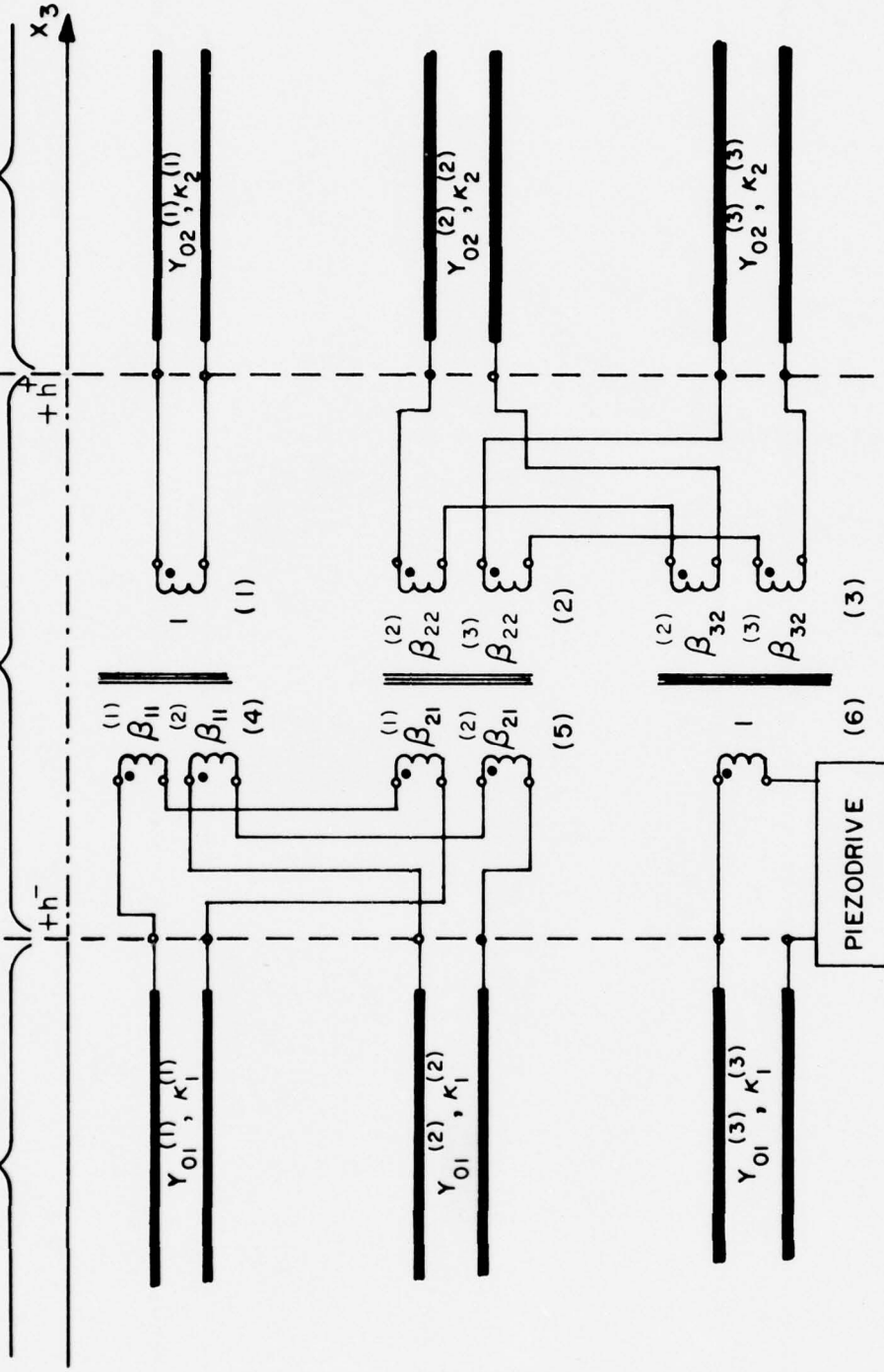

FIG. 33 EXACT ANALOG REPRESENTATION OF INTERFACIAL COUPLING. WELDED CONTACT BETWEEN X-CUT QUARTZ AND ROTATED X-CUT ADP CRYSTALS.

portrays the experimental conditions of Price & Huntington (86). An x-cut quartz crystal, (class 32), is in welded contact with a rotated x- or y- cut crystal of ADP, (class $\bar{4}2m$), so the appropriate mechanical ports are joined as shown. The quartz plate is TETM-driven. Its piezoelectric constants are such that only the mode indicated can be excited; the piezo-transformer is located in series with the mechanical winding as marked. The driven mode turns out to be a pure mode along x_3, i.e., the eigenvector describing the particle displacement for this mode is along the x_3 axis, which is the thickness direction. Because of this pure mode, the turns ratio at port (6) is unity, and no coupling to the two other modal transmission lines is present. A similar situation occurs in the rotated ADP crystal, except the pure mode is a shear, and not an extensional mode.

The resulting network is therefore simplified not because of the boundary conditions, but because of the plane wave eigenvectors in each material. Despite the simplifications, all modes remain coupled, and the precise paths of the coupling mechanisms are clearly traced in our network schematization. In reference (86) is is further shown that the coupling between ports (4) and (5) is small, and can be neglected for their purposes, so that the representation is further simplified to a consideration of coupling taking place only at ports (2), (3), (5) and (6). We arrive at their final result by setting $\beta_{21}^{(1)}$ equal to zero. This makes $\beta_{21}^{(2)}$ equal to unity, because of the normalization of the eigenvectors, from (2.26); this in turn requires $\beta_{11}^{(2)}$ to be zero and $\beta_{11}^{(1)}$ to be unity for the same reason. The network shows the situation which results in a very clear manner. Ports (4) and (1) can be connected by a direct feedthrough, are uncoupled to any

other modes, and undriven. Port (5) is connected, via port (2), to the second and third modal transmission lines in the second medium, and thence coupled to the line at port (6), which supplies the piezo-drive.

The network form of the problem sums up all of the physics of the problem in a pictorial representation wherein all of the intricacies may be traced with relative ease.

The second case of a particularization of Fig. 26 we wish to describe is given in Fig. 34. Here is shown a welded contact between a general triclinic substance, to the right, and a material having monoclinic symmetry, on the left. Representing the triclinic crystal is a mechanical interface network in its most general form, as given in either half of the network of Fig. 26. The left hand side of the interface network of Fig. 34 may be identified, for example, with a rotated Y-cut quartz plate (154). The rotation destroys the class 32 symmetry, and makes the plate appear, with respect to coordinate axes rotated around the original two-fold axis, as a crystal in class 2. We take our x_1 along the two-fold axis, and x_3, as usual, along the plate thickness. Then mode (1) is a pure shear mode, and is the only mode piezoelectrically driven in TETM.

If we take the triclinic crystal to be arbitrary, then we would have to attach the piezoelectric transformers to all transmission lines on the right side of the figure. On the other hand, a rotated Y-cut quartz crystal which has been further rotated about the x_3 (thickness) axis with respect to the laboratory frame, appears to be triclinic elastically, but only mode (1) may be driven piezoelectrically in TETM.

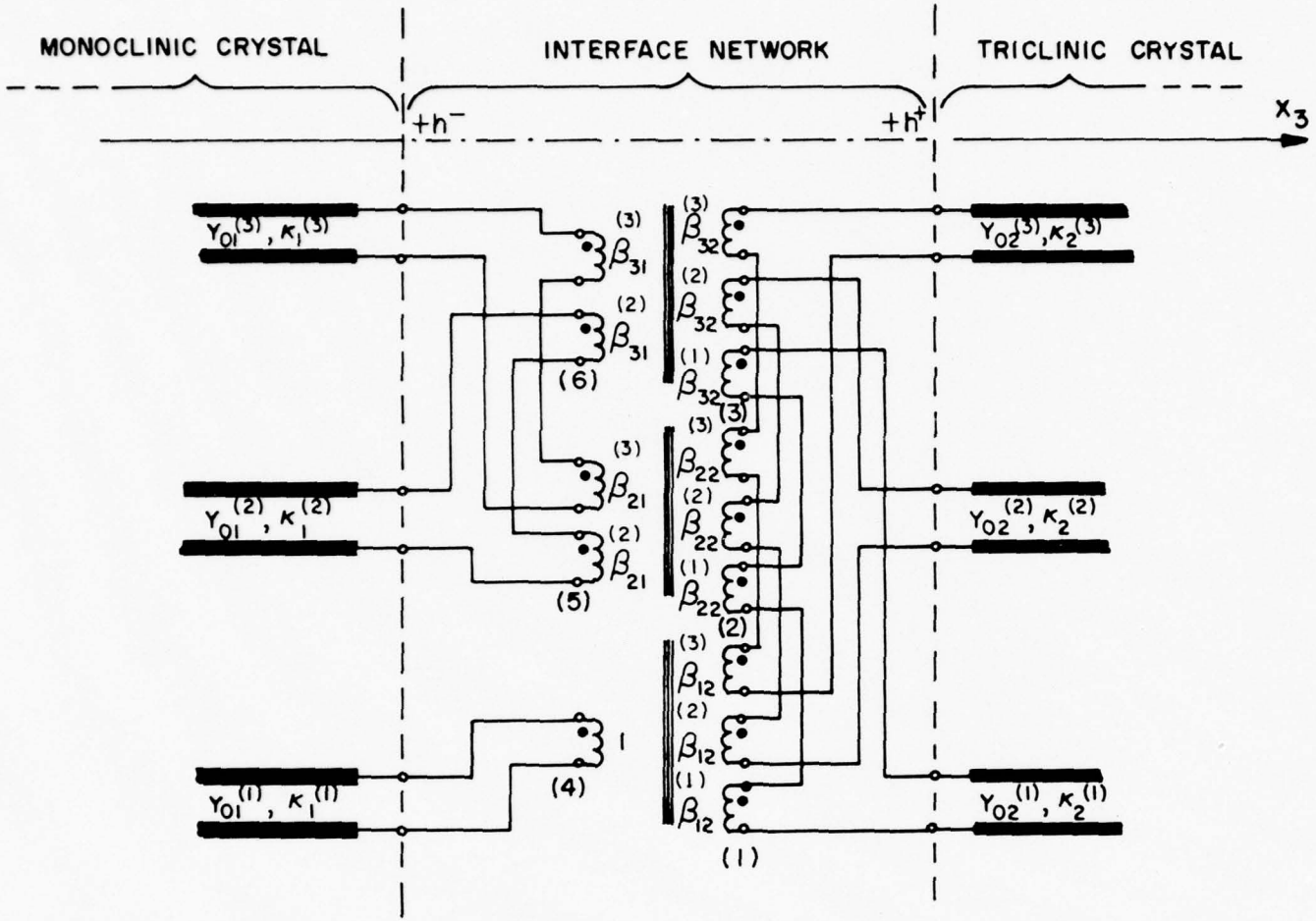

FIG. 34 EXACT ANALOG REPRESENTATION OF MECHANICAL INTERFACIAL COUPLING. WELDED CONTACT BETWEEN A TRICLINIC AND A MONOCLINIC CRYSTAL.

The network of Fig. 34 thus represents the situation where two rotated Y-cut quartz plates have been joined, with the laboratory frame coinciding with the x_i set of the left crystal, and the x_1 axis of the right crystal at an angle to the x_1 axis of the other.

Such a two-layer stack can be used as a filter element by utilizing the two electrical ports as input and output, and arranging the plate thicknesses and the orientation angles properly. Three angles are disposable. Each crystal has the rotational symbol $(YX\ell)\theta$, the angle θ describing the rotation about the crystallographic X axis. The values of θ may be chosen independently, and also the rotation angle about the thickness, of the one crystal with respect to the other, may be freely chosen.

For certain ranges of θ the phase velocities of modes (1) and (2) are close to each other and four of the transmission lines may be employed in the frequency selection process. The overall circuit for such a filter element is shown in Fig. 35. The mechanical interface network is taken from Fig. 34.

Although we shall not illustrate it, a simpler case, having attractive practical possibilities, is the case of a purely longitudinal mode in each of the two juxtaposed crystals, with the two shear modes in each coupled by the boundaries. In crystal classes 6 (class number 21) and $\bar{6}$m2 (class number 26) it can be arranged that only one modal (shear) transmission line in each crystal is TETM-driven. The degree of coupling can be adjusted by a relative rotation of the plates about the common thickness coordinate.

Practical designs stemming from considerations such as these is a fruitful area of investigation using CAD techniques. The availability

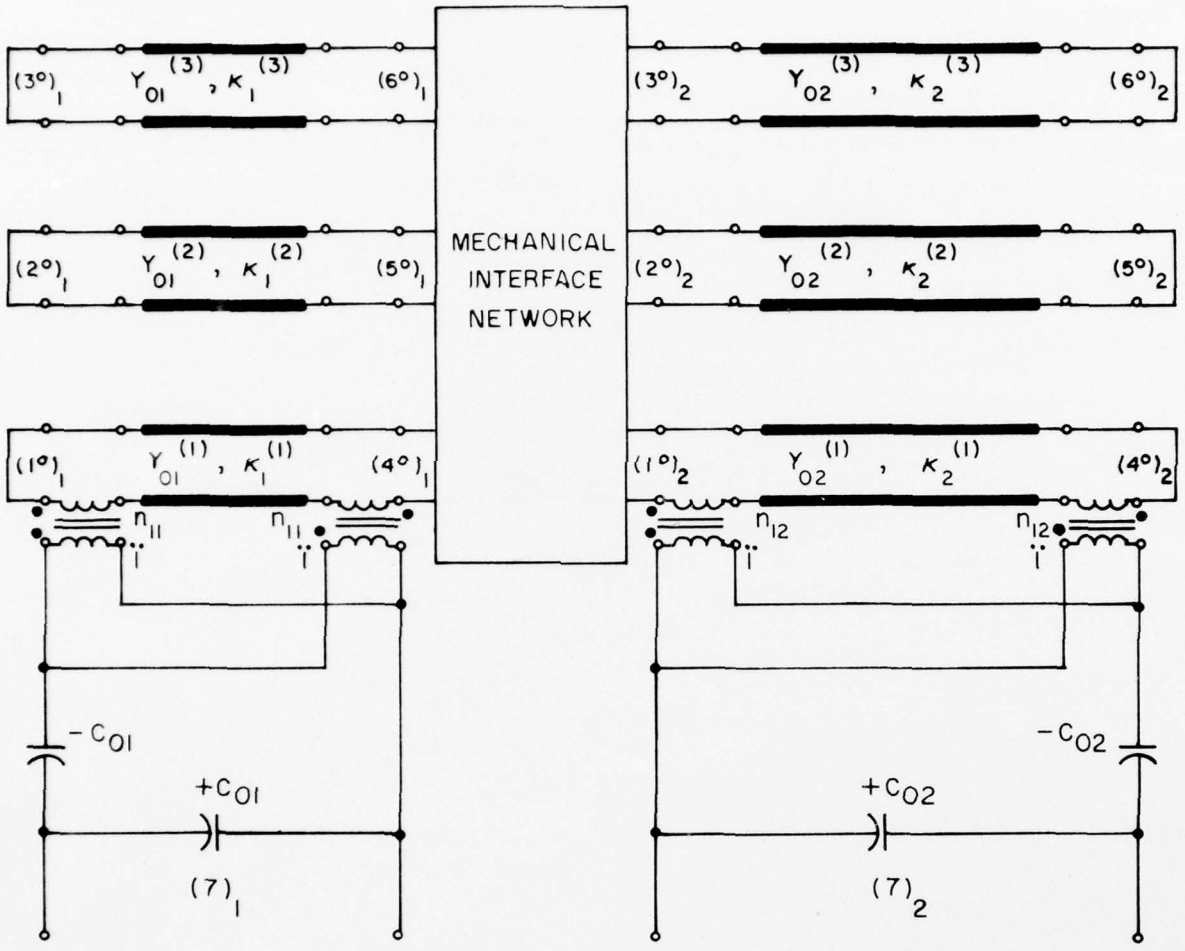

FIG. 35 EXACT ANALOG REPRESENTATION OF A TWO-LAYER STACK. ONE MODE OF EACH LAYER IS PIEZOELECTRICALLY DRIVEN IN TETM.

of the circuit formulation of the physical problem gives immediate entree to these techniques and is one of the main motivations of this work.

C. General Immittance Boundary Conditions.

In the last section, examples of various interfacial networks were described and discussed. These circuits exactly represented the physical conditions existing at the surface of contact between two adjacent strata.

We wish now to change our point of view slightly, and investigate a single surface that is loaded with an arbitrary boundary immittance. Of course, this immittance might arise as the result of juxtaposing a stack at the surface of interest, or it might come about by placing a load that is spatially lumped, upon the surface. A thin, massy, electrode would be an example of the latter that occurs very frequently in practice.

Our viewpoint, then, is not to regard the second medium in any fashion other than as it appears, at the surface of interest, to present to the first medium a set of immittance boundary conditions; that is, it couples the stress and velocity boundary conditions at ports (4), (5) and (6).

1. Let us consider the upper surface of a crystal plate as the boundary upon which the immittance conditions are to be imposed. This means, by (5.4) and (5.6), that we deal with M^{o}, K^{o} and M, K. To fix ideas, we will choose an impedance condition; the same argument can be given on the basis of admittances. At the ports (π), where $\pi = 4$,

5 and 6, we posit the general impedance relation

$$M = -\zeta K . \tag{6.1}$$

The minus sign comes about because of the conventions we have adopted for the voltages and currents, (see (5.1) and (5.2)). Zeta is a symmetric, three-by-three matrix whose elements may be complex.

Because of the relations (5.8) and (5.10) we can write

$$M = \beta M^{\circ} = -\zeta K = -\zeta \beta K^{\circ}, \tag{6.2}$$

so that

$$M^{\circ} = -\zeta^{\circ} K^{\circ}, \tag{6.3}$$

where

$$\zeta^{\circ} = \beta^{-1} \zeta \beta, \tag{6.4}$$

thus the impedances ζ° seen at ports (π°) are related to the impedances ζ by a similarity transformation. In general, ζ will be realized by some network, $\mathcal{N}(\zeta)$, that is then attached to ports (π), so the overall interface consists of the mechanical interface network of Fig. 23, plus the attached $\mathcal{N}(\zeta)$ circuit. The piezoelectric transformers would, as usual, be attached in their normal locations also. Carlin & Giordano (218) show that ζ may be diagonalized by two congruence transformations, each of which is realized by a circuit having the form of that in Fig. 23, so $\mathcal{N}(\zeta)$ is realized as two such circuits, in series. These circuits are connected, on one side, to ports (π), and on the other side to three reactances, and three resistances. Thus the general boundary network consists of only an interconnection of ideal transformers, plus three

reactances and three resistances.

In many practical cases, where the plate is a transducer radiating power, as in sonar applications, ζ may be almost purely real; in other instances, for example, mass loading effects due to electrode films, ζ is nearly purely reactive. We have seen how to represent the general case where ζ is complex. When ζ is real or imaginary only, then the cascade of the two networks, $N'(s)$ plus the mechanical interface network, is the same as a single network of the same form as the mechanical interface network having turns ratios given by the matrix product of the two transformations. Thus the overall circuit is simplified and appears as in Fig. 23, with three lumped elements attached to the three primaries, and the three other ports attached to the modal transmission lines representing the acoustic waves in the plate.

We will look at the case of lumped boundary conditions arising from mass loading the surface. After we touch on the general case we will find several specific cases where (6.4) leads to simplified networks.

If m is the mass per unit area placed at the boundary $x_3 = +h$, then the boundary conditions are

$$T_{3j} = -m\ddot{u}_j = -j\omega m v_j , \tag{6.5}$$

or

$$M = -j\omega m A K , \quad \text{at } x_3 = +h, \tag{6.6}$$

and, from (6.1), the impedance matrix is

$$\zeta = +j\omega (mA)\,\underline{1}, \tag{6.7}$$

where $\underline{1}$ is the unit matrix.

In this instance ζ is diagonal and is realized by three inductances,

each of value mA. More generally, we can take the boundary conditions as

$$T_{3j} = -m_{ji}\ddot{u}_i \quad . \tag{6.8}$$

The matrix ζ is not now diagonal, but consists of elements

$$\zeta_{ji} = +j\omega\mathcal{L}_{ji} \quad , \tag{6.9}$$

where $\mathcal{L}_{ji}$ may be realized by three inductors plus a network of the form shown in Fig. 23. This situation corresponds to an anisotropy of inertia (223). When this general ζ is inserted into (6.4) it is seen that the three transmission lines remain coupled at the boundary by the mass on the surface.

Inserting (6.7) into (6.4), however, shows that ζ° here is diagonal, so that when the inertial effect is isotropic, the three transmission lines become uncoupled mechanically from one another, and each appears with an inductance

$$\mathcal{L} = mA \tag{6.10}$$

in series with the piezoelectric transformers, as previously discussed. These piezoelectric transformers still provide coupling among the lines.

We note several limiting cases of interest. If, in (6.8), m_{11} and m_{22} are allowed to increase without bound, while m_{33} remains finite, we approach in the limit the case of transverse blockage, while if m_{33} becomes unbounded and m_{11} plus m_{22} remain finite, the condition of longitudinal blockage appears.

Also, as would be expected, when m vanishes we come back to the solid-vacuum interface considered earlier. In fact, reverting back now to a complete plate, rather than a single surface thereof, we gave exact equivalents in Figs. 10 and 17, for TETM- and LETM- driven plates that are traction-free. If in these figures the boundary short-circuits

are replaced with inductances of value mA, we have exact representations of the isotropically mass-loaded plate. This follows from (6.4) which yields a diagonal S°.

When both plate surfaces are coated with an isotropic mass, but the coatings are different on the two sides, e.g., on account of different electrode materials, and/or different electrode thicknesses, then each surface would be simply represented, mechanically, by three inductors, one attached to each transmission line at that surface. The inductance values for the two surfaces would however differ.

The foregoing is a simple example of the manner in which our networks may be utilized to describe various conditions without resorting to a new calculation every time the circumstances to be accommodated change.

If the circuit of Fig. 10 is redrawn with inductors of value mA replacing the short circuits at the surfaces, corresponding to equal masses on both surfaces, mechanical symmetry is restored, and the network may be bisected. The result follows immediately from Fig. 11 when an inductance of value mA/2 is placed in series with each modal transmission line at the end that is attached to the piezo-transformer secondary. Using either Fig. 10, or Fig. 11, with the inductors in place, the input admittance will be seen to agree exactly with that given by Yamada & Niizeki (65).

Mindlin & Lee (224) have treated mass loaded boundaries in connection with the solution of two dimensional plate equations for partially electroded crystal plates. Their main results do not concern us here, but they give the equation for the frequencies of the pure shear mode in a rotated Y-cut quartz plate equally coated on the two bounding

surfaces with massy electrodes, omitting, for clarity, the piezoelectric contribution. One may readily show that their frequency equation corresponds to that of a transmission line of length equal to h, one half the plate thickness, characteristic impedance $Z_o/2$, and wavenumber χ , that is open circuited at one end and loaded by an inductance of value $mA/2$ at the other end. Instead of this bisected version one can arrive at the same result considering a line of length 2h terminated at each end by an inductance of value mA. The presence of the mass loading has the effect of changing the effective length of the transmission line.

Similar remarks hold for the piezoelectric boundary loading, except that the effect can be made to work either to lengthen or shorten the effective transmission line length, depending upon whether TETM- or LETM- plates are used. This effect was incorporated into Lawson's description (61) of the "effective thickness" of a piezoelectric plate.

2. The foregoing has examined various boundary conditions that couple together the mechanical port variables. Here we wish to look at the case of a TETM plate excited by electrodes which are not contiguous to the plate surfaces. This arises in practice with the use of air gaps. For us, it will show the changes brought about by a different electrical boundary condition.

We take a traction-free, single plate resonator, as in Section III A, between electrodes at potentials $\pm \varphi_o$, but the electrodes have now a total separation of $2(h+d)$ instead of 2h. The plate may be located anywhere in the gap, parallel to the electrodes.

If the total gap is separated by the placement of the plate into

two portions of values d_1 and d_2, then

$$d_1 + d_2 = 2d = \text{total gap}. \tag{6.11}$$

The boundary conditions are

$$T_{3j} = 0, \quad \text{at} \quad x_3 = \pm h, \tag{3.1}$$

$$D_3 = \epsilon_0 E_0, \quad \text{at} \quad x_3 = \pm h, \tag{6.12}$$

$$\varphi = \pm \varphi_0, \quad \text{at} \quad x_3 = (+h+d_1), (-h-d_2). \tag{6.13}$$

The quantity E_0 is the value of E_3 in the vacuum region between the plates. In addition to the plate formulas we gave in Chapter III, we have the relation for the electric field

$$2\varphi_0 = \left(\varphi(+h) - \varphi(-h)\right) - 2dE_0 . \tag{6.14}$$

Using (2.20) with (6.12) permits the elimination of E_0 in favor of a_3. Then, (3.4) and (3.5) are used in (2.41), which, in turn is put into (6.14) with the result that b_3 cancels. As a result, a_3 is found to be the same as (3.6) but that the factor of unity in the denomenator is replaced by

$$\left(1 + \frac{d\,\epsilon_{33}^{S}}{h\,\epsilon_0}\right) . \tag{6.15}$$

Because a_3 enters into the expression for Y_{in}(TETM), the replacement, in (3.15), of the factor of unity by the quantity (6.15) gives the desired result.

This may be put into precisely the same form as the original by redefining the static capacitance and coupling coefficients in (3.15). Each of these is divided by (6.15) to arrive at the effective value caused by the presence of the gap. We see, by these manipulations, that the equivalent circuit of Fig. 10 still realizes Y_{in} (TETM) under these circumstances, but that the values of C_o and n_i must be changed. The change in the turns ratios takes place because n_i is proportional to $k^{(i)}$ which is altered by the presence of the gap. These results accord completely with those of Yamada & Niizeki (65) who derived an expression for the input admittance of a plate in an air gap.

D. Single-Ended and Continuous Sources of Excitation.

In previous chapters we have obtained a network that describes the behavior of a piezoelectric crystal plate that is unbounded and subject to a uniform driving field, either along, or lateral to, the thickness direction. We have, in various places, also mentioned the similarity our problems have with the microwave cavity excitation of acoustic waves in a piezoelectric solid, wherein the excitation takes place largely at a single end-face of the crystal specimen.

In this section we will indicate how the single-ended excitation that takes place in a crystal located in a microwave cavity may be represented by a modification of our circuits. In so doing we will give a further demonstration of the versatility of the equivalent network ideas presented here, and tie in additional results from the current literature.

1. Our previous networks have associated with them electrical ports across which a potential is placed. We arranged this in the LETM case

by taking a length element (2ℓ) in the lateral direction, and considered the port (7) potential as this length mulitplied by the applied lateral field. In the TETM case the potential arose in a more natural way, being directly applied to the driving electrodes.

To treat the case of excitation taking place at a single end it is appropriate to redefine the electrical port in such a fashion that an electric field appears in place of potential as the driving force. This comes about because potential difference is not a property of a point, and we desire to examine an excitation which takes place at a single surface, having no reference to the distance that separates it from the other plate surface.

Sections B & C of this chapter dealt with a single surface in the context of mechanical conditions; the piezoelectric effect may be grafted on to those networks by the procedure described there. This procedure involves an attachment of the electrical port, which takes into account both plate surfaces. In other words, while we concentrated our attention upon a single surface, as far as the mechanical properties were concerned, the electrical properties always involved both surfaces.

To recast our networks for single-ended excitation the second surface is omitted from consideration by disregarding those features that depend upon it, such as the electrical input circuit and the interconnections between the piezo transformer primaries running along the thickness coordinate. The geometry of the cavity will determine the capacitances associated with it, but we take no notice of this aspect of the problem, desiring to relate the piezoelectric excitation to the applied electric field existing within the cavity,

a quantity that is determined by separate measurement or calculation.

We take the driving field lateral to the surface of the crystal to begin the discussion. To arrive at an equivalent circuit we simply notice that in the LETM configuration, the applied voltage ($2\ell E_1$) appeared directly across the piezo-transformer primaries, in accord with the fact that the applied lateral field is continuous across the interface. By virtue of the piezoelectric effect, this led to the production of a mechanical force across the piezo-transformer secondaries of

$$2\ell E_1 n_i = A \underline{\underline{e}}^{\circ}_{13i} E_1 \quad , \tag{6.16}$$

where we have used (4.32) and (4.23). Referring to (2.38), (2.47), (2.48) and (4.16), we see that $\underline{\underline{e}}^{\circ}_{13i} E_1$ is to be associated with the "nonwavy" portion of the stress $\bar{T}^{\circ}_{3i}$, as was $e^{\circ}_{33i} \Omega_3$ in the case of TETM. Thus we write

$$2\ell E_1 n_i = A \bar{T}^{\circ}_{3i} \quad . \tag{6.17}$$

Since we desire to put the network on the basis of field strength instead of voltage, this can be done by choosing a new set of turns ratios, $\tilde{n}_{1i}$, where

$$\tilde{n}_{1i} = A \underline{\underline{e}}^{\circ}_{13i} \quad ; \tag{6.18}$$

this is to be compared to (4.32). Now the piezoelectric force is given by

$$A \bar{T}^{\circ}_{3i} = \tilde{n}_{1i} E_1 \quad , \tag{6.19}$$

so that the appearance of the field strength E_1 at the electrical

port of our new circuit produces the necessary result across the piezoelectric transformer secondary. Figure 36 shows the equivalent network for a traction-free piezoelectric plate subjected to an applied field E_1 lateral to the surface. Because the tangential component of the electric field is continuous across the interface, the driving field is of strength E_1 both within and without the crystal. Short circuits at the mechanical ports indicate the traction-free nature of the mechanical boundary conditions.

Having a representation for the case of an applied field in the x_1 direction immediately allows the case of an impressed field in the x_2 direction to be inferred. For this case (6.18) is replaced by

$$\tilde{n}_{2i} = A \underline{\underline{e}}^{\circ}_{23i} , \qquad (6.20)$$

where $\underline{\underline{e}}^{\circ}_{23i}$ is formed from (4.18) by replacing all "1" subscripts by "2". Our preceding discussions about breaking up the total stress into "wavy" and "nonwavy" portions supplied the answer to the question of how the superposition of an x_1- and an x_2- directed electric field is to be represented. Quite simply, both contributions are to be placed in series with the mechanical portion at the end of each transmission line.

The problem we are analyzing from the standpoint of our networks has been treated by Lamb & Richter (225, 226). Their results are in exact agreement with ours; they show that the total piezoelectrically induced force at the surface, due to an applied electric field having an arbitrary orientation can be broken up into components considered to be driving each of the three eigen-modes, and for each mode, the components driving it arise, in turn, as the sum of three contributions, one for

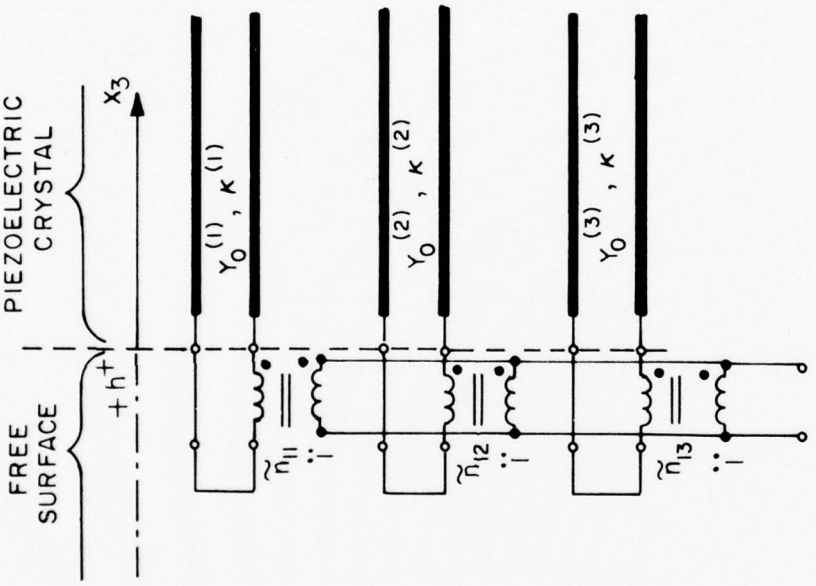

FIG. 36 EQUIVALENT NETWORK FOR ACOUSTIC WAVES GENERATED AT THE END SURFACE OF A PIEZOELECTRIC CRYSTAL BY AN IMPRESSED ELECTRIC FIELD.

each component of the impressed field. The effective piezoelectric constants for the two lateral fields, that we have called $\underline{e}^{\circ}_{13i}$ and $\underline{e}^{\circ}_{23i}$ agree completely with their formulas.

Two points remain; the first is that of the field component E_3, while the second is the case of mechanical boundary conditions other than traction-free conditions. This last point is settled by prior discussion, which leads us to open the short circuits at the mechanical ports and connect thereto a mechanical interface network of the form in Fig. 23. The other point, regarding an applied E_3 field, corresponding to the TETM excitation, is complicated by the fact that the acoustic modes themselves generate an E_3 component, but not lateral components. This is the distinction between TETM and LETM and shows up in the presence of the negative capacitor in our TETM equivalent networks.

Reference to any of our LETM networks will show that the full voltage appearing at the electrical port appears also across the piezo-transformer primaries. For the TETM plate, the corresponding networks disclose that the piezo-transformer primaries have impressed upon them a voltage which stands to the electrical port voltage in the ratio Y_{in} (TETM)/$j\omega C_o$. From (3.15), this ratio is

$$Y_{in}(TETM)/j\omega C_o = \frac{1}{\left\{1 - \sum_{p=1}^{3} (k^{(p)})^2 \frac{\tan\theta_p}{\theta_p}\right\}} \qquad (6.21)$$

If h is allowed to increase, so that θ_p become very large, then it will be seen that the ratio in (6.21) approaches unity almost everywhere. The presence of the tangent function is due to the double-ended excitation of the TETM plate. Large enough values for θ_p allow, for all intents

and purposes, the presence of the negative capacitor to be neglected, and the ratio to be considered unity.

Doing this permits us to write down the formula for the effective turns ratios of the piezo-transformers for an impressed E_3 almost by inspection. We have only to recognize that, because D_3 must be continuous, the impressed field E_3 external to the crystal will produce an internal field E_3 (inside) of value

$$E_3\,(inside) \;=\; E_3\;\epsilon_o\;/\;\epsilon_{33}^{S}\,. \tag{6.22}$$

Now we determine the turns ratios $\tilde{n}_{3i}$ so that the piezoelectric force is related to the external field E_3, since this is what is known experimentally. This relation has the form

$$A\,\bar{T}_{3i}^{\circ} \;=\; \tilde{n}_{3i}\,E_3 \;=\; A\;e_{33i}^{\circ}\;E_3\,(inside)\,, \tag{6.23}$$

so that, using (6.22)

$$\tilde{n}_{3i} \;=\; A\;e_{33i}^{\circ}\;\;\epsilon_o\,/\,\epsilon_{33}^{S}\,. \tag{6.24}$$

This also is in agreement with the results of Lamb & Richter, who make the assumption that the electric fields generated by the acoustic waves may be neglected in comparison with E_3 impressed. We may interpret these results, arrived at from our networks, and analytically by Lamb & Richter, by the complete equivalent network of Fig. 37. Here, all three field components yield piezoelectric forces that are in series in each modal transmission line end, and in series with the mechanical interface network. The interpretation of the series connection of the mechanical and piezoelectric components follows from (2.47), while the breakdown of the piezoelectric contributions follows at once from the results of

AD-A044 174 ARMY ELECTRONICS COMMAND FORT MONMOUTH N J F/G 9/1
TRANSMISSION-LINE ANALOGS FOR PIEZOELECTRIC LAYERED STRUCTURES.(U)
MAY 76 A BALLATO

UNCLASSIFIED ECOM-4413 NL

3 OF 3
ADA
044174

END
DATE
FILMED
10-77
DDC

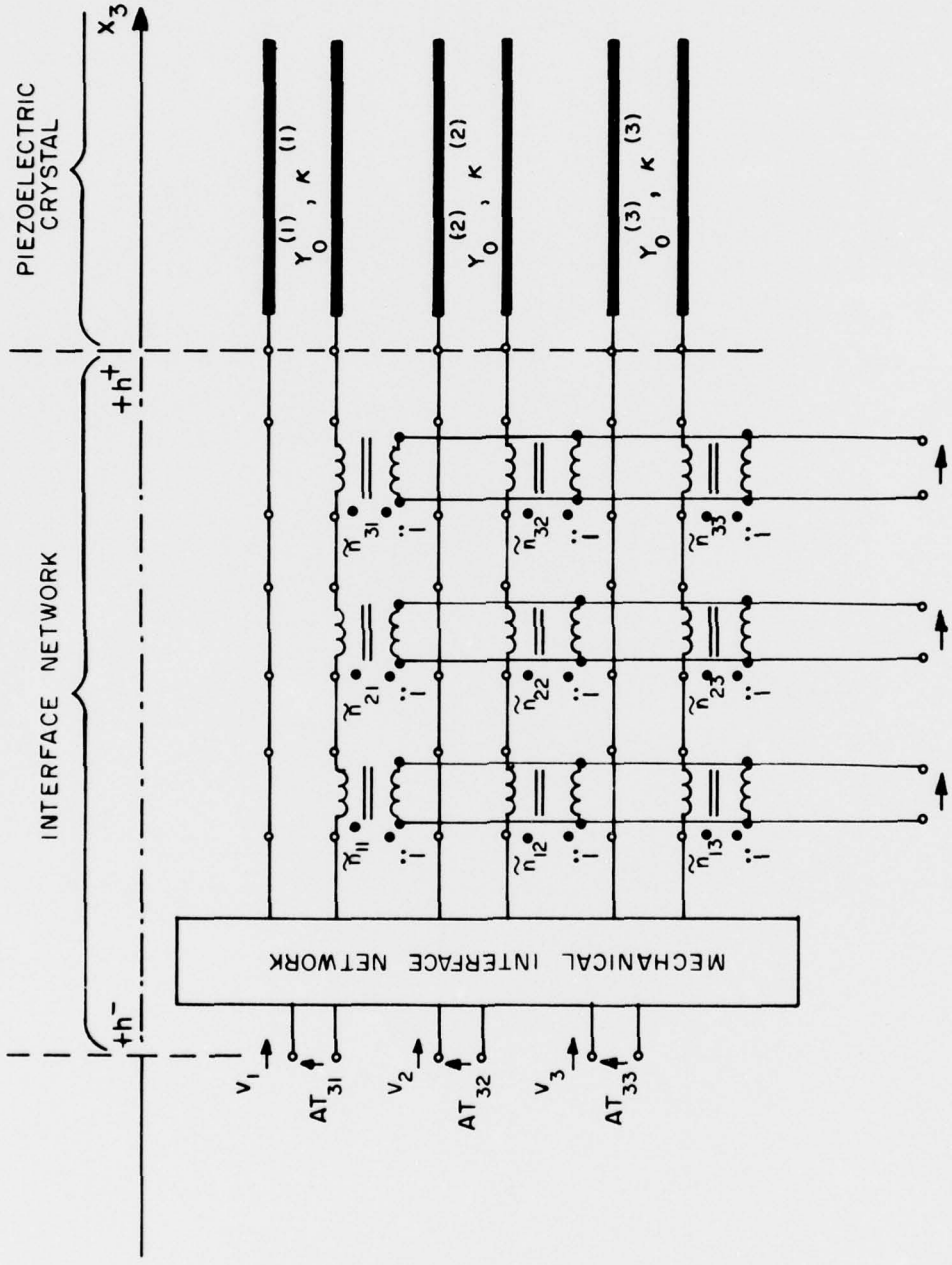

FIG. 37 PIEZOELECTRIC AND MECHANICAL INTERFACE NETWORK FOR THE SURFACE OF A CRYSTAL, EXCITED BY ARBITRARY ELECTRIC FIELDS AND MECHANICAL FORCES.

Lamb & Richter for an impressed electric field at an arbitrary direction to the crystal surface.

From this vantage point, it is not difficult to conjecture the network representing a plate equipped with an electrode arrangement that allows a uniform field to be impressed at an angle to the plate. For this case, in which the excitation is neither TETM nor LETM, the network will look like Fig. 37 at each end, but with turns ratios n_{ij} referring to potential rather than field strength, and with the three electrical ports attached to the electrical input circuit appropriate to that excitation. Thus, the ports marked with E_1 and E_2 would lead off the input circuits consisting of shunt capacitors, while that marked E_3 would attach to an input circuit containing a negative capacitor as well. Mutual capacitances between the various electrodes would additionally have to be connected between the three electrical ports as shown by Mason & Sykes (150). This network provides an answer to Redwood's question (99) concerning a circuit representing excitation by a composite field.

2. The foregoing leads naturally to a number of other conclusions. Suppose that a single crystalline medium is somehow divided into two portions by a plane surface normal to x_3, and across which the impressed field strength abruptly changes value. This is the situation depicted by Fig. 38 for one component of the field. The network representation follows from Fig. 37, for one crystal surface, by attaching to the interface a second such network. If the crystal so attached is of the same material and orientation as the original, the mechanical interfacial networks will simplify to three direct feedthroughs, as a

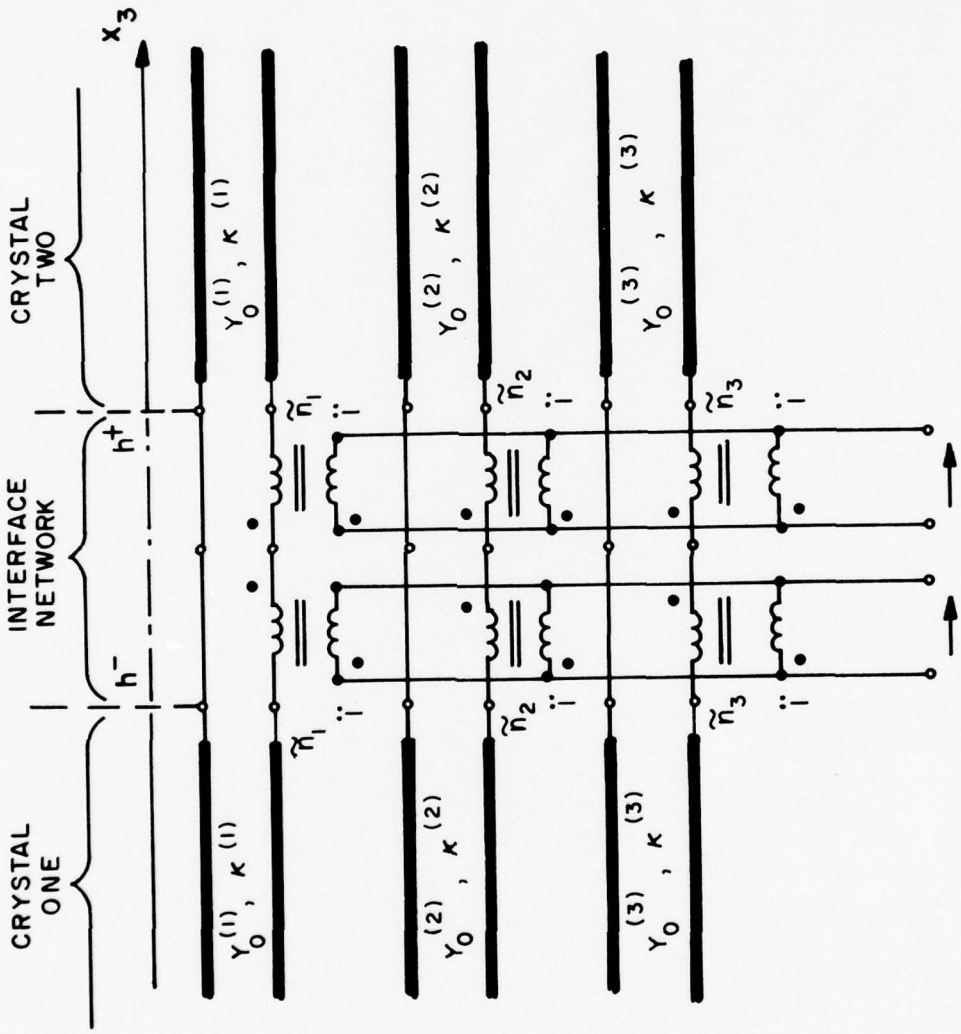

FIG.38 PIEZOELECTRIC NETWORK REPRESENTATION OF A DISCONTINUITY IN EXCITATION.

consequence of (2.26), and the circuit of Fig. 38 remains. Obviously the three components of the impressed field could be represented, as they are in Fig. 37, but this is not necessary for our discussion. Figure 38 shows that the net excitation at the interface is obtained, for each component of impressed field, and for each modal transmission line, by taking the difference between the field strengths as the effective source field strength. When the fields are of equal strength, no net piezo-excitation is present.

Exactly the same considerations apply to the situation where the impressed field remains constant across the boundary, but where the effective piezoelectric constant changes abruptly. This is a practical situation with regard to stacks of ceramics, where alternate layers are oppositely poled, or alternate between poled and unpoled. The elastic behavior, to a first approximation, is unchanged, so that Y_o and $\varkappa$ remain fixed, and the mechanical transformers reduce to feedthroughs.

The turns ratios of the contiguous transformers are negatives of one another when oppositely poled ceramics are used; this changes the dots on the transformers, so that the same field impressed at the electrical ports produces twice the piezoelectric force at the junctions of the transmission lines. The same thing is, of course, true of the junction between two plates made of the same crystal and having the same orientation except that one layer is reversed along x_3. Reversing this axis has the result of changing the sign of the pertinent transformed piezoelectric constant e^{o}_{13i} or e^{o}_{33i}, which is the same as changing the dot convention of the piezo-transformers.

More general than a change in the impressed electric field or in the piezoelectric constants is a change in the product of the two, as this product determines the force due to the change (cf. (2.38) and the discussion in Section III E). Our Fig. 38 takes this into account, in the case of an abrupt change, by making the turns ratios on the left different from those on the right, to take care of the changed piezoelectric constants, and by showing the different impressed fields applied to the proper port.

This problem is treated from another point of view, and for a single mode, by Mitchell & Redwood (83,96,97). Stacks of ceramics alternating in their poling direction occur in the papers by Sittig (80) and Stuetzer (82). Additional treatments of distributed sources are given by Holland (103,104,136) and by Leedom, et al. (98,149).

Having given the representation of Fig. 38 for an abrupt change in the piezoelectric excitation, we now indicate how the problem of continuous changes in excitation may be approached from our networks. We do this in the manner of Onoe & Okada (227), who applied the idea of a cascade of incremental transmission lines of slightly differing Y_o and γ to analyze the thickness-twist dispersion relations of a crystal plate having a varying thickness dimension. Their single modal transmission line segments must be replaced by three in our case, and the piezoelectric effect must be incorporated as we have discussed many times above. In Fig. 39 we give the desired result. The piezoelectric and mechanical interface networks have been further reduced in the schematization to boxes; it is clear from what we have presented in connection with Fig. 24 & 25, et seq., what the boxes contain. In Fig. 39 the interface networks occupy no spatial extent, whereas

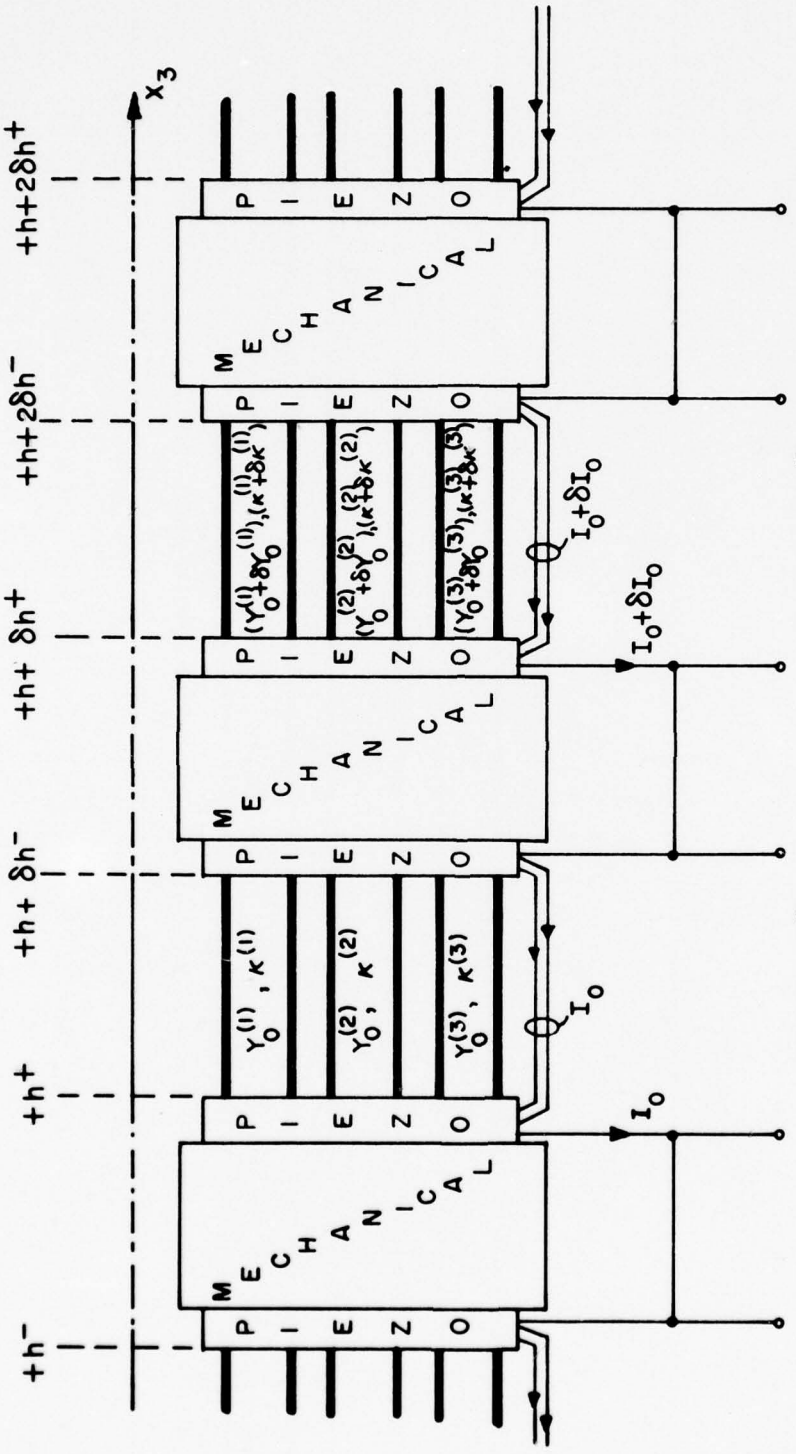

FIG. 39 INCREMENTAL ANALOG REPRESENTATION OF NONUNIFORM PIEZOELECTRIC EXCITATION IN A UNIFORM OR NONUNIFORM MEDIUM.

the transmission line segments are of incremental length. Practically speaking, this circuit would be implemented on a computer, with the physical problem modeled approximately by partitioning it into a number of segments each represented by a segment of the network shown. The fineness of the subdivisions dictates the number of segments required, which, in turn, depends upon the accuracy required in a given practical instance.

This chapter has applied the results of prior chapters to the characterization of multilayer stacks of plates, arbitrary in number and composition. Various special forms of the interfacial networks were shown. The piezoelectric excitation of acoustic waves at a single surface was also characterized in network form, as was excitation by distributed sources.

VII. Application to Devices & Computer Simulation

Rigorous network analogs have been obtained for configurations of stacked crystal plates excited piezoelectrically. At various places in the text, a number of applications of these configurations has been indicated. Realization and optimization of practical devices based upon these ideas, however, can best proceed by introducing a step intermediate between a circuit and the physical device it represents. This step consists in utilizing the network to simulate the ideal behavior of the device using CAD programs. In this way changes can be made easily without having to resort to a breadboard model each time it is desired to know the effect of some alteration in structure or composition. Since the networks are exact, they will faithfully reflect the behavior of the devices, subject only to the mild restrictions under which they were derived.

It is to a brief demonstration of these ideas that the present chapter is devoted. Here we will consider two of the simpest structures whose operation is based upon the ideas we have presented. Our object is to indicate how the structures can be expected to operate, and what avenues of future work are likely to be most fruitful in the reduction of our general results to practice.

Devices such as delay lines and pulse and code generators are best characterized in the time domain, while resonators and filters are best treated in the frequency domain. Our networks are valid and apt for both descriptions, but here we shall focus our attention upon filters to illustrate the ideas of this dissertation. Applications to the other areas

indicated, as well as to related topics, such as frequency discriminators, is relatively straightforward.

A. Double-Resonance Filter Crystals.

The first structure we will discuss is perhaps the simplest of its kind. This is the LETM-driven, traction-free resonator possessing two excitable modes having frequencies close to one another. The configuration consists of a single plate and it is used as a one-port device. A filter would be constructed from two of these elements, arranged, for example, as a half-lattice (23,25,26). In this arrangement the passband consists of those regions where the reactances of the two arms are opposite in sign. Mason & Sykes (150) describe lattice filters composed of more than one crystal in each arm; in our case each single plate is equivalent to two conventional filter crystals because of the use here of two of the three thickness modes in the plate. One can make use of this effect to reduce the number of crystals required, or to increase the filter performance by improving the shape factor or in-band ripple. Alternatively, it can be used to increase the bandwidth beyond what could be accomplished with a resonator having a single resonance of the same strength. This last application is promising with the use of crystals having high piezoelectric coupling factors, such as the refractory oxides now being investigated (181,186).

Although quartz does not possess high piezoelectric coupling, so that wide band quartz filters are not achievable without additional circuit elements, its physical properties are well known. For this reason we will use it to illustrate the double-resonance filter application; the discussion is readily applied to any other suitable substance. In quartz, the shear and quasi-shear frequencies approach one another for rotated

Y-cuts $(Y\chi\ell)\theta$, where θ is approximately -24°. Plates of substantially this orientation may be driven in LETM in such a way that the two modes of interest are of equal strength (214). The quasi-longitudinal mode is also driven, but is about 18% higher in frequency and can be neglected for our purposes.

A plate with electrodes attached for applying the lateral field is shown in Fig. 40. The angle ψ measures the field direction with respect to the z' axis. By changing ψ, the effective coupling factors of the two modes may be altered according to the graph of Fig. 41, which shows the two coefficients to be equal when $\psi = 34^{\circ}$ for a plate cut to $\theta = -23^{\circ}\,50'$.

Given on the right of Fig. 40 is the bisected form of the equivalent network of the plate, which follows from our general results, almost by inspection. The complete, bisected network of Fig. 19 has been here reduced by making one of the turns ratios equal to zero. In order to take into account the neglected third mode, the value of $\underline{C_0}$ may be augmented by the capacitance value presented to the input by the third transmission line at the frequencies of interest, which are near the nominal filter center frequency. This capacitive effect is negligible for the present case, but might not be for a substance with a high coupling coefficient for the third mode. In designing the filter, it is usually easiest to think in terms of the equivalent network parameters, and then to interpret these further in terms of the underlying physics.

For example, the lattice filter mentioned above might be designed as follows. Since the passband consists of the region where the reactances or susceptances of the two arms differ in sign, the crystal elements can be made so that they each possess equally spaced poles and zeros, the first zero of one crystal plate coinciding with the first

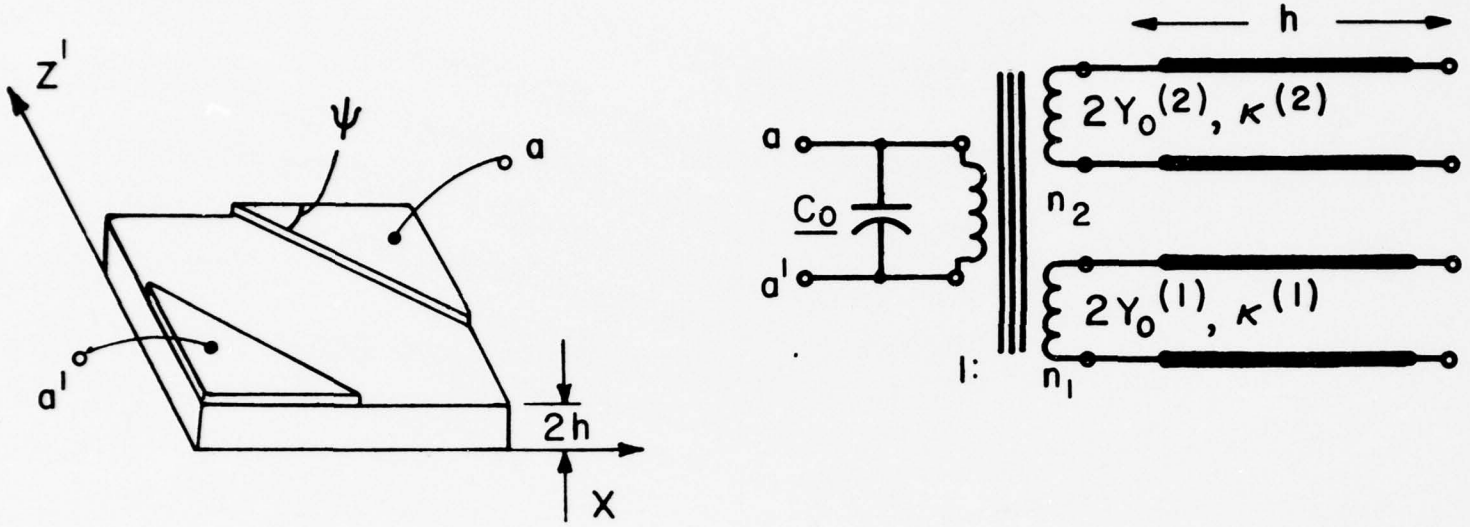

FIG. 40. LETM - DRIVEN QUARTZ PLATE, (YXℓ) θ, AND NETWORK REPRESENTATION.

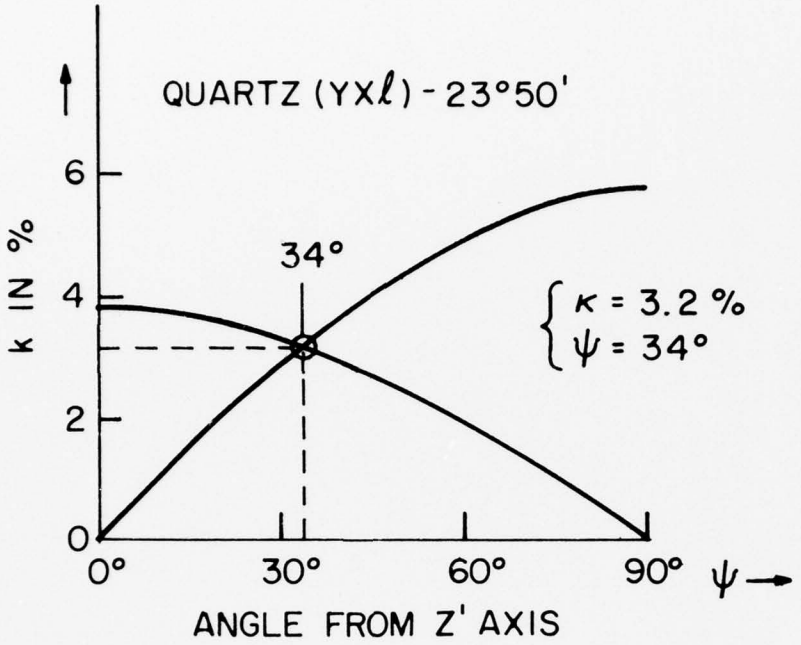

FIG. 41. EFFECTIVE LETM COUPLING COEFFICIENTS IN ROTATED Y-CUT PLATE, AS FUNCTION OF LATERAL AZIMUTH.

pole of the other. To arrange the equal spacing of the poles and zeros of each plate requires, for a given total fractional bandwidth, that the input reactance or susceptance function determined from the network of Fig. 40 be solved for the three values $k^{(1)}$, $k^{(2)}$ and $(v^{(1)}/v^{(2)})$ that simultaneously accomplish this. It is almost mandatory that this be done by computer. The resulting values may or may not be achievable with the substance chosen; this is determined by reference to curves such as those in Fig. 41 and the corresponding set for the velocities. Once the velocity ratio is known, the angle θ can be chosen, and when this has been picked, a value of ψ can also be chosen. A limitation of the technique is that $k^{(1)}$ and $k^{(2)}$ cannot be chosen independently.

After a normalized design has been arrived at, the absolute frequency is fixed by the choice of the plate thickness 2h. Figure 42 shows a graph of the computer-generated reactance function for rotated Y-cut quartz, $(YX\ell)$ $+23^{\circ}\,50'$, using $\psi = 34^{\circ}$. The reactance has been normalized to the reactance of $\underline{Co}$ at the frequency of the lower shear mode; this frequency is used to normalize the abscissa scale also. In this case the pole-zero spacings are nearly equal when the two coupling factors are equal. The total fractional bandwidth is only about 0.2% here, which is a factor of four smaller than can be attained by the use of AT-cuts of quartz alone, but is serves as an illustration of the principles involved for more practical designs based upon strongly piezoelectric materials. The requirements imposed by the filter network are readily interpreted by reference to the crystal equivalent circuit parameters, which are then determined from material constants and dimensions.

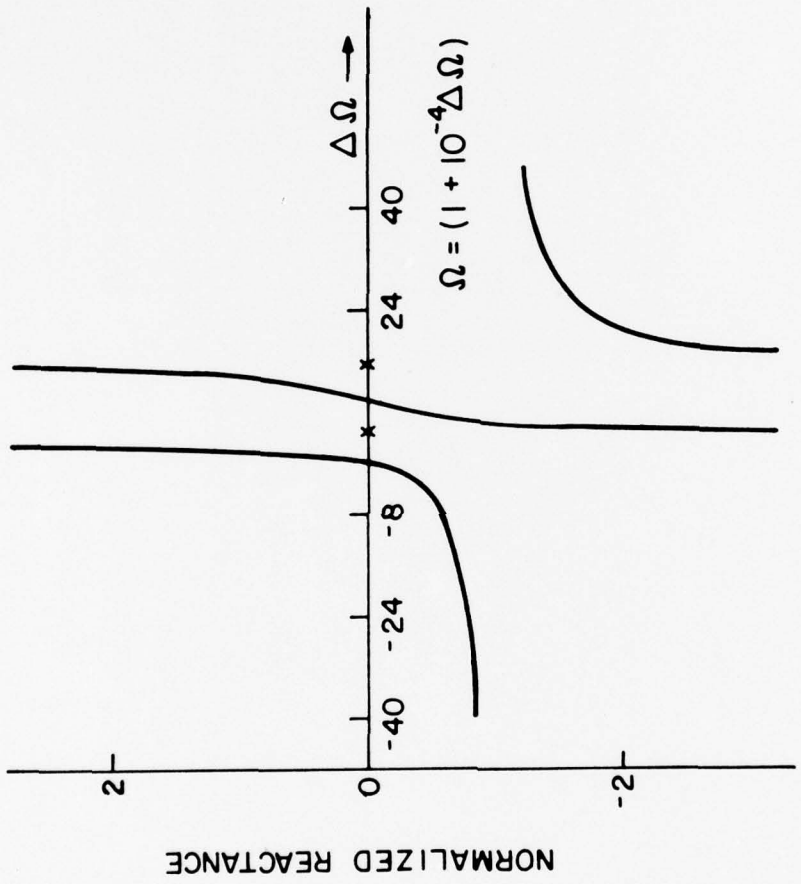

FIG. 42. NORMALIZED INPUT REACTANCE OF ROTATED Y-CUT QUARTZ PLATE (YXl) - 23°50', IN THE VICINITY OF RESONANCES OF THE SHEAR & QUASI-SHEAR MODES. LETM-DRIVEN BY A FIELD 34° FROM THE Z' AXIS.

B. Two-Layer Integral Crystal Filters

This section is devoted to a structure that is somewhat more complicated than the double-resonance crystal just considered. It has, however, possibly much greater potential for practical device realization. This structure consists of a two-layer stack of plates in welded contact, driven in TETM. We have mentioned this configuration in Section VI B in connection with the interface networks shown in Fig. 25 ff, and will make use of some of that discussion in the example we shall give below. In contrast to Section A, we now have two plates, instead of one, and will consider six modes instead of two; the device will be operated as a two-port, and will be TETM- driven. With these increased complexities it would be hard to derive much benefit from any but a most extended discussion, so we shall introduce a few compensating simplifications to enable us to see the outlines, at least, of the workings of this class of devices.

Before any simplifications are made, we will discuss the problem briefly in general. A sketch of the plate arrangement is given in Fig. 43. Where the field orientation provided a degree of freedom in the example of the first section, the relative rotation of the plates about the common x_3 axis similarly provides a means of investigating the effects of changes in the mechanical interface transformer turns ratios in the present case. The angle ψ is now taken to measure the relative rotation of the two plates from some fixed origin. The TETM driving arrangement consists of three electrodes, one at each of the traction-free surfaces, and one at the welded interface. The input and output can be taken in a number of ways; we shall consider the central electrode as common to both input and output.

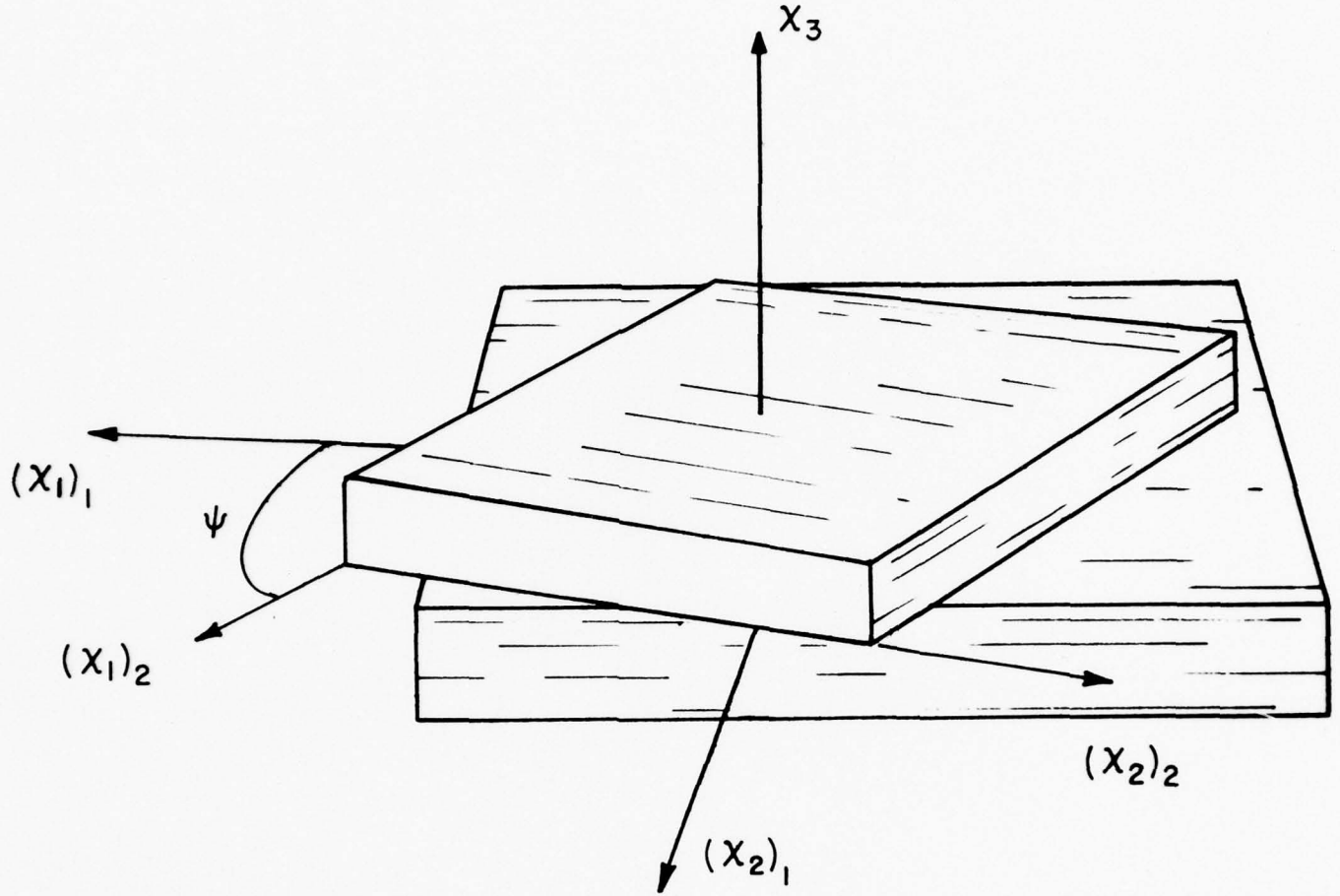

FIG. 43. TWO-LAYER STACK OF CRYSTAL PLATES SHOWING RELATIVE ROTATION ABOUT COMMON X_3 AXIS.

In this configuration we have a frequency selective device composed of two strata wherein the three modes of each layer are permitted to interact with each other via the mechanical boundary conditions. Mutual shielding or packaging is not required. The device is inherently robust because of its integral construction, and also lends itself readily to miniaturization. In fact there is no reason why integral crystal filters of this type, with two or more layers, could not be made completely compatible with integrated circuit technology.

Our illustrative example consists of computer simulated attenuation response curves of a two-layer integrated filter device. Having the overall impedance matrices for each layer, as given in Chapter V, it is not difficult to obtain the two-port impedance matrix between the electrical ports of the two-layer stack. The top and bottom faces of the plates are traction-free, so that the transmission lines representing the plates are shorted here, while the three internal mechanical ports of each plate are connected together, leaving only the electrical ports unconnected. Matrix methods pertinent to the interconnection of networks may be found in (18 & 21); we do not consider these details here but pass on to the attenuation function, A(dB).

Once the interconnected networks have been characterized by a two-port impedance matrix Z_{ij}, the attenuation may be determined provided the source and load impedance are known. Our first simplifying assumption is that these are of equal value, and are purely real:

$$Z_{source} = Z_{load} = R.$$

Then, using the equations found, e.g., in Zverev (25), the attenuation, in decibels, is

$$A(dB) = 10\log_{10}\left\{\left[Z_{11}+Z_{22}\right]^2+\left[(\det Z)/R+R\right]^2\right\}-20\log_{10}\left|2Z_{12}\right|.$$

Because our circuit impedances are all purely reactive, A(dB) is given by the same expression with reactance written for impedance, and the sign of det Z changed.

We are now ready to choose the materials to be used for the layers. Again, because of the completeness with which its material constants are known, and because it preserves so many connections with currently used devices, we pick quartz. Specifically, both plates are chosen to have precisely the same orientation, that of the AT-cut: $(Y\lambda\ell)\theta$, $\theta = +35^{\circ}15'$. This has four major consequences. First, the behavior of single plates of this cut is universally known, so that our filters can be contrasted with known results for quartz filters of standard construction. Second, the selection of the same cut makes the eigenvalues of both plates equal, so that the critical frequencies of each plate, taken separately, are in the same ratios. Third, the lower shear mode is a pure mode, so that the interface network is simplified. Finally, only the pure shear mode in each plate is TETM- drivable, so the piezoelectric interconnections are simplified.

We mentioned in Section VI B when describing Fig. 34, that it could be used to represent the mechanical interface transformer network between two rotated Y-cut plates of quartz. The entire discussion given there is pertinent to our application now, since the AT-cut is a member of this family. Figure 34 describes the mechanical network we consider here, with the piezoelectric connections made only at ports (1) and (4) of the interface and at the traction-free plate surfaces. Because both plates have the same orientation angle θ , the corresponding transmission lines on each side of the figure are identical. When the relative rotation angle ψ is zero, the device becomes identical with a single plate

of quartz, except for the central electrode. The mechanical network then degenerates into a set of three direct feed-throughs. When $\psi \neq 0^\circ$, the network of Fig. 34 is appropriate and the modal matrix components governing the transformer ratios on the right hand side are then functions of ψ if the x_i axes of the crystal on the left hand side is chosen as the reference set.

The final simplifications are that the plates are of equal thickness,

$$\omega_1/2\pi = 100 \text{ MHz},$$

and

$$R = 1/(\omega_1 C_o) = 50 \text{ ohms},$$

where ω_1 is the angular frequency at which the reference plate, taken alone, has its first admittance zero. The capacitance Co refers to the shunt capacitance of a single plate.

The effect of making the plates to be of equal thickness is to force the frequencies of both plates to be the same, so that only three, and not six modes have to be considered. This restriction is the first which should be lifted in a continuation of the work described here; two plates whose thickness differ by a few percent can be expected to exhibit a narrow-band filter characteristic.

Using all of the above-mentioned simplifying assumptions we are left with results that are easily described and analyzed. The computer-generated output is plotted in Fig. 44. Frequency normalized to ω_1 is used as the abscissa. Curves are presented for the three angles $\psi = 0^\circ$, 4° and 8°. When $\psi = 0^\circ$, the stack appears as an asymmetrically driven single plate of thickness 4h, and because of the lack of symmetry, the stack possesses resonances at integer values of Ω. The only driven mode is the lower shear mode which is a pure mode. Hence this mode is

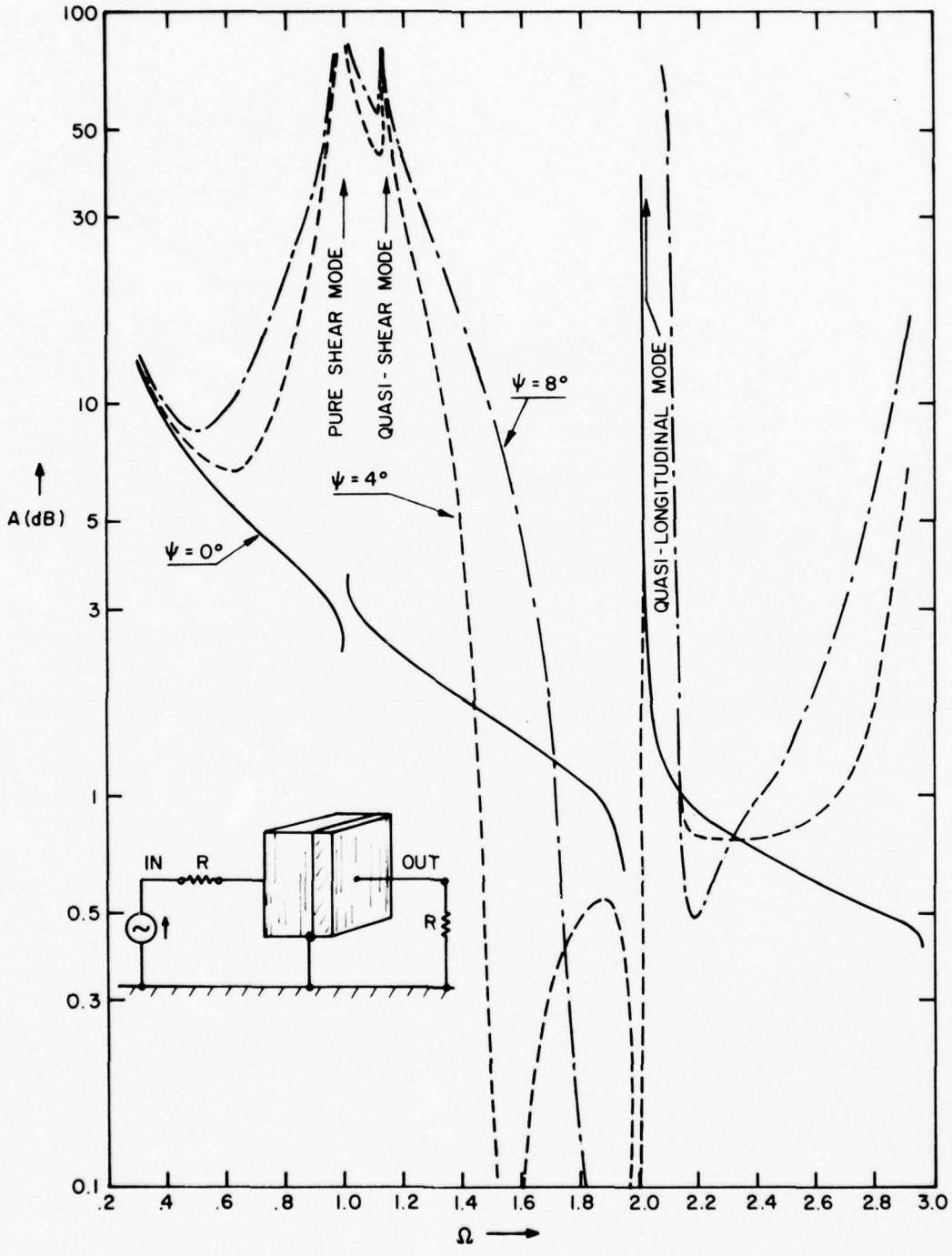

FIG. 44. ATTENUATION VERSUS FREQUENCY FOR A TWO-LAYER STACK OF 100 MHz AT-CUT RESONATORS AS FUNCTION OF RELATIVE ROTATION ψ ABOUT COMMON THICKNESS AXIS.

completely uncoupled from the others, so that any resonances due to them do not appear in the attenuation function. In both cases where $\psi \neq 0^{\circ}$, the attenuation has poles at $\Omega \approx 1.000$, 1.142 and 2.105, corresponding to modal velocities $v^{(i)}$, of $3.32\frac{8}{4}$, 3.800 and 7.007 $\times 10^{3}$ meters/second. If the plate thicknesses had not been made equal this correspondence would have been destroyed, and an important check could not be made. An easy way to explain the presence of the poles is to recognize that every time a transmission line becomes one half wavelength long, the short circuit at the traction-free boundary appears across the other end of the line and uncouples the two plates.

Notice that although the poles are fixed, the shape of the curves may be changed by varying ψ, so that one has a simple means of obtaining different filter responses. Although the purposes of our illustration are to indicate how devices based on these principles might operate and to provide an example that is still quite simple, and readily interpreted, the resulting curves for $\psi = 4^{\circ}$ and 8° are already reasonable wide band filter responses in the region just below $\Omega = 2$. Removing the restriction to equal plate thicknesses will also permit narrow band filters to be designed as integral filters.

The possible filter responses available for even the simplest two-layer structure are very large. Even if the plates are restricted to a single material, each plate cut is specified by two angles and the mutual rotation angle between the plates makes five disposable parameters to which must be added the ratio of the plate thicknesses. A large area for investigation is present here. Extensions to structures composed of more than two plates, and the use of different materials for

each of the plates further widens the possibilities of these devices for frequency selection and control.

Appendix A

The results we obtained in Chapter III are valid for TETM-driven plates of any piezoelectric crystal. It is desirable to go a little more into specific cases, because this permits us to see where simplifications may arise, and to determine certain similarities among classes of crystals. For a general background to the subject of crystal classes, and how crystal symmetry appears in the term schemes for the material constants, references (203-206) may be consulted; additional pertinent references are (158-160, 166, 179 & 180). For measured values of these constants, see (181 & 186).

We mentioned in Chapter II that tables would be given in the X Y Z frame; this referred to this appendix and to Appendix B.

Of the thirty-two crystallographic point groups, or crystal classes, twenty are piezoelectric. These are listed in Table A-1. All of the piezoelectric term schemes for these classes are different, with the exceptions that the following classes share the same schemes: 9 & 21; 12 & 24; 13 & 25; and 28 & 31. It might seem that all of these combinations would lead to a great deal of variety in the possibilities for piezoelectrically driving various modes, and in the coupling which exists between the different motions, and, indeed, there is variety enough, however, it is not overly difficult to sort it out in simple cases.

This is where it is much more advantageous to use the Christoffel procedure that was described earlier. We have used it in Table A-2, where a breakdown is given of the behavior of the different crystal

classes for plates cut with the thickness direction along either the X, Y or Z axis and driven by TETM. The table is organized according to which Γ_{ii} is, or which Γ_{ii}'s are, driven by the thickness field, and what type of coupling occurs. When displacements are coupled by elastic constants, and only one off-diagonal Γ_{ij} is involved, it is given in parentheses. It is seen that whatever happens to an X-cut of a certain crystal class, also happens to a Y-cut of that class, while a Z-cut may or may not be similarly placed in the table. The sole occupant of the "Piezo" column was noted by Bechmann (45).

In Tables A-3 to A-22 are given more detailed information regarding piezoelectric excitation of various cuts of each of the twenty piezoelectric classes. The quantities Ξ_i are essentially the factors which determine which Γ_{ii} is driven. These are given for unrotated X- , Y- , and Z- cuts; also for rotated Y- and rotated X- cuts, and for a Y- cut rotated about the Z axis; finally, they are given for the most general, doubly rotated cut. A finite value is indicated by a check mark.

By the use of these tables, it is possible to see at a glance what crystal cuts of a given class may be excited by TETM, and which Γ_{ii} is driven. Concerning this last point, it turns out that in the majority of cases ("None" column of Table A-2), the Γ_{ii} are the normal modes directly. When coupling is present, this is no longer true, but it is frequently the case that the coupling is not very large, and the Γ_{ii} are "nearly" the normal modes, and therefore one may loosely speak of them being separately driven.

CRYSTAL CLASS	HERMANN-MAUGUIN SYMBOL	CRYSTAL CLASS	HERMANN-MAUGUIN SYMBOL
1	1	16	3
3	2	18	32
4	m	19	3m
6	222	21	6
7	mm2	22	$\bar{6}$
9	4	24	622
10	$\bar{4}$	25	6mm
12	422	26	$\bar{6}$m2
13	4mm	28	23
14	$\bar{4}$2m	31	$\bar{4}$3m

TABLE A-1
THE PIEZOELECTRIC CRYSTAL CLASSES

TETM DRIVEN Γ_{ij}	TYPE OF COUPLING			
	NONE	PIEZO	ELASTIC	BOTH
NONE	6W, 10Z, 12W, 14W, 18Z, 22Z, 24W, 26Z, 28W, 31W,			
Γ_{11}	26 X		18X(Γ_{23})	
Γ_{22}			3W(Γ_{13}^*)	
Γ_{33}	7W, 9Z, 13W, 16Z, 19Z, 21W, 25W,		9X(Γ_{12}) 10X(Γ_{12})	
Γ_{11}&Γ_{22}		22X(Γ_{12})		
Γ_{22}&Γ_{33}				19X(Γ_{23})
Γ_{33}&Γ_{11}				4W(Γ_{13}^*)
Γ_{11},Γ_{22}&Γ_{33}				1W 16X

W INDICATES X-, Y-, AND Z-CUTS
X INDICATES X-, AND Y-CUTS
Z INDICATES Z-CUT
* REFERS TO IEEE AXIAL CONVENTION FOR MONOCLINIC SYSTEM

TABLE A-2
COUPLING IN PIEZOELECTRIC CRYSTAL CLASSES

CRYSTAL CLASS 1 — TABLE A-3

TETM \ CUT	X	Y	Z	(YXl)θ	(XYl)θ	(YXw)φ	(YXwl)φθ
≡1	✓	✓	✓	✓	✓	✓	✓
≡2	✓	✓	✓	✓	✓	✓	✓
≡3	✓	✓	✓	✓	✓	✓	✓

CRYSTAL CLASS 3 — TABLE A-4

TETM \ CUT	X	Y	Z	(YXl)θ	(XYl)θ	(YXw)φ	(YXwl)φθ
≡1	0	0	0	✓	0	✓	✓
≡2	✓	✓	✓	✓	✓	✓	✓
≡3	0	0	0	✓	0	✓	✓

CRYSTAL CLASS 4 — TABLE A-5

TETM \ CUT	X	Y	Z	(YXl)θ	(XYl)θ	(YXw)φ	(YXwl)φθ
≡1	✓	✓	✓	✓	✓	✓	✓
≡2	0	0	0	✓	0	✓	✓
≡3	✓	✓	✓	✓	✓	✓	✓

CRYSTAL CLASS 6 — TABLE A-6

	CUT	X	Y	Z	(YXl)θ	(XYl)θ	(YXw)φ	(YXwl)φθ
TETM	≡1	0	0	0	✓	0	0	✓
	≡2	0	0	0	0	✓	0	✓
	≡3	0	0	0	0	0	✓	✓

CRYSTAL CLASS 7 — TABLE A-7

	CUT	X	Y	Z	(YXl)θ	(XYl)θ	(YXw)φ	(YXwl)φθ
TETM	≡1	0	0	0	0	✓	0	✓
	≡2	0	0	0	✓	0	0	✓
	≡3	✓	✓	✓	✓	✓	✓	✓

CRYSTAL CLASS 9 — TABLE A-8

	CUT	X	Y	Z	(YXl)θ	(XYl)θ	(YXw)φ	(YXwl)φθ
TETM	≡1	0	0	0	✓	✓	0	✓
	≡2	0	0	0	✓	✓	0	✓
	≡3	✓	✓	✓	✓	✓	✓	✓

CRYSTAL CLASS 10 TABLE A-9

CUT		X	Y	Z	(YXl)θ	(XYl)θ	(YXw)φ	(YXwl)φθ
TETM	≡1	0	0	0	✓	✓	0	✓
	≡2	0	0	0	✓	✓	0	✓
	≡3	✓	✓	0	✓	✓	✓	✓

CRYSTAL CLASS 12 TABLE A-10

CUT		X	Y	Z	(YXl)θ	(XYl)θ	(YXw)φ	(YXwl)φθ
TETM	≡1	0	0	0	✓	0	0	✓
	≡2	0	0	0	0	✓	0	✓
	≡3	0	0	0	0	0	0	0

CRYSTAL CLASS 13 TABLE A-11

CUT		X	Y	Z	(YXl)θ	(XYl)θ	(YXw)φ	(YXwl)φθ
TETM	≡1	0	0	0	0	✓	0	✓
	≡2	0	0	0	✓	0	0	✓
	≡3	✓	✓	✓	✓	✓	✓	✓

CRYSTAL CLASS 14 — TABLE A-12

CUT		X	Y	Z	(YXl)θ	(XYl)θ	(YXw)φ	(YXwl)φθ
TETM	≡1	0	0	0	✓	0	0	✓
	≡2	0	0	0	0	✓	0	✓
	≡3	0	0	0	0	0	✓	✓

CRYSTAL CLASS 16 — TABLE A-13

CUT		X	Y	Z	(YXl)θ	(XYl)θ	(YXw)φ	(YXwl)φθ
TETM	≡1	✓	✓	0	✓	✓	✓	✓
	≡2	✓	✓	0	✓	✓	✓	✓
	≡3	✓	✓	✓	✓	✓	✓	✓

CRYSTAL CLASS 18 — TABLE A-14

CUT		X	Y	Z	(YXl)θ	(XYl)θ	(YXw)φ	(YXwl)φθ
TETM	≡1	✓	✓	0	✓	✓	✓	✓
	≡2	0	0	0	0	✓	✓	✓
	≡3	0	0	0	0	0	0	0

CRYSTAL CLASS 19 TABLE A-15

CUT / TETM	X	Y	Z	(YXl)θ	(XYl)θ	(YXw)φ	(YXwl)φθ
≡1	0	0	0	0	✓	✓	✓
≡2	✓	✓	0	✓	✓	✓	✓
≡3	✓	✓	✓	✓	✓	✓	✓

CRYSTAL CLASS 21 TABLE A-16

CUT / TETM	X	Y	Z	(YXl)θ	(XYl)θ	(YXw)φ	(YXwl)φθ
≡1	0	0	0	✓	✓	0	✓
≡2	0	0	0	✓	✓	0	✓
≡3	✓	✓	✓	✓	✓	✓	✓

CRYSTAL CLASS 22 TABLE A-17

CUT / TETM	X	Y	Z	(YXl)θ	(XYl)θ	(YXw)φ	(YXwl)φθ
≡1	✓	✓	0	✓	✓	✓	✓
≡2	✓	✓	0	✓	✓	✓	✓
≡3	0	0	0	0	0	0	0

CRYSTAL CLASS 24 — TABLE A-18

CUT		X	Y	Z	(YXl)θ	(XYl)θ	(YXw)φ	(YXwl)φθ
TETM	≡1	0	0	0	✓	0	0	✓
	≡2	0	0	0	0	✓	0	✓
	≡3	0	0	0	0	0	0	0

CRYSTAL CLASS 25 — TABLE A-19

CUT		X	Y	Z	(YXl)θ	(XYl)θ	(YXw)φ	(YXwl)φθ
TETM	≡1	0	0	0	0	✓	0	✓
	≡2	0	0	0	✓	0	0	✓
	≡3	✓	✓	✓	✓	✓	✓	✓

CRYSTAL CLASS 26 — TABLE A-20

CUT		X	Y	Z	(YXl)θ	(XYl)θ	(YXw)φ	(YXwl)φθ
TETM	≡1	✓	✓	0	✓	✓	✓	✓
	≡2	0	0	0	0	0	✓	✓
	≡3	0	0	0	0	0	0	0

CRYSTAL CLASS 28

TABLE A-21

TETM \ CUT	X	Y	Z	(YXl)θ	(XYl)θ	(YXw)φ	(YXwl)φθ
≡1	0	0	0	✓	0	0	✓
≡2	0	0	0	0	✓	0	✓
≡3	0	0	0	0	0	✓	✓

CRYSTAL CLASS 31

TABLE A-22

TETM \ CUT	X	Y	Z	(YXl)θ	(XYl)θ	(YXw)φ	(YXwl)φθ
≡1	0	0	0	✓	0	0	✓
≡2	0	0	0	0	✓	0	✓
≡3	0	0	0	0	0	✓	✓

CRYSTAL CLASS

TETM \ CUT	X	Y	Z	(YXl)θ	(XYl)θ	(YXw)φ	(YXwl)φθ
≡1							
≡2							
≡3							

Appendix B

The contents of this appendix are intended to supplement Chapter IV, as Appendix A supplements Chapter III.

For each of the piezoelectric crystal classes given in Table A-1, we present the excitation coefficients Ξ_i, appearing in the Christoffel formulation, which are responsible for LETM- driving a given mode. These coefficients are given in Tables B-1 through B-20.

As the lateral azimuth provides an extra degree of freedom, not present for TETM, the tables are somewhat more involved than the TETM counterparts. The same variety of cuts is represented, shown in the top row of each table. Along the bottom are two rows, which give the direction cosines m_i and f_i, of the plate and of the impressed electric field, respectively, that are finite in each instance.

Thus, for example, the rotated Y-cut, designated $(yx\ell)\theta$ has m_2 and m_3 finite, and there are three separate choices, within this heading, for the direction cosines, f_i, of the lateral field: f_1 finite, with f_2 and f_3 zero; f_2 and f_3 finite, with f_1 zero; finally, all three f_i may be finite. The Ξ_i may be zero or finite depending upon the particular choice. A finite value is represented by a checkmark.

CRYSTAL CLASS 1 — TABLE B-1

CUT →	X			Y			Z			(YXl)θ			(XYl)θ			(YXw)φ			(YXwl)φθ	
LETM = 1	✓	✓	✓	✓	✓	✓	✓	✓	✓	✓	✓	✓	✓	✓	✓	✓	✓	✓	✓	✓
LETM = 2	✓	✓	✓	✓	✓	✓	✓	✓	✓	✓	✓	✓	✓	✓	✓	✓	✓	✓	✓	✓
LETM = 3	✓	✓	✓	✓	✓	✓	✓	✓	✓	✓	✓	✓	✓	✓	✓	✓	✓	✓	✓	✓
f_i	2	3	$^2_3$	1	3	$^1_3$	1	2	$^1_2$	1	$^2_3$	$^1_{2_3}$	2	$^1_3$	$^1_{2_3}$	3	$^1_2$	$^1_{2_3}$	$^1_2$	$^1_{2_3}$
m_i	m1			m2			m3			m2,m3			m3,m1			m1,m2			m1,m2,m3	

CRYSTAL CLASS 3 — TABLE B-2

CUT →	X			Y			Z			(YXl)θ			(XYl)θ			(YXw)φ			(YXwl)φθ	
LETM = 1	✓	O	✓	✓	✓	✓	O	✓	✓	✓	✓	✓	✓	O	✓	✓	✓	✓	✓	✓
LETM = 2	O	✓	✓	O	O	O	✓	O	✓	✓	✓	✓	O	✓	✓	✓	✓	✓	✓	✓
LETM = 3	✓	O	✓	✓	✓	✓	O	✓	✓	✓	✓	✓	✓	O	✓	✓	✓	✓	✓	✓
f_i	2	3	$^2_3$	1	3	$^1_3$	1	2	$^1_2$	1	$^2_3$	$^1_{2_3}$	2	$^1_3$	$^1_{2_3}$	3	$^1_2$	$^1_{2_3}$	$^1_2$	$^1_{2_3}$
m_i	m1			m2			m3			m2,m3			m3,m1			m1,m2			m1,m2,m3	

CRYSTAL CLASS 4 — TABLE B-3

CUT →	X			Y			Z			(YXl)θ			(XYl)θ			(YXw)φ			(YXwl)φθ	
LETM = 1	O	✓	✓	O	O	O	✓	O	✓	✓	✓	✓	O	✓	✓	✓	✓	✓	✓	✓
LETM = 2	✓	O	✓	✓	✓	✓	O	✓	✓	✓	✓	✓	✓	O	✓	✓	✓	✓	✓	✓
LETM = 3	O	✓	✓	O	O	O	✓	O	✓	✓	✓	✓	O	✓	✓	✓	✓	✓	✓	✓
f_i	2	3	$^2_3$	1	3	$^1_3$	1	2	$^1_2$	1	$^2_3$	$^1_{2_3}$	2	$^1_3$	$^1_{2_3}$	3	$^1_2$	$^1_{2_3}$	$^1_2$	$^1_{2_3}$
m_i	m1			m2			m3			m2,m3			m3,m1			m1,m2			m1,m2,m3	

CRYSTAL CLASS 6 — TABLE B-4

CUT →		X			Y			Z			(YXl)θ			(XYl)θ			(YXw)φ			(YXwl)φθ	
LETM	≡1	O	O	O	O	✓	✓	O	✓	✓	O	✓	✓	✓	O	✓	✓	O	✓	✓	✓
	≡2	O	✓	✓	O	O	O	✓	O	✓	✓	O	✓	O	✓	✓	✓	O	✓	✓	✓
	≡3	✓	O	✓	✓	O	✓	O	O	O	✓	O	✓	✓	O	✓	O	✓	✓	✓	✓
f_i		2	3	$^2_3$	1	3	$^1_3$	1	2	$^1_2$	1	$^2_3$	$^1_{2_3}$	2	$^1_3$	$^1_{2_3}$	3	$^1_2$	$^1_{2_3}$	$^1_2$	$^1_{2_3}$
m_i		m1			m2			m3			m2,m3			m3,m1			m1,m2			m1,m2,m3	

CRYSTAL CLASS 7 — TABLE B-5

CUT →		X			Y			Z			(YXl)θ			(XYl)θ			(YXw)φ			(YXwl)φθ	
LETM	≡1	O	✓	✓	O	O	O	✓	O	✓	✓	O	✓	O	✓	✓	✓	O	✓	✓	✓
	≡2	O	O	O	O	✓	✓	O	✓	✓	O	✓	✓	✓	O	✓	✓	O	✓	✓	✓
	≡3	O	O	O	O	O	O	O	O	O	O	✓	✓	O	✓	✓	O	✓	✓	✓	✓
f_i		2	3	$^2_3$	1	3	$^1_3$	1	2	$^1_2$	1	$^2_3$	$^1_{2_3}$	2	$^1_3$	$^1_{2_3}$	3	$^1_2$	$^1_{2_3}$	$^1_2$	$^1_{2_3}$
m_i		m1			m2			m3			m2,m3			m3,m1			m1,m2			m1,m2,m3	

CRYSTAL CLASS 9 — TABLE B-6

CUT →		X			Y			Z			(YXl)θ			(XYl)θ			(YXw)φ			(YXwl)φθ	
LETM	≡1	O	✓	✓	O	O	O	✓	✓	✓	✓	✓	✓	✓	✓	✓	✓	O	✓	✓	✓
	≡2	O	O	O	O	✓	✓	✓	✓	✓	✓	✓	✓	✓	✓	✓	✓	O	✓	✓	✓
	≡3	✓	O	✓	✓	O	✓	O	O	O	✓	✓	✓	✓	✓	✓	O	✓	✓	✓	✓
f_i		2	3	$^2_3$	1	3	$^1_3$	1	2	$^1_2$	1	$^2_3$	$^1_{2_3}$	2	$^1_3$	$^1_{2_3}$	3	$^1_2$	$^1_{2_3}$	$^1_2$	$^1_{2_3}$
m_i		m1			m2			m3			m2,m3			m3,m1			m1,m2			m1,m2,m3	

CRYSTAL CLASS 10 — TABLE B-7

CUT →	X			Y			Z			(YXl)θ			(XYl)θ			(YXw)φ			(YXwl)φθ	
LETM = 1	0	✓	✓	0	✓	✓	✓	✓	✓	✓	✓	✓	✓	✓	✓	✓	0	✓	✓	✓
LETM = 2	0	✓	✓	0	✓	✓	✓	✓	✓	✓	✓	✓	✓	✓	✓	✓	0	✓	✓	✓
LETM = 3	✓	0	✓	✓	0	✓	0	0	0	✓	✓	✓	✓	✓	✓	0	✓	✓	✓	✓
f_i	2	3	2_3	1	3	1_3	1	2	1_2	1	2_3	1_{2_3}	2	1_3	1_{2_3}	3	1_2	1_{2_3}	1_2	1_{2_3}
m_i	m1			m2			m3			m2,m3			m3,m1			m1,m2			m1,m2,m3	

CRYSTAL CLASS 12 — TABLE B-8

CUT →	X			Y			Z			(YXl)θ			(XYl)θ			(YXw)φ			(YXwl)φθ	
LETM = 1	0	0	0	0	0	0	0	✓	✓	0	✓	✓	✓	0	✓	0	0	0	✓	✓
LETM = 2	0	0	0	0	0	0	✓	0	✓	✓	0	✓	0	✓	✓	0	0	0	✓	✓
LETM = 3	✓	0	✓	✓	0	✓	0	0	0	✓	0	✓	✓	0	✓	0	✓	✓	✓	✓
f_i	2	3	2_3	1	3	1_3	1	2	1_2	1	2_3	1_{2_3}	2	1_3	1_{2_3}	3	1_2	1_{2_3}	1_2	1_{2_3}
m_i	m1			m2			m3			m2,m3			m3,m1			m1,m2			m1,m2,m3	

CRYSTAL CLASS 13 — TABLE B-9

CUT →	X			Y			Z			(YXl)θ			(XYl)θ			(YXw)φ			(YXwl)φθ	
LETM = 1	0	✓	✓	0	0	0	✓	0	✓	✓	0	✓	0	✓	✓	✓	0	✓	✓	✓
LETM = 2	0	0	0	0	✓	✓	0	✓	✓	0	✓	✓	✓	0	✓	✓	0	✓	✓	✓
LETM = 3	0	0	0	0	0	0	0	0	0	0	✓	✓	0	✓	✓	0	✓	✓	✓	✓
f_i	2	3	2_3	1	3	1_3	1	2	1_2	1	2_3	1_{2_3}	2	1_3	1_{2_3}	3	1_2	1_{2_3}	1_2	1_{2_3}
m_i	m1			m2			m3			m2,m3			m3,m1			m1,m2			m1,m2,m3	

CRYSTAL CLASS 14 — TABLE B-10

CUT →	X			Y			Z			(YXl)θ				(XYl)θ			(YXw)φ			(YXwl)φθ	
LETM ≡1	O	O	O	O	✓	✓	O	✓	✓	O	✓	✓	✓	O	✓	✓	O	✓	✓	✓	
LETM ≡2	O	✓	✓	O	O	O	✓	O	✓	✓	O	✓	O	✓	✓	✓	O	✓	✓	✓	
LETM ≡3	✓	O	✓	✓	O	✓	O	O	O	✓	O	✓	✓	O	✓	O	✓	✓	✓	✓	
f_i	2	3	$^2_3$	1	3	$^1_3$	1	2	$^1_2$	1	$^2_3$	$^1_{2_3}$	2	$^1_3$	$^1_{2_3}$	3	$^1_2$	$^1_{2_3}$	$^1_2$	$^1_{2_3}$	
m_i	m1			m2			m3			m2,m3			m3,m1			m1,m2			m1,m2,m3	

CRYSTAL CLASS 16 — TABLE B-11

CUT →	X			Y			Z			(YXl)θ				(XYl)θ			(YXw)φ			(YXwl)φθ	
LETM ≡1	✓	✓	✓	✓	O	✓	✓	✓	✓	✓	✓	✓	✓	✓	✓	✓	✓	✓	✓	✓	
LETM ≡2	✓	O	✓	✓	✓	✓	✓	✓	✓	✓	✓	✓	✓	✓	✓	✓	✓	✓	✓	✓	
LETM ≡3	✓	O	✓	✓	O	✓	O	O	O	✓	✓	✓	✓	✓	✓	O	✓	✓	✓	✓	
f_i	2	3	$^2_3$	1	3	$^1_3$	1	2	$^1_2$	1	$^2_3$	$^1_{2_3}$	2	$^1_3$	$^1_{2_3}$	3	$^1_2$	$^1_{2_3}$	$^1_2$	$^1_{2_3}$	
m_i	m1			m2			m3			m2,m3			m3,m1			m1,m2			m1,m2,m3	

CRYSTAL CLASS 18 — TABLE B-12

CUT →	X			Y			Z			(YXl)θ				(XYl)θ			(YXw)φ			(YXwl)φθ	
LETM ≡1	O	O	O	O	O	O	O	✓	✓	O	✓	✓	✓	✓	✓	O	✓	✓	✓	✓	
LETM ≡2	✓	O	✓	✓	O	✓	✓	O	✓	✓	O	✓	✓	✓	✓	O	✓	✓	✓	✓	
LETM ≡3	✓	O	✓	✓	O	✓	O	O	O	✓	O	✓	✓	O	✓	O	✓	✓	✓	✓	
f_i	2	3	$^2_3$	1	3	$^1_3$	1	2	$^1_2$	1	$^2_3$	$^1_{2_3}$	2	$^1_3$	$^1_{2_3}$	3	$^1_2$	$^1_{2_3}$	$^1_2$	$^1_{2_3}$	
m_i	m1			m2			m3			m2,m3			m3,m1			m1,m2			m1,m2,m3	

CRYSTAL CLASS 19 — TABLE B-13

CUT →	X			Y			Z			(YXl)θ			(XYl)θ			(YXw)φ			(YXwl)φθ	
LETM ≡1	✓	✓	✓	✓	O	✓	✓	O	✓	✓	O	✓	✓	✓	✓	✓	✓	✓	✓	✓
LETM ≡2	O	O	O	O	✓	✓	O	✓	✓	O	✓	✓	✓	✓	✓	✓	✓	✓	✓	✓
LETM ≡3	O	O	O	O	O	O	O	O	O	O	✓	✓	O	✓	✓	O	✓	✓	✓	✓
f_i	2	3	$^2_3$	1	3	$^1_3$	1	2	$^1_2$	1	$^2_3$	$^1_{2_3}$	2	$^1_3$	$^1_{2_3}$	3	$^1_2$	$^1_{2_3}$	$^1_2$	$^1_{2_3}$
m_i	m1			m2			m3			m2,m3			m3,m1			m1,m2			m1,m2,m3	

CRYSTAL CLASS 21 — TABLE B-14

CUT →	X			Y			Z			(YXl)θ			(XYl)θ			(YXw)φ			(YXwl)φθ	
LETM ≡1	O	✓	✓	O	O	O	✓	✓	✓	✓	✓	✓	✓	✓	✓	✓	O	✓	✓	✓
LETM ≡2	O	O	O	O	✓	✓	✓	✓	✓	✓	✓	✓	✓	✓	✓	✓	O	✓	✓	✓
LETM ≡3	✓	O	✓	✓	O	✓	O	O	O	✓	✓	✓	✓	✓	✓	O	✓	✓	✓	✓
f_i	2	3	$^2_3$	1	3	$^1_3$	1	2	$^1_2$	1	$^2_3$	$^1_{2_3}$	2	$^1_3$	$^1_{2_3}$	3	$^1_2$	$^1_{2_3}$	$^1_2$	$^1_{2_3}$
m_i	m1			m2			m3			m2,m3			m3,m1			m1,m2			m1,m2,m3	

CRYSTAL CLASS 22 — TABLE B-15

CUT →	X			Y			Z			(YXl)θ			(XYl)θ			(YXw)φ			(YXwl)φθ	
LETM ≡1	✓	O	✓	✓	O	✓	O	O	O	✓	✓	✓	✓	✓	✓	O	✓	✓	✓	✓
LETM ≡2	✓	O	✓	✓	O	✓	O	O	O	✓	✓	✓	✓	✓	✓	O	✓	✓	✓	✓
LETM ≡3	O	O	O	O	O	O	O	O	O	O	O	O	O	O	O	O	O	O	O	O
f_i	2	3	$^2_3$	1	3	$^1_3$	1	2	$^1_2$	1	$^2_3$	$^1_{2_3}$	2	$^1_3$	$^1_{2_3}$	3	$^1_2$	$^1_{2_3}$	$^1_2$	$^1_{2_3}$
m_i	m1			m2			m3			m2,m3			m3,m1			m1,m2			m1,m2,m3	

CRYSTAL CLASS 24 — TABLE B-16

CUT →	X			Y			Z			(YXl)θ			(XYl)θ			(YXw)φ			(YXwl)φθ	
LETM ≡1	0	0	0	0	0	0	0	✓	✓	0	✓	✓	✓	0	✓	0	0	0	✓	✓
LETM ≡2	0	0	0	0	0	0	✓	0	✓	✓	0	✓	0	✓	✓	0	0	0	✓	✓
LETM ≡3	✓	0	✓	✓	0	✓	0	0	0	✓	0	✓	✓	0	✓	0	✓	✓	✓	✓
f_i	2	3	2_3	1	3	1_3	1	2	1_2	1	2_3	1_{2_3}	2	1_3	1_{2_3}	3	1_2	1_{2_3}	1_2	1_{2_3}
m_i	m1			m2			m3			m2,m3			m3,m1			m1,m2			m1,m2,m3	

CRYSTAL CLASS 25 — TABLE B-17

CUT →	X			Y			Z			(YXl)θ			(XYl)θ			(YXw)φ			(YXwl)φθ	
LETM ≡1	0	✓	✓	0	0	0	✓	0	✓	✓	0	✓	0	✓	✓	✓	0	✓	✓	✓
LETM ≡2	0	0	0	0	✓	✓	0	✓	✓	0	✓	✓	✓	0	✓	✓	0	✓	✓	✓
LETM ≡3	0	0	0	0	0	0	0	0	0	0	✓	✓	0	✓	✓	0	✓	✓	✓	✓
f_i	2	3	2_3	1	3	1_3	1	2	1_2	1	2_3	1_{2_3}	2	1_3	1_{2_3}	3	1_2	1_{2_3}	1_2	1_{2_3}
m_i	m1			m2			m3			m2,m3			m3,m1			m1,m2			m1,m2,m3	

CRYSTAL CLASS 26 — TABLE B-18

CUT →	X			Y			Z			(YXl)θ			(XYl)θ			(YXw)φ			(YXwl)φθ	
LETM ≡1	0	0	0	0	0	0	0	0	0	0	✓	✓	0	✓	✓	0	✓	✓	✓	✓
LETM ≡2	✓	0	✓	✓	0	✓	0	0	0	✓	0	✓	✓	0	✓	0	✓	✓	✓	✓
LETM ≡3	0	0	0	0	0	0	0	0	0	0	0	0	0	0	0	0	0	0	0	0
f_i	2	3	2_3	1	3	1_3	1	2	1_2	1	2_3	1_{2_3}	2	1_3	1_{2_3}	3	1_2	1_{2_3}	1_2	1_{2_3}
m_i	m1			m2			m3			m2,m3			m3,m1			m1,m2			m1,m2,m3	

CRYSTAL CLASS 28

TABLE B-19

CUT →	X			Y			Z			(YXl)θ			(XYl)θ			(YXw)φ			(YXwl)φθ	
LETM ≡1	0	0	0	0	✓	✓	0	✓	✓	0	✓	✓	✓	0	✓	✓	0	✓	✓	✓
LETM ≡2	0	✓	✓	0	0	0	✓	0	✓	✓	0	✓	0	✓	✓	✓	0	✓	✓	✓
LETM ≡3	✓	0	✓	✓	0	✓	0	0	0	✓	0	✓	✓	0	✓	0	✓	✓	✓	✓
f_i	2	3	2_3	1	3	1_3	1	2	1_2	1	2_3	1_{2_3}	2	1_3	1_{2_3}	3	1_2	1_{2_3}	1_2	1_{2_3}
m_i	m1			m2			m3			m2,m3			m3,m1			m1,m2			m1,m2,m3	

CRYSTAL CLASS 31

TABLE B-20

CUT →	X			Y			Z			(YXl)θ			(XYl)θ			(YXw)φ			(YXwl)φθ	
LETM ≡1	0	0	0	0	✓	✓	0	✓	✓	0	✓	✓	✓	0	✓	✓	0	✓	✓	✓
LETM ≡2	0	✓	✓	0	0	0	✓	0	✓	✓	0	✓	0	✓	✓	✓	0	✓	✓	✓
LETM ≡3	✓	0	✓	✓	0	✓	0	0	0	✓	0	✓	✓	0	✓	0	✓	✓	✓	✓
f_i	2	3	2_3	1	3	1_3	1	2	1_2	1	2_3	1_{2_3}	2	1_3	1_{2_3}	3	1_2	1_{2_3}	1_2	1_{2_3}
m_i	m1			m2			m3			m2,m3			m3,m1			m1,m2			m1,m2,m3	

CRYSTAL CLASS

CUT →	X			Y			Z			(YXl)θ			(XYl)θ			(YXw)φ			(YXwl)φθ	
LETM ≡1																				
LETM ≡2																				
LETM ≡3																				
f_i	2	3	2_3	1	3	1_3	1	2	1_2	1	2_3	1_{2_3}	2	1_3	1_{2_3}	3	1_2	1_{2_3}	1_2	1_{2_3}
m_i	m1			m2			m3			m2,m3			m3,m1			m1,m2			m1,m2,m3	

BIBLIOGRAPHY

1. R. D. Mindlin and M. G. Salvadori, "Analogies," in Handbook of Experimental Stress Analysis, M. Hetényi, Ed. (J. Wiley & Sons, Inc., New York, 1950), Chap. 16, pp. 700-827.

2. J. C. Maxwell, A Treatise on Electricity and Magnetism, (Dover, New York, 1954), 3rd ed., Vol. II, Chap. VII, p. 228, Fig. 34a.

3. Lord Kelvin, (Sir Wm. Thomson), Baltimore Lectures on molecular dynamics and the wave theory of light. (Cambridge U. Press, London, 1904), Lecture XI, pp. 122-131.

4. C. Truesdell and R. Toupin, "The Classical Field Theories," in Handbuch der Physik, S. Flügge, Ed., (Springer, Berlin, 1960), Vol. III/1, pp. 226-793.

5. J. Mac Cullagh, "An Essay Towards a Dynamical Theory of Crystalline Reflexion and Refraction," Trans. Roy. Irish Acad. Sci. (Dublin), Vol. 21, 1839, pp. 17-50.

6. A. S. Goldhaber and M. M. Nieto, "Terrestrial and Extraterrestrial Limits on The Photon Mass," Revs. Mod. Phys., Vol. 43, No. 3, July 1971, pp. 277-296.

7. Z. Bay and J. A. White, "Frequency Dependence of the Speed of Light in Space," Phys. Rev. D., Third Series, Vol. 5, No. 4, 15 Feb. 1972, pp. 796-799.

8. B. A. Auld, "Application of Microwave Concepts to the Theory of Acoustic Fields and Waves in Solids," IEEE Trans. on Microwave Theory and Techniques, Vol. MTT-17, No. 11, Nov. 1969, pp. 800-811.

9. S. -T. Peng, "Rigorous Analogies Between Elastic and Electromagnetic Systems," to be published.

10. A. Sommerfeld, Lectures on Theoretical Physics, (Academic Press, New York, 1964), Vol. II, Chap. III, p. 111.

11. E. C. Jordan, Electromagnetic Waves and Radiating Systems, (Prentice-Hall, Englewood Cliffs, N.J., 1950), Chap. 11, pp. 378-390.

12. S. Ramo and J. R. Whinnery, Fields and Waves in Modern Radio, (Wiley, New York, 1953), 2nd ed., Chap. 5, pp. 207-229.

13. R. F. Harrington, Time-Harmonic Electromagnetic Fields, (McGraw-Hill, New York, 1961), Chap. 1, pp. 12-14.

14. R. Plonsey and R. E. Collin, Principles and Applications of Electromagnetic Fields, (McGraw-Hill, New York, 1961), Chap. 9, pp. 326-341.

15. R. Plonsey and R. E. Collin, Principles and Applications of Electromagnetic Fields, (McGraw-Hill, New York, 1961), Chap. 10, pp. 361-369.

16. E. A. Guillemin, Communication Networks, (Wiley, New York, 1935), Vol. II, Chap. I, pp. 6-9.

17. H. Unz, "Oliver Heaviside (1850-1925)," IEEE Trans. on Education, Vol. E-6, Sept. 1963, pp. 30-33.

18. E. A. Guillemin, Introductory Circuit Theory, (Wiley, New York, 1953).

19. E. A. Guillemin, Synthesis of Passive Networks: theory and methods appropriate to the realization and approximation problems, (Wiley, New York, 1957).

20. W. Cauer, Synthesis of Linear Communication Networks, (McGraw-Hill, New York, 1958), 2nd ed., Vols. I & II.

21. H. J. Carlin and A. B. Giordano, Network Theory: an introduction to reciprocal and nonreciprocal circuits, (Prentice-Hall, Englewood Cliffs, N.J., 1964).

22. H. Ruston and J. Bordogna, Electric Networks: functions, filters, analysis, (McGraw-Hill, New York, 1966).

23. W. P. Mason, Electromechanical Transducers and Wave Filters, (van Nostrand, New York, 1948), 2nd ed.

24. D. C. Youla, "A Tutorial Exposition of some Key Network-Theoretic Ideas Underlying Classical Insertion-Loss Filter Design," Proc. IEEE, Vol. 59, No. 5, May 1971, pp. 760-799.

25. A. I. Zverev, Handbook of Filter Synthesis, (Wiley, New York, 1967).

26. W. Herzog, Siebschaltungen mit Schwingkristallen,(Dieterich'sche Verlagsbuchhandlung, Wiesbaden, 1949).

27. D. I. Kosowski and C. R. Hurtig, "Recent Developments in Crystal Filters," Proc. 17th Annual Frequency Control Symposium, U. S. Army Electronics Research and Development Laboratory, Fort Monmouth, New Jersey, May 1963, pp. 566-586.

28. J. Groszkowski, Frequency of Self-Oscillation, (Macmillan, New York, 1964).

29. E. Hafner, "Theory of Oscillator Design," Proc. 17th Annual Frequency Control Symposium, U. S. Army Electronics Research and Development Laboratory, Fort Monmouth, NJ, May 1963, pp. 508-536.

30. P. I. Richards, "Resistor-Transmission-Line Circuits," Proc. IRE, Vol. 36, No. 2, Feb. 1948, pp. 217-220.

31. H. J. Carlin, "Distributed Circuit Design With Transmission Line Elements," Proc. IEEE, Vol. 59, No. 7, July 1971, pp. 1059-1081.

32. T. Koga, "Synthesis of a Resistively Terminated Cascade of Uniform Lossless Transmission Lines and Lumped Passive Lossless

Two-Ports," IEEE Trans. on Circuit Theory, Vol. CT-18, No. 4, July 1971, pp. 444-455.

33. IEEE Transactions on Circuit Theory, Vol. CT-18, No. 1, Jan. 1971, Special Issue on Computer-Aided Circuit Design.

34. G. Green, "On the Propagation of Light in Crystallized Media," Trans. Cambridge Phil. Soc., Vol. 7, Part 2, 1839, pp. 121-140.

35. G. Green, "On the Laws of Reflexion and Refraction of Light at the Common Surface of Two Noncrystallized Media," Trans. Cambridge Phil. Soc., Vol. 7, Part 1, 1838, pp. 1-24.

36. E. B. Christoffel, "Ueber die Fortpflanzung von Stössen durch elastische feste Körper," Annali di Matematica (Milano), Series II, Vol. VIII, 1877, pp. 193-243.

37. Lord Kelvin, (Sir Wm. Thomson), Baltimore Lectures on molecular dynamics and the wave theory of light. (Cambridge U. Press, London, 1904).

38. M. J. P. Musgrave, "On the Propagation of Elastic Waves in Aelotropic Media. I. General Principles," Proc. Roy. Soc. (London), Vol. A226, 1954, pp. 339-355.

39. M. J. P. Musgrave, "On the Propagation of Elastic Waves in Aelotropic Media. II. Media of Hexagonal Symmetry," Proc. Roy. Soc. (London), Vol. A226, 1954, pp. 356-366.

40. G. F. Miller and M. J. P. Musgrave, "On the Propagation of Elastic Waves in Aelotropic Media. III. Media of Cubic Symmetry," Proc. Roy. Soc. (London), Vol. A236, 1956, pp. 352-383.

41. M. J. P. Musgrave, "The Propagation of Elastic Waves in Crystals and other Anisotropic Media," in Reports on Progress in Physics, (Physical Society, London, 1959), Vol. XXII, pp. 74-96.

42. M. J. P. Musgrave, "Elastic Waves in Anisotropic Media," in Progress in Solid Mechanics, I. N. Sneddon and R. Hill, Eds., (Interscience, New York, 1961), Vol. II, Chap. II, pp. 61-85.

43. A. W. Lawson, "Comment on the Elastic Constants of Alpha-Quartz," Phys. Rev., Vol. 59, 1941, pp. 838-839.

44. J. V. Atanasoff and P. J. Hart, "Dynamical Determination of the Elastic Constants and Their Temperature Coefficients for Quartz," Phys. Rev., Vol. 59, Jan. 1941, pp. 85-96.

45. R. Bechmann, "Über Dickenschwingungen piezoelektrischer Kristallplatten," Archiv der Elektrischen Übertragung, Vol. 6, Sept. 1952, pp. 361-368.

46. R. Bechmann, "Über Dickenschwingungen piezoelektrischer Kristallplatten," Nachtrag, Archiv der Elektrischen Übertragung, Vol. 7, July 1953, pp. 354-356.

47a. R. Bechmann and S. Ayers, "Thickness Modes of Plates Excited Piezoelectrically," Research Report No. 13471, Post Office Research Station, Dollis Hill, London, May 1952, pp. 15.

47b. R. Bechmann and S. Ayers, "Thickness Modes of Plates Excited Piezoelectrically," in Piezoelectricity, (Her Majesty's Stationery Office, London, 1957), Report No. 2, Part 2, pp. 33-41.

48. J. J. Kyame, "Wave Propagation in Piezoelectric Crystals," J. Acoust. Soc. Amer., Vol. 21, No. 3, May 1949, pp. 159-167.

49. H. Pailloux, "Piézoélectricité Calcul des Vitesses de Propagation," J. Phys. Rad., Vol. 19, May 1958, pp. 523-525.

50. V. Alda, K. Hruška and J. Tichý, "Propagation of Waves Through Infinite Piezoelectric Medium," Czech. J. Phys., Vol. 13, 1963, pp. 345-366. (In Czech).

51. K. Hruška, "The Rate of Propagation of Ultrasonic Waves in ADP in Voigt's Theory," Czech. J. Phys., Vol. B16, 1966, pp. 446-453.

52. K. Hruška, "Relation Between the General and the Simplified Condition for the Velocity of Propagation of Ultrasonic Waves a Piezoelectric Medium," Czech. J. Phys., Vol. B18, 1968, pp. 214-221.

53. C. G. Knott, "Reflexion and Refraction of Elastic Waves, with Seismological Applications," Phil. Mag., Fifth Series, Vol. 48, No. 290, July 1899, pp. 64-97.

54. R. D. Mindlin, "Waves and Vibrations in Isotropic, Elastic Plates," in Structural Mechanics, J. N. Goodier and N. J. Hoff, Eds., (Pergamon Press, New York, 1960), pp. 199-232.

55. I. Koga, "Thickness Vibrations of Piezoelectric Oscillating Crystals," Physics, Vol. 3, Aug. 1932, pp. 70-80.

56. I. Koga, "Vibration of Piezoelectric Oscillating Crystal," Phil. Mag., Seventh Series, Vol. 16, No. 104, Aug. 1933, pp. 275-283.

57. Lord Rayleigh, (J. W. Strutt), "On the Free Vibrations of an Infinite Plate of Homogeneous Isotropic Elastic Matter," Proc. London Math. Soc., Vol. XX, No. 357, 1889, pp. 225-234.

58. H. Ekstein, "High Frequency Vibrations of Thin Crystal Plates," Phys. Rev., Vol. 68, Nos. 1 and 2, July 1945, pp. 11-23.

59. E. G. Newman and R. D. Mindlin, "Vibrations of a Monoclinic Crystal Plate," J. Acoust. Soc. Amer., Vol. 29, No. 11, Nov. 1957, pp. 1206-1218.

60. W. G. Cady, "The Piezoelectric Resonator and the Effect of Electrode Spacing upon Frequency," Physics, Vol. 7, No. 7, July 1936, pp. 237-259.

61. A. W. Lawson, "The Vibration of Piezoelectric Plates," Phys. Rev., Vol. 62, July 1942, pp. 71-76.

62. H. Ekstein, "Forced Vibrations of Piezoelectric Crystals," Phys. Rev., Vol. 70, Nos. 1 and 2, July 1946, pp. 76-84.

63. R. D. Mindlin, "Forced Thickness-Shear and Flexural Vibrations of Piezoelectric Crystal Plates," J. Appl. Phys., Vol. 23, No. 1, Jan. 1952, pp. 83-88.

64. H. F. Tiersten, "Thickness Vibrations of Piezoelectric Plates," J. Acoust. Soc. Amer., Vol. 35, No. 1, Jan. 1963, pp. 53-58.

65. T. Yamada and N. Niizeki, "Admittance of Piezoelectric Plates Vibrating Under the Perpendicular Field Excitation," Proc. IEEE, Vol. 58, No. 6, June 1970, pp. 941-942.

66. J. J. Kyame, "Conductivity and Viscosity Effects on Wave Propagation in Piezoelectric Crystals," J. Acoust. Soc. Amer., Vol. 26, No. 6, Nov. 1954, pp. 990-993.

67. M. J. P. Musgrave, "Elastic Waves in Anisotropic Media," in Progress in Solid Mechanics, I. N. Sneddon and R. Hill, Eds., (Interscience, New York, 1961), Vol. II, Chap. II, Sec. 11, pp. 75-77.

68. A. R. Hutson and D. L. White, "Elastic Wave Propagation in Piezoelectric Semiconductors," J. Appl. Phys., Vol. 33, No. 1, 1962, pp. 40-47.

69. G. Arlt, "Resonance-Antiresonance of Conducting Piezoelectric Resonators," J. Acoust. Soc. Amer., Vol. 37, No. 1, Jan. 1965, pp. 151-157.

70. J. Lamb and J. Richter, "Anisotropic Acoustic Attenuation with New Measurements for Quartz at Room Temperatures," Proc. Roy. Soc. (London), Vol. A293, 1966, pp. 479-492.

71. R. Holland, "Representation of Dielectric, Elastic, and Piezoelectric Losses by Complex Coefficients," IEEE Trans. on Sonics and Ultrasonics, Vol. SU-14, No. 1, Jan. 1967, pp. 18-20.

72. G. K. Guttwein, T. J. Lukaszek, and A. D. Ballato, "Practical Consequences of Modal Parameter Control in Crystal Resonators," Proc. 21st Annual Frequency Control Symposium, U. S. Army Electronics Command, Fort Monmouth, New Jersey, April 1967, pp. 115-137.

73. W. E. Newell, "Face-Mounted Piezoelectric Resonators," Proc. IEEE, Vol. 53, No. 6, June 1965, pp. 575-581.

74. W. E. Newell, "Ultrasonics in Integrated Electronics," Proc. IEEE, Vol. 53, No. 10, Oct. 1965, pp. 1305-1309.

75. Clevite Corporation Staff, Piezoelectric Technology Data for Engineers, Piezoelectric Division, Clevite Corporation, Bedford Ohio 44146, 1965, pp. 45.

76. J. van Randeraat, Ed., Piezoelectric Ceramics, Electronic Components and Materials Division, N. V. Philips' Gloeilampenfabrieken, Einhoven, The Netherlands, June 1968, pp. 118.

77. T. F. Hueter and R. H. Bolt, Sonics, (Wiley, New York, 1955), Sec. 4.12, pp. 136-146.

78. R. Holland, "The Linear Theory of Multielectrode Piezoelectric Plates," 1966 WESCON Convention Record, Vol. 10, part 3, paper 3/3, pp. 15.

79. E. P. EerNisse, "Resonances of One-Dimensional Composite Piezoelectric and Elastic Structures," IEEE Trans. on Sonics and Ultrasonics, Vol. SU-14, No. 2, April 1967, pp. 59-67.

80. E. K. Sittig, "Transmission Parameters of Thickness-Driven Piezoelectric Transducers Arranged in Multilayer Configurations," IEEE Trans. on Sonics and Ultrasonics, Vol. SU-14, No. 4, Oct. 1967, pp. 167-174.

81. E. K. Sittig, A. W. Warner, and H. D. Cook, "Bonded Piezoelectric Transducers for Frequencies Beyond 100 MHz," Ultrasonics, Vol. 7, No. 2, April 1969, pp. 108-112.

82. O. M. Stuetzer, "Piezoelectric Pulse and Code Generators," IEEE Trans. on Sonics and Ultrasonics, Vol. SU-14, No. 2, April 1967, pp. 75-88.

83. R. F. Mitchell and M. Redwood, "Frequency Response of a Distributed Piezoelectric Source of Sound," Electronics Letters, Vol. 4, No. 6, Mar. 1968, pp. 107-109.

84. R. Holland and E. P. EerNisse, Design of Resonant Piezoelectric Devices, (M.I.T. Press, Cambridge, Mass., 1969), Sec. 2.4, pp. 89-95.

85. D. I. Bolef and M. Menes, "Measurement of Elastic Constants of RbBr, RbI, CsBr, and CsI by an Ultrasonic cw Resonance Technique," J. Appl. Phys., Vol. 11, No. 6, June 1960, pp. 1010-1017.

86. W. J. Price and H. B. Huntington, "Acoustical Properties of Anisotropic Materials," J. Acoust. Soc. Amer., Vol. 22, No. 1, Jan. 1950, pp. 32-37.

87. W. G. Cady, Piezoelectricity, (McGraw-Hill, New York, 1946), also (Dover, New York, 1964), Chap. VIII, p. 185 and Chap. XIII, p. 312.

88. E. G. Cook, "Transient and Steady-State Response of Ultrasonic Piezoelectric Transducers," IRE Nat. Convention Record, Vol. 4, Part 9, 1956, pp. 61-69.

89. J. C. Slater, "Transducer for Producing Sound at Microwave Frequencies," U. S. Patent No. 2,773,996, filed 13 Sept. 1946, issued 11 Dec. 1956.

90. D. L. Arenberg, "Ultrasonic Apparatus," U. S. Patent No. 2,883,660, filed 27 Oct. 1953, issued 21 April 1959.

91. H. E. Bömmel and K. Dransfeld, "Excitation of Very-High-Frequency Sound in Quartz," Phys. Rev. Lett., Vol. 1, No. 7, April 1958, pp. 234-236.

92. H. E. Bömmel and K. Dransfeld, "Attenuation of Hypersonic Waves in Quartz," Phys. Rev. Lett., Vol. 2, No. 7, April 1959, pp. 298-299.

93. H. E. Bömmel and K. Dransfeld, "Excitation and Attenuation of Hypersonic Waves in Quartz," Phys. Rev., Vol. 117, No. 5, Mar. 1960, pp. 1245-1252.

94. E. H. Jacobsen, "Experiments with Phonons at Microwave Frequencies," in Quantum Electronics, C. H. Townes, Ed., (Columbia U. Press, New York, 1960), pp. 468-484.

95. E. H. Jacobsen, "Sources of Sound in Piezoelectric Crystals," J. Acoust. Soc. Amer., Vol. 32, No. 8, Aug. 1960, pp. 949-953.

96. R. F. Mitchell and M. Redwood, "The Generation of Sound in Non-Uniform Piezoelectric Materials," Ultrasonics, Vol. 7, No. 2, April 1969, pp. 123-124.

97. R. F. Mitchell and M. Redwood, "Generation and Detection of Sound by Distributed Piezoelectric Sources," J. Acoust. Soc. Amer., Vol. 47, No. 3, (Part 1), 1970, pp. 701-710.

98. D. A. Leedom, R. Krimholtz, and G. L. Matthaei, "Equivalent Circuits for Transducers Having Arbitrary Even- or Odd- Symmetry Piezoelectric Excitation," IEEE Trans. on Sonics and Ultrasonics, Vol. SU-18, No. 3, July 1971, pp. 128-141.

99. M. Redwood, "Transient Performance of a Piezoelectric Transducer," J. Acoust. Soc. Amer., Vol. 33, No. 4, April 1961, pp. 527-536.

100. M. Redwood, "Experiments with the Electrical Analog of a Piezoelectric Transducer," J. Acoust. Soc. Amer., Vol. 36, No. 10, Oct. 1964, pp. 1872-1880.

101. R. G. Peterson and M. Rosen, "Use of Thick Transducers to Generate Short-Duration Stress Pulses in Thin Specimens," J. Acoust. Soc. Amer., Vol. 41, No. 2, 1967, pp. 336-345.

102. R. W. Holland, "Application of Green's Functions and Eigenmodes in the Design of a Piezoelectric Ceramic Devices," Ph.D. Thesis, Electrical Engineering, Massachusetts Institute of Technology, Jan. 1966, pp. 383.

103. R. Holland, "The Equivalent Circuit of an N-Electrode Piezoelectric Bar," Proc. IEEE, Vol. 54, No. 7, July 1966, pp. 968-975.

104. R. Holland, "The Equivalent Circuit of a Symmetric N-Electrode Piezoelectric Disk," IEEE Trans. on Sonics and Ultrasonics, Vol. SU-14, No. 1, Jan. 1967, pp. 21-33.

105. J. C. Slater, Microwave Electronics, (Van Nostrand, Princeton, New Jersey, 1950), Preface, pp. v-ix.

106. J. C. Slater, Microwave Transmission, (Dover, New York, 1959), Chap. I, pp. 7-42.

107. C. G. Montgomery, R. H. Dicke and E. M. Purcell, Eds., Principles of Microwave Circuits, (Dover, New York, 1965).

108. N. Marcuvitz, Ed., Waveguide Handbook, (Dover, New York, 1965).

109. R. E. Collin, Field Theory of Guided Waves, (McGraw-Hill, New York, 1960), p. 105, p. 463, etc.

110. W. L. Weeks, Electromagnetic Theory for Engineering Applications, (Wiley, New York, 1964).

111. R. -S. Chu and T. Tamir, "Guided-Wave Theory of Light Diffraction by Acoustic Microwaves," IEEE Trans. on Microwave Theory and Techniques, Vol. MTT-17, No. 11, Nov. 1969, pp. 1002-1020.

112. Lord Rayleigh, (J. W. Strutt), The Theory of Sound, (Dover, New York, 1945), 2nd ed., Vol. I and Vol. II.

113. W. P. Mason, "A Study of the Regular Combination of Acoustic Elements, with Applications to Recurrent Acoustic Filters, Tapered Acoustic Filters, and Horns," Bell System Tech. J., Vol. 6, No. 2, April 1927, pp. 258-294.

114. W. P. Mason, "Electrical Wave Filters Employing Quartz Crystals as Elements," Bell System Tech. J., Vol. 13, 1934, pp. 405-452.

115. M. Redwood and J. Lamb, "On the Measurement of Attenuation in Ultrasonic Delay Lines," Proc. IEE (London), Vol. 103, Part B, Nov. 1956, pp. 773-780.

116. A. A. Oliner, "An Equivalent Network for Elastic Waves at a Solid-Liquid Interface, With Applications," Polytechnic Institute of Brooklyn, Electrophysics Memo PIBEP-68-016, Farmingdale, New York, Aug. 1968, pp. 22.

117. A. A. Oliner, "Microwave Network Methods for Guided Elastic Waves," IEEE Trans. on Microwave Theory and Techniques, Vol. MMT-17, No. 11, Nov. 1969, pp. 812-826.

118. A. A. Oliner, R. C. M. Li, and H. L. Bertoni, "Microwave Network Approach to Guided Acoustic Surface Wave Structures," Research and Development Technical Report ECOM-0418-F, Final Report on Contract DAAB07-69-C-0418. Polytechnic Institute of Brooklyn, Farmingdale, New York, August 1971, pp. 231.

119. S. Butterworth, "On a Null Method of Testing Vibration Galvanometers," Proc. Phys. Soc. (London), Vol. 26, 1914, pp. 264-273.

120. W. G. Cady, "The Piezo-Electric Resonator," Proc. IRE, Vol. 10, 1922, pp. 83-114.

121. K. S. Van Dyke, "The Electric Network Equivalent of a Piezo-Electric Resonator," (Abstract), Phys. Rev., Vol. 25, No. 6, June 1925, p. 895.

122. D. W. Dye, "The Piezo-Electric Quartz Resonator and its Equivalent Electrical Circuit," Proc. Phys. Soc. (London), Vol. 38, 1926, pp. 399-458.

123. K. S. Van Dyke, "The Piezo-Electric Resonator and its Equivalent Network," Proc. IRE, Vol. 16, 1928, pp. 742-764.

124. Y. Watanabe, "Der piezoelektrische Resonator in Hochfrequenzschwingungskreisen," Elektrische Nachrichten-Technik, Vol. 5, No. 2, Feb. 1928, pp. 45-64.

125. Y. Watanabe, "The Piezo-Electric Resonator in High-Frequency Oscillation Circuits," Part I, Proc. IRE, Vol. 18, No. 4, April 1930, pp. 695-717.

126. Y. Watanabe, "The Piezo-Electric Resonator in High-Frequency Oscillation Circuits," Parts II, III, IV, Proc. IRE, Vol. 18, No. 5, May 1930, pp. 862-893.

127. A. Ballato, "Resonance in Piezoelectric Vibrators," Proc. IEEE, Vol. 58, No. 1, Jan. 1970, pp. 149-151.

128. W. P. Mason, "An Electromechanical Representation of a Piezoelectric Crystal Used as a Transducer," Proc. IRE, Vol. 23, No. 10, Oct. 1935, pp. 1252-1263.

129. S. Butterworth, "On Electrically-maintained Vibrations," Proc. Phys. Soc. (London), Vol. 27, 1915, pp. 410-424.

130. W. P. Mason, "A Dynamic Measurement of the Elastic, Electric and Piezoelectric Constants of Rochelle Salt," Phys. Rev., Vol. 55, April 1939, pp. 775-789.

131. D. A. Berlincourt, D. R. Curran, and H. Jaffe, "Piezoelectric and Piezomagnetic Materials and Their Function in Transducers," in Physical Acoustics: Principles and Methods, W. P. Mason, Ed., (Academic Press, New York, 1964) Vol. I, Part A, Chap. 3, pp. 169-270.

132. W. Roth, "Piezoelectric Transducers," Technical Report No. 43, Research Laboratory of Electronics, Massachusetts Institute of Technology, Cambridge, Massachusetts, July 1947, pp. 36.

133. W. Roth, "Piezoelectric Transducers," Proc. IRE, Vol. 37, No. 7, July 1949, pp. 750-758.

134. R. Bechmann, "Dickenschwingungen piezoelektrisch erregter Kristallplatten," Hochfrequenztecknik u. Elektroakustik, Vol. 56, 1940, pp. 14-21.

135. R. Holland and Eer Nisse, "Variational Evaluation of Admittance of Multielectroded Three-Dimensional Piezoelectric Structures," IEEE Trans. on Sonics and Ultrasonics, Vol. SU-15, No. 2, April 1968, pp. 119-132.

136. R. Holland and E. P. Eer Nisse, Design of Resonant Piezoelectric Devices, (M.I.T. Press, Cambridge, Mass., 1969).

137. R. Bechmann, "Some Application of the Linear Piezoelectric Equations of State," Trans IRE Prof. Group on Ultrasonic Engrg., Vol. PGUE-3, May 1955, pp. 43-62.

138. R. Bechmann, "Elastic, Piezoelectric and Dielectric Constants of Polarized Barium Titanate Ceramics and Some Applications of the Piezoelectric Equations," J. Acoust. Soc. Amer., Vol. 28, No. 3, May 1956, pp. 347-350.

139. "IRE Standards on Piezoelectric Crystals: Determination of the Elastic, Piezoelectric, and Dielectric Constants - The Electromechanical Coupling Factor, 1958," Proc. IRE, Vol. 46, No. 4, April 1958, pp. 764-778. (IEEE Standard No. 178).

140. "IRE Standards on Piezoelectric Crystals: Measurements of Piezoelectric Ceramics, 1961," Proc. IRE, Vol. 49, No. 7, July 1961, pp. 1161-1169. (IEEE Standard No. 179).

141. M. Onoe, H. F. Tiersten, and A. H. Meitzler, "Shift in the Location of Resonant Frequencies Caused by Large Electromechanical Coupling in Thickness-Mode Resonators," J. Acoust. Soc. Amer., Vol. 35, No. 1, Jan. 1963, pp. 36-42.

142. M. Onoe and H. Jumonji, "Useful Formulas for Piezoelectric Ceramic Resonators and Their Application to Measurement of Parameters," J. Acoust. Soc. Amer., Vol. 41, No. 4, (Part 2), 1967, pp. 974-980.

143. H. Schüssler, "Darstellung elektromechanischer keramischer Wandler als Dickenscherschwinger mit piezoelektrischer und piezomagnetischer Anregung," Archiv der Elektrischen Übertragung, Vol. 22, No. 8, Aug. 1968, pp. 399-406.

144. M. Marutake, "Approximate Method of Calculating Electromechanical Coupling Factor," Proc. IRE, Vol. 49, May 1961, p. 967.

145. M. Marutake, "Approximate Method of Calculating Electromechanical Coupling Factor II," Proc. IRE, Vol. 50, Feb. 1962, pp. 214-215.

146. J. K. Stevenson and M. Redwood, "The Motional Reactance of a Piezoelectric Resonator - A More Accurate and Simpler Representation for use in Filter Design," IEEE Trans. on Circuit Theory, Vol. CT-16, No. 6, Nov. 1969, pp. 568-572.

147. J. Williams and J. Lamb, "On the Measurement of Ultrasonic Velocity in Solids," J. Acoust. Soc. Amer., Vol. 30, No. 4, April 1958, pp. 308-313.

148. C. Franx, "On Activity Dips of AT Crystals at High Level of Drive," Proc. 21st Annual Frequency Control Symposium, U.S. Army Electronics Command, Fort Monmouth, New Jersey, April 1967, pp. 436-454.

149. R. Krimholtz, D. A. Leedom, and G. L. Matthaei, "New Equivalent Circuits for Elementary Piezoelectric Transducers," Electronics Lett., Vol. 6, June 1970, pp. 398-399.

150. W. P. Mason and R. A. Sykes, "Electrical Wave Filters Employing Crystals with Normal and Divided Electrodes," Bell System Tech. J., Vol. 19, 1940, pp. 221-248.

151. H. B. Huntington, The Elastic Constants of Crystals, (Academic Press, New York, 1958), pp. 52-53.

152. E. G. Cook and H. E. Van Valkenburg, "Thickness Measurement by Ultrasonic Resonance," J. Acoust. Soc. Amer., Vol. 27, No. 3, May 1955, pp. 564-569.

153. H. J. McSkimin, "Notes and References for the Measurement of Elastic Moduli by Means of Ultrasonic Waves," J. Acoust. Soc. Amer., Vol. 33, No. 5, May 1961, pp. 606-615.

154. "Standards on Piezoelectric Crystals, 1949," Proc. IRE, Vol. 37, No. 12, Dec. 1949, pp. 1378-1395. (IEEE Standard No. 176).

155a. "Standard Definitions and Methods of Measurement for Piezoelectric Vibrators," IEEE Standard No. 177, May 1966, (Inst. of Elec. and Elx. Engrs., New York, 1966).

155b. IRE Standards on Piezoelectric Crystals - The Piezoelectric Vibrator: Definitions and Methods of Measurement, 1957," Proc. IRE, Vol. 45, No. 3, Mar. 1957, pp. 353-358.

156. W. H. Horton and S. B. Boor, "Comparison of Crystal Measurement Equipment," Proc. 19th Annual Frequency Control Symposium, U. S. Army Electronics Command, Fort Monmouth, New Jersey, April 1965, pp. 436-468.

157. W. Thomson (Lord Kelvin) and P. G. Tait, Treatise on Natural Philosophy, (Cambridge U. Press, London, 1912) 3rd ed., Parts I and II.

158. W. Voigt, Lehrbuch der Kristallphysik, (B. G. Teubner, Leipzig, 1928).

159. A. E. H. Love, A Treatise on the Mathematical Theory of Elasticity, (Dover, New York, 1944), 4th ed.

160. W. G. Cady, Piezoelectricity, (McGraw-Hill, New York, 1946), also (Dover, New York, 1964).

161. R. A. Heising, Ed., Quartz Crystals for Electrical Circuits: Their Design and Manufacture, (van Nostrand, New York, 1946).

162. W. P. Mason, Piezoelectric Crystals and Their Application to Ultrasonics, (van Nostrand, New York, 1950).

163. R. D. Mindlin, An Introduction to the Mathematical Theory of Elastic Plates, Monograph prepared for U. S. Army Signal Corps Engrg. Labs., Fort Monmouth, New Jersey, 1955. Signal Corps Contract No. DA-36-039 sc 56772.

164. P. W. Forsbergh, Jr., "Piezoelectricity, Electrostriction and Ferroelectricity," in Handbuch der Physik, S. Flügge, Ed. (Springer, Berlin, 1956), Vol. XVII, pp. 264-392.

165. R. Bechmann, et al., in Piezoelectricity, (Her Majesty's Stationery Office, London, 1957), pp. 369.

166. J. F. Nye, Physical Properties of Crystals: their representation by tensors and matrices. (Clarendon Press, Oxford, 1957).

167. W. M. Ewing, W. S. Jardetzky, and F. Press, Elastic Waves in Layered Media, (McGraw-Hill, New York, 1957).

168. H. W. Katz, Ed., Solid State Magnetic and Dielectric Devices, (Wiley, New York, 1959), Chap. 3, "Electrostrictive and Magnetostrictive Systems," pp. 87-130.

169. H. W. Katz, Ed., Solid State Magnetic and Dielectric Devices, (Wiley, New York, 1959), Chap. 5, "Electromechanical Applications," pp. 170-232.

170. H. W. Katz, Ed., Solid State Magnetic and Dielectric Devices, (Wiley, New York, 1959), Chap. 11, "Magnetic and Dielectric Measurements," pp. 457-500.

171. L. M. Brekhovskikh, Waves in Layered Media, (Academic Press, New York, 1960).

172. R. F. S. Hearmon, An Introduction to Applied Anisotropic Elasticity, (Oxford Univ. Press, London, 1961).

173. H. Kolsky, Stress Waves in Solids, (Dover, New York, 1963).

174. L. Brillouin, Tensors in Mechanics and Elasticity, (Academic Press, New York, 1964).

175. R. Bechmann, "Piezoelectricity - Frequency Control," Proc. 18th Annual Frequency Control Symposium, U. S. Army Electronics Laboratories, Fort Monmouth, New Jersey, 1964, pp. 43-92.

176. W. P. Mason, "Use of Piezoelectric Crystals and Mechanical Resonators in Filters and Oscillators," in Physical Acoustics: Principles and Methods, W. P. Mason, Ed., (Academic Press, New York, 1964), Chap. 5, pp. 335-415.

177. Proceedings of the IEEE, Vol. 53, No. 10, Oct. 1965, Special Issue on Ultrasonics.

178. Y. C. Fung, Foundations of Solid Mechanics, (Prentice-Hall, Englewood Cliffs, New Jersey, 1965).

179. S. Bhagavantam, Crystal Symmetry and Physical Properties, (Academic Press, New York, 1966).

180. W. P. Mason, Crystal Physics of Interaction Processes, (Academic Press, New York, 1966).

181. R. Bechmann and R. F. S. Hearmon, "Elastic, Piezoelectric, Piezo-optic, and Electro-optic Constants of Crystals," in Landolt-Börnstein, Numerical Data and Functional Relationships in Science and Technology, K. -H. Hellwege, Ed., New Series, Group III, Vol. 1. (Springer, Berlin, 1966), pp. 160.

182. E. A. Gerber and R. A. Sykes, "State of the Art - Quartz Crystal Units and Oscillators," Proc. IEEE, Vol. 54, No. 2, Feb. 1966, pp. 103-116.

183. E. A. Gerber and R. A. Sykes, "Quartz Frequency Standards," Proc. IEEE, Vol. 55, No. 6, June 1967, pp. 783-791.

184. F. I. Fedorov, Theory of Elastic Waves in Crystals, (Plenum, New York, 1968).

185. IEEE Transactions on Microwave Theory and Techniques, Vol. MTT-17, No. 11, Nov. 1969, Special Issue on Microwave Acoustics.

186. R. Bechmann, R. F. S. Hearmon and S. K. Kurtz, "Elastic, Piezoelectric, Piezo-optic, Electro-optic Constants and Nonlinear Dielectric Susceptibilities of Crystals," in Landolt-Börnstein, Numerical Data and Functional Relationships in Science and Technology, K. -H. Hellwege, Ed., New Series, Group III, Vol. 2. (Springer, Berlin, 1969), pp. 232.

187. H. F. Tiersten, Linear Piezoelectric Plate Vibrations: elements of the linear theory of piezoelectricity and the vibrations of piezoelectric plates, (Plenum, New York, 1969).

188a. G. Bradfield, "Ultrasonic Transducers, 1. Introduction to Ultrasonic Transducers, Part A," Ultrasonics, Vol. 8, No. 2, April 1970, pp. 112-123.

188b. G. Bradfield, "Ultrasonic Transducers, 1. Introduction to Ultrasonic Transducers, Part B," Ultrasonics, Vol. 8, No. 3, July 1970, pp. 177-189.

189. M. J. P. Musgrave, Crystal Acoustics: introduction to the study of elastic waves and vibrations in crystals, (Holden-Day, San Francisco, 1970).

190. R. Bechmann, "General Formulae for the Transformation of the Elastic, Piezoelectric and Dielectric Constants," USA SRDL technical report 2051, U.S. Army Signal Research and Development Laboratory, Fort Monmouth, New Jersey, May 1959, pp. 88.

191. L. D. Landau and E. M. Lifshitz, Electrodynamics of Continuous Media, (Pergamon, London, 1960), Art. 17, pp. 78-79.

192. F. B. Hildebrand, Methods of Applied Mathematics, (Prentice-Hall, Englewood Cliffs, New Jersey, 1952), p. 39.

193. E. A. Guillemin, The Mathematics of Circuit Analysis, (Wiley, New York, 1949), Chap. III, Art. 10, pp. 111-118.

194. S. A. Basri, "A Method for The Dynamic Determination of The Elastic, Dielectric, and Piezoelectric Constants of Quartz," National Bureau of Standards Monograph 9, U. S. Dept. of Commerce, June 1960, pp. 22.

195. L. B. Felsen and N. Marcuvitz, "Modal Analysis and Synthesis of Electromagnetic Fields," Report R-446-55(a) and (b), Contract No. AF-19(604)-890, Polytechnic Institute of Brooklyn, Brooklyn, New York, Feb. 1956, pp. 40. AD93662.

196. A. E. H. Love, A Treatise on the Mathematical Theory of Elasticity, (Dover, New York, 1944), 4th ed., Chap. VII, Art. 125, pp. 177-178.

197. P. M. Morse and H. Feshbach, Methods of Theoretical Physics, (McGraw-Hill, New York, 1953), Art. 2.2, pp. 142-151, and Art. 3.4, pp. 318-337.

198. R. F. Harrington, Time - Harmonic Electromagnetic Fields, (McGraw-Hill, New York, 1961), Chap. 1, pp. 1-36; Chap. 2, pp. 37-94.

199. J. F. Havlice, W. L. Bond and L. B. Wigton, ""Elastic" Poynting Vector in a Piezoelectric Medium," IEEE Trans. on Sonics and Ultrasonics, Vol. SU-17, No. 4, Oct. 1970, pp. 246-249.

200. R. Bechmann, "Contour Modes of Plates Excited Piezoelectrically and Determination of Elastic and Piezoelectric Coefficients," IRE Convention Record, Part 6, Audio and Ultrasonics, 1954, pp. 77-85.

201. H. G. Baerwald, "Eigen Coupling Factors and Principal Components, The Thermodynamic Invariants of Piezoelectricity," IRE Convention Record, Vol. 8, Part 6, March 1960, pp. 205-211.

202. E. A. Guillemin, Introductory Circuit Theory, (Wiley, New York, 1953), Chap. 2, Art. 5, pp. 79-81.

203. A. R. von Hippel, Dielectrics and Waves, (Wiley, New York, 1954), Sec. 26, pp. 193-198, Sec. 27, pp. 198-202.

204. M. J. Buerger, Elementary Crystallography: An introduction to the fundamental geometrical features of crystals, (Wiley, New York, 1956).

205. S. K. Dickinson, Jr., "Guide to the Interpretation of Space Group Symbols," report AFCRL-65-279, Air Force Cambridge Research Laboratories, Bedford, Massachusetts, April 1965, pp. 44.

206. L. D. Landau and E. M. Lifshitz, Statistical Physics, (Pergamon, London, 1969), 2nd ed., Chap. XIII, pp. 401-423.

207. R. Bechmann, "Improved High - Precision Quartz Oscillators Using Parallel Field Excitation," Proc. IRE, Vol. 48, No. 3, Mar. 1960, pp. 367-368.

208. R. Bechmann, "Parallel Field Excitation of Thichness Modes of Quartz Plates," Proc. of the 14th Annual Frequency Control Symposium, U. S. Army Signal Research and Development Laboratory, Fort Monmouth, New Jersey, May-June 1960, pp. 68-88.

209. V. Ianouchevsky, "Parallel Field Excitation," Proc. IRE, Vol. 48, No. 6, June 1960, p. 1165.

210. R. Bechmann, "Excitation of Piezoelectric Plates By Use of a Parallel Field with Particular Reference to Thickness Modes of Quartz," Proc. IRE, Vol. 48, No. 7, July 1960, pp. 1278-1280.

211. W. Ianouchevsky, "The Stability and Q-Factor of Quartz-Crystals Excited by the Parallel Field Technique," (Observatoire de Paris, Paris, April 1963), Final Report to U. S. Dept. of Army, Contract No. DA-91-591-EUC-1752, May 1961 to April 1963. AD 410296.

212. W. Ianouchevsky, "High Q Crystal Units," Proc. 17th Annual Frequency Control Symposium, U. S. Army Electronics Research and Development Laboratory, Fort Monmouth, New Jersey, May 1963, pp. 233-247.

213. A. W. Warner, "Use of Parallel-Field Excitation in the Design of Quartz Crystal Units," Proc. 17th Annual Frequency Control Symposium, U. S. Army Electronics Research and Development Laboratory, Fort Monmouth, New Jersey, May 1963, pp. 248-266.

214a. A. D. Ballato and R. Bechmann, "Piezoelectric Crystal Element," U. S. Patent No. 3,202,846, filed 3 April 1963, issued 24 Aug. 1965.

214b. A. D. Ballato and R. Bechmann, "Piezoelectric Crystal Elements," U. K. Patent No. 1,028,102, filed 26 March 1964, issued 4 May 1966.

215. H. Schweppe, "Excitation of Two Adjacent Resonances With a Chosen Frequency Separation in a Ceramic Piezoelectric Resonator," IEEE Trans. on Sonics and Ultrasonics, Vol. SU-17, No. 1, Jan. 1970, pp. 12-17.

216a. IEEE Standards on Piezoelectricity, draft version, Section 4, April 1970, pp. 16.

216b. H. F. Tiersten, "Open Circuited Thickness Vibrations," unpublished notes, 1970, pp. 7.

217. E. A. Guillemin, Synthesis of Passive Networks: theory and methods appropriate to the realization and approximation problems, (Wiley, New York, 1957), Chap. 3, Art. 7, pp. 96-99.

218. H. J. Carlin and A. B. Giordano, Network Theory: an introduction to reciprocal and nonreciprocal circuits, (Prentice-Hall, Englewood Cliffs, N.J., 1964), Sec. 3.16, pp. 190-207.

219. E. A. Guillemin, The Mathematics of Circuit Analysis, (Wiley, New York, 1949), Chap. II, Art. 7, pp. 48-53.

220. W. G. Cady, "Composite Piezoelectric Resonator," IRE Transactions on Ultrasonic Engineering, Vol. PGUE-3, May 1955, pp. 1-15.

221. G. J. Kühn, "Symmetry of Energy-Transfer Ratios for Elastic Waves at a Boundary Between Two Media," J. Acoust. Soc. Amer., Vol. 36, No. 3, Mar. 1964, pp. 423-427.

222. L. M. Brekhovskikh, Waves in Layered Media, (Academic Press, New York, 1960), Chap. I, Sec. 3.4, pp. 25-27.

223. A. E. H. Love, A Treatise on the Mathematical Theory of Elasticity, (Dover, New York, 1944), 4th ed., Sec. 209, pp. 299-300.

224. R. D. Mindlin and P. C. Y. Lee, "Thickness-Shear and Flexural Vibrations of Partially Plated, Crystal Plates," Int. J. Solids Structures, Vol. 2, 1966, pp. 125-139.

225. J. Lamb and J. Richter, "Cavity Resonator for Piezoelectric Surface Excitation," J. Acoust. Soc. Amer., Vol. 41, No. 4, (Part 2), 1967, pp. 1043-1051.

226. J. Lamb and J. Richter, "New Type of Cavity Resonator for Piezoelectric Surface Excitation of Acoustic Waves at Microwave Frequencies," Electronics Lett., Vol. 2, No. 2, Feb. 1966, pp. 73-74.

227. M. Onoe and K. Okada, "Analysis of Contoured Piezoelectric Resonators Vibrating in Thickness-Twist Modes," Proc. 23rd Annual Frequency Control Symposium, U. S. Army Electronics Command, Fort Monmouth, New Jersey, May 1969, pp. 26-38.